LOW FREQUENCY WAVES IN A NARROW FJORD

Richard G. Dorrestein

Florida University

Prepared for:
Office of Naval Research

October 1972

ENGINEERING AND INDUSTRIAL EXPERIMENT STATION

College of Engineering

University of Florida

Gainesville

LOW FREQUENCY WAVES IN A NARROW FJORD

(EYJAFJÖRDUR, ICELAND)

Submitted to:

Department of the Navy
Office of Naval Research
Contract Nonr 580(17)

Submitted by:

Engineering and Industrial Experiment Station
College of Engineering
University of Florida
Gainesville

October 1972

UNCLASSIFIED

Security Classification

DOCUMENT CONTROL DATA - R & D

Security classification of title, body of abstract and indexing annotation must be entered when the overall report is classified

1. ORIGINATING ACTIVITY (Corporate author)

University of Florida

2a. REPORT SECURITY CLASSIFICATION

Unclassified

2b. GROUP

3. REPORT TITLE

Low Frequency Waves in a Narrow Fjord (Eyjafjordur, Iceland)

4. DESCRIPTIVE NOTES (Type of report and inclusive dates)

Final Report October 1972

5. AUTHOR(S) (First name, middle initial, last name)

Richard G. Dorrestein

6. REPORT DATE	7a. TOTAL NO. OF PAGES	7b. NO. OF REFS
Oct. 1972	191	19

8a. CONTRACT OR GRANT NO	9a. ORIGINATOR'S REPORT NUMBER(S)
NONR 580(17)	
b. PROJECT NO.	
c.	9b. OTHER REPORT NO(S) (Any other numbers that may be assigned this report)
d.	N/A

10. DISTRIBUTION STATEMENT

Distribution of this document is unlimited.

11. SUPPLEMENTARY NOTES	12. SPONSORING MILITARY ACTIVITY
	N/A

13. ABSTRACT

SEE ATTACHMENT

DD FORM 1 NOV 65 1473 (PAGE 1)

S/N 0101-807-6801

S-i

Security Classification

SUMMARY

Eyjafjördur is a relatively narrow and rather regularly shaped, more or less straight fjord on the North Coast of Iceland. Its total length is 60 km, depths are mainly 40 to 100 meters.

In the winters 1966 to 1968, a number of tide records were taken at five to seven stations along the fjord during periods of high depression activity, when long waves of all periods penetrated into the fjord from the sea.

For 14 selected time periods, eight of them of duration 24 hours, 48 minutes, approximating two cycles of the predominant M_2 tide, sets of simultaneous segments of the records from one to six stations could be analyzed.

The method of direct Fourier analysis appeared to be inadequate due to the large "contamination" of the Fourier components by the side-lobes of the large low-frequency water level variations in the whole fjord (not those of the astronomical tides, but: , which appeared to be directly associated with the variations of atmospheric pressure in the period range one to three days. After "pre-tapering" the records with a cosine square taper, however, subsequent Fourier analysis gave quite satisfactory results. For the digitalization, the records were sampled at intervals of two minutes. Spectra, cross-spectra and coherencies were thus computed up to the Nyquist frequency $(4 \text{ min.})^{-1} = 4\text{-}1/6$ mHz.

The results could be rather well fitted with the theoretical description of the one-dimensional long wave motion in narrow hypothetical fjords whose width b and mean depth d are given as certain powers of the distance x to the head of the fjord:

$$b = \text{const. } x^m \quad , \qquad d = \text{const. } x^n \quad ,$$

where m and n are positive constants and $n < 2$. For this category of fjords, the linearized differential equation in x for the complex amplitude of a harmonic water motion has the solution:

$$\text{const. } s^{\alpha} J_{-\alpha}(s) \quad , \qquad (1)$$

in which $J_{-\alpha}(s)$ is the Bessel function of the first kind of order $-\alpha$, $\alpha = \frac{1-m-n}{2-n}$, and in which the distance x and the angular frequency ω appear exclusively combined in the variable

$$s = \omega \int_0^x \frac{d\xi}{\sqrt{gd(\xi)}}$$

(+ possible small friction term). This implicates that the function $s^{\alpha} J_{-\alpha}(s)$ not only describes the relative behavior of amplitude and phase at given ω as a function of x, but also essentially the amplitude and phase at a given location x, with respect to the head $x = 0$, as function of the frequency ω.

Most of the spectra from the stations along the main fjord show more or less pronounced peaks at or near the frequencies .135, .30 and .47 mHz (periods 123, 55 and 35 minutes, respectively), corresponding with the first three modes of natural longitudinal oscillations in the fjord. Except for a few more (minor) peaks, all spectral levels decrease below noise level for frequencies beyond 1.8 mHz.

The station Olafsfjördur, situated on the head of a small side fjord of that name, gave completely different spectra, showing peaks at or near .76, 1.65 and 2.43 mHz, reflecting the natural modes of the side fjord.

From the frequencies of the peaks, the parameter α in the Bessel-type expression (1) that gives the best fit could be derived: $\alpha = -0.05$ for the main fjord; α = circa - 0.3 for Ólafsfjördur.

In most of the cases, the spectra of the stations on the main fjord show good to reasonable coherency with the spectrum of Akureyri at the head of the fjord for frequencies up to about 0.6 mHz, in some cases also up to about 1.2 mHz, so that several reasonable plots could be made of amplitude ratios and phase differences for any one of the main fjord stations and Akureyri, against the component number k. These plots show features that are characteristic for each station. They could be rather well fitted by the expression (1); for α, the best fitting values between 0 and + 0.3 were found for the inner parts of the main fjord.

All estimated α - values are not in contradiction with m- and n- values roughly estimated from the geometry of the fjord.

Using the data of eight spectra from Akureyri, a detailed analysis was made to estimate the expected shape of the "real" spectral peak at .135 mHz occurring at that station if there is a "white" input spectrum at sea near the mouth of the fjord. This resulted in an estimated half-power band width of .0085 mHz, a Q-factor of 16, and a maximum amplitude amplification factor of 24.

If seaward radiation of energy from the fjord is ignored, the estimated value of a bottom friction parameter, with the calculated low average tidal current velocities in the fjord (order of 3 cm/s) would lead to a very low Chezy coefficient C of only about $10 m^{\frac{1}{2}}/sec$ ($g/C^2 = 0.1$). It is therefore probable that the mentioned seaward energy radiation is the main factor determining the "quality" of the resonances in the fjord.

TABLE OF CONTENTS

SUMMARY

Eyjafjördur is a relatively narrow and rather regularly shaped, more or less straight fjord on the North Coast of Iceland. Its total length is 60 km, depths are mainly 40 to 100 meters.

In the winters 1966 to 1968, a number of tide records were taken at five to seven stations along the fjord during periods of high depression activity, when long waves of all periods penetrated into the fjord from the sea.

For 14 selected time periods, eight of them of duration 24 hours, 48 minutes, approximating two cycles of the predominant M_2 tide, sets of simultaneous segments of the records from one to six stations could be analyzed.

The method of direct Fourier analysis appeared to be inadequate due to the large "contamination" of the Fourier components by the side-lobes of the large low-frequency water level variations in the whole fjord (not those of the astronomical tides, but:), which appeared to be directly associated with the variations of atmospheric pressure in the period range one to three days. After "pre-tapering" the records with a cosine square taper, however, subsequent Fourier analysis gave quite satisfactory results. For the digitalization, the records were sampled at intervals of two minutes. Spectra, cross-spectra and coherencies were thus computed up to the Nyquist frequency $(4 \text{ min.})^{-1}$ = 4-1/6 mHz.

The results could be rather well fitted with the theoretical description of the one-dimensional long wave motion in narrow hypothetical fjords whose width b and mean depth d are given as certain powers of the distance x to the head of the fjord:

$$b = \text{const. } x^m \quad , \qquad d = \text{const. } x^n \quad ,$$

where m and n are positive constants and $n < 2$. For this category of fjords, the linearized differential equation in x for the complex amplitude of a harmonic water motion has the solution:

$$\text{const. } s^{\alpha} J_{-\alpha}(s) \quad , \qquad (1)$$

in which $J_{-\alpha}(s)$ is the Bessel function of the first kind of order $-\alpha$, $\alpha = \frac{1-m-n}{2-n}$, and in which the distance x and the angular frequency ω appear exclusively combined in the variable

$$s = w \int_0^x \frac{d\xi}{\sqrt{gd(\xi)}}$$

(+ possible small friction term). This implicates that the function $s^{\alpha} J_{-\alpha}(s)$ not only describes the relative behavior of amplitude and phase at given ω as a function of x, but also essentially the amplitude and phase at a given location x, with respect to the head $x = 0$, as function of the frequency ω.

Most of the spectra from the stations along the main fjord show more or less pronounced peaks at or near the frequencies .135, .30 and .47 mHz (periods 123, 55 and 35 minutes, respectively), corresponding with the first three modes of natural longitudinal oscillations in the fjord. Except for a few more (minor) peaks, all spectral levels decrease below noise level for frequencies beyond 1.8 mHz.

The station Ólafsfjördur, situated on the head of a small side fjord of that name, gave completely different spectra, showing peaks at or near .76, 1.65 and 2.43 mHz, reflecting the natural modes of the side fjord.

From the frequencies of the peaks, the parameter α in the Bessel-type expression (1) that gives the best fit could be derived: $\alpha = -0.05$ for the main fjord; α = circa - 0.3 for Olafsfjördur.

In most of the cases, the spectra of the stations on the main fjord show good to reasonable coherency with the spectrum of Akureyri at the head of the fjord for frequencies up to about 0.6 mHz, in some cases also up to about 1.2 mHz, so that several reasonable plots could be made of amplitude ratios and phase differences for any one of the main fjord stations and Akureyri, against the component number k. These plots show features that are characteristic for each station. They could be rather well fitted by the expression (1); for α, the best fitting values between 0 and + 0.3 were found for the inner parts of the main fjord.

All estimated α - values are not in contradiction with m- and n- values roughly estimated from the geometry of the fjord.

Using the data of eight spectra from Akureyri, a detailed analysis was made to estimate the expected shape of the "real" spectral peak at .135 mHz occurring at that station if there is a "white" input spectrum at sea near the mouth of the fjord. This resulted in an estimated half-power band width of .0085 mHz, a Q-factor of 16, and a maximum amplitude amplification factor of 24.

If seaward radiation of energy from the fjord is ignored, the estimated value of a bottom friction parameter, with the calculated low average tidal current velocities in the fjord (order of 3 cm/s) would lead to a very low Chezy coefficient C of only about $10 m^{\frac{1}{2}}/sec$ ($g/C^2 = 0.1$). It is therefore probable that the mentioned seaward energy radiation is the main factor determining the "quality" of the resonances in the fjord.

1. Introduction

1.1. Purpose of Study

The theory of the behavior of long waves penetrating from the sea into narrow channels, bays or fjords is relatively well known, especially so if the effects of bottom and lateral friction and of back radiation of energy toward the sea can be considered as of relatively small importance so that they can be linearized. One treatment on this subject was published some years ago as Technical Paper No. 213, Engineering Progress at the University of Florida, Vol. XV, No. 12, December 1961.

Relatively few field measurements with subsequent analyses are known to have been made, however, to check the theoretical concepts and, if possible, to estimate the magnitude of the effects of friction and seaward radiation in real situations. For some bays which have suitable dimensions for a large amplification of astronomical tides, studies have been made, e.g. for the Bay of Fundy. In Japan, much theoretical and empirical work was, and is, done concerning the properties of tsunami waves as they enter into bays and bights.

The purpose of the study reported here was to check theoretical concepts concerning the properties of long waves in narrow channels, etc. in a case of a rather simply shaped, rather deep and really narrow fjord for which a relatively simple theory should be valid in pretty good approximation. Eyjafjördur, a fjord on the north coast of Iceland was selected for this purpose.

The simple theory assumes that all long wave activity in the fjord is of oceanic origin so that no energy is transferred from the atmosphere to long waves within the fjord proper, and the fjord acts as a passive system on a

random input, except for the main tides. If, moreover, non-linear effects in the fjord caused by friction of the bottom and by the currents would be negligible, the fjord would act as a linear passive system so that, after spectral analysis, the coherencies of water levels between pairs of stations should be near to unity and the amplitude ratios and phase differences for any pair of stations should be the same functions of wave frequency for all records.

1.2 Main Tidal Data and Some Meteorological Conditions

The dimensions of the fjord are such that the semidiurnal and diurnal tides have only minor differences in amplitude and phase at different locations in the fjord. The most important constituent is the semidiurnal M_2 tide, amplitude (half of tidal range) 44 cm. The other constituents with amplitudes exceeding 1 cm are:

semidiurnal	S_2	amplitude	14 cm;
semidiurnal	N_2	amplitude	9 cm;
semidiurnal	K_2	amplitude	3 cm;
diurnal	K_1	amplitude	7 cm;
diurnal	O_1	amplitude	2 cm;
diurnal	P_1	amplitude	2 cm.

The north coast of Iceland is subject in some winters to the incursion of ice but Eyjafjördur is usually free from ice. Gales are frequent in winter. They are usually blowing from directions between north and east and are usually accompanied by heavy snowstorms. It is mainly in these situations and mainly without daylight that a number of tide recorders were in action and were looked after regularly by the attendants.

1.3 The Geometry of the Fjord

All the calculations following in this report are based on

roughly. Data were taken from the British Admiralty Chart nr. 3001 with a map of Eyjafjördur, scale 1:120.000.

A longitudinal coordinate x was defined along the axis of the main fjord, starting from x = 0 at the head of the fjord (Akureyi S); the mouth or seaward boundary of the fjord (in this case rather arbitrarily defined as a line running roughly W - E at 66°11' North) is then situated at x = 60 km. As functions of x, the width b was taken and the mean depth d was approximated from the chart, mostly with intervals of 3 km. Rough graphs of the functions b(x) and d(x) are given in the Figures 1A and 1B. Fig. 1B is a double logarithmic plot, allowing to obtain an idea of the magnitudes of the parameters m and n to be introduced in par 2.2.

As will be elucidated in par 2.1, it is appropriate to consider the transformation from x to the variable,

$$\int_0^x d\xi \, (gd(\xi))^{-\frac{1}{2}} \quad ,$$

representing the theoretical travel time of a long wave propagating from the head of the fjord to the location x. This was done by a graphical integration. For each of the stations along the main fjord from which records were analyzed, the following table gives the quantity

$$\frac{S_r}{k} = \frac{2\pi}{1488 \times 60 \times \sqrt{9.81}} \int_0^x \frac{d\xi}{\sqrt{d(\xi)}} = 2.24 \times 10^{-5} \int_0^x \frac{d\xi}{\sqrt{d(\xi)}} \quad ;$$

the meaning of the proportionality factor will become clear later.

Station	x(km)	$\frac{S_r}{k}$ (dimensionless)
Akureyri South	0	0
Akureyri North	2	.010 (rough)
Dagverdareyri	10½	.040
Hjalteyri	20½	.073[5]
Hrisey	37½	.124
(Mouth of Olafsfjördur)	(51-53½)	.164 (rough)
(Mouth)	60	.183 (rough)

A similar estimate of parameters, but a very rough one, has been made for the little side fjord of Olafsfjördur. This led to the following values: total length about 5 km; slopes of double logarithmic b(x) and d(x) plots m = about 0.3, n = from 1 (at head) to 2 (at mouth); S_r/k for whole fjord .035, or a factor 5.3 smaller than for the main fjord.

1.4 List of Notations

		Unit
a_k , b_k	Fourier coefficients	mm water
a'_k, b'_k	Fourier coefficients after "pre-tapering"	mm water
b(x)	width of water surface	m or km
c, c_1, c_2...	any constant	-
d(x)	average depth across the fjord or channel	
f/2T	frequency of harmonic wave motion	mHz = $10^{-3}s^{-1}$
f(t)	(in Appendix 1) ordinate of record to be analyzed	-
g	acceleration of gravity = 9.81	ms^{-2}
h(x,t),h( )	level of water surface above zero position	mm
k	number of Fourier component for "standard duration" of record (1488 min)	-
k'	same for other durations	-

		Unit
m	exponent in $b = x^m$, or: positive integer	-
n	exponent in $d = x^n$, or: positive integer	-
q(x,t)	volume transport through a cross-section, positive seaward	$m^3 s^{-1}$
q	friction or dissipation parameter (Chapter 2, Eq. (12))	-
r	modulus of amplitude ratio with respect to head of channel (Akureyri S)	-
s	variable (Chapter 2, Eq. (9))	-
s_r	real part of s	-
s_1, s_2 ...	zeros of Bessel-type solution without friction	-
s	(in Appendix 1) number of Fourier component	-
t	time	s, min or h
v(x,t)	longitudinal velocity of water, averaged over cross-section, positive seaward	ms^{-1}
$v_m(x)$	velocity occurring in friction term	$m\ s^{-2}$
x	distance along channel axis from head of channel, positive seaward	m or km
A(x) = b(x) · d(x)	cross-sectional area of channel	m^2
B(f,k)	"blurring function" (par. 4.4)	-
C	Chézy coefficient	$m^{\frac{1}{2}} s^{-1}$
$C_{12,k}$	co-spectral density for stations 1 & 2	mm^2/mHz
E	expectation or expected value of a variate	-
H(x)	complex amplitude of harmonic wave action	mm water
$H_a(x)$	normalized solution of differential equation (Chapter 2, Eq. (16))	-
P(|k-f|)	spectral window function (par. 4.4)	-
Q(x)	complex amplitude of harmonic discharge, positive seaward	$m^3 s^{-1}$

		Unit
$Q_{12,k}$	quad-spectral density for stations 1 & 2	mm^2/mHz
$2T$	duration of record	s, min or h
$2T_o$	"standard duration" of record = 1488 min	-
$W(f)$	spectral density	mm^2/mHz
W_k	$2T\beta_k$	
α	parameter of Bessel-type solution	-
β_k, $\beta_{k'}$	variance of water level associated with kth Fourier component	mm^2
γ	coefficient of bottom friction = g/C^2 (Chapter 2, Eq. (2))	-
$\gamma^2(f), \gamma^2 k$	coherency	-
ρ	phase difference	radian
$\tau=t/T$	$-1 \leq \tau \leq +1$	-
ω	angular frequency of wave motion	radian s^{-1}

In some places in the text, other symbols are temporarily introduced.

For the convenience of the reader:

1 mHz = $(1000\ s)^{-1}$ = $16\ 2/3\ min)^{-1}$ = 3.6 cycles per hour

1 k-unit = $(1488\ min)^{-1}$ = $(89280\ s)^{-1}$ = .0112 mHz

1 cycle per hour corresponds with k = 24.8

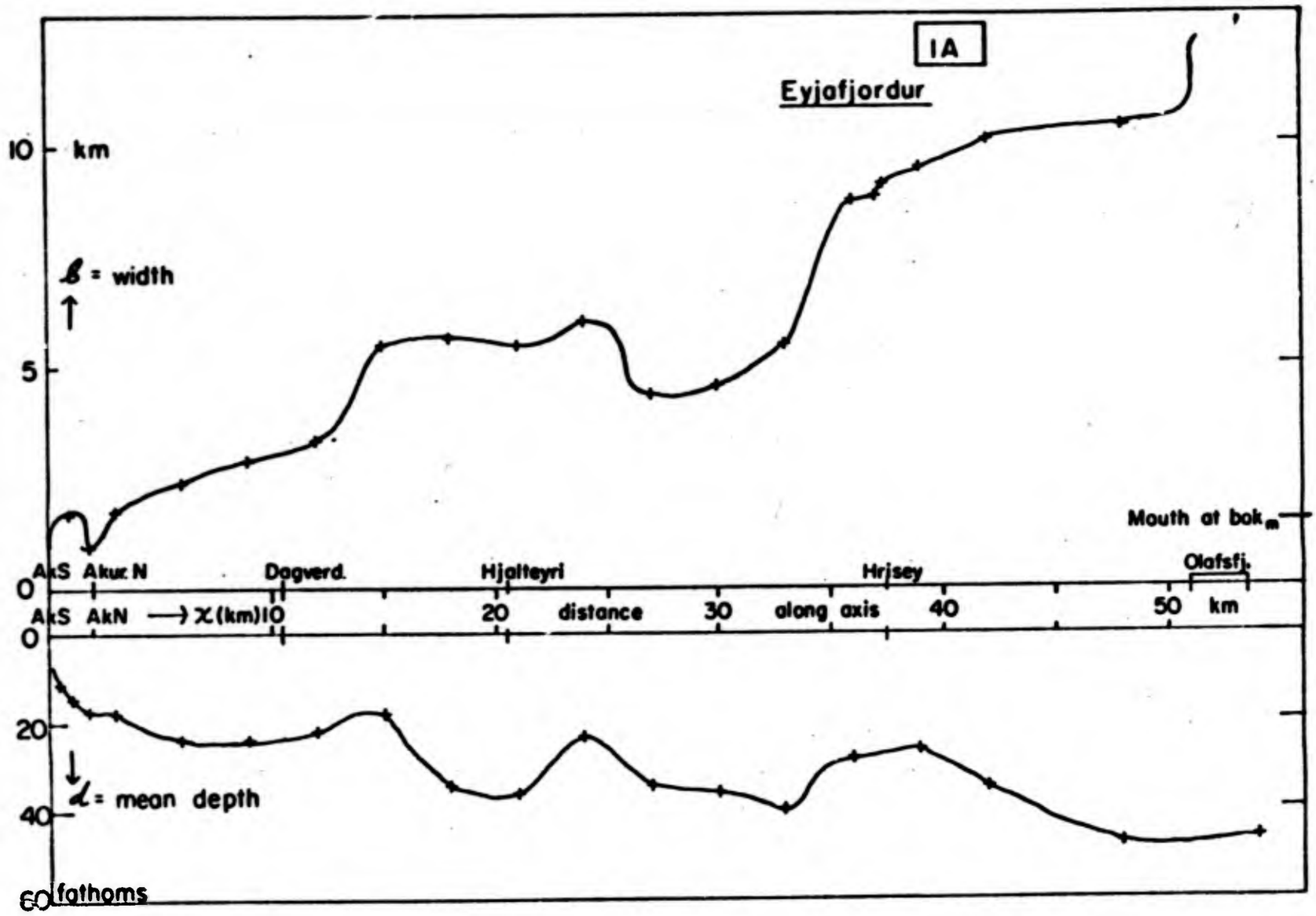
1A
Eyjafjordur
10
km
B = width
5
0
AkS
Akur. N
Dagverd.
Hjalteyri
Hrisey
Olafsfj.
Mouth at bok m
AkS
AkN
X (km) 10
20
distance
30
along axis
40
50
km
0
20
d = mean depth
40
fathoms

Figure 1A

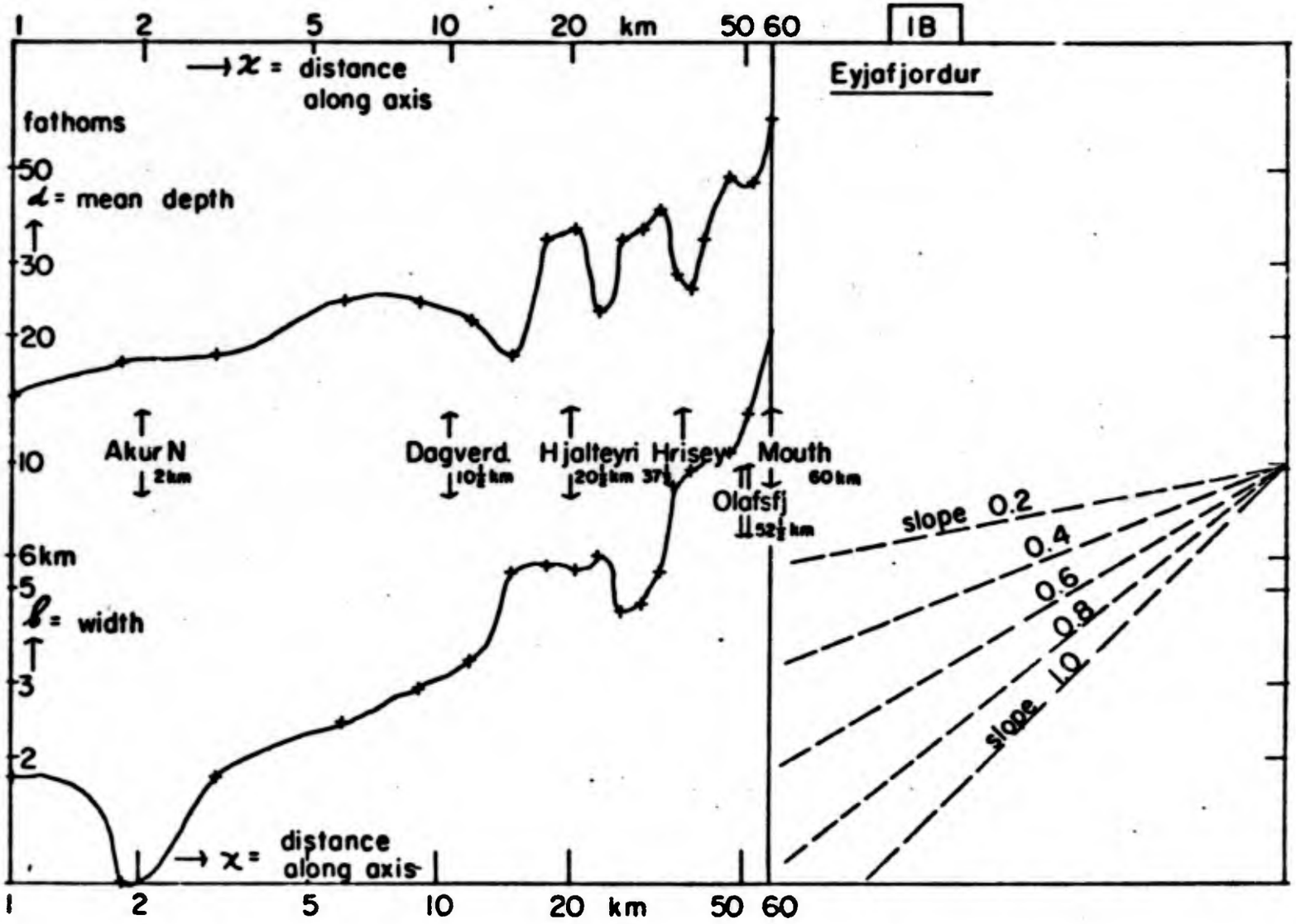
1B
Eyjafjordur
1 2 5 10 20 km 50 60
→x = distance along axis
fathoms
50
d = mean depth
30
20
10
Akur N
2km
Dagverd.
10½km
Hjalteyri
20½km
Hrisey
37½
Mouth
60km
Olafsfj
52½km
6km
5
ℓ = width
3
2
slope 0.2
0.4
0.6
0.8
1.0
→x = distance along axis
1 2 5 10 20 km 50 60

Figure 1B

2. Theory

A theoretical treatment of the penetration and amplification of long waves in narrow bays or channels was given in the paper "Amplification of Long Waves in Bays", Engineering Progress at the University of Florida, Vol. XV, No. 12, Technical Paper No. 213, December, 1961. In the following, a modification and an extension of that treatment is given. The just mentioned paper will be referred to as ALW.

2.1 The Differential Equations

The governing equations are

ALW(1):
$$\frac{\partial q}{\partial x} + b \frac{\partial h}{\partial t} = 0 \qquad (1)$$

ALW(2) modified:
$$\frac{\partial v}{\partial t} = - g \frac{\partial h}{\partial x} - \gamma \frac{|v|}{d} v \qquad (2)$$

where the dimensionless coefficient γ can be identified with g/C^2, C being the Chézy coefficient.

After linearization of the friction term on the right of (2), this equation can be approximately put in the form

ALW(4) modified:
$$\frac{\partial q}{\partial t} = - gbd \frac{\partial h}{\partial x} - \gamma \frac{v_m}{d} q \qquad (4)$$

where $v_m(x)$ is a time independent positive velocity to be determined later.

If we now consider the water motion to be harmonic in time with angular frequency ω (with the implication of a negligible net water flow in the fjord), Equations (4) and (1) yield:

ALW(6):
$$\frac{dQ}{dx} + i\omega bH = 0 \qquad (6)$$

ALW(7) modified:
$$\frac{dH}{dx} + \frac{i\omega + \gamma v_m/d}{gbd} Q = 0 \qquad (7)$$

If the total water motion would be "monochromatic", it is known that for v_m should be taken $8/3\pi$ times the local amplitude of v.

If, however, we consider a relatively small component of the water motion in the presence of a large tidal motion, v_m, in the equation for the small component could be best taken $6/\pi$ times the local amplitude of the large tidal motion, as will be shown in Chapter 9.

Since the friction term with γ is relatively small in the cases we shall consider it is convenient to introduce a modified (complex) depth parameter by

$$d^* = d\left(1 - \frac{i\gamma v_m}{\omega d}\right)^{-1} \tag{7a}$$

(with $d^* = d$, if friction is neglected) and (7) can be transformed to

$$\frac{dH}{dx} + \frac{i\omega}{gbd^*} Q = 0 \tag{7b}$$

Elimination of Q from (6) and (7b) then leads to the differential equation for H:

ALW(8) modified:
$$\frac{d^2H}{dx^2} + \frac{1}{bd^*}\frac{d}{dx}(bd^*) \times \frac{dH}{dx} + \frac{\omega^2}{gd^*} H = 0 \tag{8}$$

To simplify this equation, we again introduce a dimensionless variable s by

ALW(9) modified:
$$\frac{ds}{dx} = \frac{\omega}{\sqrt{gd^*}}, \quad s = \omega \int_0^x \frac{d\xi}{\sqrt{gd^*(\xi)}} \tag{9}$$

and obtain

ALW(10) modified:
$$\frac{d^2H}{ds^2} + \frac{1}{b\sqrt{d^*}}\frac{d}{ds}(b\sqrt{d^*}) \times \frac{dH}{ds} + H = 0 \tag{10}$$

where we have to remember, however, that b and d are considered as given functions of x, not directly as given functions of s.

Equation (7b) can be written

ALW(11) modified: $$Q = ib\sqrt{gd^*}\, x \frac{dH}{ds} \qquad (11)$$

The new variable s, according to (9) and (7a) can be approximated as follows if the imaginary part of d^x is relatively small:

$$s = \omega \int_0^x \frac{d\xi}{\sqrt{gd}} \left(1 - \frac{1}{2} i\gamma \frac{v_m}{\omega d}\right)$$

$$= \omega \int_0^x \frac{d\xi}{\sqrt{gd}} - \frac{1}{2} i\gamma \int_0^x d\xi \frac{v_m}{d\sqrt{gd}} = s_r (1 - iq) \qquad (12)$$

where s_r represents the real part of s and q (positive) << 1 is half the parameter f that was used in ALW (see ALW(12)).

As we will see later, the analysis of the Eyjafjördur records allow certain estimates of q to be made.

2.2 The Bessel-Type Solutions

In the paper ALW, solutions of the differential equations for H and Q were presented for a number of special cases. We shall now consider the solution in a more general case, in which the previously treated cases A, B, C, D are all included. The treatment to be given now can, in principle, be found in earlier publications by others, e.g. Schönfeld [1], but as far as evident, has never before been elaborated and applied to an actual bay, channel or fjord.

The category of narrow bays to be considered here is characterized by the following expressions defining the width and mean depth as functions of

the longitudinal distance x:

$$b = \text{const. } x^m, \qquad d = \text{const. } x^n, \qquad d^* = \text{const. } x^n \tag{13}$$

where m and n are positive constants or zero and n is smaller than 2. In fact, the second and third equalities cannot hold at the same time, unless v_m/d in (7a) would be independent of x for a given ω. We assume that the imaginary part of d^* is always small so that <u>both</u> equalities can be assumed to be approximately true. Under the assumptions (13) the differential Equation (10) can be solved analytically. The hope exists that the long wave motion in Eyjafjördur can be approximated by the motion in a hypothetical fjord with characteristics given by (13), where the parameters m and n may be fitted according to the results of the observations.

Using (13) we have, from (12):

$$s = \text{const. } x^{1 - n/2},$$

$$b\sqrt{d^*} = \text{const. } s^{\frac{2m + n}{2-n}},$$

$$\frac{1}{b\sqrt{d^*}} \frac{d}{ds} (b\sqrt{d^*}) = \frac{2m + n}{2-n} \times \frac{1}{s} .$$

If we put

$$\frac{2m + n}{2-n} = 1 - 2\alpha, \qquad \alpha = \frac{1-m-n}{2-n} \left(\leq \frac{1}{2}\right) \tag{14}$$

the differential Equation (10) becomes

$$\frac{d^2H}{ds^2} + \frac{1 - 2\alpha}{s} \frac{dH}{ds} + H = 0 \tag{15}$$

The remarkable thing about this new equation is that it is an ordinary differential equation in the variable s only, so that in the solutions x and

ω appear exclusively combined in s.

We note that the differential equations obtained for four cases in the paper ALW indeed are special cases of (15):

Case A: $m = 0, n = 0, = \frac{1}{2}$ ..... Equation ALW (10A)

Case B: $m = 1, n = 0, = 0$ ..... Equation ALW (10B)

Case C: $m = 0, n = 1, = 0$ ..... Equation ALW (10C)

Case D: $m = 1, n = 1, = -1$ ..... Equation ALW (10D)

In the discussion of the solutions of (15) we shall often refer to the "Tables of Functions with Formulae and Curves" by E. Jahnke and F. Emde, 4th Edition, Dover Publ. 1945, by the indication "JE" plus page number.

The general solution of (15), accoring to JE 146 middle, can be expressed as:

$$H = s\{c_1 J_\alpha(s) + c_2 N_\alpha(s)\}$$

$$\text{or as } H = s^\alpha \{c_1 J_{-\alpha}(s) + c_2 N_{-\alpha}(s)\} ,$$

where J and N are Bessel functions of the first kind and second kind, respectively, and c_1 and c_2 are arbitrary constants. If α is not an integer, the following combination is the most convenient one:

$$H = s^\alpha \{c_2 J_\alpha(s) + c_2 J_{-\alpha}(s)\} .$$

One of the basis solutions shall have to be rejected by the imposed boundary condition that Q (see (11)) goes to zero as s goes to zero. For small s, J_α behaves as s^α, $J_{-\alpha}$ (α not a positive integer) behaves as $s^{-\alpha}$, N_0 behaves as ln s, N_α and $N_{-\alpha}$ for α being a negative integer, -n behaves as $s^{-n} = s^\alpha$. Q in our case for small s being const. $s^{1-2\alpha} \frac{dH}{ds}$, all Bessel functions that behave as s^α must be rejected (unless $\alpha = 0$) since they would

lead to a leading term s^0 in Q so that Q would not approach zero as s goes to zero. Only $J_{-\alpha}(s)$ remains; since α is never a positive integer, $s^{\alpha}J_{-\alpha}(s)$ behaves for small s as const. (1 - const. s^2), giving a leading term in Q proportional to $s^{2(1-\alpha)}$ which is zero for s zero, for all values of α under consideration.

The general solution with the condition Q zero for s zero is thus given by

$$H = \text{const. } s^{\alpha}J_{-\alpha}(s).$$

We introduce the letter H_{α} for the solutions that are normalized to unity for s zero. In fact (JF 128):

$$H_{\alpha}(s) = \frac{(-\alpha)!}{2^{\alpha}} s^{\alpha}J_{-\alpha}(s) \tag{16}$$

and for small values of s:

$$H_{\alpha}(s) = 1 - \frac{s^2}{4(1-\alpha)} \tag{17}$$

The function H_{α} as function of s (Eq. (12)) describes the relative behavior of amplitude and phase of a monochromatic long wave, angular frequency ω, along the channel. However, if we consider the amplitude and phase at a fixed place in the channel $x = x_1$, say, with respect to the amplitude and phase at the closed head of the channel x = 0, as a function of ω, we see that this function is also essentially given by $H_{\alpha}(s)$ when in (12) x is fixed and ω is variable. It is not <u>quite</u> true since, for x fixed, the small parameter q in (12) is not a well-defined function of ω and contains, moreover, the velocities v_m.

The functions $H_{\alpha}(s)$ form a family of functions which are clearly analytic

in an area of the complex s-plane including the positive real axis. Along this axis, they are real and have, for $\alpha < \frac{1}{2}$, a damped oscillatory character, with an infinite number of zeros: $s_1, s_2, \ldots, s_n, \ldots$

Some members of the family are quite familiar functions:

$$H_{\frac{1}{2}}(s) = \cos s;\ H_{-\frac{1}{2}}(s) = \frac{\sin s}{s};\ H_{-3/2}(s) = 3\left(\frac{\sin s}{s^3} - \frac{\cos s}{s^2}\right).$$

Along a line $s = s_r(1-iq)$ (see Eq. (12)) with q so small that qs_r is still $\ll 1$, we have approximately

$$H(s_r - iqs_r) = H(s_r) - iqs_r \left(\frac{dH}{ds}\right)_{s=s_r} - \frac{1}{2}(qs_r)^2 \left(\frac{d^2H}{ds^2}\right)_{s=s_r} \qquad (18)$$

from which we see that the modulus of $H(s_r - iqs_r)$ differs to second order in qs_r only from the modulus of $H(s_r)$ whenever $H(s_r)$ is not zero, but that near the zeros s_n where $H(s_n) = 0$, we have minima of the modulus of H approximated by

$$|H(s_n - iqs_n)| = qs_n \left(\ldots\right)_{s=s_n} \cdot \{1 + \text{Order}\,(ss_n)^2\} \qquad (19)$$

With α decreasing from its maximum value $+\frac{1}{2}$, for real and positive s the secondary maxima and minima of H_α decrease in absolute magnitude and the zeros increase. Figs. 2A, 2B and 2C give graphs of the first three zeros s_1, s_2 and s_3, the ratios s_2/s_1 and s_3/s_1, of the first two secondary maxima $|H|$ and of the expressions $\left|s\frac{dH}{ds}\right|$ for $s = s_1$ and $s = s_2$, all plotted against α, and found by connecting the points computed for various special values of α by smooth lines.

In Fig. 2C, a diagram showing the parameter α as a function of m and n according to Eq. (14) is inserted.

To illustrate the general behavior of the functions $H_\alpha(s)$, Fig. 2D gives a few plots for the function $H_0(s) \equiv J_0(s)$. Both the modulus and the argument of both $J_0(s_r)$ and $J_0\{s_r(1 - .199\ i)\}$, where s_r is real, have been plotted against s_r. The data for the second function was taken from Hayashi's "Fünfstellige Funktionentafeln", Springer, Berlin, 1930, p. 106.

We shall make use of the functions $H_\alpha(s)$ in the interpretation of the analyses of the records.

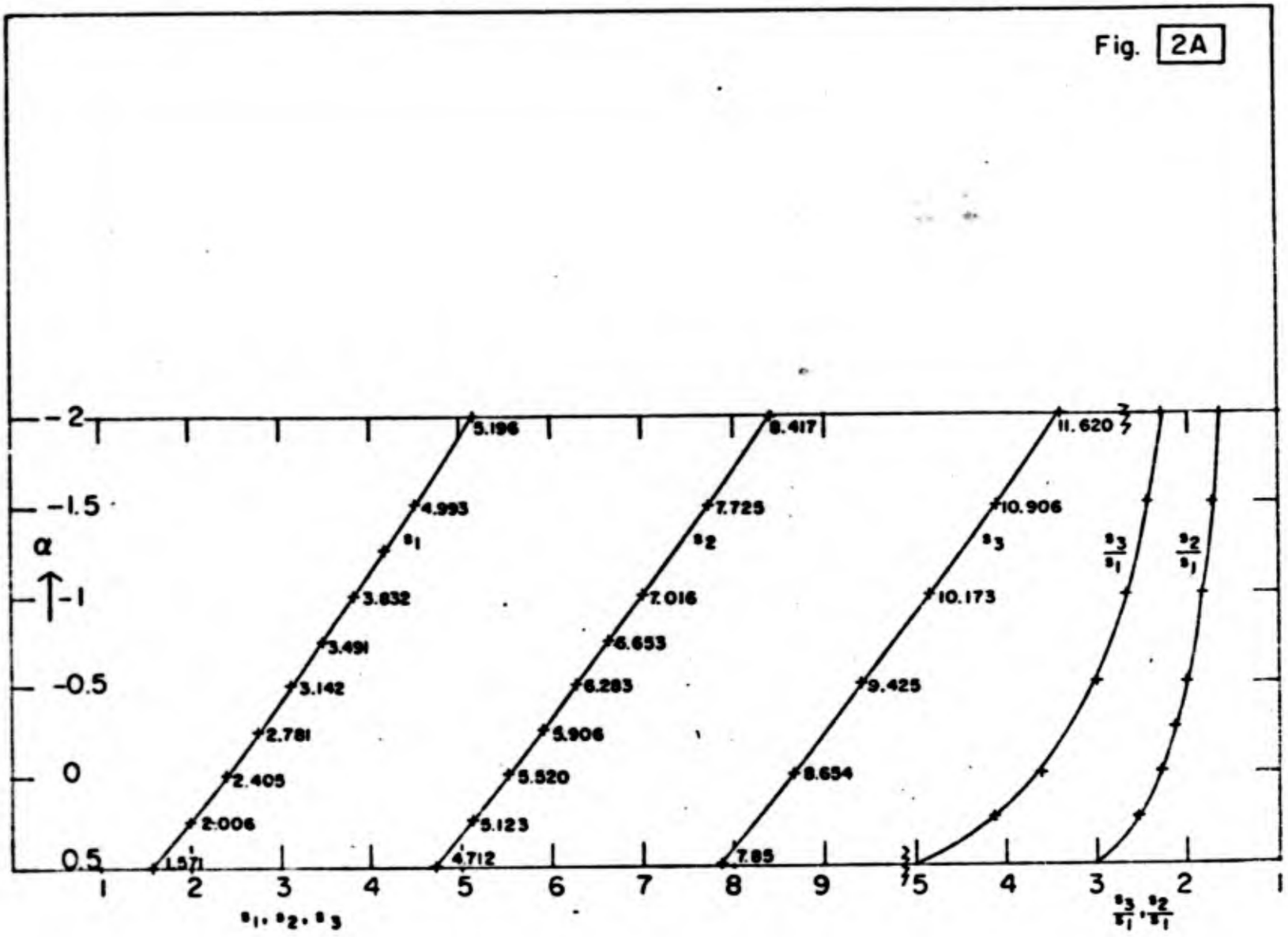
Fig. 2A
α
-2
-1.5
-1
-0.5
0
0.5
1.571
2.006
2.405
2.781
3.142
3.491
3.832
4.193
5.196
4.712
5.123
5.520
5.906
6.283
6.653
7.016
7.417
7.85
8.654
9.425
10.173
10.906
11.620
1 2 3 4 5 6 7 8 9
s1, s2, s3
5 4 3 2 1
s3/s1, s2/s1

Figure 2A

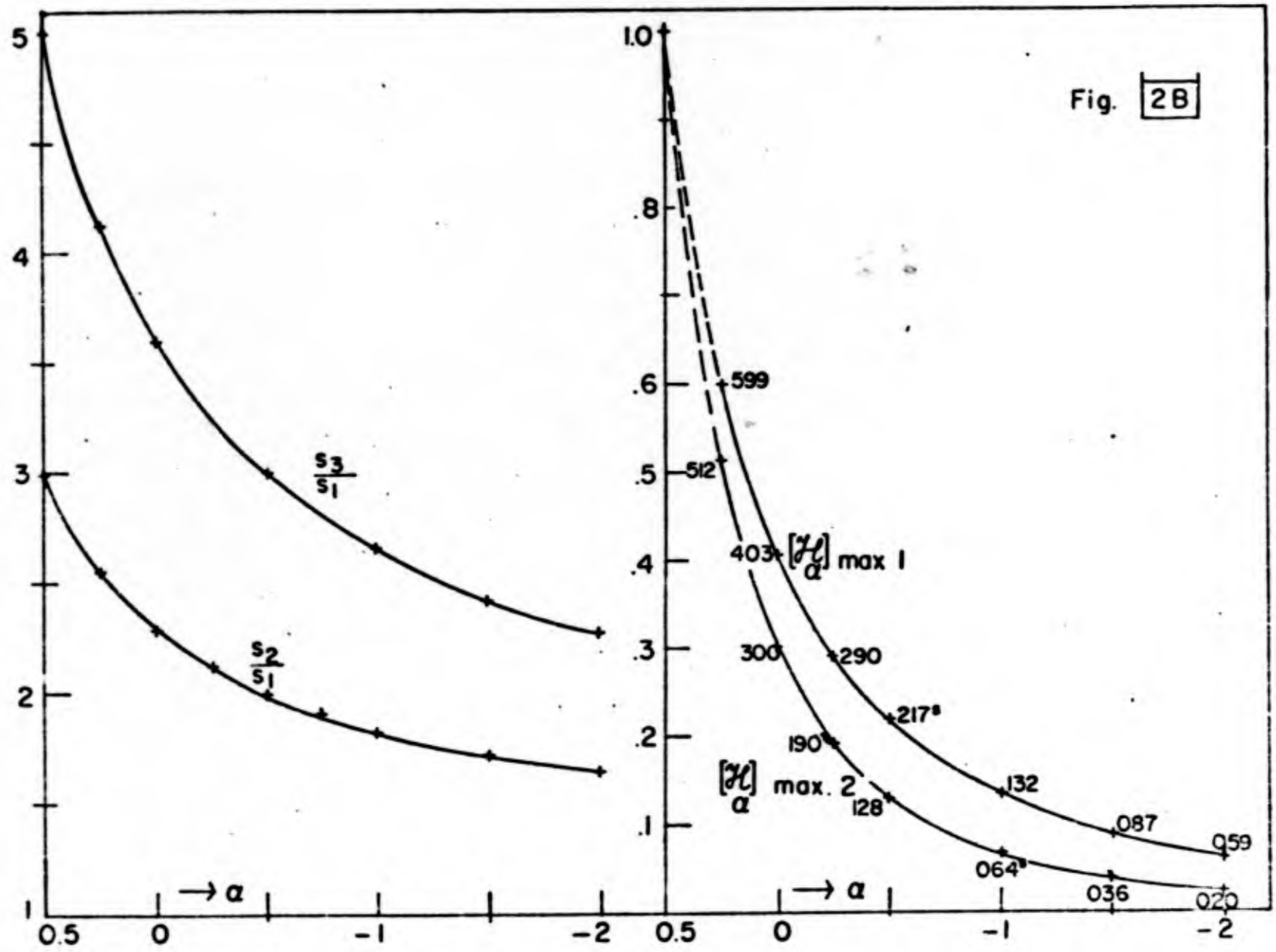
Fig. 2B
5
4
3
2
1
1.0
.8
.6
.5
.4
.3
.2
.1
$\frac{S_3}{S_1}$
$\frac{S_2}{S_1}$
→ α
0.5
0
-1
-2
599
512
403
300
290
217
190
132
128
087
064
059
036
020
$[\eta]_\alpha$ max 1
$[\eta]_\alpha$ max. 2

Figure 2B

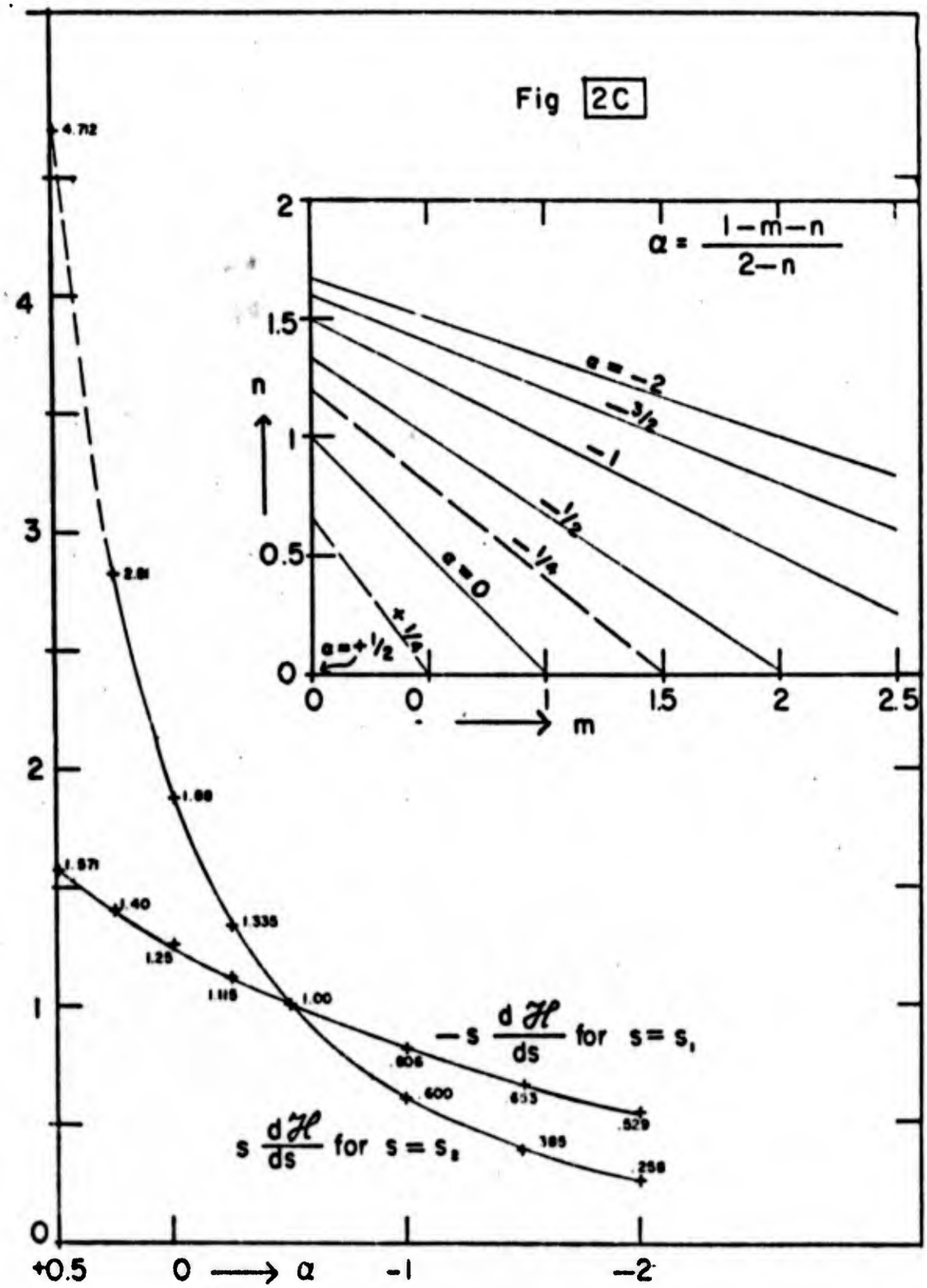
Fig 2C
$\alpha = \frac{1-m-n}{2-n}$
n
m
a = −2
−3/2
−1
−1/2
−1/4
a = 0
a = +1/2
$-s\frac{d\mathcal{H}}{ds}$ for $s = s_1$
$s\frac{d\mathcal{H}}{ds}$ for $s = s_2$
+0.5
0 ⟶ α
−1
−2

Figure 2C

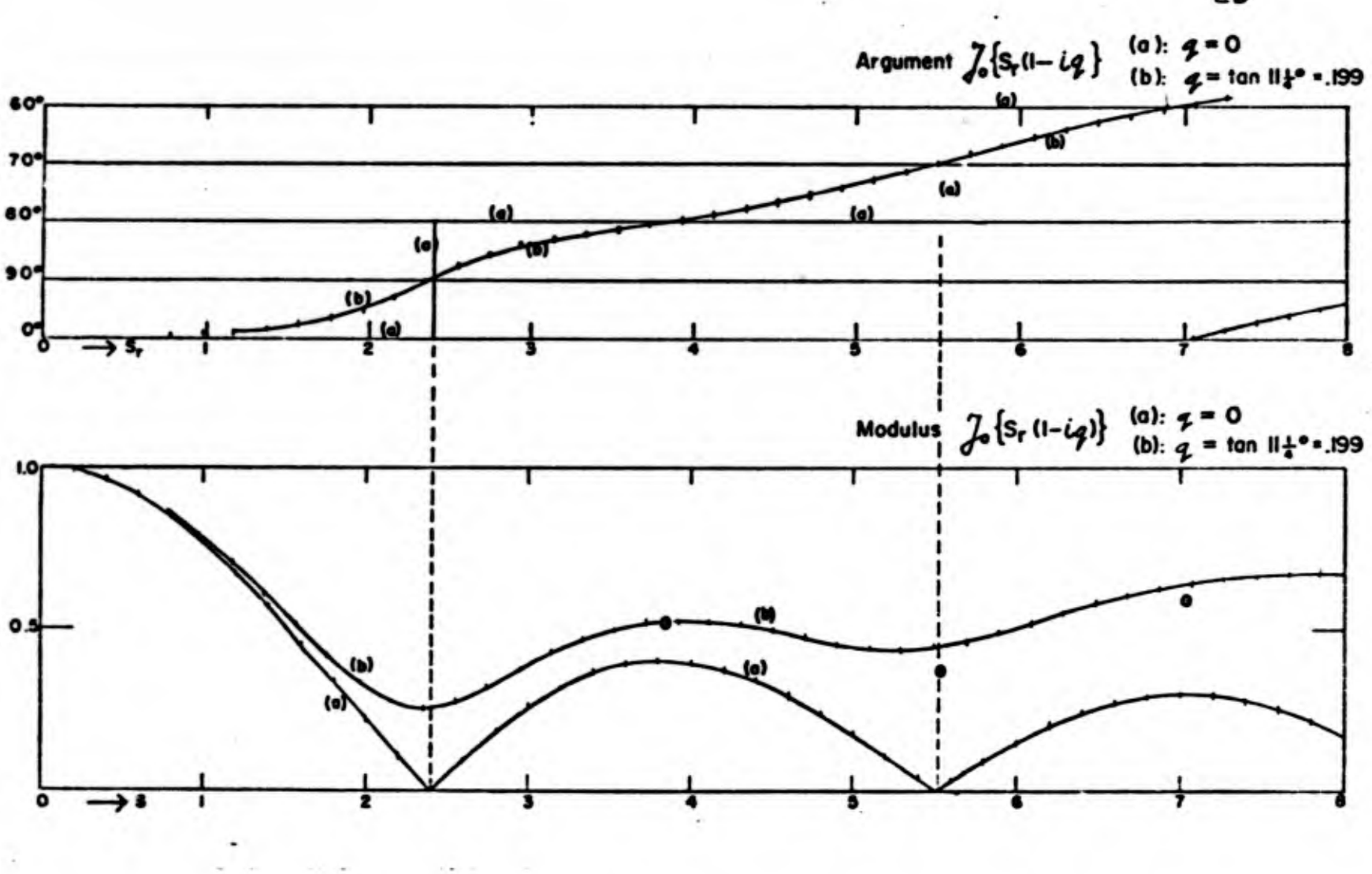
2D
Argument $J_0\{S_r(1-iq\}$
(a): $q = 0$
(b): $q = \tan 11\frac{1}{4}° = .199$
60°
70°
80°
90°
0°
0
$\rightarrow S_r$
1
2
3
4
5
6
7
8
(a)
(b)
Modulus $J_0\{S_r(1-iq)\}$
(a): $q = 0$
(b): $q = \tan 11\frac{1}{4}° = .199$
1.0
0.5
0
$\rightarrow S$

Figure 2D

3. Instruments and Installation

The location of the gauge stations are shown on page 39, the chart of Eyjafjordhur. The west side of the fjord is more densely populated and has many pier installations easily accessible making supervision easy. All the recording stations were therefore established on the west side of the fjord. For recording of the long waves, Stevens tide recorders with electric clocks were used. Height scale was 1:10 and paper speed 144 inches per day. The recorders were in operation for 72 hours continuously whenever north to north-easterly winds of force nine or more were forecasted.

The recorders were installed in a case placed on top of a steel pipe permitting float and counterweight to move freely in the well with the rising and falling tide. The well itself was securely fastened to a pier or quay wall.

The well is conical at the lower end upon which a heavy conical bottom-lid of steel provided with a rubber gasket to make a tight seal rests. A chain connects the bottom lid with the top of the well, which has an opening through which the bottomlid may be lifted up for inspection and cleaning of the orifice in the well and in the bottomlid which filters out sea and swell.

This arrangement proved inadequate at some places, where the well was very much exposed to strong wave activity which lifted the bottomlid up from its seat.

Lead weights were therefore placed on top of the lid. In some cases, that was still not enough. A pipe was therefore welded to the outside of the well. A chain led through the pipe and was fastened to an eye bolt on the top side of the bottomlid. At the upper end a rigging-screw was attached to tighten up the chain, so that the bottomlid provided a watertight seal.

This proved satisfactory in all cases and did not cause too much inconvenience for cleaning of the orifice.

Since it is essential that the time scale on each record is known as accurately as possible (maximum permissable error 1/2 minute, say, but preferably less), the attendants at all stations were provided with accurate chronometer watches (Bulova). The attendants were asked to make time marks on the records, at least three times per 24 hours with minimum intervals of a couple of hours, with indication of the exact time as read from their watches plus the deviation of the watch, all in hours, minutes and seconds. Moreover they were asked to determine the deviation of their watch using a radio time signal at least daily during recordings.

4. Principles of Analyzing Method

In this paragraph, only principles of the analyses will be explained. The details of the computation procedures are given in the Appendix I to this report.

The most conspicuous feature of all records is the semidiurnal tide. The shorter period long waves, even those which might be amplified in the fjord by resonance, which have periods of 2 hours or less, represent only a small fraction of the total variance of the water levels.

4.1 Direct Fourier Analysis

The method of analysis promising to extract the maximum of information from the available data in this case was thought to be straightforward Fourier analysis of strictly simultaneous segments of records, together with the determination of the corresponding "cross-spectral" estimates. Whenever possible, the duration of these segments was chosen to be: 24 Hrs. 48 min. = 1488 minutes, closely approximating two cycles of the predominant M_2 - tide. For this duration, no traces of this tide will appear in other Fourier components than the second one, and the contamination of the third and higher Fourier components by the major tides was expected to be sufficiently small.

Let a record to be analyzed be given by $h(\tau)$ for $\tau = t/T$ running from -1 to +1; 2T is the total duration of the record. We then put

$$h(\tau) - \text{mean} = \sum_{k=1}^{k_{max}} a_k \cos k\pi\tau \sum_{k=1}^{k_{max}} b_k \sin k\pi\tau \quad , \qquad (1)$$

with the Fourier components a_k, b_k, given by

$$a_k = \int_{-1}^{+1} h(\tau) \cos k\pi\tau \, d\tau, \quad b_k = \int_{-1}^{+1} h(\tau) \sin k\pi\tau \, d\tau^{(1)} \qquad (2)$$

For a record of 1488 minutes duration, the series is extended until $k_{max} = 372$, corresponding with 4 minutes as the period of the last Fourier component.

The contribution to the total variance of $h(\tau)$ that is given by the kth Fourier component is, obviously, $\frac{1}{2}(s_k^2 + b_k^2)$. This quantity will be denoted here by β_k. If we divide this by the elementary frequency step, being $(2T)^{-1}$, we obtain a measure of the spectral density $W(f)$:

$$W_k = 2T\beta_k = T(a_k^2 + b_k^2). \qquad (3)$$

This shall be called here the "Fourier spectrum". (2)

For each record analyzed, the values of a_k, b_k and w_k were computed and printed out.

As far as the signal $h(\tau)$ in a given frequency band, or range of k-values, can be considered as a sample drawn from a (stationary) Gaussian random signal, the coefficients a_k and b_k have a normal probability distribution with mean zero and equal variance, without correlation with other a's and b's. Then $\beta_k \geq 0$ has an exponential distribution or, in other words, is distributed according to an X^2-distribution with two degrees of freedom. This means that for each of those β_k-values, the relative variance around the expected value $E(\beta_k)$ is equal to one, which is quite large. For ranges of k-values in which the expectation $E(\beta_k)$ does not vary much, the spectral estimates can be improved by averaging a number of adjacent β_k-values.

---

(1) Note that in this report the signal to be analyzed is denoted by $h(\tau)$ and the frequency by $f/2T$, whereas in the appendix the signal is $f(t)$, and note that in this report the number of the Fourier component is denoted by k, whereas in the appendix, it is denoted by s.

(2) The so-called "periodogram" [2], [3] is a plot of this quantity, or of this quantity multiplied by a constant factor, as a function of the period $2T/k$.

It should be admitted that, in fact, in no frequency range the signals $h(\tau)$ can be considered to remain statistically stationary over durations of 24 hours, for one thing because the meteorological (wind) conditions vary notably over such durations, especially during the passage of storm depressions as in the cases under consideration. This fact will be simply ignored here, however. The spectral method of analysis, then, will provide information about some average conditions during the time interval considered but gives no information at all about possible variations that occurred in the course of that time interval.

In order to correlate pairs of records (1 and 2, say) the "cross-spectral contributions" were also computed, as given by

$$C_{12,k} = T(a_{1k}a_{2k} + b_{1k}b_{2k}) \qquad \text{(cospectrum)} \qquad (4)$$

$$Q_{12,k} = T(a_{1k}b_{2k} - a_{2k}b_{1k}) \qquad \text{(quadspectrum)} \qquad (4)$$

If the usual formula for the coherency

$$= \frac{C_{12,k}^2 + Q_{12,k}^2}{W_{1k}\, W_{2k}} \qquad (5)$$

is applied to the above defined Fourier components, the results is identically unity. In fact, both signals could always theoretically be said to be completely coherent if the complex frequency response function relating both signals would be allowed to jump irregularly between the frequencies $k/2T$ to $(k + 1)/2T$ for any positive k. In that case, for the frequency $k/2T$ the modulus of the frequency response function could be found from $(s_{2k}/s_{1k})^{\frac{1}{2}}$ and the tangens of the phase angle from $Q_{12,k}/C_{12,k}$. However, for a physical system as in this case, the frequency response function must have a continuous character,

in the sense that for $k \gg 1$, its variation over the frequency interval $k/2T$ to $(k + 1)/2T$ should be relatively small (except perhaps near resonance peaks). In order to obtain more accurate estimates of the spectra and in order to obtain still estimates of coherency of the signals between pairs of stations, the program also contained the averaging of β-, C- and Q-values over groups of m consecutive k-values and the computation of γ^2-values from these averages. Form, the values 5, 11 and 21 were taken. (The results for m = 11 and 21, however, were not used).

A rough impression of the degree of coherency between the records of two stations can also be obtained by looking at the variations of β_{2k}/β_{1k} and of arctg $(Q_{12,k}/C_{12,k})$ with k.

As are the quantities β, C and Q, $\gamma^2(f)$ is a statistical variable. Its statistical properties seem difficult to obtain. However, when the number of degrees of freedom is of moderate size, say > 20, and $\gamma^2(f)$ is in the range (0.35, 0.95) its expectation and variance have been determined by means of a recipe given in [4]: see also section 7.4.

A number of records were analyzed in the way described above. Inspection of the results obtained showed, however, that this method as such was not satisfactory and that a modification was necessary, as will be explained in the next paragraphs.

4.2 Fourier Analysis After "Pre-tapering" the Records

In the year 1969, a few trials were performed with Fourier analysis of sets of simultaneous records, according to the lines described in the previous paragraph 4.1, but after the signals ($h(\tau)$ minus average) had been multiplied by the simple "taper" function $\cos^2 \frac{\pi}{2} \tau \equiv \frac{1}{2} + \frac{1}{2} \cos \pi\tau$. The effect of such a pre-tapering is at least twofold:

1o. The weight of the extremities of the record (at $\tau = -1$ and $+1$) in the analysis is reduced to zero, that of the first and last quarter of the record is reduced and the weight of the middle part of the record is relatively enhanced; the overall level of all β-values is reduced;

2o. The "contamination" of the strong, low-frequency components (order $(1\ \text{day})^{-1}$) which appear in the higher frequencies is considerably lower than in the case of no pre-tapering; in other words, the amounts of energy, really associated with frequencies of order $(1\ \text{day})^{-1}$, that show up in Fourier components at much higher frequencies are considerably reduced.

There were two reasons for these trials with pre-tapering:

1o. For the records of 24 hours, 48 minute duration, to reduce the contamination effects of the relatively strong semidiurnal and diurnal tidal components with periods deviating from 12 hours, 24 minutes and 24 hours, 48 minutes, respectively, on the higher frequencies;

2o. To obtain a method for adequately analyzing sets of segments with durations a few hours shorter than 24 hours 48 minutes; this was desirable because of the numerous defects in some of the records, in which sets of simultaneous segments of reasonable quality with 18 to 22 hours duration could be selected, but not so for sets of 24 hours 48 minute duration.

A pre-tapering with the taper $\frac{1}{2} + \frac{1}{2} \cos \pi\tau$ is exactly equivalent with a simple tranformation of the directly obtained Fourier components a_k, b_k, as can be easily seen when we consider the Fourier components a'_k, b'_k, of the function $(\frac{1}{2} + \frac{1}{2} \cos \pi\tau).\ h(\tau)$ (with $h(\tau)$ assumed to have mean zero):

$$a'_k = \frac{1}{4} a_{k-1} + \frac{1}{2} a_k + \frac{1}{4} a_{k+1} \qquad (k \geq 1)\ ,$$

$$b'_k = \frac{1}{4} b_{k-1} + \frac{1}{2} b_k + \frac{1}{4} b_{k+1} \qquad (k \geq 1)\ . \tag{6}$$

If $h(\tau)$ in a given k-range can be considered as a sample drawn from a (stationary) Gaussian random signal, it follows that a'_k and b_k', again, are normally distributed with mean zero and equal variance, that a'_k and b_k' are not correlated and that $\beta'_k = \frac{1}{2}(a'^2_k + b_k'^2)$, again, has an exponential probability distribution.

Then it follows also (since the original Fourier components are mutually independent) that the following relation exists between the expectations of β- and β'-values.

$$E(\beta_k') = \frac{1}{16} E(\beta_{k-1}) + \frac{1}{4} E(\beta_k) + \frac{1}{16} E(\beta_{k+1}),$$

which in case the expected values of β_{k-1}, β_k and β_{k+1} are equal reduces to

$$E(\beta_k') = \frac{3}{8} E(\beta_k) . \qquad (7)$$

The ratio 3/8 found here is in accordance with the fact that the variance of the record in all frequency ranges, except perhaps for the lowest frequencies, is multiplied by a factor approximating the mean value of $\cos^4 \frac{\pi}{2} \tau$ between $\tau = -1$ and $\tau = +1$, which is 3/8.

Consecutive values of a_k' and of b_k' and also of β_k' are clearly no more independent. A simple calculation shows, if the variances of a'_{k-1}, a_k', a'_{k+1}, a'_{k+2} and a'_{k+3} are equal, that the correlation coefficient between a'_k and a'_{k+1} is 2/3 and that oetween a'_k and a'_{k+2} is 1/6. A similar rule holds for the b's. Similarly, if the expectations of β_{k-1}, β_k', β'_{k+1}, β_{k+2} and β'_{k+3} are equal, the correlation coefficient between β'_k and β'_{k+1} appears to be 4/9 and that between β'_k and β'_{k+2} is 1/36.

4.3 The "Saw-Tooth Effect"

From a comparison of the results of a few analyses of records with

24 hour, 28 minute duration without and with pre-tapering, the somewhat alarming discovery was then made that the reduction factor between corresponding averages of ten consecutive β- and β'-values appeared to be much smaller than 3/8 in all cases, except for the very lowest k-values 1, 2 and 3. This factor, instead of being about 3/8, varied between 1/5 and 1/30.

The explanation of this discrepancy was then readily found after an inspection of the original records. In spite of the fact that the duration of the segments analyzed was very nearly two periods of by far the most important constituent of the astronomical tide, M_2, all these segments showed a considerable difference in water level at the beginning and at the end of the segment. These differences varied between 6 and 30 cm in absolute value (with tidal ranges from 50 to 100 cm). For any one of the segments, the differences for various stations were equal within a few centimeters.

These large differences are very much in excess of what could be contributed by the other astronomical tidal components which mainly have periods not deviating much either from 12 hours 24 minutes or from 24 hours 48 minutes. In fact, these differences demonstrate large variations of water level with periods of the order of one to a few days occurring in the whole fjord, which variations appeared to show a very narrow correlation with the variations in atmospheric pressure that occurred during the records. This will be illustrated later in an example in Appendix 4.

The awkward effect of such a difference of ordinates at the beginning and at the end of a segment on the result of a direct Fourier analysis is well known: it is due to the fact that the signal $h(\tau)$, given in the interval $-1 \leq \tau \leq +1$, for the Fourier analysis essentially is considered as a function of the angle $\phi = \pi\tau$, and that the latter function is discontinuous at $(p + 1)\pi$

(p is integer), unless the original function $h(\tau)$ has the same value at $\tau = -1$ and $\tau = +1$.

This "saw-tooth effect" can be demonstrated by considering the Fourier coefficients a_k^*, b_K^*, of the function $h^*(\tau) = \frac{1}{2} c\tau$, applying Equations (1) and (2). If the constant c is put equal to the difference of ordinates for the segment considered (that at beginning minus that at end), addition of this function $\frac{1}{2} c\tau$ to the given signal $h(\tau)$ is one way to remove the apparent discontinuity just mentioned, with only a negligible effect on the spectral density of the signal at all frequencies that are high compared with (duration of segment)$^{-1}$.

Since $h^*(\tau) = \frac{1}{2} c\tau$ is uneven, all a^x-values are zero but for b_k^x we have

$$b_k^* = (-1)^{k-1} \cdot \frac{c}{k\pi} , \qquad (k \geq 1) \qquad (8)$$

In a number of cases, the correction term b_k^x , with the constant c taken equal to the difference of ordinates at the beginning and at the end of the record, was applied to the coefficients b_k from the direct Fourier analysis. It was found then that in almost all cases for k = 4 and higher, the corrected Fourier sine coefficients $(b_k + b_k^x)$ were much smaller in absolute value than the original ones (b_k), and that consequently the corrected values of β, viz. $\frac{1}{2} \{a_k^2 + (b_k + b_k^*)^2\}$, were generally considerably smaller than the uncorrected values of β_k. The "saw-tooth" effect on the b_k-values, in fact, was so strong that for a given set of simultaneous segments in most of the cases, the b_k-values for all stations, either were positive for even k and negative for uneven k, or just the opposite: negative for even k and positive for uneven k, according to the sign of the difference of ordinates at beginning and end of the records.

This demonstrates that the method of direct Fourier analysis without applying some correction for these records really represents a pitfall and is absolutely inadequate.

The correction procedure described above is one method to improve the estimation of the spectra. This procedure compensates for the unnatural discontinuity of the signal $h(\tau)$ at $\tau = \pm 1$, which gives rise to an error in the Fourier sine coefficients decaying as k^{-1} according to Eq. (8). We are left, however, with an equally unnatural discontinuity of the derivative of $h(\tau)$ at $\tau = \pm 1$, which cannot very clearly be deduced from the record, and which can be shown to generate an error in the Fourier cosine coefficients decaying as k^{-2} for $k \gg 1$.

The pre-tapering procedure described in the previous paragraph 4.2 is probably a better way to obtain reliable estimates of the spectra. If the taper function $\cos^2 \frac{\pi}{2} \tau \equiv \frac{1}{2} + \frac{1}{2} \cos \pi\tau$ is applied to the "saw-tooth" function $h^*(\tau) = \frac{1}{2}c\tau$, subsequent Fourier analysis yields cosine coefficients a^{x1} which are zero again, and sine coefficients b_k^x given by

$$b_k^{*1} = (-1)^k \cdot \frac{c}{2\pi k(k^2-1)} \qquad (k \geq 2) \tag{8a}$$

a result readily derived, e.g., by applying Equation (6) to Equation (8).

It is seen that b_k^{x1} decays as k^{-3} for large k and is smaller than b_k^x by a factor roughly $2k^2$.

For the actual analyses, it generally turned out that b_k^{x1} (with the constant c taken equal to the difference of ordinates at the beginning and at the end of the record) was much smaller in absolute value than b_k, except for the lowest k-values 1, 2 and 3. For k exceeding about 12, the calculated

β_k^{*1}-values fall below the expected noise level of β_k' (see par. 5.3). This means that the Fourier spectra derived from the analyses of the pre-tapered records are hardly affected by the preceding application of the "saw-tooth" correction, and that these spectra are really significant.

It should be observed, however, that the pre-tapering strongly distorts the Fourier spectrum for the very lowest k-values 1, 2 and 3, and this in a rather complicated way, dependent of the phase of the main tidal constituents with respect to the time of beginning and end of the record. The pre-tapering, therefore, is obviously <u>not</u> a good procedure to estimate the main tides - but this was not a purpose of the analyses.

The conclusion is, after all, that the pre-tapering as introduced in par. 4.2, or an alternative procedure, is essential to arrive at a sensible analysis, not only for the records with durations deviating from two periods of the M_2-tide, but for the records with duration equal to two periods of the M_2-tide as well. Among the family of taper functions that might be used as well, the $\cos^2$-taper is attractive by its simple properties.

All of the analyzed records, therefore, were pre-tapered in this way. The remainder of the procedure is the same as that described in par. 4.1.

4.4. <u>The "Blurring Functions" B(f,k) and the Spectral Window Function P(|k-f|)</u>

In this paragraph, we give a rather complete set of formulas describing the relation between the amplitudes in the "real" spectrum and the Fourier components, without and with the pre-tapering according to par. 4.2.

Consider a hypothetical infinitely sharp spectral line with frequency f/2T, where f is an arbitrary positive constant. The corresponding signal will be described by a linear combination of cos $f\pi\tau$ and sin $f\pi\tau$ in the interval $-1 \leq \tau = t/T \leq 1$. Let the "blurring functions" be defined as follows:

$B_c(f,k)$ = kth Fourier cosine coefficient for $h(\tau) = \cos f\pi\tau$; $B_s(f,k)$ = kth Fourier sine coefficient for $h(\tau) = \sin f\pi\tau$. The sine coefficient for $\cos f\pi\tau$ and the cosine coefficient for $\sin f\pi\tau$ are obviously zero.

By straightforward calculation, we then have, without taper:

$$B_c(k,f) = (-1)^{k-1} \frac{\sin f\pi}{\pi} \left[\frac{1}{k-f} - \frac{1}{k+f} \right] \tag{9}$$

$$B_s(k,f) = (-1)^{k-1} \frac{\sin f\pi}{\pi} \left[\frac{1}{k-f} + \frac{1}{k+f} \right]; \tag{10}$$

with taper $\cos^2 \frac{\pi}{2}\tau$:

$$B_c(f,k) = (-1)^{k} \frac{\sin f\pi}{2\pi} \left[\frac{1}{(k-f-1)(k-f)(k-f+1)} - \frac{1}{(k+f-1)(k+f)(k+f+1)} \right] \tag{9a}$$

$$B_s(f,k) = (-1)^{k} \frac{\sin f\pi}{2\pi} \left[\frac{1}{(k-f-1)(k-f)(k-f+1)} + \frac{1}{(k+f-1)(k+f)(k+f+1)} \right] \tag{10a}$$

Several special cases will be discussed.

1o. Frequency f approaches zero. Since the function $h(\tau) = \frac{1}{2}c\tau$ is equivalent with $c(2\pi f)^{-1}$. $\sin f\pi\tau = \frac{1}{2}c\tau$ if f goes to zero, the limits of the expressions (10) and (10a) after multiplication by $c(2\pi f)^{-1}$ for $f \to 0$ must be given by (8) and (8a) respectively. This is the case.

2o. Frequency number f approaches a positive integer, k_o. Without taper, (9) shows that $B_c(k_o,k) = 0$ for all $k \neq k_o$, and by taking the limit, that $B_c(k_o,k_o) = 1$. Similarly for $B_s(k_o,k)$. With taper, (9a) shows that $B_c(k_o,k) = 0$ for all $k < k_o - 1$ and $> k_o + 1$ and, by taking the limit, that $B_c(k_o,k_o - 1) = B_c(k_o,k_o + 1) = \frac{1}{4}$ and $B_c(k_o,k_o) = \frac{1}{2}$, in accordance with (6). Similarly for $B_s(k_o,k)$.

3o. Contamination of higher components from low frequencies: $k \gg 1$ and $k \gg f$. Expressions (9) to (10a) then give the following asymptotic expressions.

Without taper:

$$B_c(f,k) \approx (-1)^{k-1} \cdot \frac{2f \sin f\pi}{\pi k^2} \qquad (11)$$

$$B_s(f,k) \approx (-1)^{k-1} \cdot \frac{2 \sin f\pi}{\pi k} \qquad (12)$$

With taper:

$$B_c(f,k) \approx (-1)^{k-1} \cdot \frac{3f \sin f\pi}{\pi k^4} \qquad (11a)$$

$$B_s(f,k) \approx (-1)^{k-1} \cdot \frac{\sin f\pi}{\pi k^3} \qquad (12a)$$

The last two formulas express again the enormous reduction of the contamination in the higher components from low frequency signals, as was already discussed in par. 4.3.

4o. "Short-distance blurring" for the higher components: $|k-f| \ll k+f$ and $f \gg 1$. Under these conditions, the second term in the square hooks of all four expressions (9) to (10a) become negligible as compared with the first terms, to the effect that only two functions remain; without taper:

$$B(f,k) \approx (-1)^{k-1} \cdot \frac{\sin f\pi}{\pi\,(k-f)} \quad ; \qquad (13)$$

with taper:

$$B(f,k) \approx (-1)^{k} \cdot \frac{\sin f\pi}{2\pi(k-f-1)(k-f)(k-f+1)} \cdot \qquad (13a)$$

Except for the sign, both functions are only functions of the difference $|k-f|$. If we have a (stationary) Gaussian random signal with a well defined

"real" spectral density in the frequency range considered, and if we introduce a function $P(|k-f|)$ by:

$$\text{without taper:} \quad |B(f,k)|^2 = P(|k-f|), \tag{14}$$

$$\text{with taper} \quad : \quad \frac{8}{3}\,|B(f,k)|^2 = P(|k-f|), \tag{14a}$$

this function $P(|k-f|)$ can be interpreted as the fraction of the energy in the real spectrum associated with frequency f/2T that shows up in the kth Fourier component. (The factor 8/3 in (14a) is a consequence of the relation (7)). $P(|k-f|)$ is then equivalent with the "spectral window" in the general theory of spectral analysis of Gaussian stationary time series; see [5]. It can be shown that the sum of $P(|k-f|)$ over all k's, with f fixed, approximates unity, as it must be. A graph of $P(|k-f|)$ against k-f is shown in Fig. 4a.

It was already noted in par. 4.2 (Eq. 6) and in the case 2o given in this paragraph, that energy at a f· ·ency number f being an integer, k_o, by the pre-tapering is distributed over the three Fourier components $k_o - 1$, k_o and $k_o + 1$. In other cases, however, for example if the frequency number lies halfway between two k-values, say $f = k_o + \frac{1}{2}$, the pre-tapering gives considerably less "short distance blurring" than without using a taper, as is seen in the next table deduced by putting $f = k_o + \frac{1}{2}$ in Equations (13) and (13a) and using (14) and (14a):

$\lvert k - f \rvert$	$p(\lvert k-f \rvert)$ in promilles	
	without taper	with taper
½	405	480
1½	45	19
2½	16	1
3½	8	-
4½	5	-
≥ 5½	21	-

We have found empirically the following relations to hold true for all f >> 1:

$$\sum_k P(k-f) = 1, \tag{15}$$

mean frequency shift:

$$\sum_k (k-f) \cdot P(k-f) = 0, \tag{16}$$

mean square frequency shift:

$$\sum_k (k-f)^2 \cdot P(k-f) = \frac{1}{3} \quad . \tag{17}$$

The sums are to be taken over all k-values.

Without taper, (15) and (16) are also true, but the sum in (17) obviously diverges.

The spectral window function $P(|k-f|)$ in the case $|k-f| << k + f$ and $f >> 1$ will be used later in ection 8.2.2.

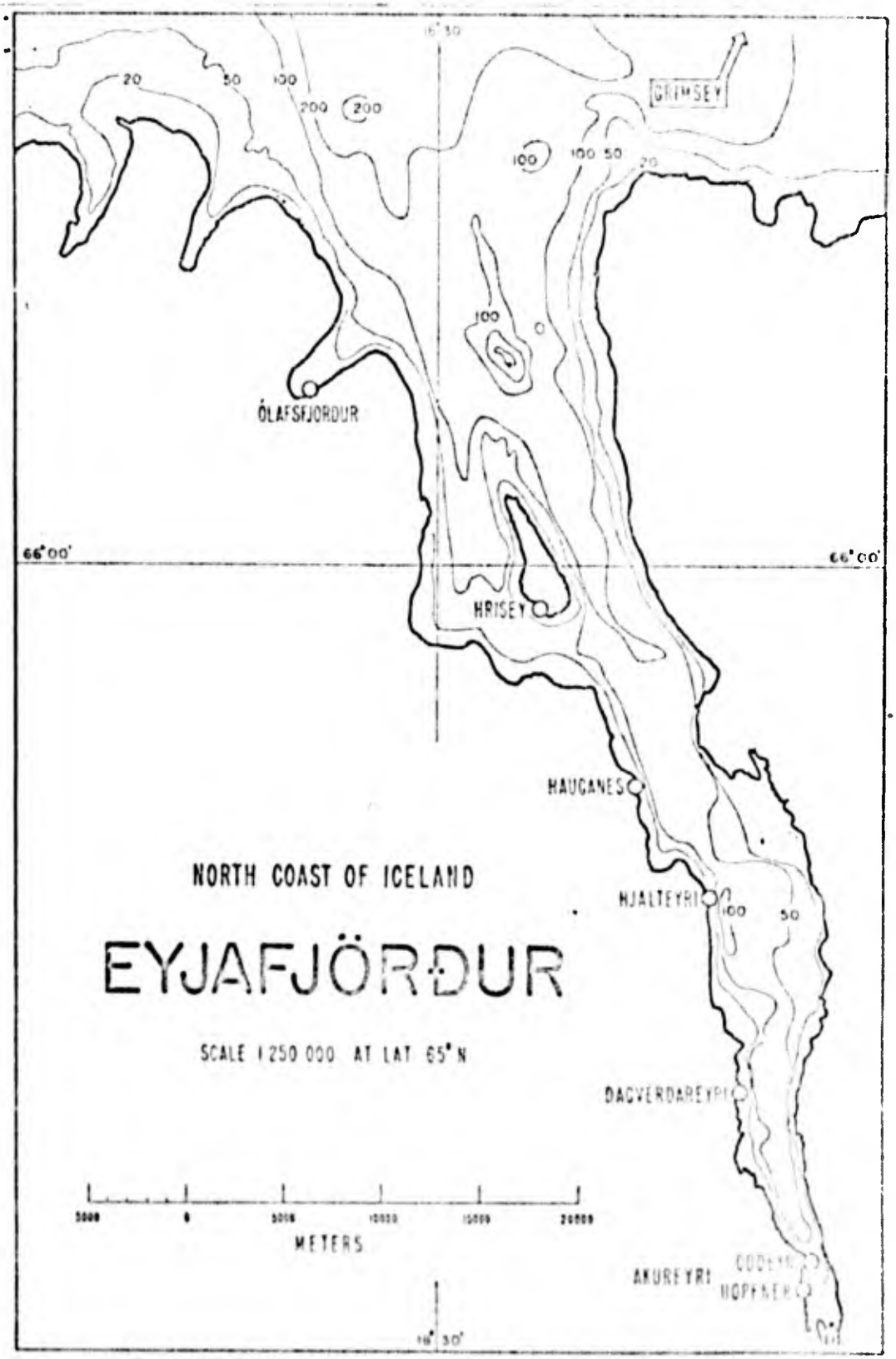
GRIMSEY
ÓLAFSFJÖRDUR
HRISEY
HAUGANES
HJALTEYRI
AKUREYRI
66°00'
NORTH COAST OF ICELAND
EYJAFJÖRÐUR
SCALE 1 250 000 AT LAT 65° N
METERS

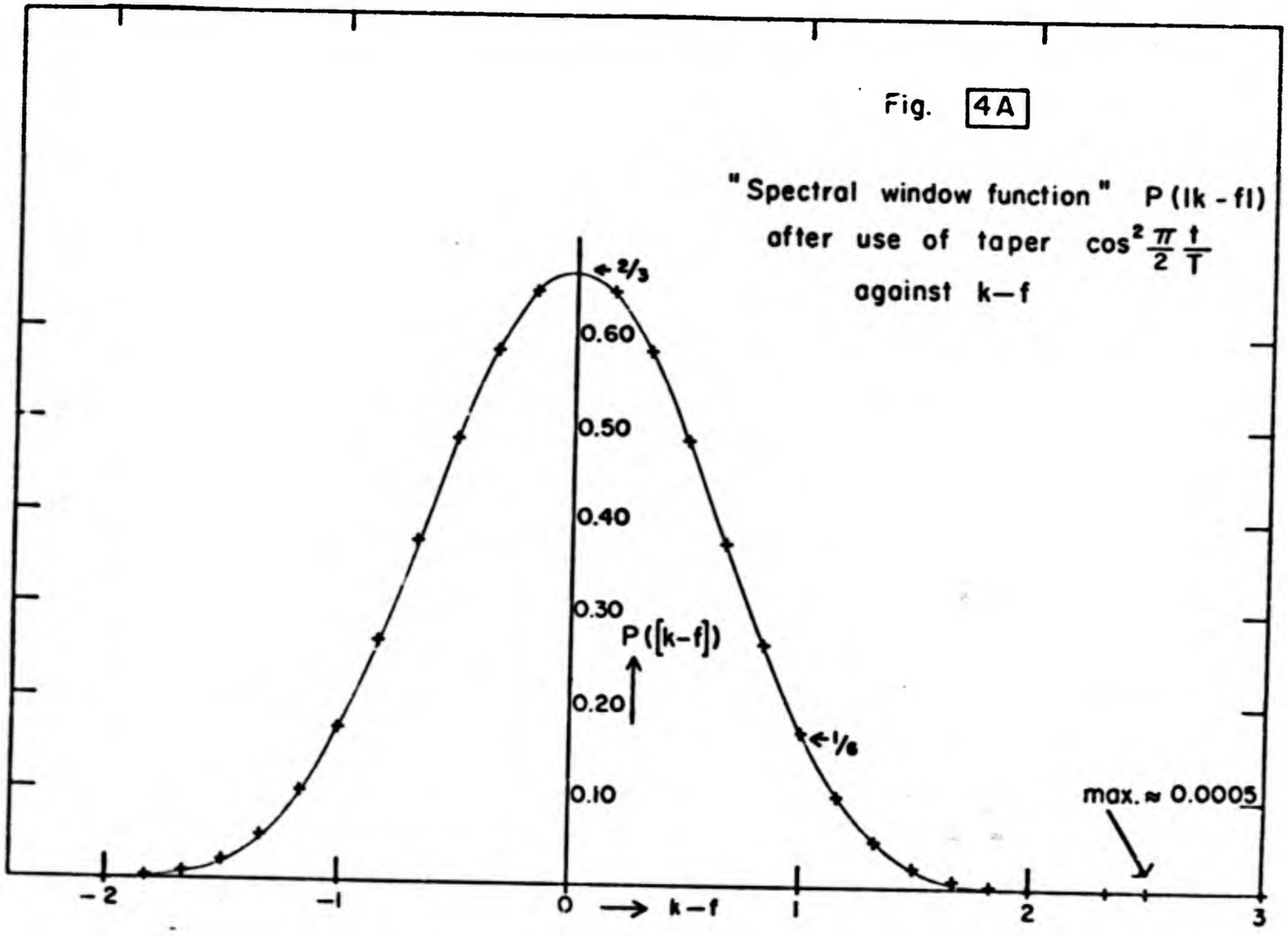
Fig. 4A
"Spectral window function" P(|k - f|)
after use of taper $\cos^2 \frac{\pi}{2} \frac{t}{T}$
against k—f
2/3
0.60
0.50
0.40
0.30
P([k-f])
0.20
1/6
0.10
max. ≈ 0.0005
-2
-1
0
k-f
1
2
3

5. Records Analyzed; Generalities of the Spectra

5.1 The Records

Simultaneous records from five to seven stations were received from the following periods:

8 - 11 December 1966,

20 - 23 February 1967,

14 - 20 March, 1967,

26 - 29 October 1967,

16 - 19 March 1968.

A sample record for each of six stations is given in Fig. 5A. The appearance of the Olafjordur records deviates from that of the other stations in that the former show considerable wave activity at periods of two to ten minutes while such rather short waves are practically absent in the latter records. This is clearly reflected in the spectra, see par. 6.3.

The choice of simultaneous segments to be analyzed from various stations was rather seriously limited by occasional apparent defects and interruptions in the records. The segments selected with their times and the stations are given by crosses in the next table. (see following page).

The table shows a few slight overlaps in time: for records three and four and records seven and eight.

Relevant data on winds and atmospheric pressures are given in Appendix 3.

Generally speaking the records from Hrisey had the highest quality; next to Hrisey is Akureyri S. For Olafsfjordur, only a few records were fit to be analysed, unfortunately from periods that no good records were available from Akureyri S and some of the other stations. The instrument at Hauganes apparently suffered from serious troubles of mechanical nature all the time;

No.	Year	Local Time	Duration	Stations* Ola	Hri	Hja	Dag	AkN	AkS	Tidal Range (approx.) cm.
1	1966	9 Dec.15.00 - 10 Dec.15.48	24 hr. 48 min. 2 T_o				x	x	x	94
2	1967	20 Feb.13.24 - 21 Feb.14.12	" " "				x	x	x	62
3	1967	21 Feb.14.12 - 22 Feb.15.00	" " "		x	x	x	x	x	72
4	1967	22 Feb.10.12 - 23 Feb.11.00	" " "		x	x	x	x		88
5	1967	14 Mar.16.12 - 15 Mar.17.00	" " "		x	x	x	x	x	93
6	1967	17 Mar.08.12 - 18 Mar.09.00	" " "		x	x		x	x	77
7	1967	18 Mar.14.00 - 19 Mar.14.48	" " "		x	x			x	58
8	1967	19 Mar.12.12 - 20 Mar.13.00	" " "		x	x		x	x	53
9	1968	17 Mar.11.35 - 18 Mar.09.55	22 hr. 20 min. 1.8 T_o		x				x	
10	1968	18 Mar.23.08 - 19 Mar.14.00	14 hr. 52 min. 1.2 T_o	x	x			x		
11	1968	18 Mar.08.16 - 18 Mar.23.08	14 hr. 52 min. 1.2 T_o	x						
12	1967	28 Oct.11.16 - 29 Oct.09.36	22 hr. 20 min. 1.8 T_o	x	x		x			
13	1967	26 Oct.18.00 - 27 Oct.12.36	18 hr. 36 min. 1.5 T_o		x		x			
14	1966	10 Dec.20.48 - 11 Dec.09.12	12 hr. 24 min. 1.0 T_o	x		x	x	x		

* Ola - Olafsfjordur
Hri - Hrisey
Hja - Hjalteyri
Dag - Dagverdareyri
AkN - Akureyri (Oddeyri)
AkS - Akureyri (Hafnarbryggja)

These abbreviations will be used further in the report.

no records from Hauganes could be analyzed. The latter was also true for the records from Grimsey; here the apparent trouble was the extremely wide and irregular variations in chart speed, caused by the strong frequency variations of the electric power supply.

5.2 The Spectra; Generalities

All spectral results to be discussed in the following paragraphs were derived from pre-tapered Fourier analysis following the procedure described in paragraphs 4.2 and 4.1.

Many plots were made of spectral densities, amplitude ratios and other parameters against the number of the Fourier component as abscissa. This number is given as "k" for the segments numbers one to eight inclusive with duration $2T_o$ = 24 hrs. 48 min; for the other records it is denoted by "k'". All computations were executed and printed out for the full frequency range considered, viz., from nearly zero to the Nyquist frequency $(4 \text{ min.})^{-1}$ = 4-1/6 mHz (k from zero to 372) but most of the graphs were only made for a limited range of the lower frequencies (ref. also the next paragraph).

The spectral densities are denoted either by W_k, $W_{k'}$, in mm^2 mean square water level variation per mHz (= 10^{-3} cycles/second), or by β_k, $\beta_{k'}$, in mm^2 mean square water level variation per frequency step $(2T_o)^{-1}$ or $(2T)^{-1}$; $(2T_o)^{-1}$ = .0112 mHz. The relation is $W_k = 2T_o\beta_k$ for records numbers 1 - 8 and $W_{k'} = 2T\beta_{k'}$ for the other records. The factor 3/8 in Eq. (7) has been accounted for in the computation of all spectra.

The numbers encircled on the graphs refer to the number of the time period in the table above.

The very high peaks caused by the astronomical tides in the lowest frequencies, k = 1, 2 and 3, were omitted from all plots. The analyses of the spectra and cross-spectra executed so far give no reason to believe that the

water level variations in the fjord with frequencies higher than about 05 mHz (periods below six hours) cannot be adequately described as random variations in the sense of the Gaussian random process. In other words, the shorter period tidal constituents are believed to give a negligibly small contribution to the observed water level variations.

5.3 Noise Level of Spectra

The spectra for all stations show some characteristic features at the lower frequencies (below 1 mHz). With the exception of the Olafsfjordur spectra, they also show a general decrease with increasing frequency above 1 mHz, to a level of the order of 0.5 mm^2/mHz which gives the impression of being merely "instrumental noise". (The computer output for W_k was given in units of 0.080 mm^2/mHz).

It is obvious that computed spectral densities below a certain level will not be significant but will be the result of the many sources of errors that are necessarily made during the whole procedure from the measurement in Iceland to the print-out of the computer.

It is relevant, therefore, to make an estimate of the minimum level of insturmental noise that can be expected. For one source of errors, the combined inaccuracy of the curve tracing during the recording in Iceland and of the reading of the ordinates during the digitizing of the analog records, this can be done. It may be safely assumed that the root mean square of this error is of the order 0.2 mm at least, corresponding with 4 mm^2 water level variance. If the tracing and reading errors would be uncorrelated this variance would give a white noise over the total frequency interval considered (0 to 4-1/6 mHz) with a spectral density obviously given by 4/4-1/6 = 1 mm^2/mHz. It is rather

probable that those errors have a certain persistence along the record; this would reduce the spectral densities in the higher frequencies and increase them in the lower frequencies. Still it appears justified from this rough esitmate to interpret W-values below 1 mm^2/mHz as mainly instrumental noise.

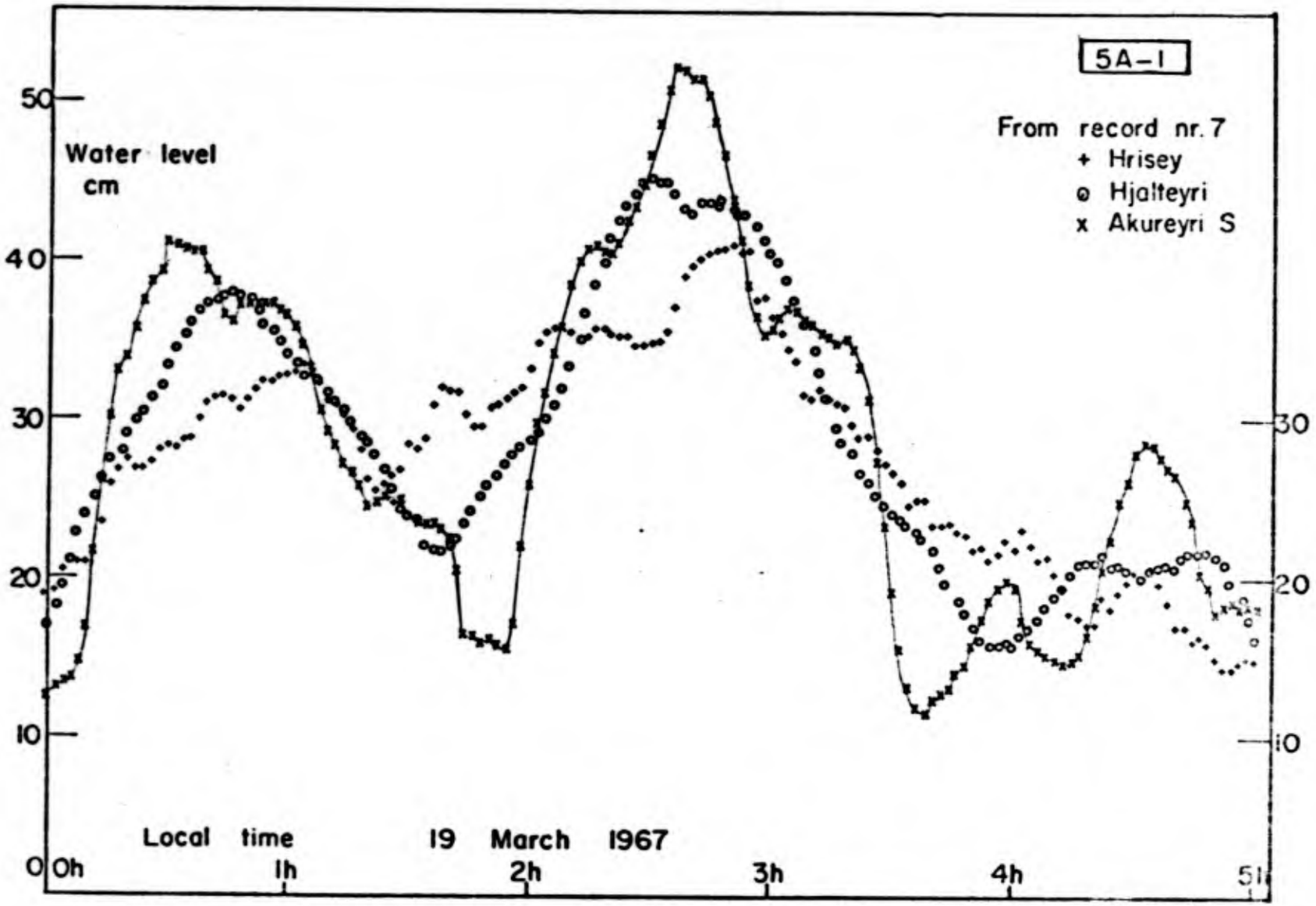
5A-1
From record nr. 7
+ Hrisey
o Hjalteyri
x Akureyri S
Water level
cm
50
40
30
20
10
0
Local time
19 March 1967
0h
1h
2h
3h
4h
5h

Figure 5A-1

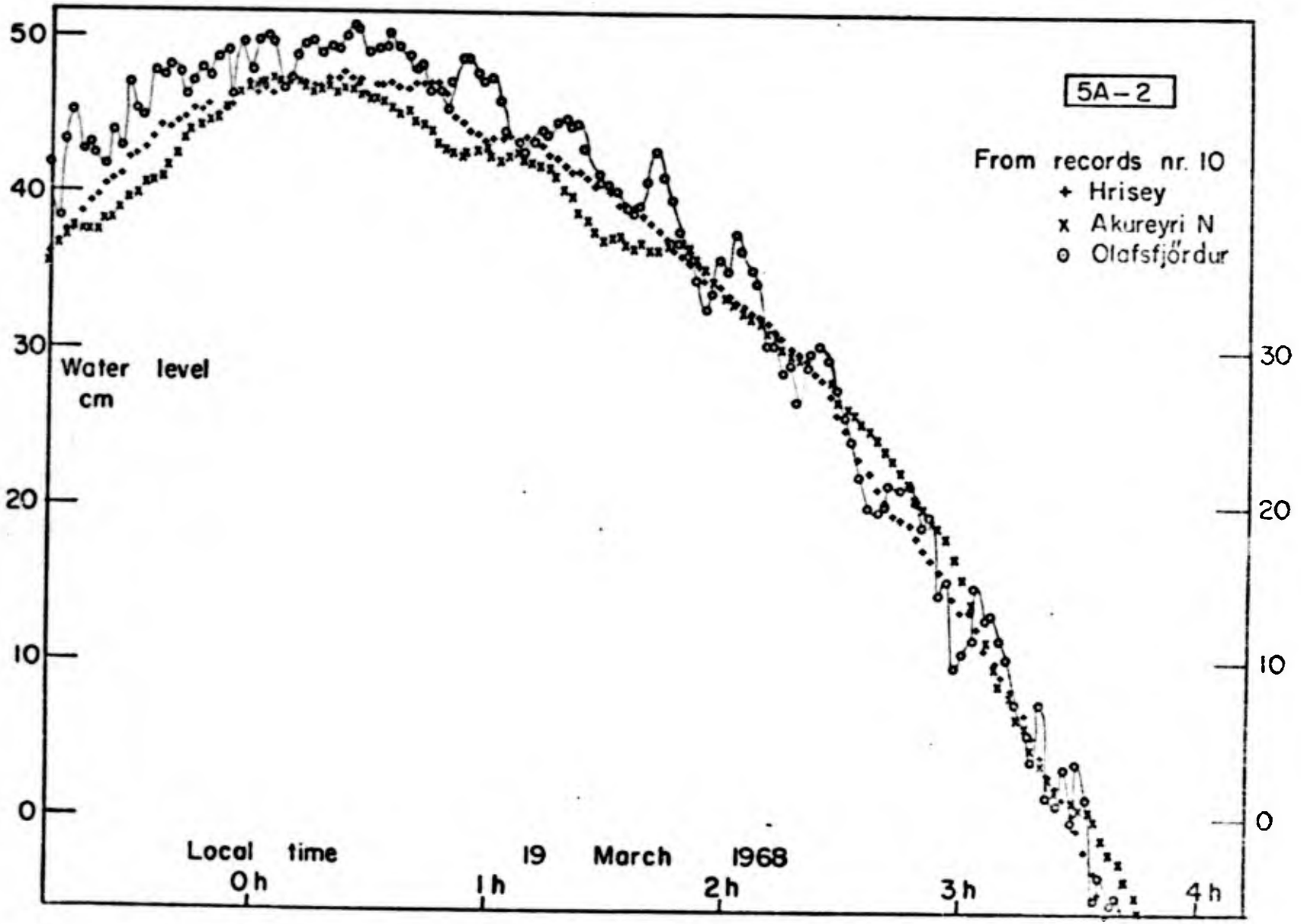
5A-2
From records nr. 10
+ Hrisey
x Akureyri N
o Olafsfjördur
Water level
cm
50
40
30
20
10
0
Local time
19 March 1968
0 h
1 h
2 h
3 h
4 h

Figure 5A-2

6. Autospectra

6.1. General

This word will be used to denote the normal spectra referring to one station only, to make a clear distinction from the cross-spectra referring to pairs of stations.

Only part of the computed autospectra have been plotted, mainly those for Aks, Hja, Hri and Ola. Explanatory notes for the various plots are given in Appendix 2. A short discussion is given in the following.

As could be expected, for each station the spectra show a high degree of variability from record to record. This variability has, at least, two causes: first, the natural variability due to the small number of "degrees of freedom" per spectral estimate (cf. par. 4.1.). The validity of conclusions to be drawn from the spectra will, therefore, be highly improved if we consider all available spectra together and look for features that are common to all or at least most of the spectra.

For each of the stations, some characteristic common features of the spectra can be readily discerned then.

First, the Ola spectra are quite different from those of the other stations. The Ola spectra will be dealt with separately.

6.2. The "Main Fjord" Stations

Hereby we mean the stations situated on the main fjord from Akureyri to Hrisey.

Note: one k-unit corresponds with .0112 mHz.

1o. (Figs 6A). For the lower frequencies nearly all spectra of Aks, Hja and Hri show pronounced peaks at or near k - 12; several spectra show more

or less pronounced peaks at or near k = 27 and at or near k = 42. In general the magnitude of these peaks increases in the order Hri - Hja - AkS. Clearly here we see the first, second and third mode of natural longitudinal oscillations in the fjord.

2o. (Figs 6A). All Hri spectra are low for K = 15 to 17 and for k = 37 to 39; all Hja spectra are low for k = 28 to 32. This points to the occurrence of modes of the natural oscillations.

3o. (Figs 6B). The AkS spectra have, moreover, relative maxima for k = 75 to 90 and for k = 120 to 140 and pronounced relative minima for k = 60 to 70 and others for k = 110 to 115. All of the AkS spectra show the minimum at k = 60 to 70 (period 21-24 minutes). No explanation for this was found.

4o. (Fig. 6C). The Hja spectra indicate the presence of an additional maximum for k = 80 to 90, just as AkS. Thus here we probably have another mode of natural oscillation.

5o. (Fig. 6C). The Hri spectra do not indicate a maximum for k = 80 to 90 but do indicate maxima for k = 115 to 130 and (not presented here) for k = 190 to 240 (of order 5 to 20 mm^2/mHz).

6o. Except for the maxima mentioned above, the level of all spectra (not presented here) is in general of the order mm^2/mHz or lower for k exceeding about 160. The lowest general level in wide k-ranges above 160 is 0.2 to 0.5 mm^2/mHz, which is believed to be pure instrumental noise (cf. par. 5.3).

For Akureyri S an attempt was made to arrive at a more accurate estimation of the shape of the three peaks mentioned in 1o above. For each of three k-ranges, 7 to 17, 18 to 35 and 36 to 53 (incl.), first for each spectrum

the relative distribution of energy was determined by dividing ϱ_k by its average value in that k-range for that spectrum. This was done to eliminate the large variations in the "input" spectrum. Then for each k-range the averages of these relative distributions were taken and plotted (see graph 6F). It can be shown (see Appendix 5) that this estimator procedure has a bias to the effect that the peaks will tend to be less pronounced than they really are (in Section 8.2.1 later on a better procedure is described), but the method may serve to give an optimum fit of the first three resonant frequencies of the fjord. From graph 6F we estimate: $k_1 = 12.0$, $k_2 = 27$ and $k_3 = 42$, respectively, corresponding with natural frequencies .135 mHz, .302 mHz and .470 mHz, respectively and natural periods 124 minutes, 55 minutes and 35 minutes, respectively.

Now, from the ratios between these resonant freqnencies we may estimate the parameter α if we want to fit a Bessel-type equation for the water motion in the whole fjord, according to Fig. 2B. The result then is:

$$s_2/s_1 = k_2/k_1 = 27/12 = 2.25 \text{ gives } \alpha = -0.05;$$

$$s_3/s_1 = k_3/k_1 = 42/12 = 3.50 \text{ gives } \alpha = -0.06.$$

Both estimates are in good agreement.

One of the combinations of values of the geometric parameters m and n (cf. par. 2.2) that lead to $\alpha = -0.05$, is $m = 0.68$, $n = 0.40$ (see Fig. 2C). If we look at Fig. 1B the double logarithmic plots of b(x) and d(x), we see that taking these values as the average slopes of these curves over the whole fjord would not be an unreasonable guess, but more than this cannot be said.

We may also consider once more the k-values themselves of the spectral

peaks. If it would be allowed to take the value .182 as the ratio s_r/k for the whole fjord (see Table in Par. 1.3) we would have

$$k_1 = 12.0, \quad k_2 = 27, \quad k_3 = 42;$$

$$s_1 = 2.18, \quad s_2 = 4.9, \quad s_3 = 7.7.$$

Then, from Fig. 2A the following values for α would follow: +0.15, +0.38 and >0.5, respectively. On the other hand, if the ratio s_r/k is taken a little higher than .182, namely .208, we obtain from the resonant k-values:

$$s_1 = 2.50, \quad s_2 = 5.62, \quad s_3 = 8.74,$$

all three values being consistent with $\alpha = -0.05$ according to Fig. 2A, an excellent mutual fit.

The result just described may be interpreted as a confirmation of the well known fact (see [6], [7]) that for a channel open to the sea with a width not quite negligibly small the "effective length" for resonance exceeds the actual length by a certain amount.

6.3. Olafsfjordur

For this station Fourier spectra were computed for only 4 segments, all with durations shorter than 24 hours 48 minutes; see the table in par. 5.1. The spectra obtained were plotted in Figures 6D and 6E on a common frequency scale, of 8.04 cm. per mHz and 6.43 cm. per mHz, respectively; see also explanation in Appendix 2.

The spectra show the following, more or less common, features.

1o. (Fig. 6D). A narrow pronounced peak with average position 0.76^5 mHz (period 21.8 minutes), a less consistent and more diffuse peak in the

51

region 1.55 to 1.80 mHz (periods 11 to 9-1/2 minutes) and a less consistent and lower peak at 2.40 - 2.46 mHz (period about 7 minutes). The first peak can be safely attributed to the first mode of natural longitudinal oscillation of the little fjord of Ola, and the other two peaks may be attributed to the higher modes.

2o. (Fig. 6D). For the frequencies .135 mHz, .302 mHz and .470 mHz, where the other stations show peaks, the spectral density at Ola is quite low.

3o. Contrary to the other stations, the Ola spectra do not show a general decrease of level to values below 1 mm^2/mHz for frequencies above 1 mHz but they show, instead, a general increase of level from 2 mHz to the Nyquist frequency 4-1/6 mHz. This implicates that considerable "folding" occurs here and that the spectra will continue to be at a rather high level for frequencies beyond 4-1/6 mHz.

All these results suggest that the non-tidal water level variations at Ola will be rather unrelated with simultaneous non-tidal water level variations at the other stations. If we assume that the first three peaks mentioned in 1o above correspond with the first three modes of longitudinal oscillation in the little fjord we can estimate the parameter α for the best fitting Bessel-type equation from Fig. 2B, as was done for the main fjord in the previous paragraph. We then find:

$$s_2/s_1 = 1.60 \text{ to } 1.70/0.76^5 = 2.08 \text{ to } 2.22$$

gives $\alpha = -0.34$ to -0.10;

$$s_3/s_1 = 2.43/0.76^5 = 3.17$$

gives $\alpha \simeq -0.32$;

both estimates being in sufficient mutual agreement.

A rough estimate from the geometry of the little fjord (par. 1.3) indicated the parameter m to be rather small, about 0.3, and the parameter n to be 1.0 at least. A combination m = 0.3, n = 1.0, indeed, leads to $\alpha = -0.30$ (see Fig. 2C).

If we take $\alpha = -0.30$, the zeros of the corresponding Bessel function are (Fig. 2A):

$$s_1 = 2.85, \qquad s_2 = 5.99, \qquad s_3 = 9.12.$$

Dividing these values by the k-values corresponding with the peak frequencies 0.76^5, circa 1.65 and 2.43 mHz, we obtain for s_r/k (whole side fjord): .042, .041 and .042, respectively; i.e., exactly a factor 5 less than the corresponding value of the main fjord (par. 6.2). This result is in quite good agreement with the very rough estimate from the fjord geometry (par. 1.3) which gave a factor of 5.2.

So far, some interesting conclusions were already drawn from the study of the autospectra alone. More conclusions can be derived from the examination of the relations between spectra of pairs of stations. This will be done in the next chapter.

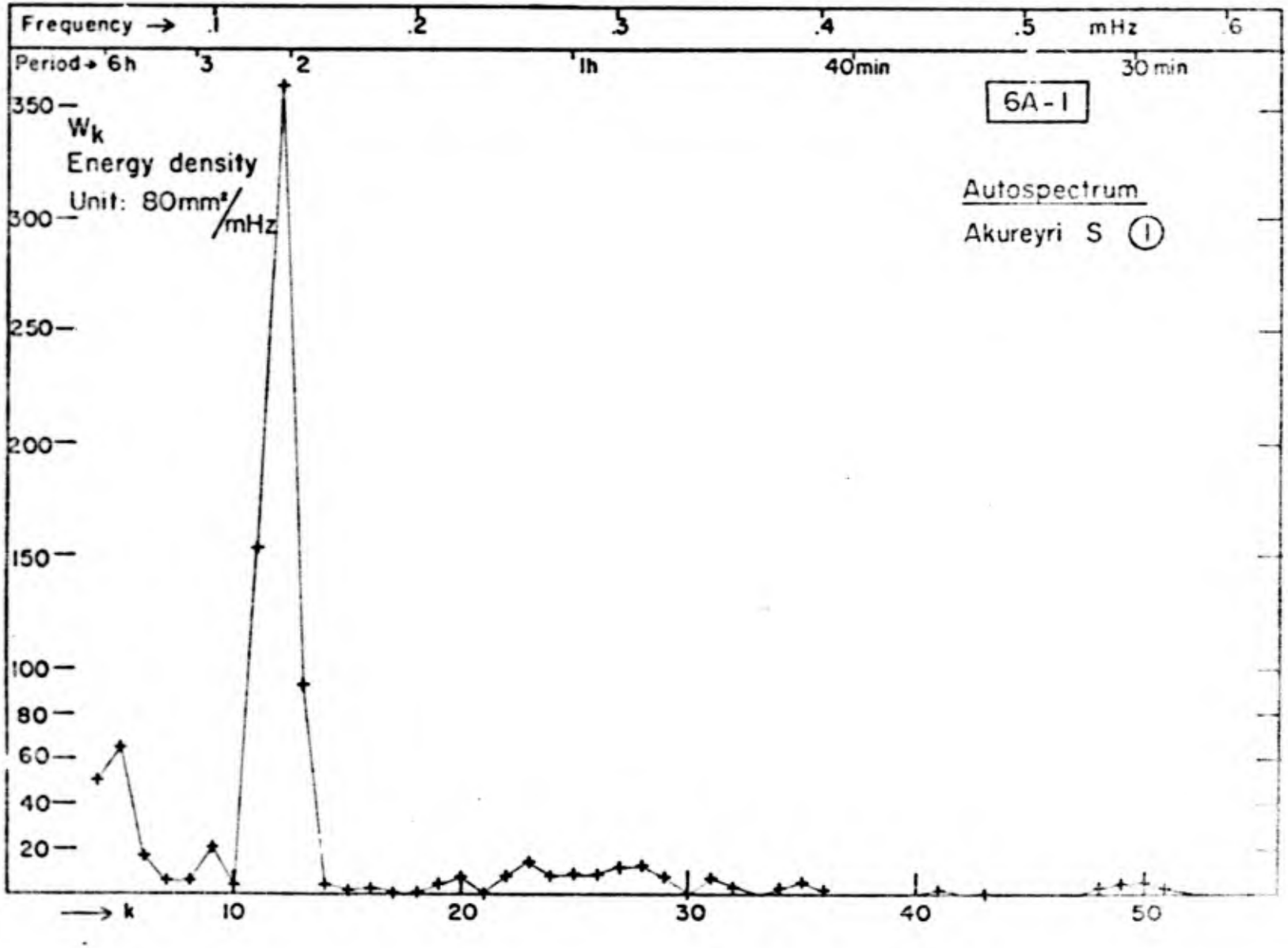
Frequency → .1 .2 .3 .4 .5 mHz .6
Period → 6h 3 2 1h 40min 30 min
6A-1
Autospectrum
Akureyri S (1)
W_k
Energy density
Unit: 80mm²/mHz
350
300
250
200
150
100
80
60
40
20
→ k
10
20
30
40
50

Figure 6A-1

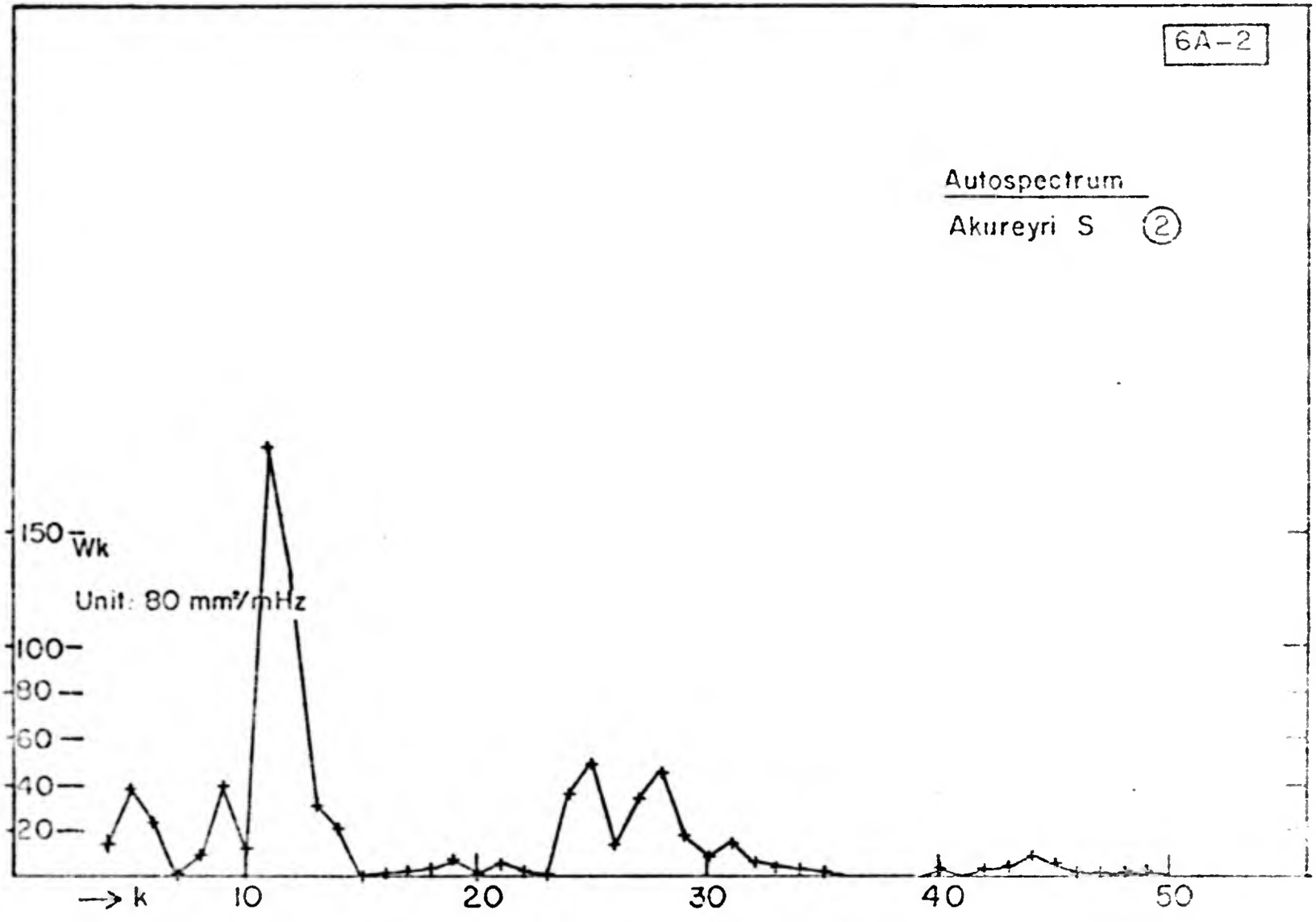
6A-2
Autospectrum
Akureyri S ②
150 $\bar{W}_k$
Unit: 80 mm²/mHz
100
80
60
40
20
→ k
10
20
30
40
50

Figure 6A-2

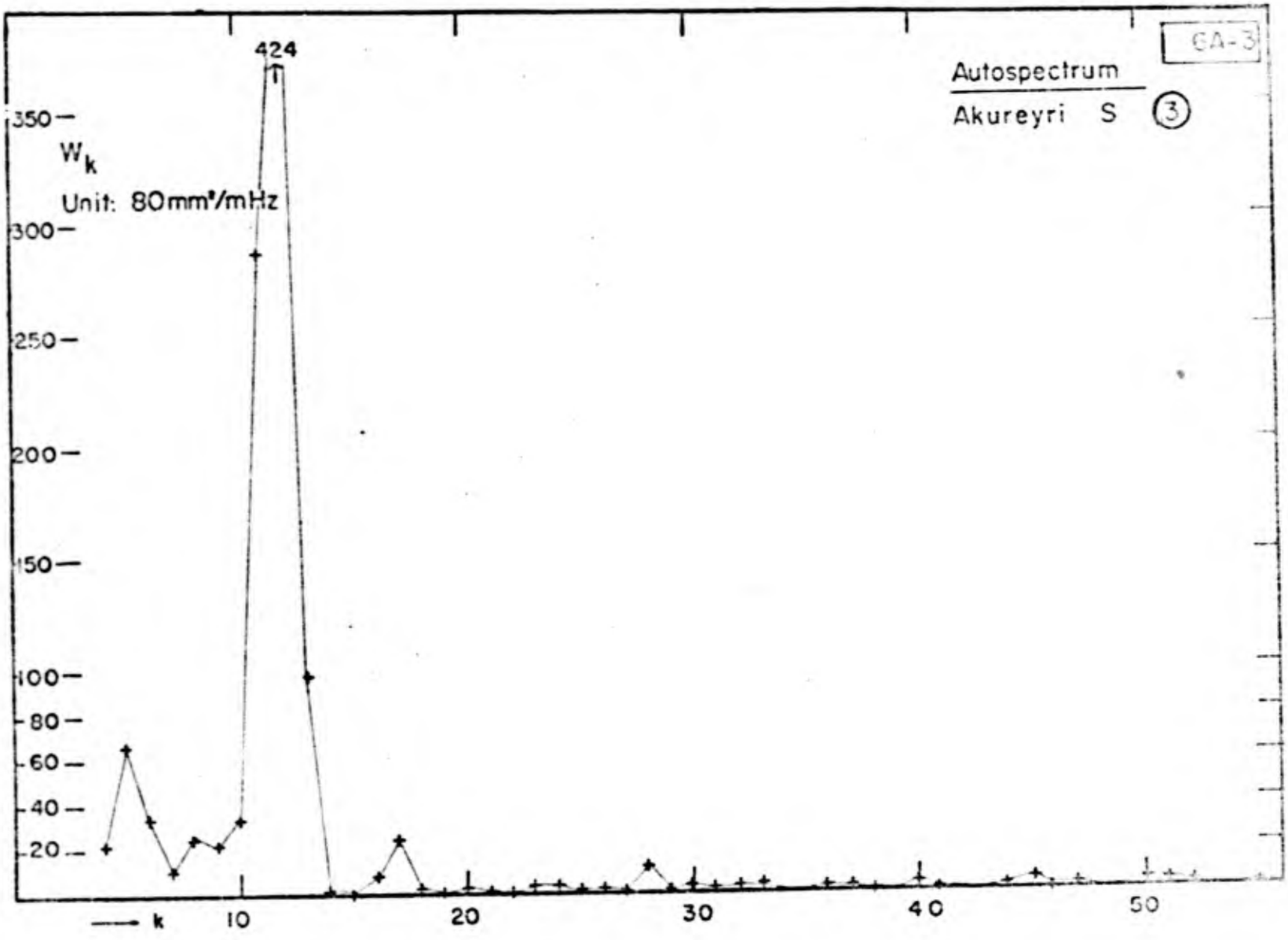
6A-3
Autospectrum
Akureyri S ③
424
350
W_k
Unit: 80mm²/mHz
300
250
200
150
100
80
60
40
20
k
10
20
30
40
50

Figure 6A-3

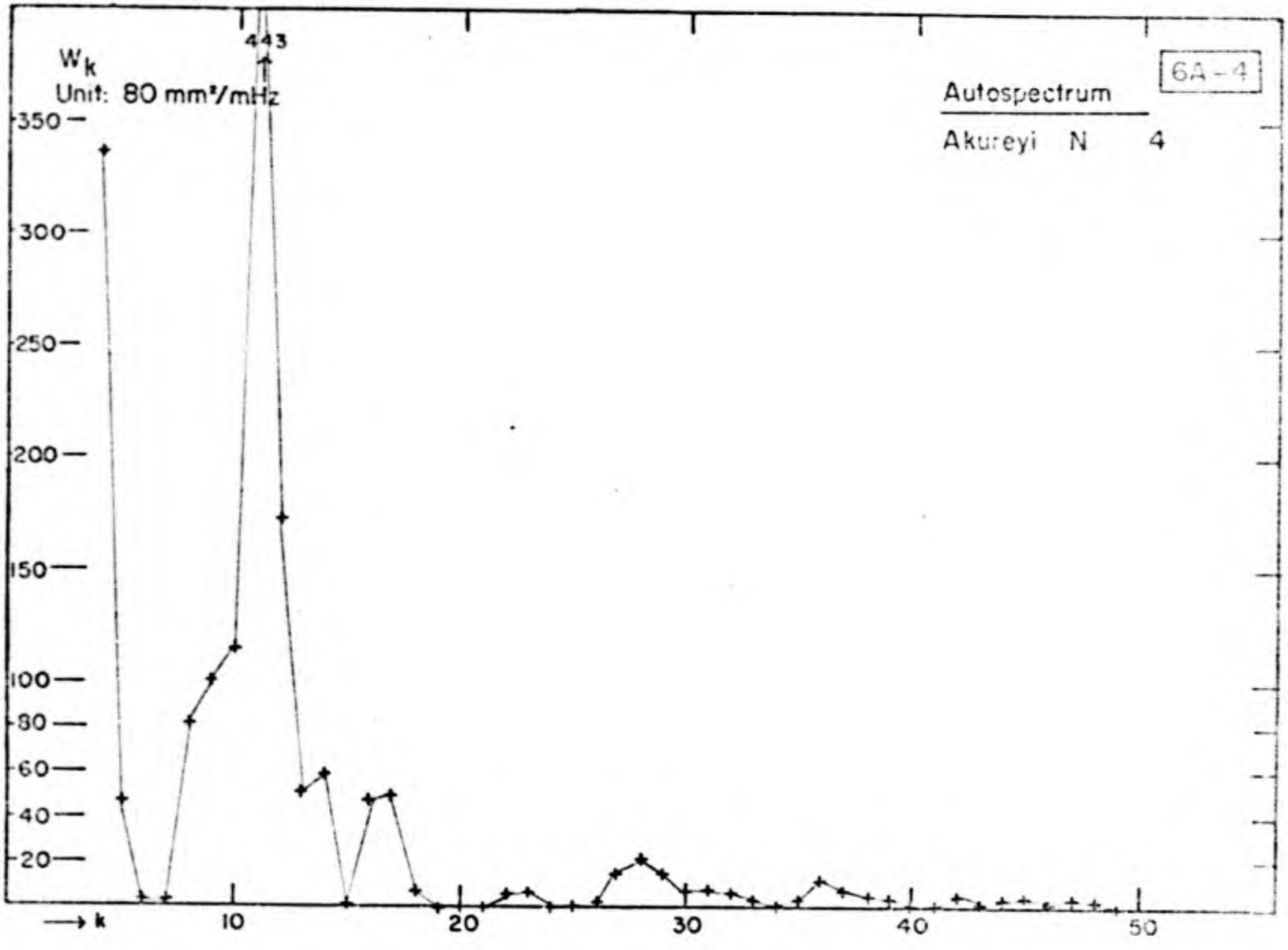
443
W_k
Unit: 80 mm²/mHz
6A-4
Autospectrum
Akureyi N 4
350
300
250
200
150
100
80
60
40
20
→ k
10
20
30
40
50

Figure 6A-4

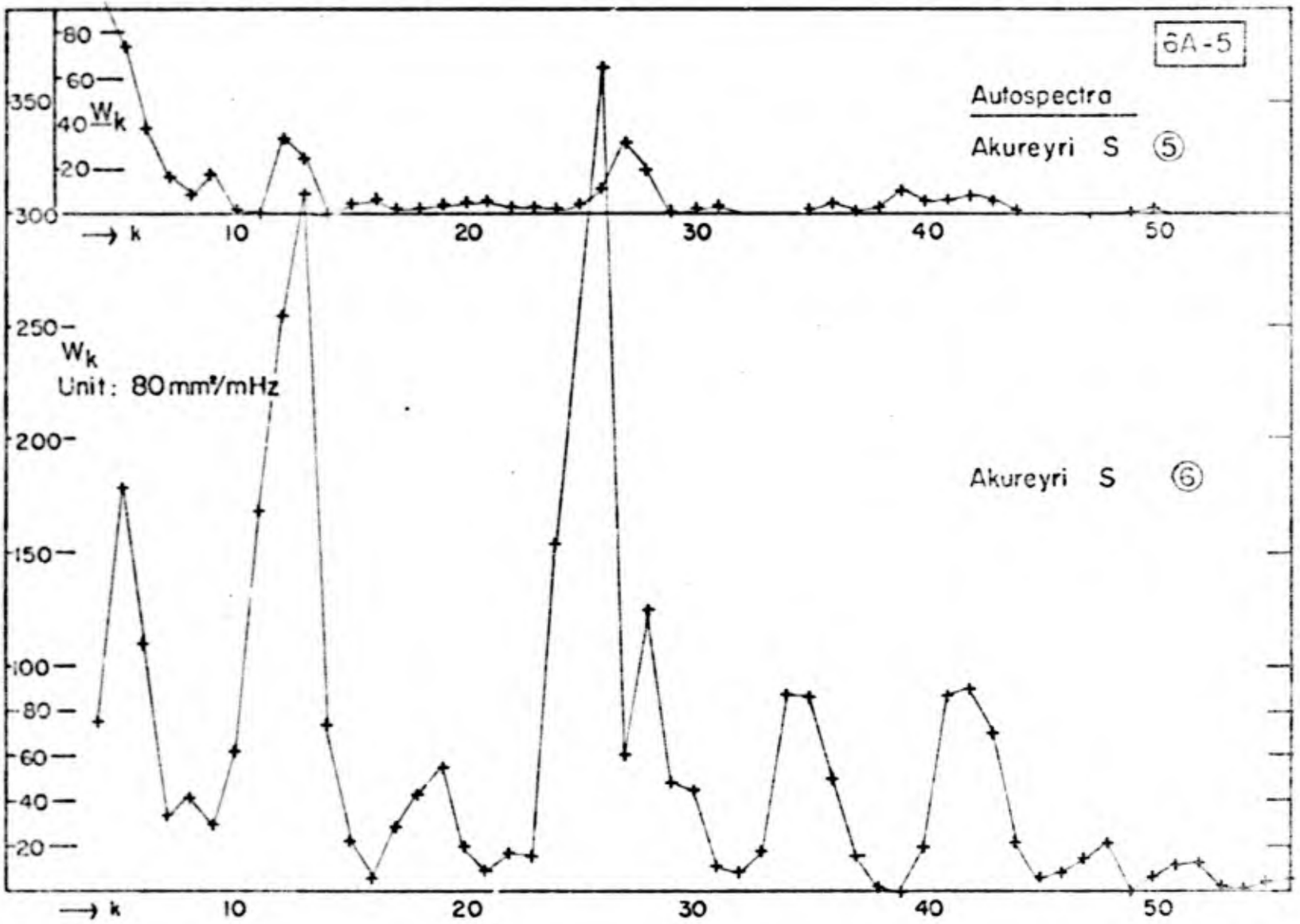
6A-5
Autospectra
Akureyri S ⑤
Akureyri S ⑥
W_k
Unit: 80 mm²/mHz
→ k
80
60
40
20
350
300
250
200
150
100
80
60
40
20
10
20
30
40
50

Figure 6A-5

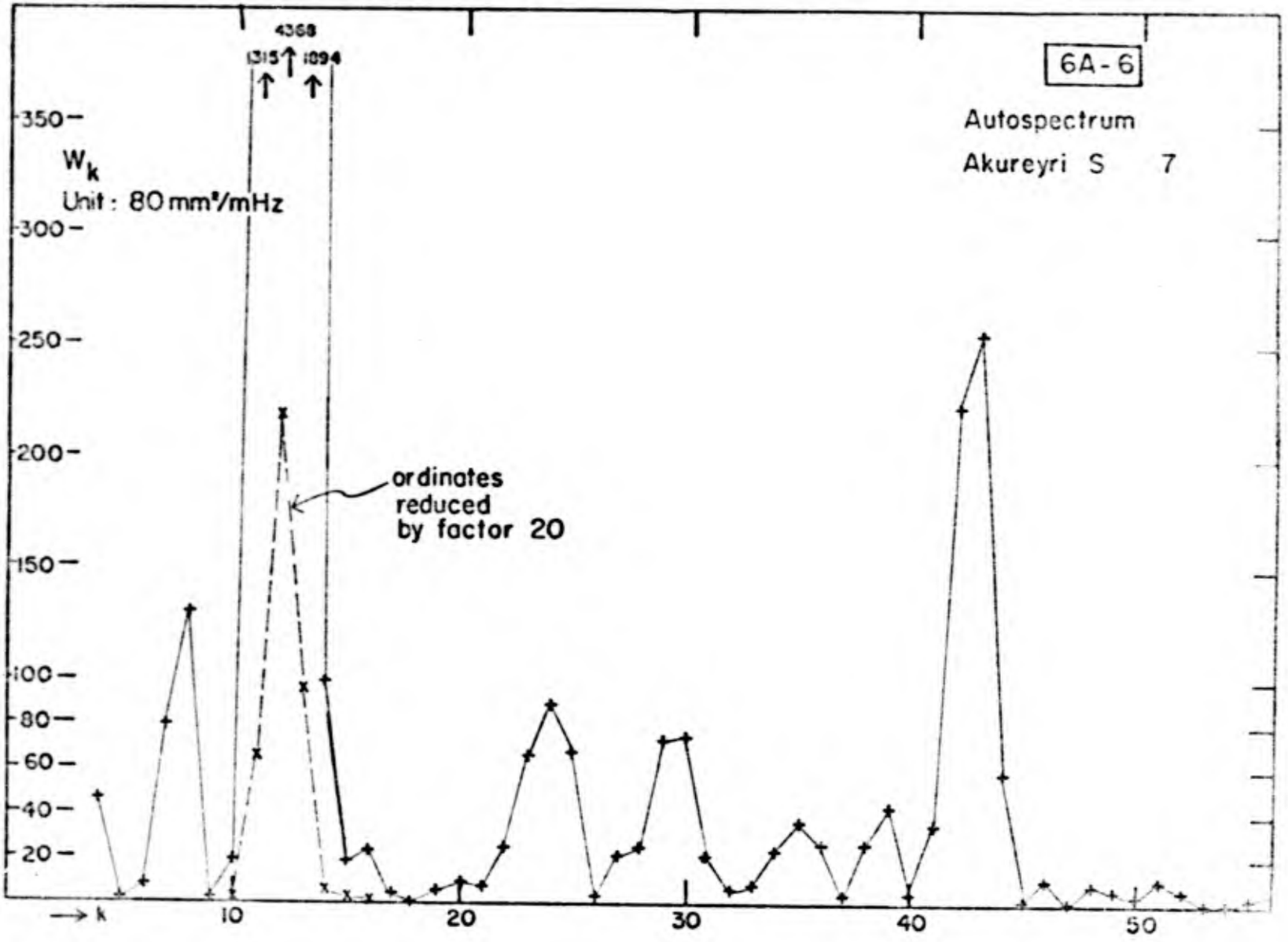
6A-6
Autospectrum
Akureyri S 7
4368
1315
1094
350
300
250
200
150
100
80
60
40
20
W_k
Unit : 80 mm²/mHz
ordinates
reduced
by factor 20
→ k
10
20
30
40
50

Figure 6A-6

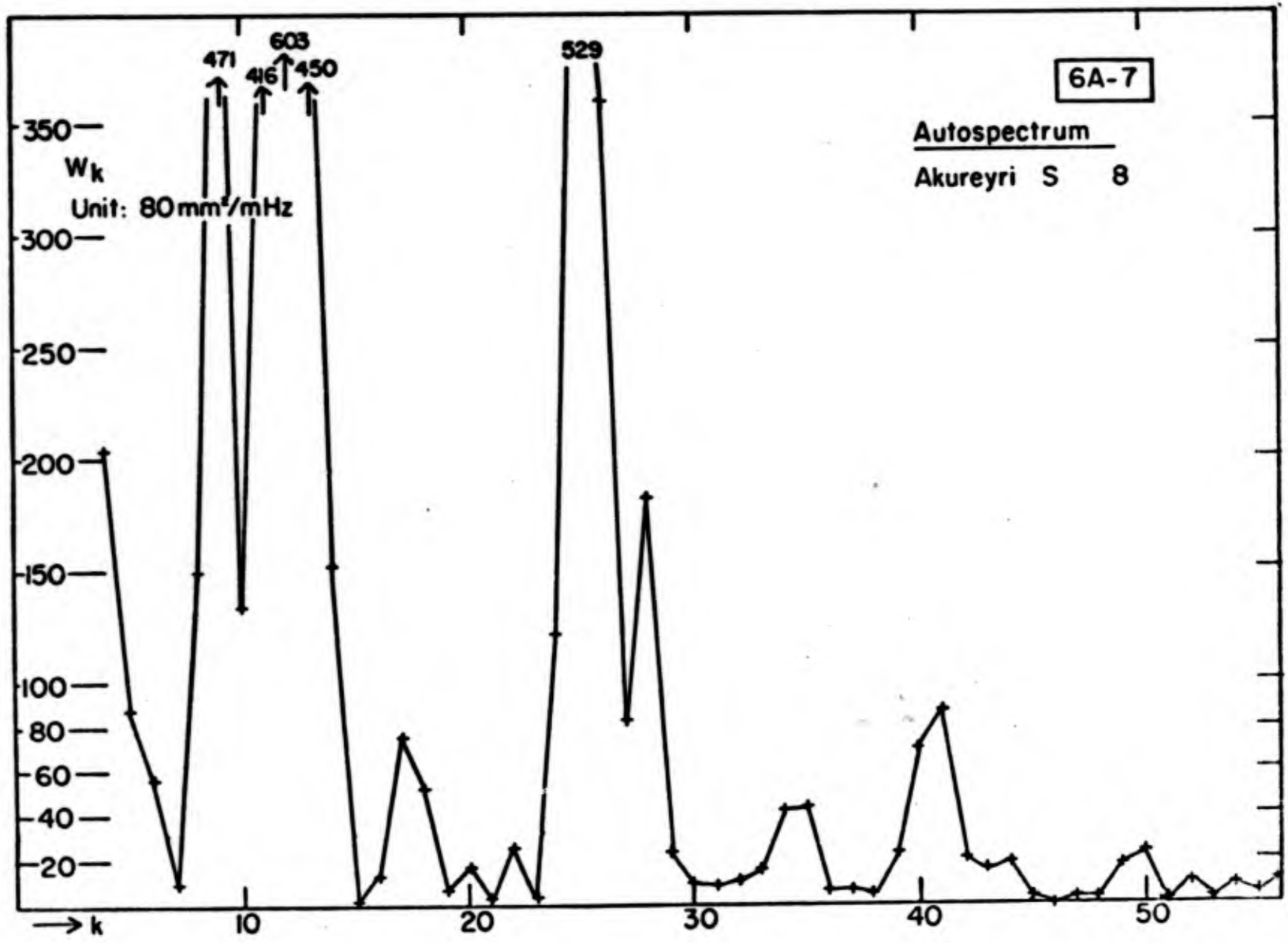
6A-7
Autospectrum
Akureyri S 8
Wk
Unit: 80mm²/mHz
471
603
416
450
529
350
300
250
200
150
100
80
60
40
20
→k
10
20
30
40
50

Figure 6A-7

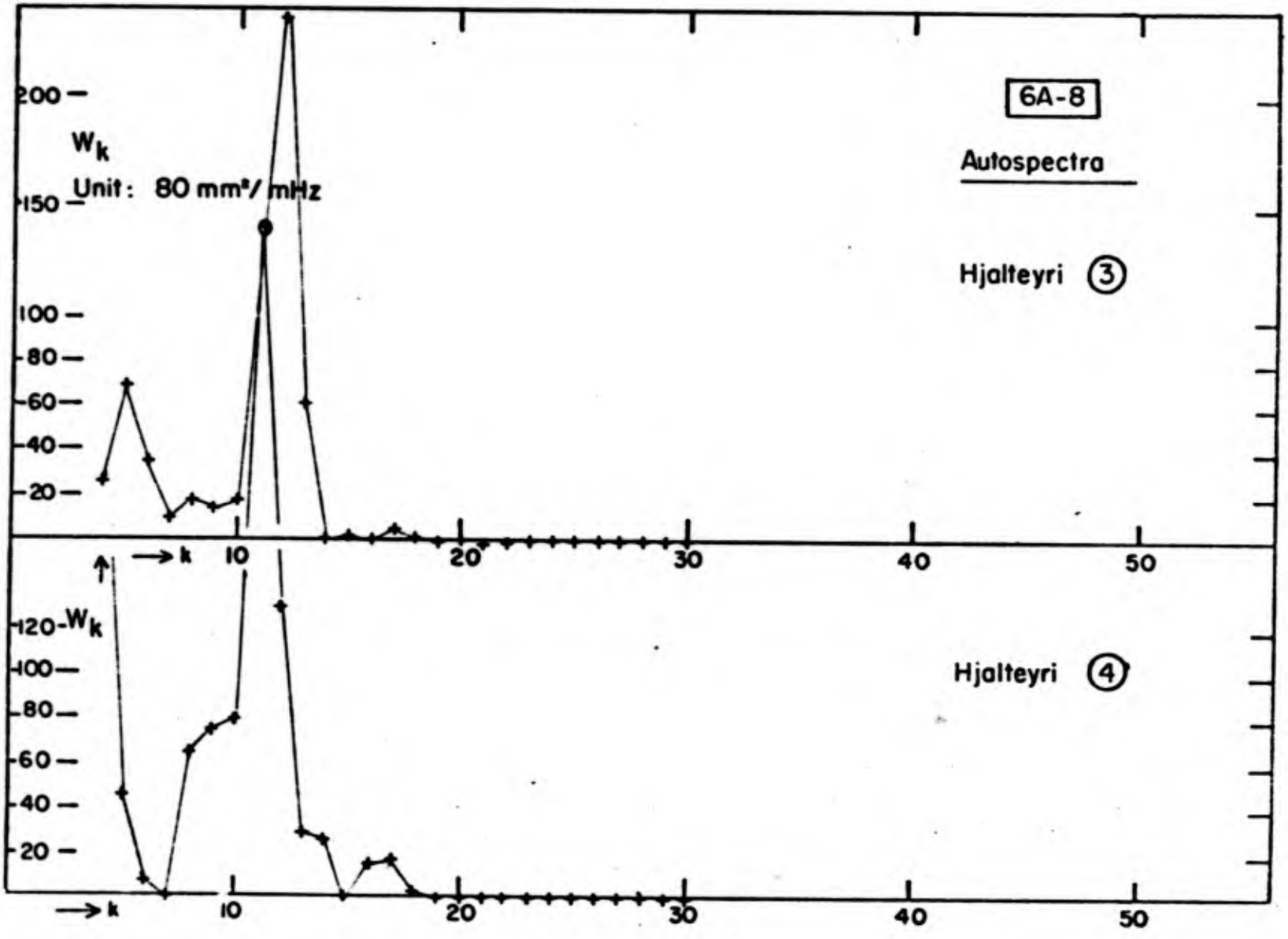
6A-8
Autospectra
Hjalteyri ③
Hjalteyri ④
W_k
Unit: 80 mm²/ mHz
200
150
100
80
60
40
20
120
k
10
20
30
40
50

Figure 6A-8

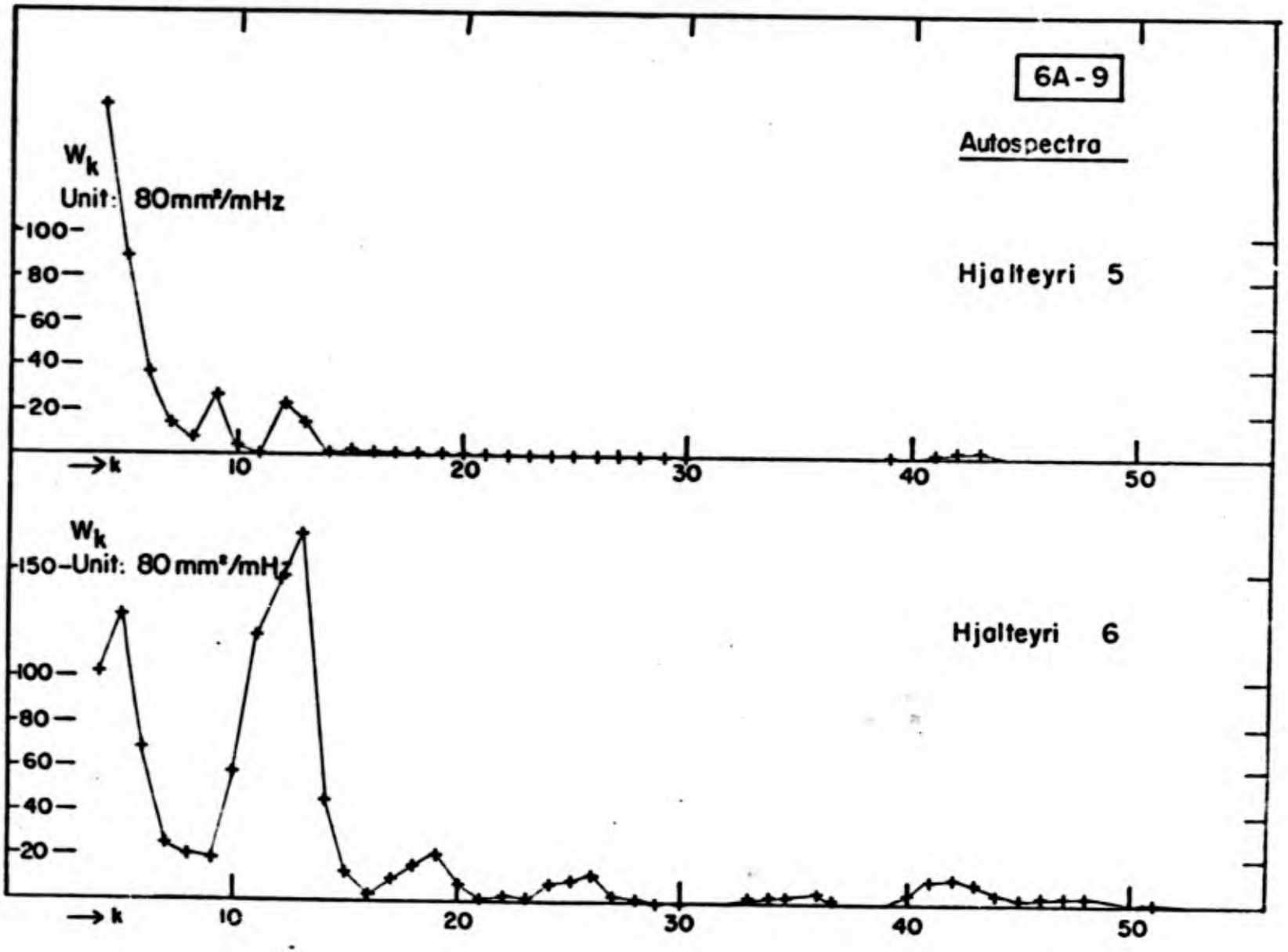
6A-9
Autospectra
W_k
Unit: 80mm²/mHz
100
80
60
40
20
→k
10
20
30
40
50
Hjalteyri 5
W_k
150
Unit: 80 mm²/mHz
100
80
60
40
20
→k
10
20
30
40
50
Hjalteyri 6

Figure 6A-9

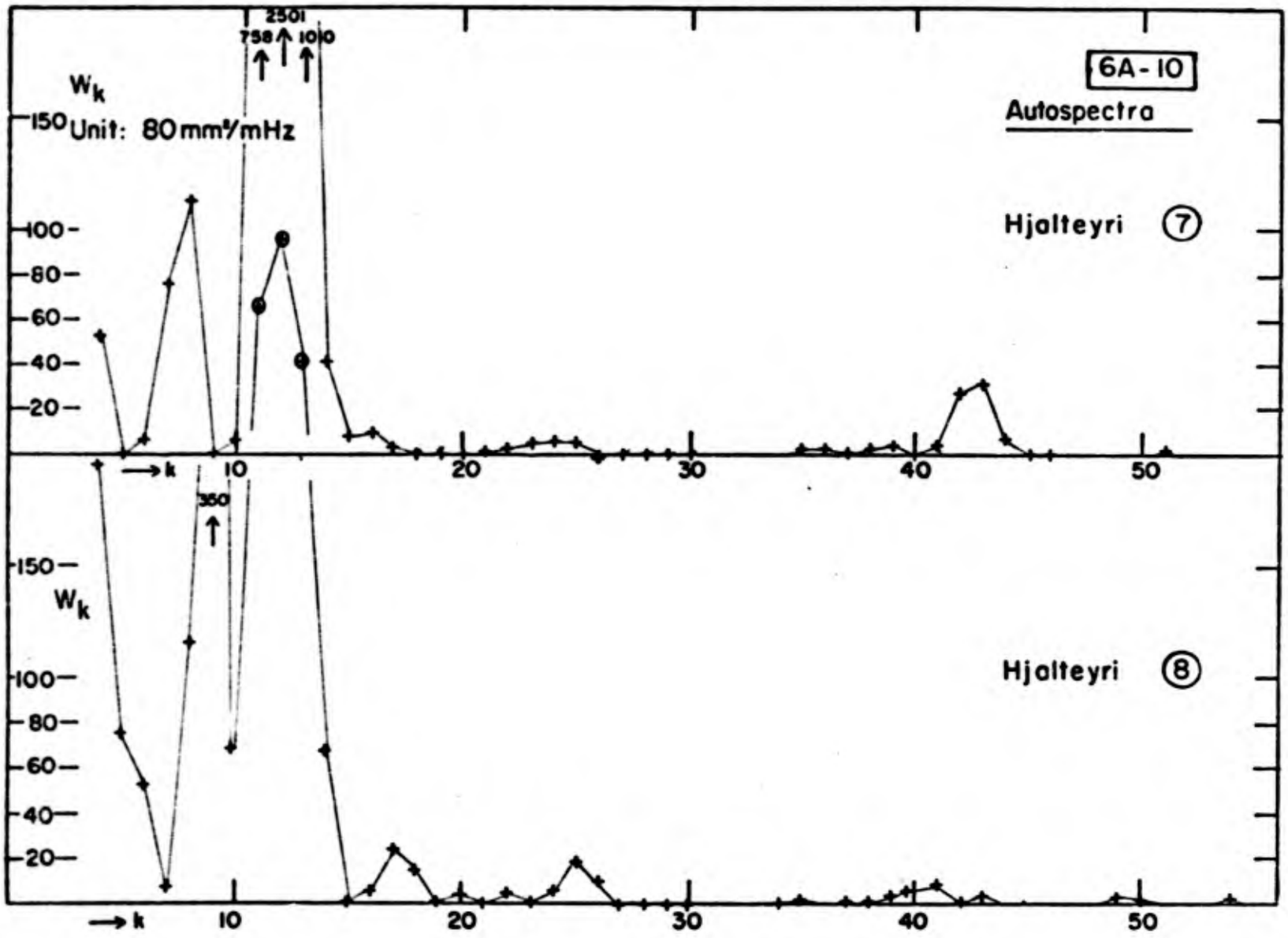
6A-10
Autospectra
Hjalteyri ⑦
Hjalteyri ⑧
Wk
Unit: 80 mm²/mHz
250
758
1010
350
150
100
80
60
40
20
10
20
30
40
50
→k

Figure 6A-10

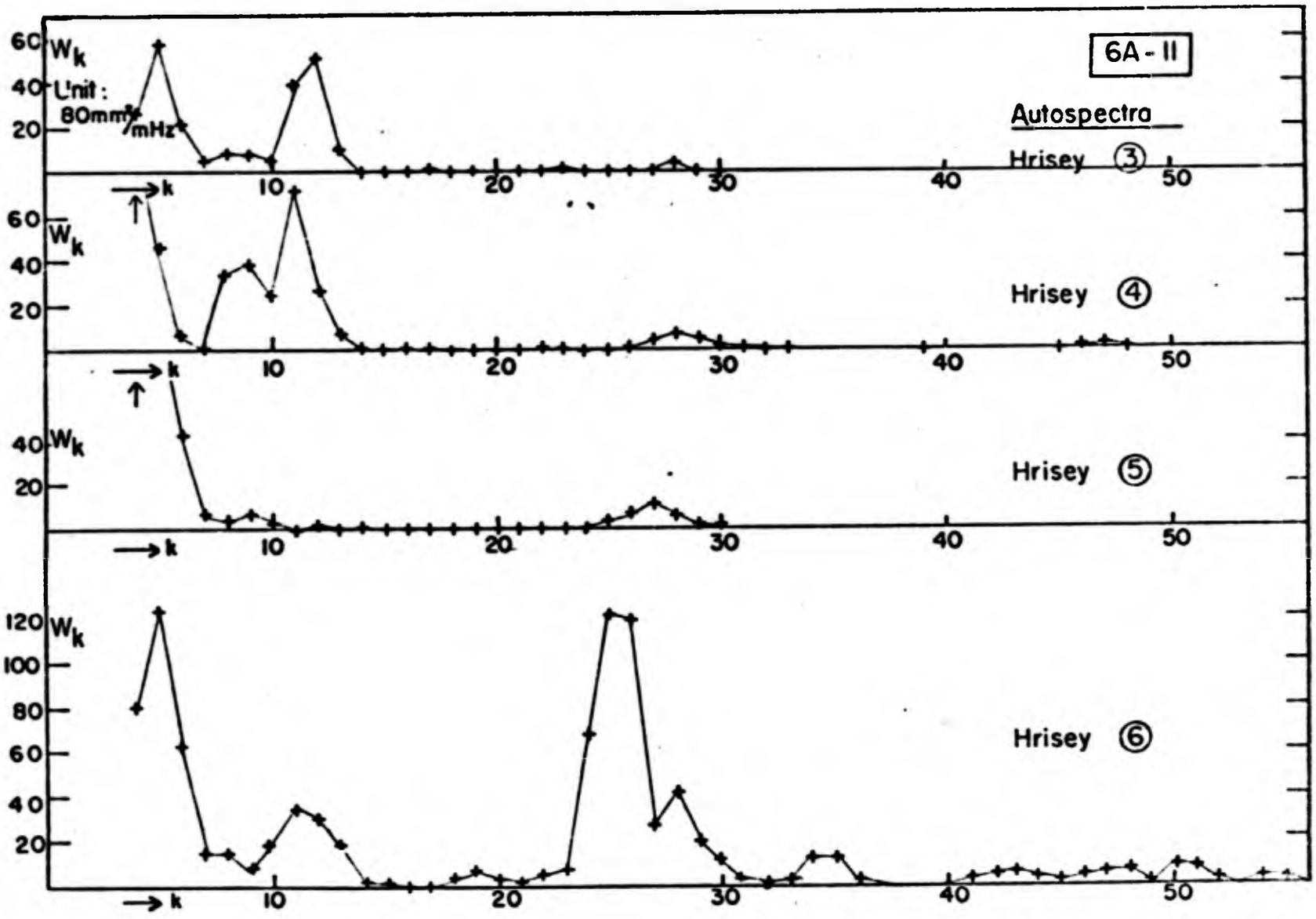
6A - II
Autospectra
Unit : 80mm²/mHz
W_k
k
Hrisey ③
Hrisey ④
Hrisey ⑤
Hrisey ⑥

Figure 6A-11

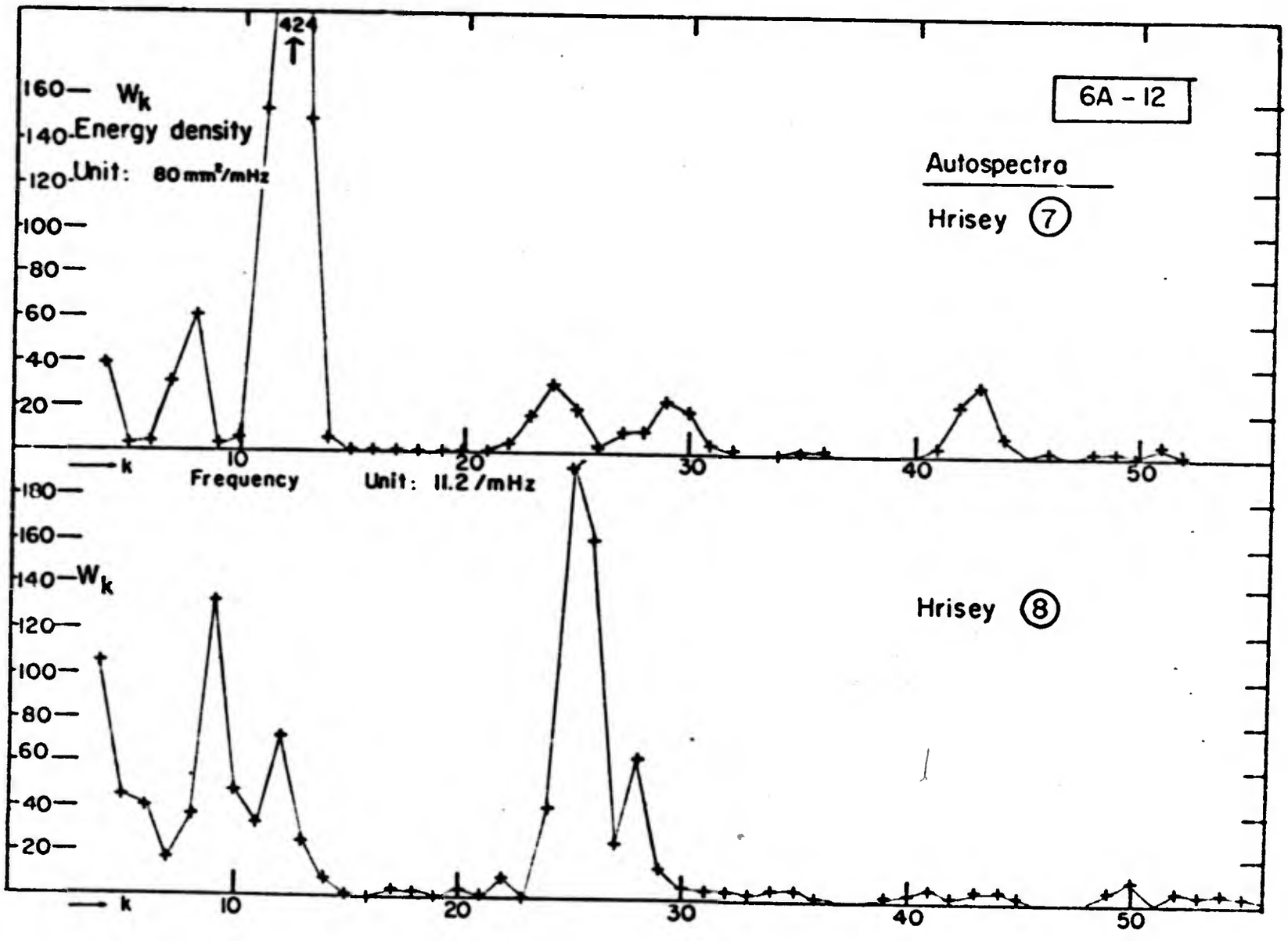
424
160— W_k
140-Energy density
120-Unit: 80 mm²/mHz
100—
80—
60—
40—
20—
6A - 12
Autospectra
Hrisey (7)
k
10
20
30
40
50
Frequency
Unit: 11.2 /mHz
180—
160—
140—W_k
120—
100—
80—
60—
40—
20—
Hrisey (8)
k
10
20
30
40
50

Figure 6A-12

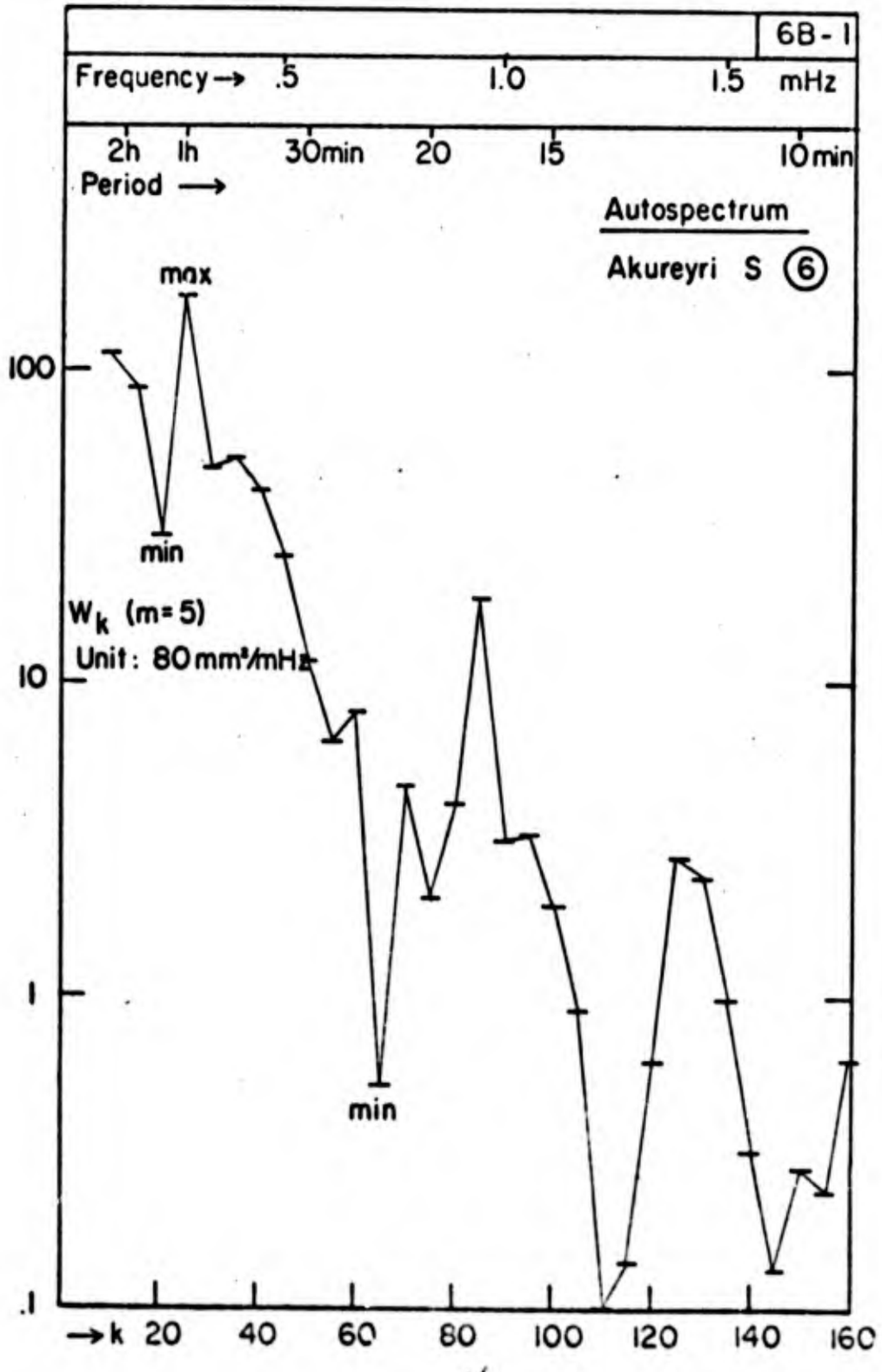
6B-1
Frequency → .5 1.0 1.5 mHz
2h 1h 30min 20 15 10min
Period →
Autospectrum
Akureyri S ⑥
max
min
W_k (m=5)
Unit: 80 mm²/mHz
100
10
1
.1
min
→k 20 40 60 80 100 120 140 160

Figure 6B-1

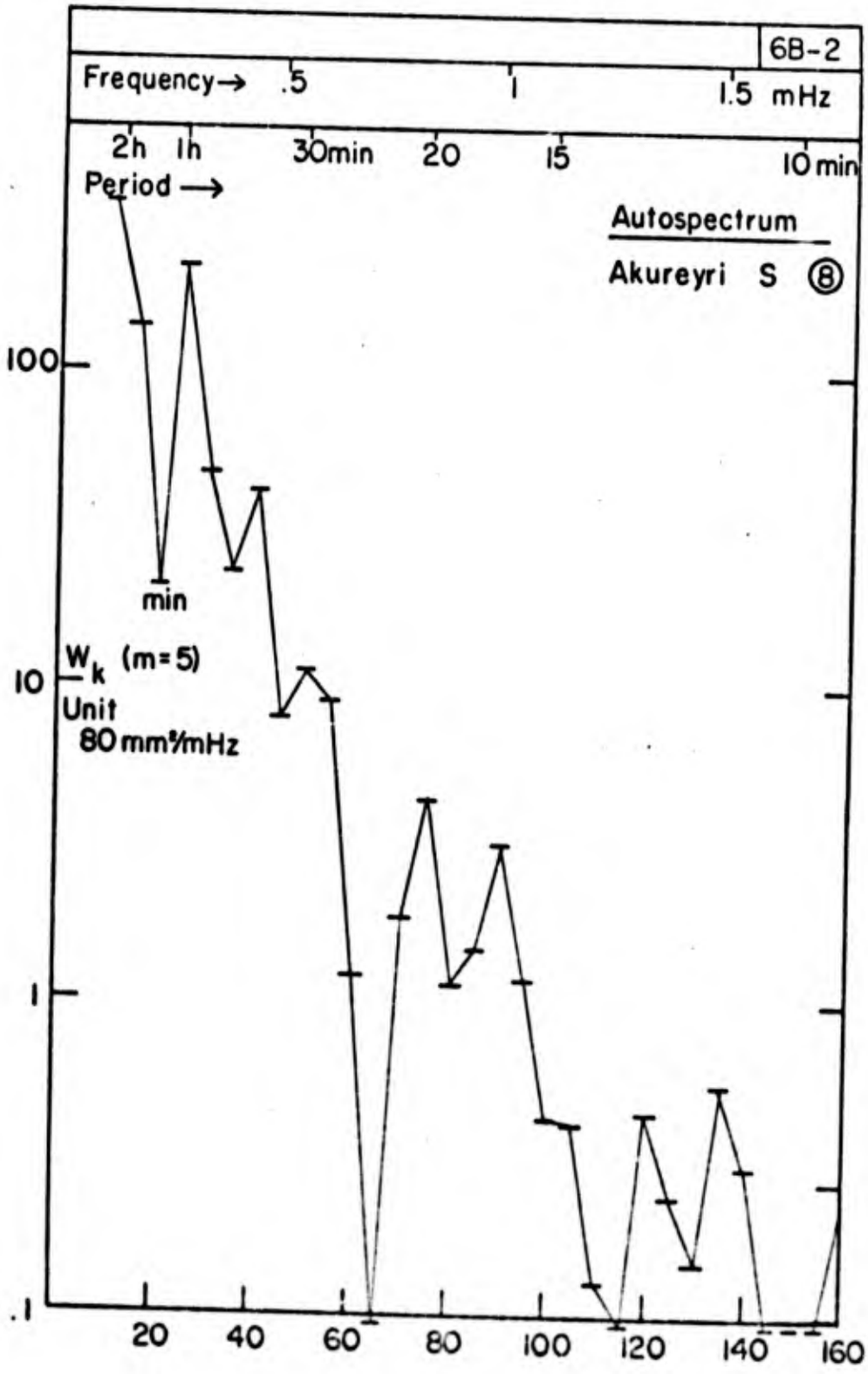
68-2
Frequency→ .5 1 1.5 mHz
2h 1h 30min 20 15 10 min
Period →
Autospectrum
Akureyri S ⑧
100
min
10
W_k (m=5)
Unit
80 mm²/mHz
1
.1
20 40 60 80 100 120 140 160

Figure 68-2

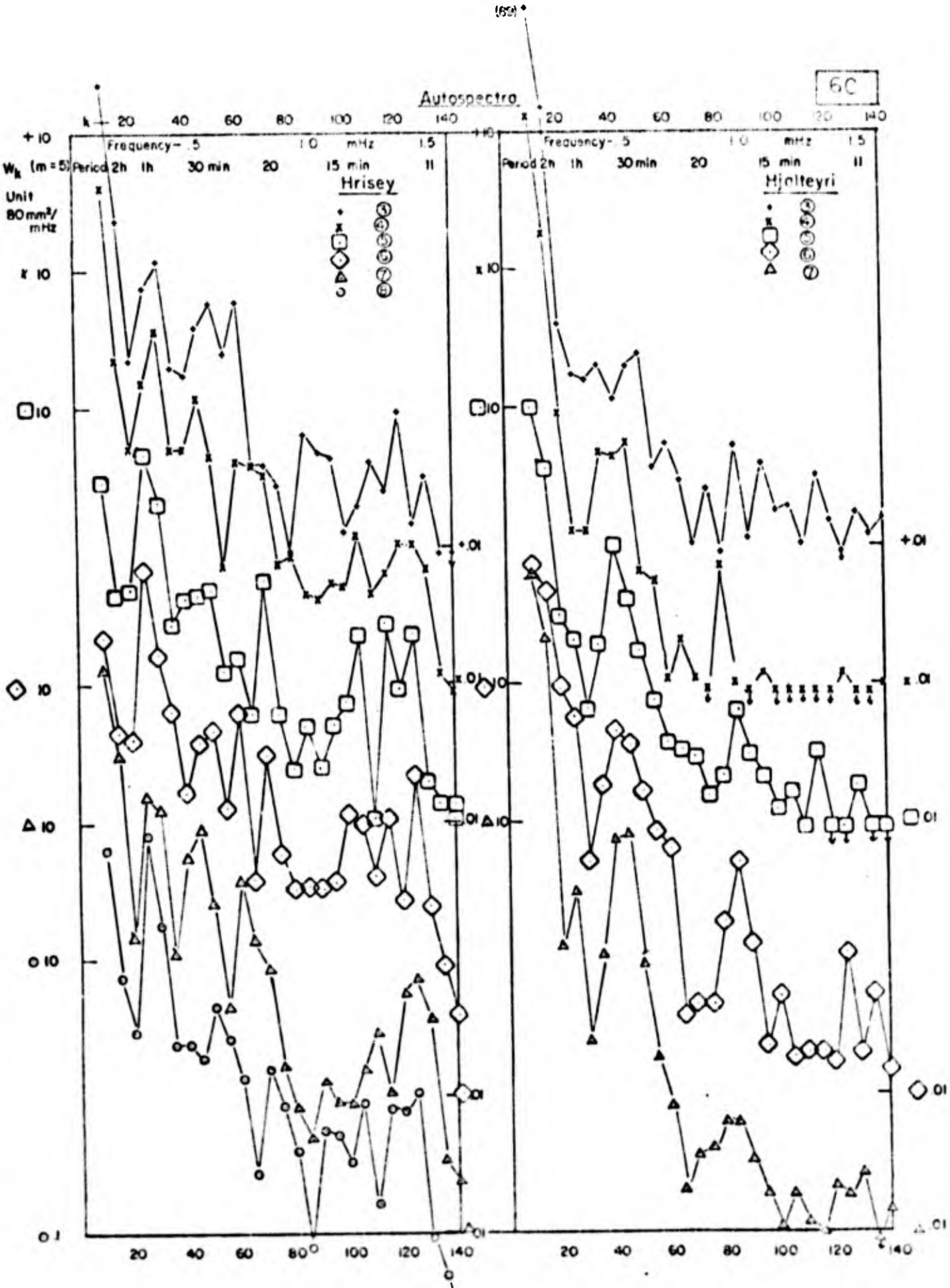
6C
Autospectra
Frequency- .5 1.0 mHz 1.5
Period 2h 1h 30 min 20 15 min 11
Hrisey
Hjalteyri
Unit
80 mm²/ mHz
k — 20 40 60 80 100 120 140
x 10
□10
◇10
△10
○10
○1

Figure 6C

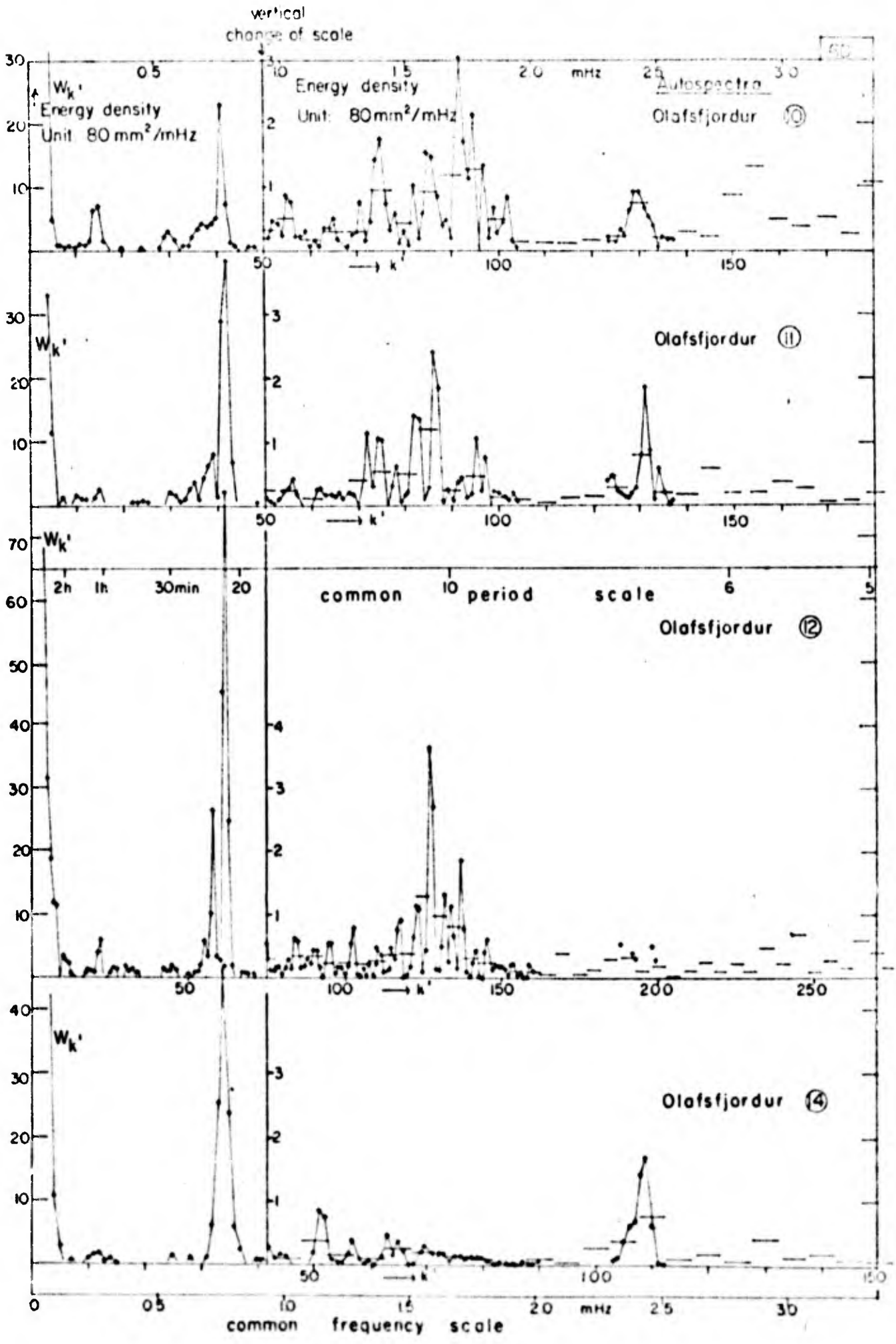
vertical change of scale
Autospectra
Energy density
Unit: 80 mm²/mHz
Olafsfjordur (10)
Olafsfjordur (11)
Olafsfjordur (12)
Olafsfjordur (14)
common period scale
2h
1h
30min
common frequency scale
mHz
k'

Figure 60

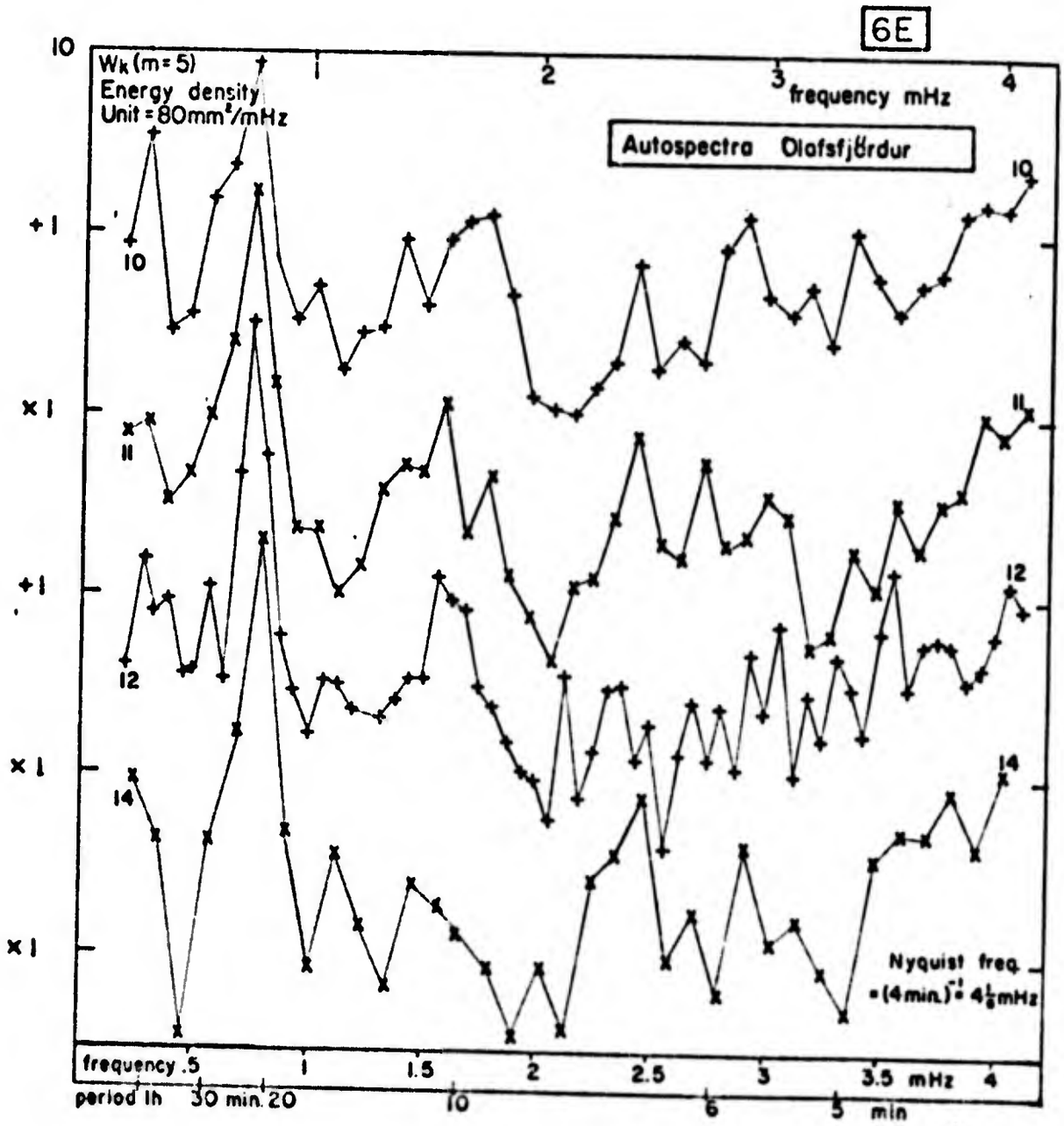
6E
Wk (m=5)
Energy density
Unit = 80mm²/mHz
frequency mHz
Autospectra Olafsfjörður
10
11
12
14
+1
×1
+1
×1
×1
Nyquist freq.
=(4min.)⁻¹= 4½mHz
frequency .5
1
1.5
2
2.5
3
3.5 mHz
4
period 1h
30 min.
20
10
6
5 min

Figure 6E

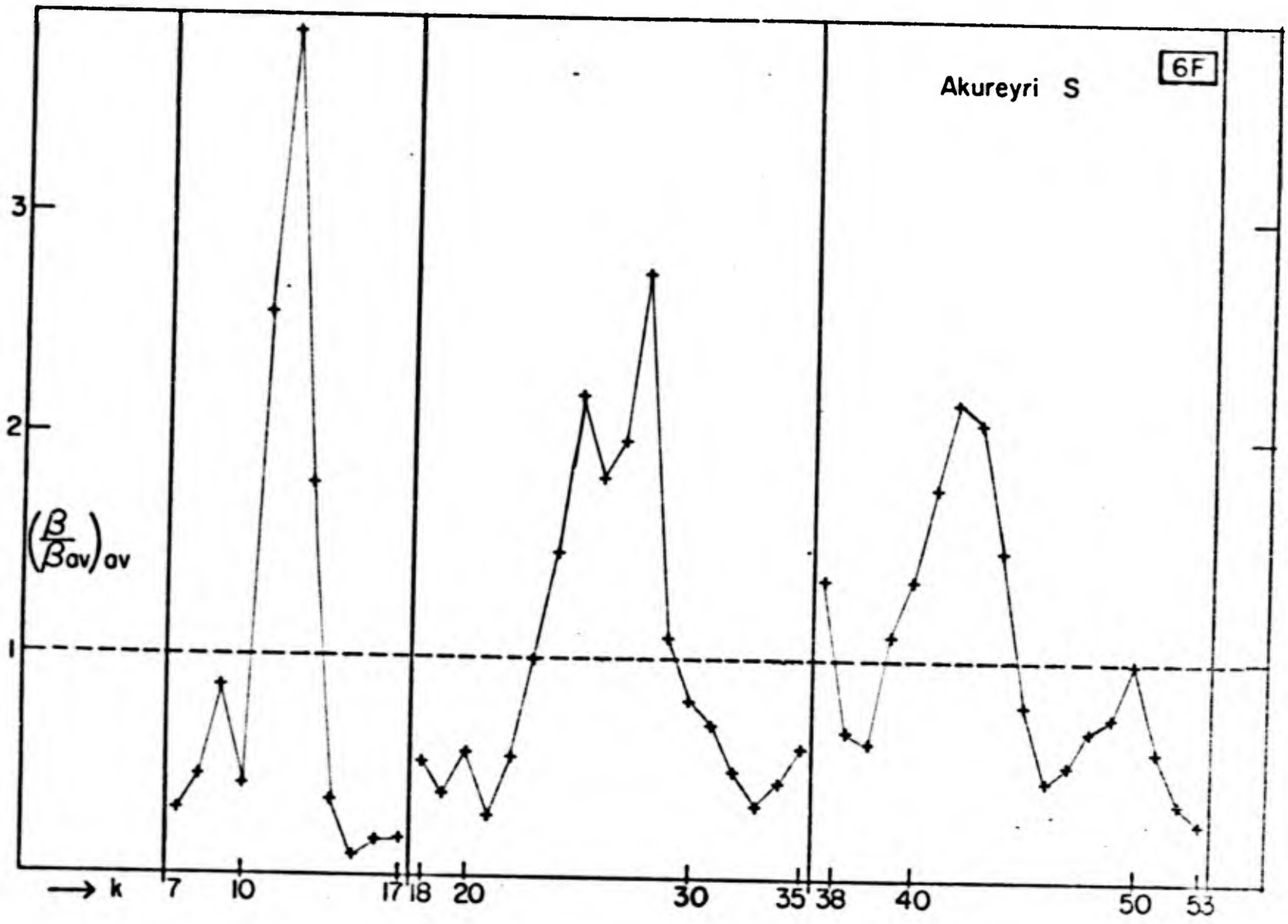
6F
Akureyri S
3
2
1
$\left(\frac{\beta}{\beta_{av}}\right)_{av}$
→ k
7
10
17
18
20
30
35
38
40
50
53

Figure 6F

7. Amplitude Ratios and Phase Differences

7.1. General

As was already explained in the introduction of this report (Section 1.1), if we may neglect the energy transferred from the atmosphere to long waves within the fjord proper and if we may also neglect non-linear effects in the fjord, then the water in the fjord would act as a linear passive system on the long waves entering from the sea. Then the coherencies between water level variations at pairs of stations should approximate unity and the amplitude ratios and phase differences for any pair of stations should be the same functions of wave frequency for all records.

The autospectra of the stations in the main fjord (Figures 6A-6C) discussed in the previous Chapter 6 already indicate the existence of strong correlations between the water level variances at different stations along the main fjord, at least for frequencies up to roughly 1 mHz.

In reality, however, we cannot expect that the water in the fjord will merely act as a linear passive system on the long waves entering from the sea. We must rather expect that the water level records analyzed for any station in the fjord can be considered as being the sum of two parts:

1o. a signal that is coherent with the similar coherent parts of the water level variation at all other locations in the fjord (including its boundary with the sea), i.e., a signal with, for any wave frequency, components having constant amplitude ratios and phase differences with respect to the similar components at another location in the fjord;

2o. a rest signal not satisfying this condition, which may be labeled simply as "noise".

The theory given in Chapter 2 obviously refers to the first (coherent) signal only.

The second signal, again, will be composed of a part reflecting real water level variations due to locally excited wave activity and to non-linear effects, and an error signal due to the many sources of errors made during the whole recording and analyzing procedure.

It appears that a systematic analysis of amplitude ratios and phase differences for pairs of stations in the fjord will be the most appropriate method to test the degree of validity of the assumption of a linear passive system, i.e., to obtain an impression of the relative magnitudes of the coherent and incoherent parts of the water level variations, because it is possible in this way to eliminate both sources of the large variability of the "input" spectra at sea, as explained in Section 6.1. If the assumption is nearly true, i.e., if the incoherent parts of the signals are relatively small, plots of amplitude ratio and phase difference for the Fourier components of a given pair of stations against the number k or k' should have a smooth appearance and should be identical for all records. Incomplete coherency between the records will show up in such plots by irregular fluctuations in the ordinates of successive points.

In cases of sufficient coherency between the water levels at two stations over a certain frequency range, the plots of amplitude ratio and phase difference also give us an adequate tool to check the validity of the Bessel type approximation for the wave motion in the fjord as elucidated in Section 2.2. If, for a given frequency ω, the differential equation (15) of that section for the complex amplitude H of the wave motion, with its solution given by const. $s^{\alpha} J_{-\alpha}(s)$, would be approximately valid, we would obviously have for the complex amplitude ratio for two stations i and j:

$$\frac{H_i}{H_j} = \frac{s_i^{\alpha} J_{-\alpha}(s_i)}{s_j^{\alpha} J_{-\alpha}(s_j)}.$$

If the second station is taken to be Akureyri S (the head of the fjord), for which we adopt here the suffix A, we would have for the complex amplitude ratio for a station i on the main fjord and Akureyri S, after introducing the normalized solution $H_\alpha(s)$ (Section 2.2, Eq. (16)):

$$\frac{Hi}{H_A} = \frac{H_\alpha(s_i)}{H_\alpha(o)} = H_\alpha(s_i). \tag{1}$$

The variable s_i is given by (Section 2.1, Eq. (12)):

$$s_i = s_{ri}(1-iq_i), \tag{2}$$

with a real part

$$s_{ri} = w \int_0^{xi} \frac{d\xi}{\sqrt{gd(\xi)}}, \tag{3}$$

thus being strictly proportional to ω,

and an imaginary part

$$-is_{ri}q_i = -1/2i \int_0^{xi} d\xi \; \frac{\gamma v_m}{d\sqrt{gd}}, \tag{4}$$

provided the quantity q_i is small compared with unity, and in which d is a function of ξ but γ and v_m must be assumed to contain both ξ and ω.

According to Equation (1) then, the behavior of the complex amplitude ratio Hi/H_A as function of the frequency ω would have to coincide with the behavior of the normalized function $H_\alpha/(s_i)$ along a line in the complex s_i-plane starting from the origin and deviating relatively little from the real s_i-axis, with the relation between ω and s_i being given by Equations (2) to (4). According to Eq. (4), the imaginary part $-is_{ri}q_i$ for a given ω will increase monotonically with the distance x_i, but for a given x_i it will probably not vary much with the frequency ω. This means that the just mentioned

line in the complex s_i-plane will have the tendency to run parallel with the real axis (except for very small s_{ri}), so that q_i will decrease with increasing ω. If friction could be neglected altogether, the parameter s_i would be real and simply proportional to ω.

The Figures 7A to 7I are plots of amplitude ratio r and phase difference ϕ for some station and Akureyri S against the Fourier component number k or k'. They will be called "ratio plots", for shortness. They are presented only for those cases and for those frequency ranges in which the coherencies were sufficiently high to make these plots meaningful. Curves have been drawn in a subjective way through the points, to show, or to suggest, a possible shape of the curve if there would be no incoherent contributions to the signals at both stations.

Only results derived by means of pre-tapered Fourier analysis (ref. Sections 4.2 and 4.1) were used. The amplitude ratios r_{ik} were calculated from the computer output W_{ik} and W_{Ak} as $r_{ik} = (W_{ik}/W_{Ak})^{1/2}$, or similarly from average W-values over five consecutive k- (or k'-) numbers; the phase differences ϕ were calculated from the computer output C_{iAk} and Q_{iAk} as $\phi = \text{arctg}(Q_{iAk}/C_{iAk})$ (with consideration of the signs), or similarly from average C- and Q-values over five consecutive k- (or k'-) numbers. Positive ϕ-values (<180°) imply a phase lag of Akureyri S with respect to the first station. Further explanatory notes for the various plots are given in Appendix 2. As before, one k-unit corresponds with .0112 mHz.

The degree of irregular scatter of the points around the curves, in particular the amplitude ratio curves, gives an impression of the relative magnitude of the incoherent parts of the signals. In general, it will be seen that this scatter is relatively small for the lower frequencies and that it increases with decreasing W-values and with increasing wave frequency.

Where curves could be reasonably drawn, it will also be seen that these curves derived from different records for one station are very similar, but that

they are different for different stations; all this is according to expectation.

7.2. The "Main Fjord" Stations

Almost all of the material to be discussed in this chapter refers to the stations along the "main fjord".

Even in the lower frequencies, from about 0.05 to 0.6 mHz (periods 6 hours to 30 minutes) most of the plots (Figures 7A, C, D,G, H) show an amount of scatter which is by no means negligible, indicating that the incoherent parts of the water level variations as analyzed, in this frequency range, were of the same order of magnitude as the coherent parts. The scatter is relatively small in this frequency range for the records no. six and seven only (Figures 7A-4, 7A-5, 7A-11, 7A-12, 7H-5). For these two cases the coherencies are still reasonably good for frequencies up to about 1.2 mHz (Figures 7B-1 to 7B-4, 7H-5).

Note that for most of the records there is some correlation between the scatter in the plots for Hrisey, Hjalteyri and Dagverdareyri (as far as they are given), apparently owing to the choice of Akureyri S as common reference station. Look, e.g., for records no. three (Figs. 7A-1, 7A-7 and 7G-3) at the outlying points at k - 4, 15, 29, 49 (all of them too high) and at k = 16 and 41 (too low). In principle, it would be possible, by a symmetrical treatment of the records of the various stations, to arrive at slightly better estimates for the coherent amplitude ratios than by the subjective tracing of curves as was done here, but the gain would be small.

The amplitude ratio and phase difference curves found for the various stations with respect to Akureyri S, in general, are consistent with the concept of one-dimensional long waves in the fjord, with decreasing wave-lengths as the number k increases. The sometimes rather sharp minima of the amplitude ratio curves, in several instances being clearly associated with a rather sudden shift in phase difference from about 0° to 180° (for the first minima), or from

about 180° to 0° (for the second minima) indicate the wave frequencies for which the (vertical) wave motion has a node at the station concerned. It will be seen that the node associated with the first mode of natural longitudinal oscillation in the fjord with k = 12 (ref. section 6.2), which node must be assumed to occur near the seaward boundary, moves inward with increasing k: for k = 15 to 16 the node occurs near Hrisey, for k = about 29 it is near Hjalteyri and for k about 47 it is near Dagverdareyri. Similarly, the node associated with the second mode of natural longitudinal oscillation with k = 27 (ref. Section 6.2), with increasing k has moved for k about 39 to Hrisey and for k about 70 to Hjalteyri.

It is clear that the characteristic features of the amplitude ratio and phase difference curves move to larger k-values as the station considered is closer to Akureyri, and that these features then become more and more obscured by the increasing amount of scatter.

The phase shifts associated with the minima of the amplitude ratio curves should be theoretically always in the positive sense with increasing k (from 0°, <u>via</u> +90° to 180°, from 180° <u>via</u> -90° to 0°) and this is, indeed, more or less clearly seen in the plots, though in a few cases the reverse is suggested.

For the lower frequencies up to about .6 mHz the amplitude ratio and phase difference curves found for each of the stations with respect to Akureyri S, indeed, might be approximated by a Bessel-type expression [$H_\alpha(s)$] with the complex argument $s = s_r(1-iq)$ having a real part s_r proportional to the wave frequency and a realtively small imaginary part $-is_rq$, according to Equations (1), (2), (3), (4) of Section 7.1; compare also Fig. 2D. If such a Bessel-type solution is fitted, the k-values, k_1, k_2, ... for which r has minima must practically correspond with the zeros s_1, s_2, ... of the real function $H_\alpha(s_r)$.

The parameter α then can be estimated, in principle, in at least three different ways:

1. by taking the ratios k_2/k_1, k_3/k_1, ... which should equal s_2/s_1, s_3/s_1, ..., respectively, and reading off α from Fig. 2B; this appears to be the most accurate method; it ignores knowledge on the geometry of the fjord;

2. by multiplying k_1, k_2, ... by the geometric parameter s_r/k for the station (ref. Section 1.3) to find the zeros s_1, s_2, ..., respectively, and reading off α from Fig. 2A; this method is less accurate;

3. by taking the ordinates of the secondary maxima of the amplitude ratio curves and reading off α from Fig. 2B; this method, however, appears to be less effective.

The values found for α then give best fits obviously relating to that part of the fjord lying between the station considered and the head (Akureyri) only.

If a value of α has been estimated, a value for the dissipation parameter q can be most conveniently estimated from the levels of the minima of the r(k) curve. If these minima are low enough we have approximately, according to Eq. (19) of Section 2.2, for the n-th minimum $r_{min\ n}$:

$$r_{min\ n} \approx qs_n \left[\frac{dH_\alpha}{ds} \right]_{s = s_n} \qquad (5)$$

Figure 2C can be used.

It will appear later that the third method just described for estimating the parameter α, viz., from the ordinates of the secondary maxima of the r(k) curve, needs the application of a correction for a dissipation term. From Eq. (18) of Section 2.2 we have for the j-th secondary maximum $r_{max\ j}$, corresponding with an s-value $s_j(1-iq)$, where s_j (real) denotes the value of s_r at which $H_\alpha(s_r)$ has its j-th extremum:

$$r_{max\ j} \approx [H_\alpha(s_j) - 1/2(\rho s_j)^2 \left(\frac{d^2 H_\alpha}{ds^2}\right)_{s=s_j}]. \qquad (6)$$

In fact, the last term always makes $r_{max\ j}$ larger than $[H_\alpha(s_j)]$; this was already illustrated by Fig. 2D.

We shall now consider the results for specific stations more closely.

7.2.1. Hrisey-Akureyri S

See Figures 7A-1 to 7A-6 including 7B-1, 7B-2, 7C-1, 7D-1, 7E-1 and 7F-1. Among these, Figures 7A-2 and 7D-1 refer to Akureyri N as reference station because there was no adequate record for Akureyri S.

Minima of the amplitude ratio curves are situated at k about 15, about 39, about 85 and about 140 (see, especially, Fig. 7E-1). The Bessel-type solution would predict minima at roughly equal distances in the frequency scale, thus additional minima at k about 60-65 and 110-115. Actually, however, pronounced maxima are seen right in both these k-ranges. With reference to the autospectra presented in Figures 6B and 6C it appears that the unexpected maxima for k = 60-65 and 110-115 are associated with dips in the Akureyri spectra, rather than with peaks in the Hrisey spectra. As already stated in Section 6.2 (3°), it must be admitted that no explanation was found for these rather consistent minima in the Akureyri spectra.

If we now restrict ourselves to the lower frequency range up to 0.6 mHz, the following table gives some values estimated from the curves drawn in Figures 7A and 7C. (see following page for table)

Notes:

1) Since in Fig. 7A-2 Akureyri N is the reference station, r-values read from this figure were multiplied by the average amplitude ratio for Akureyri N-Akureyri S at k = 15, 39, 27 and 51 respectively (ref. Section 7.2.4).

Figure	Records No.	k_1	k_1*	k_2	k_2*	$r_{min\ 1}$	$r_{min\ 2}$	$r_{max\ 1}$	$r_{max\ 2}$
7A-1	3	15-1/2	15-1/2	39-1/2	38-1/2	(.17)	(.29)	(.64)	-
7A-2	4[1]	15-1/2	15	37-1/2	(40)	.13[1]	.16[1]	.61[1]	(.65)[1]
7A-3	5	15	15	40	(40)	.11	.21	.75	-
7A-4	6	15	15-1/2	39-1/2	37-1/2	.14	.14	.67	.67
7A-5	7	15-1/2	15	38	39	.16	.17	.68	.69
7A-6	8	15-1/2	-	38	38	.16	.17	.71	(.71)
7C-1	9	(14)[2]	-	(39)[2]	-	(.20)	(.14)	(.64)	-
Averages		15.2	15.2	38.8	38.3	.14	.17	.68	.68

Explanation:

k_1, k_2 = estimated k-values for which amplitude ratio r is minimum;
k_1*, k_2* = estimated k-values for which phase difference is +90° or -90°;
$r_{min\ 1}$, $r_{min\ 2}$ = estimated minimum ordinates of amplitude ratio curves;
$r_{max\ 1}$, $r_{max\ 2}$ = same for maximum ordinates,

Values in parentheses are less accurate. In the averaging double weight was given to the values of records 6 and 7 and the values in parentheses were neglected.

2) Since the duration of the records No. 9 was 1.8 cycles of the M_2-tide, relevant k'-values were multiplied by 2.0/1.8 = 1.11.

The averaging of the estimates from various records does not imply that the parameters concerned are necessarily always the same; on the contrary, it must be assumed that there are some variations with time, due, e.g., to the variations in amplitude and phase of the main tide and the accompanying tidal currents, and to variations in the amplitudes in the shorter period long waves as well. The table, however, confirms the belief that the parameters vary very little.

If a Bessel-type expression is to be fitted the following values for α are found by the methods described in Section 7.2.

Method 1: $k_2/k_1 = 38.6/15.2 = 2.54$ gives $\alpha = +0.24$.

Method 2: since s_r/k was determined to be 0.124 (see Section 1.3) we derive

$s_1 = 0.124 \times 15.2 = 1.89$ gives $\alpha = +0.32$;

$s_2 = 0.124 \times 38.6 = 4.79$ gives $\alpha = +0.46$.

The result from Method 1 is probably the best estimate. Both results of Method 2 can be made to fit exactly with this if s_r/k would be a little higher: 0.133.

With $\alpha = +0.24$, a reasonable guess at the geometric parameters m and n for the part of the fjord between Hrisey and Akureyri (cf. Section 2.2) from Fig. 2C, with reference to Fig. 1B, would be m = 0.40, n = 0.15.

We can estimate the dissipation parameter q from $r_{min\ 1} = 0.14$ and $r_{min\ 2} = 0.17$ (see table above), putting $\alpha = +0.24$ and using Eq. (5) of Section 7.2 and Fig. 2C:

$r_{min\ 1} = 0.14$ corresponding with s_1 2.02, gives q = 0.101,

$s_1 q = 0.20$;

$r_{min\ 2} = 0.17$, corresponding with s_2 5.14, gives q = 0.061,

$s_2 q = 0.31$.

Owing to the scatter of the points in the r-plots it is suspected that both estimates of r_{min}, and thus of q, are on the high side. A closer analysis of the dissipation of wave energy in the fjord will be given in Chapter 9.

With an estimated value of 0.08 for q, an additional check on the value of α can be obtained from the mean ordinate of the first secondary maximum of the r-curve, i.e., the third method given in Section 7.2, see Eq. (6) of that section, repeated here with the subscript max 1:

$$r_{max\ 1} \approx [H_\alpha (s_{max\ 1}) - 1/2(qs_{max\ 1})^2 (\frac{d^2 H_\alpha}{ds^2})_{s = s_{max\ 1}}]$$
$$\cdot \frac{d^2 H_\alpha}{ds^2}$$

From $r_{max\ 1} \approx 0.68$ (see table above, $qs_{max\ 1} \approx 0.08 \times 3.4 = 0.27$, at $s = 3.4$ is about +0.62, we obtain about -0.03 for the second term on the right and $[H_\alpha(3.4)]$ becomes 0.65. Fig. 2B then gives $\alpha = +0.30$, which is only a little higher than the value +0.24 found earlier.

Conclusion. For the long-wave motion with frequencies up to about 0.6 mHz in the fjord between Hrisey and Akureyri a Bessel-type expression can be reasonably will fitted if α is between +0.20 and +0.30 and the parameter $s_r q$ (Section 7.2, Eq. (4)) is 0.2 to 0.3.

7.2.2. Hjalteyri - Akureyri S

See Figures 7A-7 to 7A-13 inclusive, 7B-3, 7B-4 and 7E-2. Among these, Figures 7A-8 and 7A-10 refer to Akureyri N as reference station; in the former case no adequate record for Akureyri S was available.

Minima of the amplitdue ratio curves are found at k about 29 and about 70. Systematic minima at certain higher k-values are not discernable in Fig. 7E-2; coherencies appear to be almost non-significant for k exceeding about 100.

The following table gives some values estimated from the curves drawn in Figures 7A and 7B. The meaning of the symbols in this table is the same as that in the table given in the previous Section 7.2.1. (see table on following page).

As in the previous Section 7.2.1, the table suggests that the parameters do not vary much under varying external conditions.

If a Bessel-type expression is to be fitted in this case the following values for α are found by the methods described in Section 7.2.

Method 1: k_2/k_1 = 70-1/2/29.0 = 2.43 gives α = +0.15.

Method 2: since s_r/k was determined to be 0.073^5 (see Section 1.3) we derive

$s_1 = 0.073^5 \times 29.0 = 2.14$ gives α = +0.17;

$s_2 = 0.073^5 \times 70\text{-}1/2 = 5.20$ gives α = +0.20.

There is a satisfactory agreement. Both results of Method 2 can be made to fit exactly with the result of method 1 if s_r/k would be taken 0.075.

With α = +0.15, a reasonable guess at the geometric parameters m and n for the part of the fjord between Hjalteyri and Akureyri (cf. Section 2.2) from Fig. 2C, with reference to Fig. 1B, would be m = 0.53, n = 0.20.

We can estimate the dissipation parameter q from $r_{min\ 1}$ = 0.07 (see table above) and using Eq. (5) of Section (7.2) and Fig. 2C, putting α = +0.15: $r_{min\ 1}$ = 0.07, corresponding with s_1 2.17 gives q = 0.052, $s_1 q$ = 0.11.

The latter value is smaller than those found for Hrisey; this should be expected from Eq. (4) of Section 7.1 since the distance Akrueyri - Hjalteyri is shorter than the distance Akureyri - Hrisey.

The value of q is so small that method no. three given in Section 7.2 for estimating α can be applied in the simple form $r_{max\ 1} \approx [H_\alpha]_{max\ 1}$. If $r_{max\ 1}$ = 0.41, Fig. 2B then gives α = +0.02, which is a little smaller than the value 0.15 found earlier.

Figure	Records No.	k_1	k_1*	k_2	k_2*	$r_{min\ 1}$	$r_{min\ 2}$	$r_{max\ 1}$	$r_{max\ 2}$
7A-7	3	(28-1/2)	-	-	-	(.17)	-	(.38)	-
7A-8	4[1]	28-1/2	29	-	-	.05[1]	-	.36[1]	-
7A-9	5	28	28	-	-	.05	-	.47	-
7A-10	5[1]	28	28	-	-	.05[1]	-	.43[1]	-
7A-11 7B-3	6	29	29-1/2	(70-1/2)	(71)	.08	(.09)	.43	-
7A-12 7B-4	7	30	-	(70-1/2)	(71)	.07	(.13)	.39	-
7A-13	8[2]	(29-1/2)	-	-	-	(.03)	-	(.33)	-
Averages		29.1	29.0	(70-1/2)	(71)	.07	-	.41	-

Explanation:
Values in parentheses are less accurate. In the averaging double weight was given to the values of records 6 and 7, the values of each of Figures 7A-9 and 7A-10 had a half weight and the values in parentheses were neglected except those for k_2 and k_2*.

Notes:
1. Since in Figures 7A-8 and 7A-10 Akureyri N is the reference station, r-values read from these figures were multiplied by the average amplitude ratio for Akureyri N - Akureyri S at k = 29 and 46, respectively (ref. section 7.2.4).

2. The phase differences determined for records no. 8 suggested a small time shift error of the records; the amplitude ratios, however, wer considered to be hardly affected by this error.

Conclusion. For the long-wave motion with frequencies up to about 0.8 mHz in the fjord between Hjalteyri and Akureyri a Bessel-type expression can be reasonably well fitted if α is between 0 and +0.15 and $s_r q$ is about 0.1.

7.2.3. Dagverdareyri - Akureyri S

See Figures 7G-1 to 7G-5 inclusive, among which Fig. 7G-4 refers to Akureyri N as reference station.

The only characteristic feature that shows up clearly in all five amplitude ratio curves is the minimum at k somewhere between 45 and 50; three of the plots give an indication of a second minimum at k between 85 and 95. Moreover all curves show an anomalous character for k between 60 and 70 which apparently is connected with the unexplained dip in the autospectra of Akureyri (see Section 6.2 (3o), see also Section 7.2.1, second paragraph).

Some values of parameters estimated from the curves are given in the next table, where the meaning of symbols is the same as that in the earlier tables of Section 7.2.1 and 7.2.2.

Figure	Record No.	k_1	k_1*	k_2	$r_{min\ 1}$	$r_{min\ 2}$	$r_{max\ 1}$
7G-1	1	49	(57)	(92)	.13	(.31)	-
7G-2	2	47	(55)	88	.21	(.43)	-
7G-3	3	47	(65)	87	.19	.32	-
7G-4	4[1]	45	54	-	.20[1]	-	-
7G-5	5	(59)	(66)	-	(.28)	-	-
Averages		47	-	88	.18	.32	-

Note[1]: Since in Fig. 7G-4 Akureyri N is the reference station, the value of $r_{min\ 1}$ as read from this figure was multiplied by the average amplitude ratio for Akureyri N - Akureyri S at k = 45 (ref. the next Section 7.2.4).

There is some indication here that the parameters vary a little from record to record.

If if is attempted to fit a Bessel-type expression here, the following values for α are found by the methods described in Section 7.2.

Method 1: $k_2/k_1 = 88/47 = 1.88$ gives $\alpha = -0.8$.

Method 2: since s_r/k was estimated to be 0.040 (see Section 1.3) we derive $s_1 = 0.040 \times 47 = 1.88$ gives $\alpha = +0.32$.

Apparently both estimates for α show a large discrepancy. The second estimate does not deviate much from the estimates found for Hjalteyri and Hrisey and therefore is probably the better one. If $\alpha = +0.32$ we should have (from Fig. 2B) $k_2/k_1 = 2.64$ and if $k_1 = 47$ is correct, k_2 should thus be 124. In that case the minima found near k = 90 would be a consequence of the unexplained minima of the autospectra of Akureyri S at k = 60 to 70 and 110 to 115, see Section 6.2 (3o).

With $r_{min\ 1} = 0.18$ and $\alpha = +0.32$ the dissipation parameter q can be estimated (Eq. (5) of Section 7.2 and Fig.2C):

$r_{min\ 1} = 0.18$, corresponding with s_1 1.88 gives $q = 0.125$,
$qs_1 = 0.23$.

The latter value exceeds that found for Hjalteyri, whereas we should expect a smaller value. It seems that the minimum ordinates in the plots 7G were considerably over-estimated due to the relatively higher degree of scatter of the points in these plots.

Conclusion. For the long-wave motion with frequencies up to about 0.6 mHz in the fjord between Dagverdareyri and Akureyri a Bessel-type expression can be reasonably well fitted if α is about 0.3.

7.2.4. Akureyri N - Akureyri S

See Figures 7H-1 to 7H-6 inclusive; see also the explanation in Appendix 2.

The common features shown in the plots are not unexpected, in view of the very short distance between these two stations. The coherencies are relatively high up to rather high frequencies, especially in Fig. 7H-5 (records no. 6). The amplitude ratios slowly decrease with increasing k. Five plots show a minimum at k between 130 and 150, associated with a phase shift. This means that for the southern extremity of the fjord, south of the "narrows" of Oddeyri, the existence of a proper oscillation with frequency 1.5 to 1.6 mHz (period 10 to 11 minutes), with a minimum amplitude off Akureyri N (Oddeyri), has been demonstrated.

The next table gives values of k_1 at which the minimum of the amplitude ratio occurrs and of $r_{min\ 1}$, the corresponding minimum ordinate, as estimated from the figures.

Figure	Records nr	k_1	$r_{min\ 1}$
7H-1	1	-	-
7H-2	2	142	.34
7H-3	3	(135)	(.47)
7H-4	5	(135)	(.45)
7H-5	6	144	.31
7H-6	8	132	.46

Amplitude ratios for a set of k-values, as read from the figures are given in the following table. (see following page).

Values interpolated from the figures in the last line have been used as correction factors in some of the plots dealt with in the previous sections.

Fourier component number k							
Figure	20	40	60	80	100	120	140
7H-1	.99	.94	.80	.64	.53	-	-
7H-2	.96	.87	.76	.65	.52	.41	.35
7H-3	.96	.87	.77	.68	.59	.51	.48
7H-4	.98	.94	.86	.75	.62	.49	.45
7H-5	.96	.86	.73	.59	.44	.35	.31
7H-6	.96	.87	.77	.67	.56	.48	.47
Averages	.97	.89	.78	.66	.54	.45	.41

7.3. Olafsfjordur

Only two plots of the amplitude ratio with respect to one of the Akureyri stations could be made; see Figures 7D-2 for records no. 10 and 7I-1 for records no. 14, both with Akureyri N as reference station. Both plots refer to the frequencies up to 0.63 mHz, i.e., below the frequency 0.76^5 mHz of the first consistent peak in the autospectra of Ola; around the latter frequency the amplitudes at Ola were up to 20 times higher than the amplitudes at AkN.

Both plots are of moderate quality but they definitely show common features: minima at about 0.14, 0.34 and 0.47 mHz, separated by maxima, and ratios higher than one for frequencies higher than 0.52 mHz.

For frequencies below 0.6 mHz the features of the amplitude ratio curve for Ola must be expected to reflect properties of the main fjord, rather than properties of the little side fjord. It can be safely assumed that the amplitude ratios for the mouth of the side fjord - which is rather close to the mouth of the main fjord (cf. Section 1.3) - and Akureyri can be found by multiplying

the amplitude ratios for the stations Ola and Akureyri by a function of frequency that monotonically decreases from unity at zero frequency to some value of the order of one-quarter at 0.63 mHz. (This function should look like $H_\alpha(s)$ with α -0.3 (see Section 6.3) between s = 0 and s 0.8 times the first zero).

Then the minima in the r-curve for the mouth of the side fjord would be expected at slightly higher frequencies than the minima in the r-curve for the station Olafsfjordur, with negligilbe frequency shifts for the first and second minima and a larger shift for the third minimum. On the other hand, each of the minima in the r-curve for the mouth of the side fjord must be expected to occur at a frequency between the corresponding frequency of a peak in the autospectra of Akureyri and the corresponding frequency of a minimum in the r-curve for Hrisey. The following table confirms the correctness of these considerations.

	Characteristic frequencies		
Peaks in autospectra AkS (cf. section 6.2)	.135 mHz (k=12	.30 mHz (k=27)	.47 mHz (k=42)
Minima of r for Olafsfj.	.14 (± .01)mHz	.34(± .02)mHz	.47(± .02)mHz
Minima of r for Hrisey (cf. section 7.2.1)	.170 mHz(k=15.2)	.43mHz(k=38.6)	-

More quantitative information than this can hardly be deduced from the available observational material.

7.4 Note on Estimates of Coherency

In this report coherencies between pairs of simultaneous spectra at two stations 1 and 2 were calculated as:

$$\gamma k^2 = \frac{\overline{C}_{12,k}{}^2 + \overline{Q}_{12,k}{}^2}{\overline{W}_{1k}\,\overline{W}_{2k}} \quad ; \qquad (7)$$

see Section 4.1, Equations (3), (4) and (5), the overbars here indicating an averaging over m consecutive k-values: from k-2 to k+2 if m is taken 5. These coherencies referring to m = 5 have been given, as percentages, along the top side of several of the ratio plots.

It was already indicated in Section 4.1 that expression (7) gives positively biased estimates for the really coherent parts of both signals concerned; in the limiting case m = 1, expression (7) even gives always 100 percent.

For completely incoherent signals it can be easily shown from Eqs. (3) and (4) of Section 4.1 that expression (7) has an expected value of at least 1/m for un-tapered Fourier spectra. For two pre-tapered Fourier spectra of uncorrelated signals the situation is a little more complicated but the expected value for γ^2_k then will probably be even higher.

An experimental check on this was made by considering a sample of 150 arbitrary γ^2-values taken from the computer output, all for m = 5 and for k-values larger than 200, where the spectral estimates are so small that they can be assumed to represent pure "instrumental noise" (see Section 5.3) and therefore can be assumed to be completely incoherent. The average of these γ^2-values turned out to be 32 percent; 21 values, or roughly one seventh part, turned out to be 60 percent or higher, 4 values were even 80 percent or higher, the highest value was 91 percent. This result makes clear that for m = 5, coherencies γ^2 calculated according to Eq. (7) that even exceed 60 percent do not guarantee that there is any coherency at all.

Munk and Cartwright [19] mention an approximate unbiased estimate of the true coherency γ^2 in case one of the signals is noise-free. It is:

$$\gamma_k^{*2} = \gamma^2 k - \frac{1}{m-1}(1 - \gamma^2_k), \qquad (8)$$

where γ^2_k is given by (7), and where it is assumed that the complex amplitude ratio for the coherent part of the signals is constant over the m k-values considered. (In fact, M. and C. were discussing ensemble averages for <u>one</u> k-value). According to (8), for example, γ^2_k = 60 percent for m = 5 would correspond with an unbiased estimate γ_k^{*2} = 50 percent.

The conclusion is that, for m = 5, individual γ^2_k-values according to Eq. (7) do not tell much about true coherency, unless γ^2_k exceeds 80 percent at least.

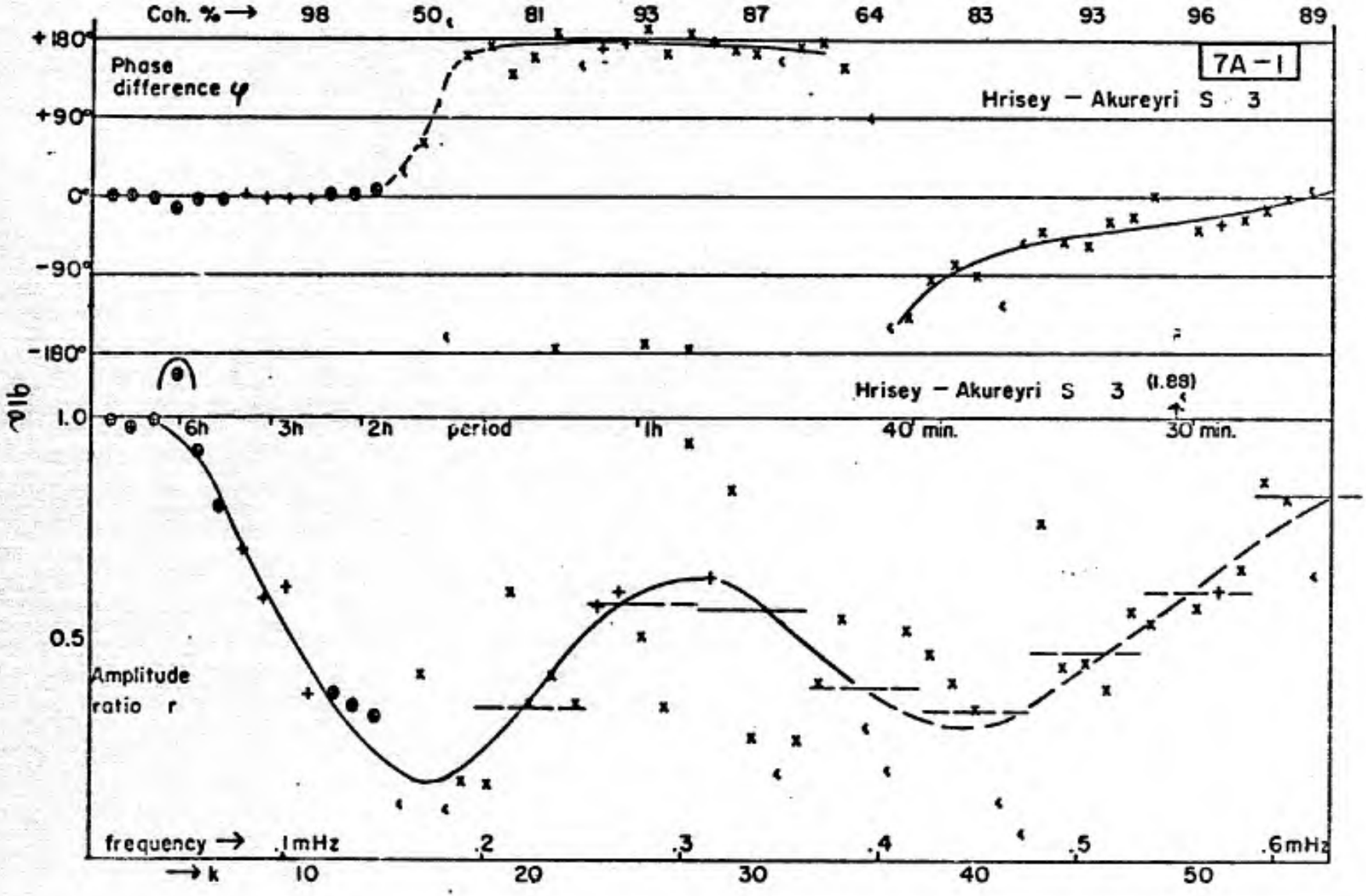
Coh. % →
98
50
81
93
87
64
83
93
96
89
+180°
+90°
0°
-90°
-180°
Phase
difference φ
7A-1
Hrisey – Akureyri S 3
Hrisey – Akureyri S 3
(1.88)
φ/b
1.0
0.5
6h
3h
2h
period
1h
40 min.
30 min.
Amplitude
ratio r
frequency →
.1mHz
.2
.3
.4
.5
.6mHz
→ k
10
20
30
40
50

Figure 7A-1

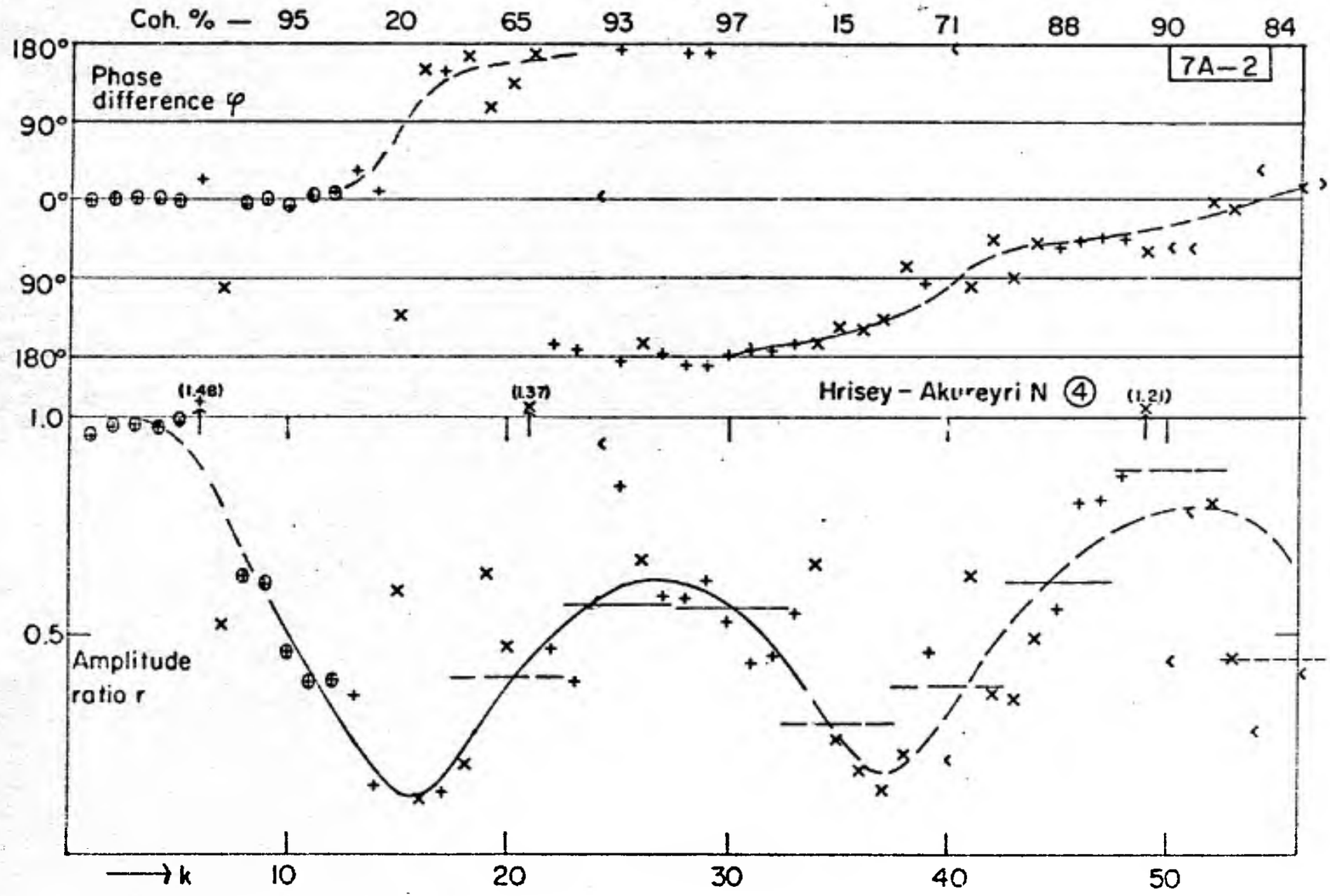
Coh. % — 95 20 65 93 97 15 71 88 90 84
180°
Phase
difference φ
7A—2
90°
0°
90°
180°
(1.48)
(1.37)
Hrisey – Akureyri N ④
(1.21)
1.0
0.5
Amplitude
ratio r
→ k
10
20
30
40
50

Figure 7A-2

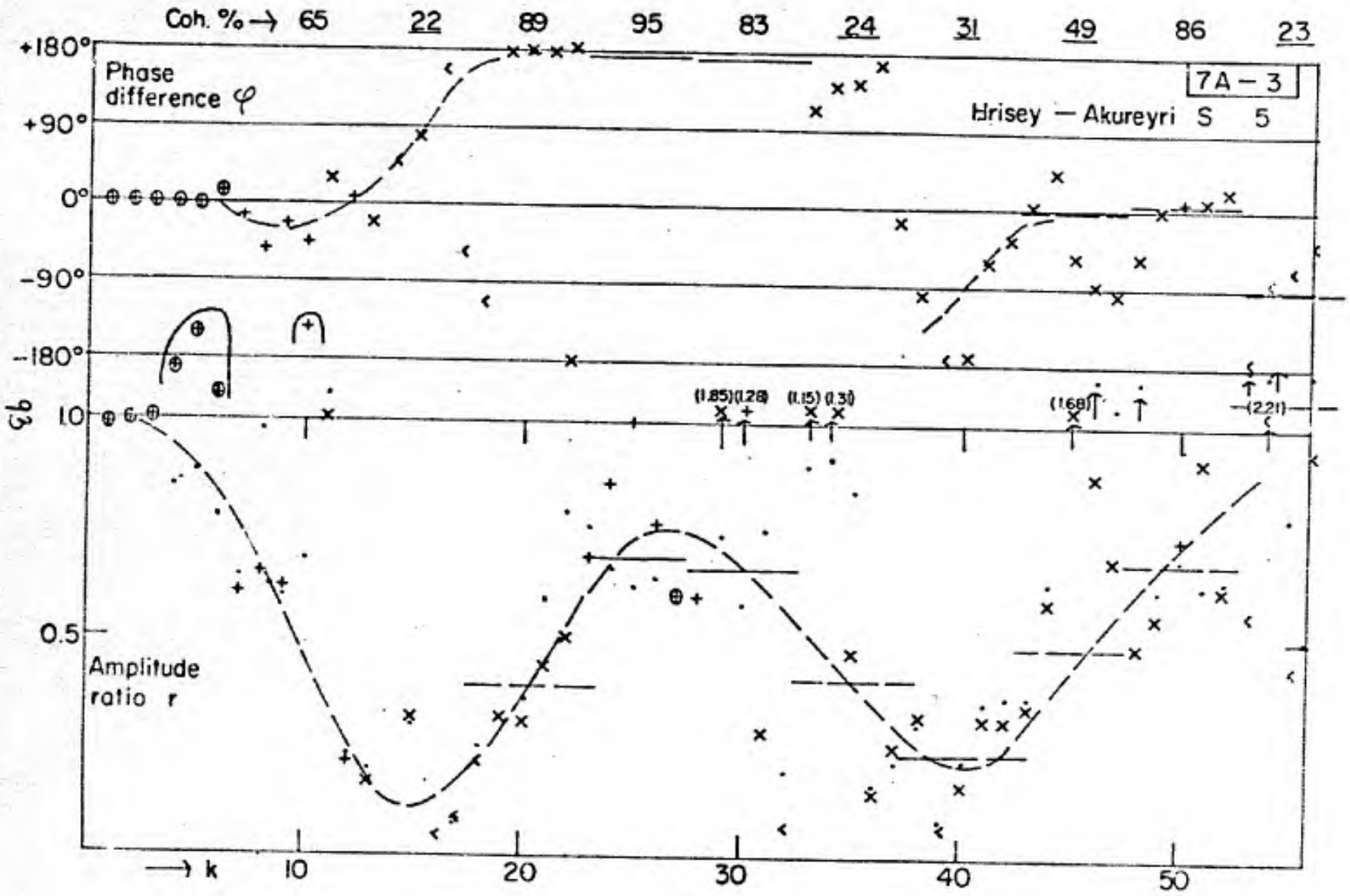
Coh. % → 65 22 89 95 83 24 31 49 86 23
+180°
+90°
0°
-90°
-180°
Phase difference φ
7A – 3
Hrisey — Akureyri S 5
(1.85)(1.28) (1.15) (1.31)
(1.68)
(2.21)
1.0
0.5
Amplitude ratio r
→ k
10
20
30
40
50

Figure 7A-3

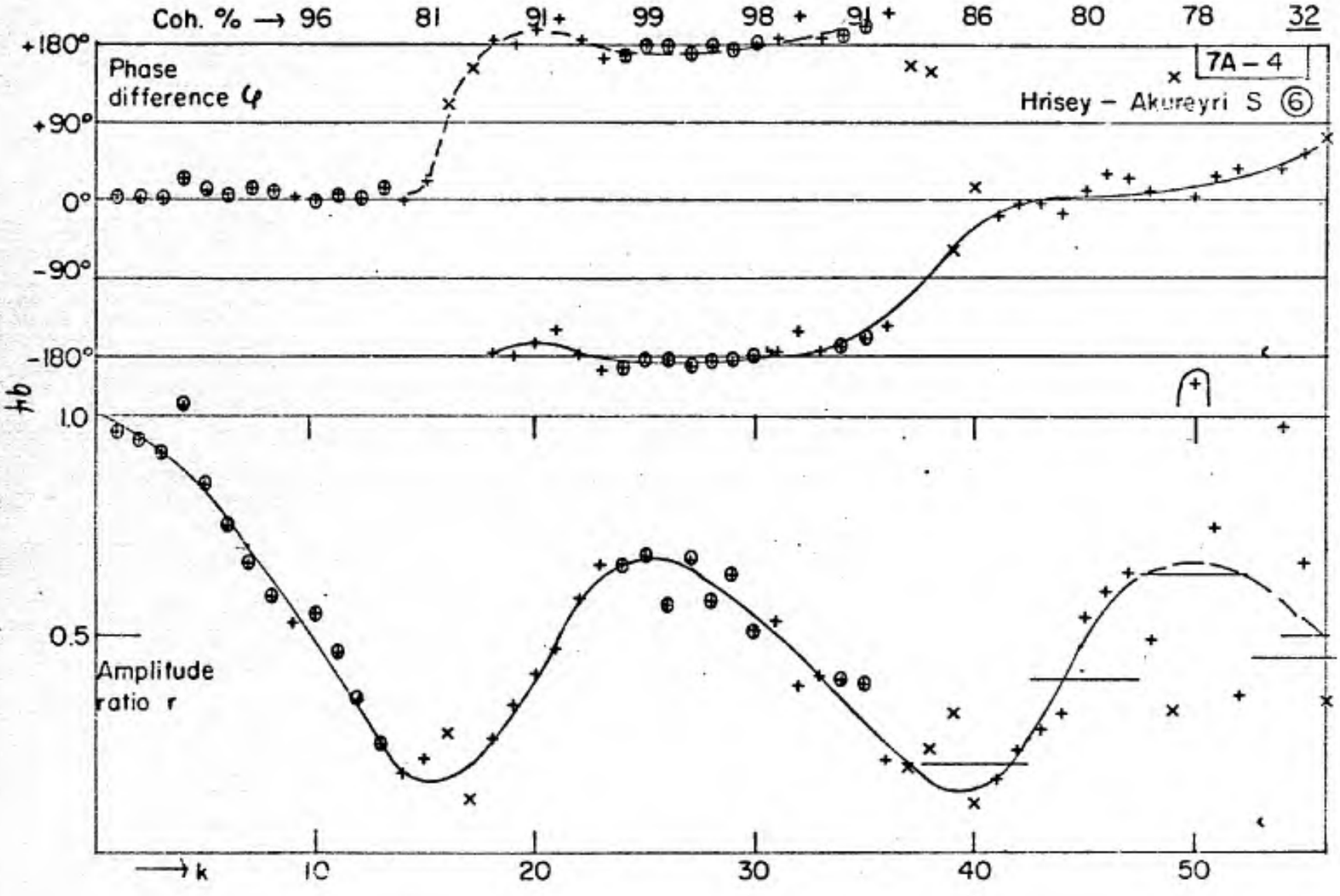
Coh. % → 96 81 91 99 98 91 86 80 78 32
+180°
Phase
difference φ
7A – 4
Hrisey – Akureyri S ⑥
+90°
0°
-90°
-180°
Hb
1.0
0.5
Amplitude
ratio r
→k
10
20
30
40
50

Figure 7A-4

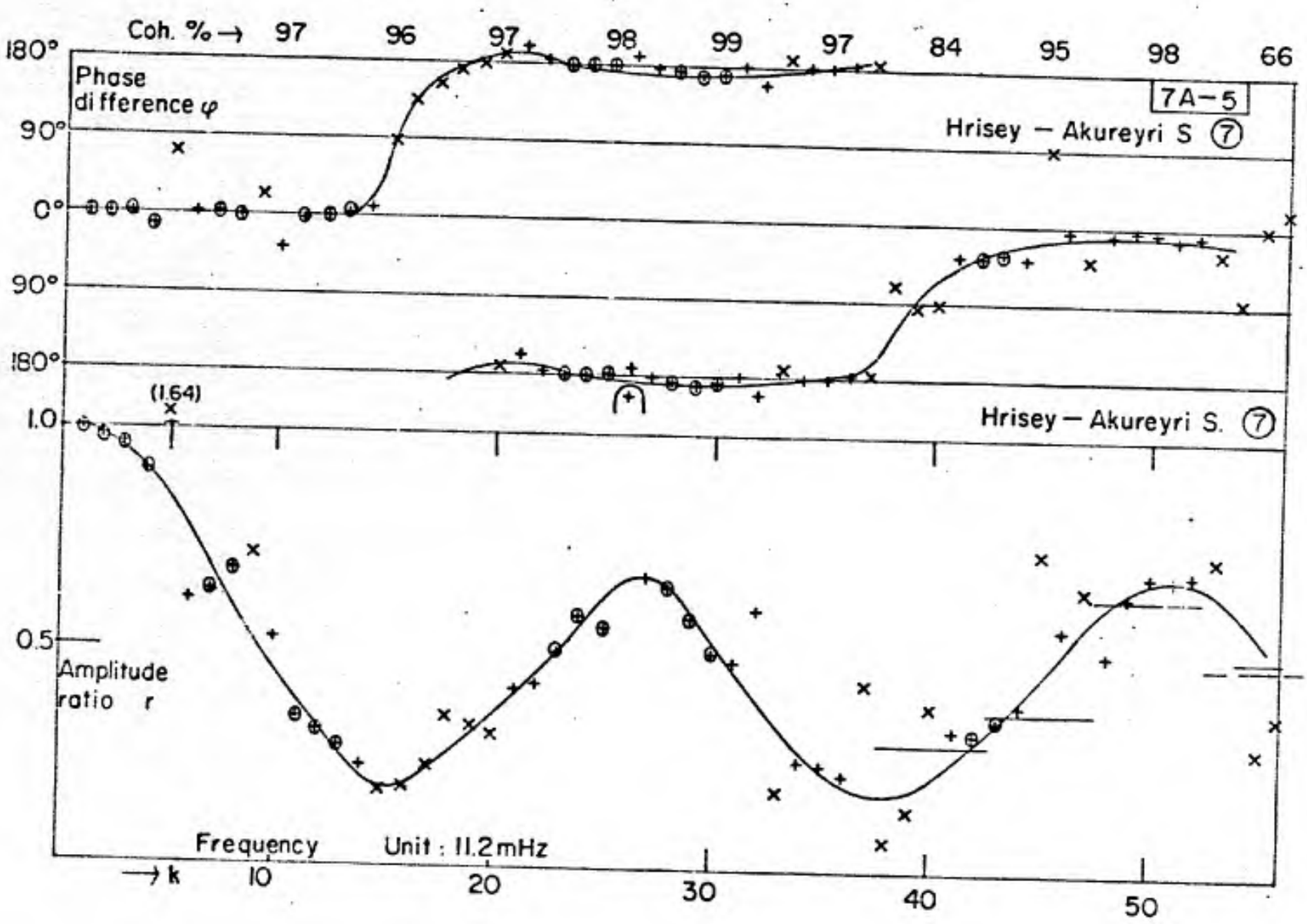
Coh. % →
97
96
97
98
99
97
84
95
98
66
180°
Phase
difference φ
90°
0°
90°
180°
7A-5
Hrisey — Akureyri S ⑦
(1.64)
1.0
Hrisey — Akureyri S. ⑦
0.5
Amplitude
ratio r
Frequency
Unit : 11.2mHz
→ k
10
20
30
40
50

Figure 7A-5

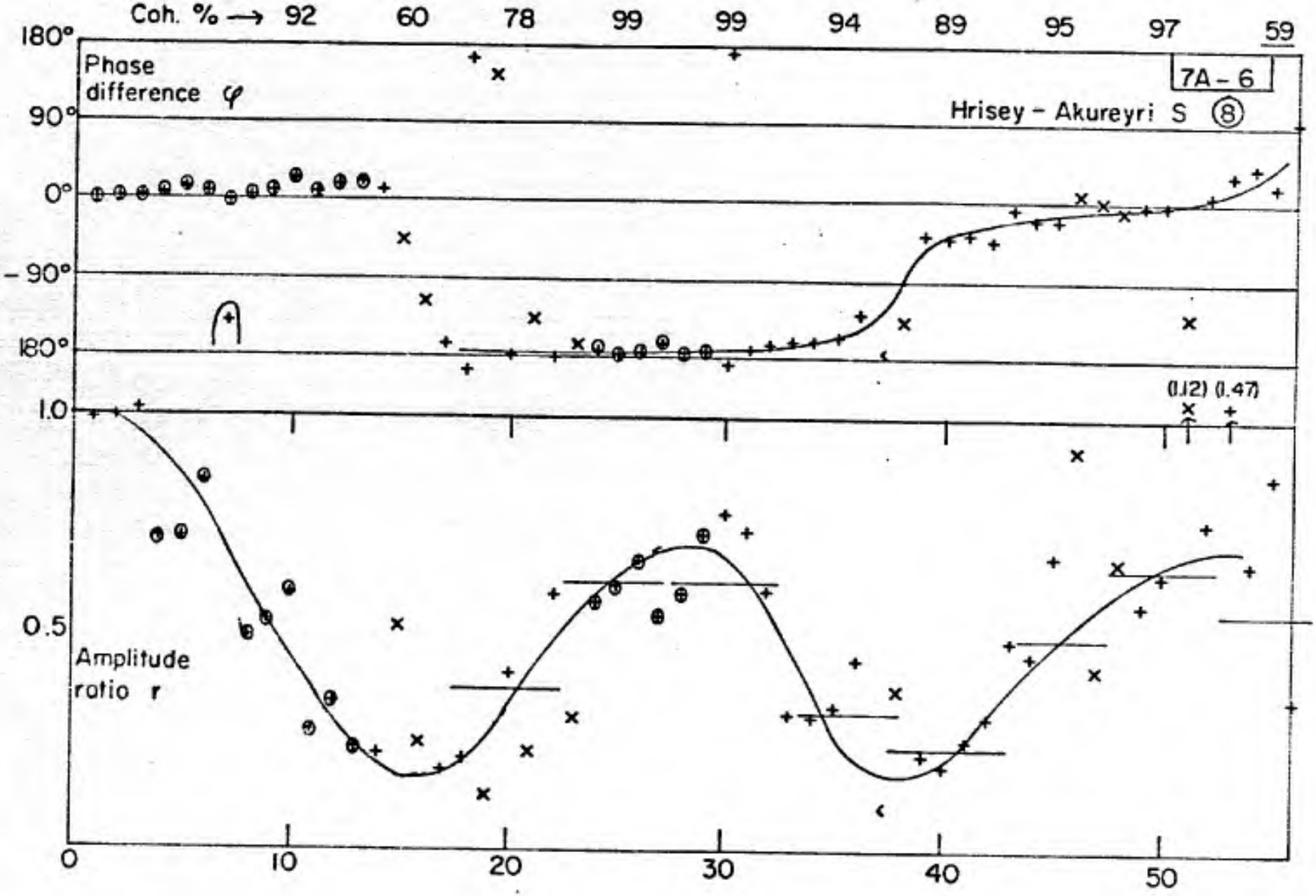
Coh. % → 92 60 78 99 99 94 89 95 97 59
180°
90°
0°
-90°
180°
Phase difference φ
7A - 6
Hrisey - Akureyri S ⑧
(0.12) (0.47)
1.0
0.5
Amplitude ratio r
0
10
20
30
40
50

Figure 7A-6

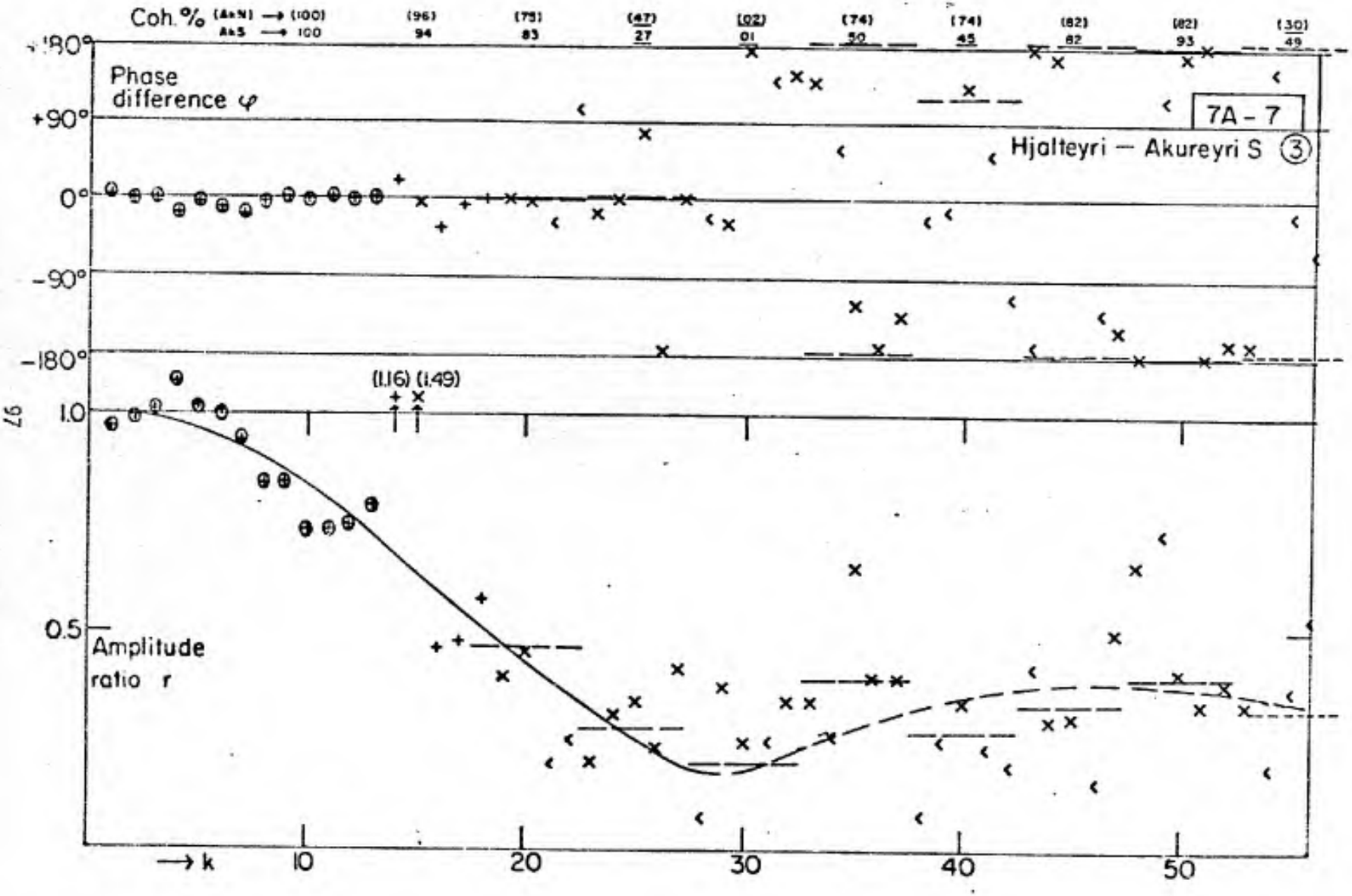
Coh. % (A+N) → (100)
A+S → 100
(96) 94
(75) 83
(47) 27
(02) 01
(74) 50
(74) 45
(82) 82
(82) 93
(30) 49
+180°
+90°
0°
-90°
-180°
Phase difference φ
7A - 7
Hjalteyri — Akureyri S ③
(1.16) (1.49)
1.0
0.5
Amplitude ratio r
→ k
10
20
30
40
50

Figure 7A-7

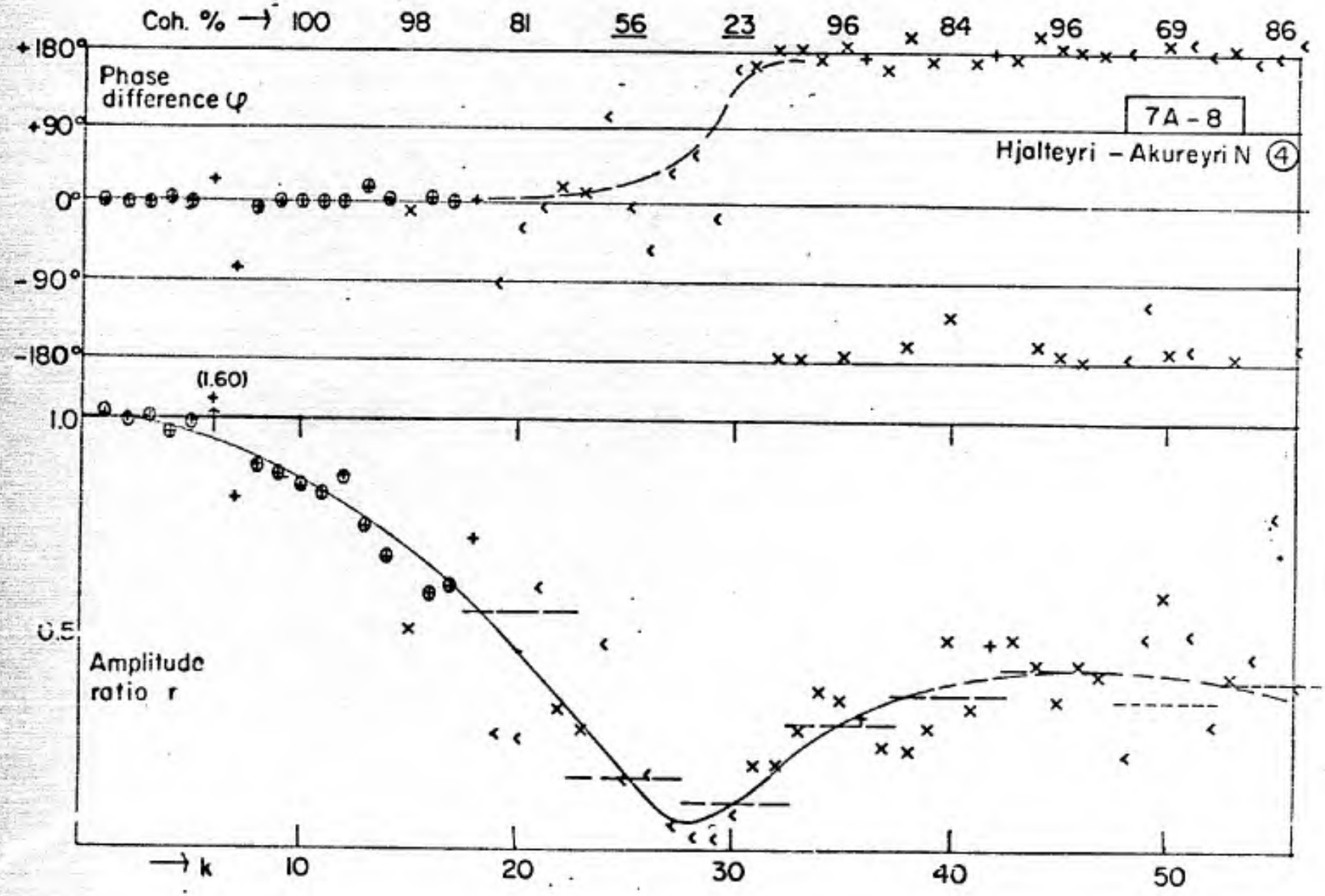
Coh. % → 100 98 81 56 23 96 84 96 69 86
+180°
Phase
difference φ
+90°
0°
-90°
-180°
7A - 8
Hjalteyri – Akureyri N ④
(1.60)
1.0
0.5
Amplitude
ratio r
→ k
10
20
30
40
50

Figure 7A-8

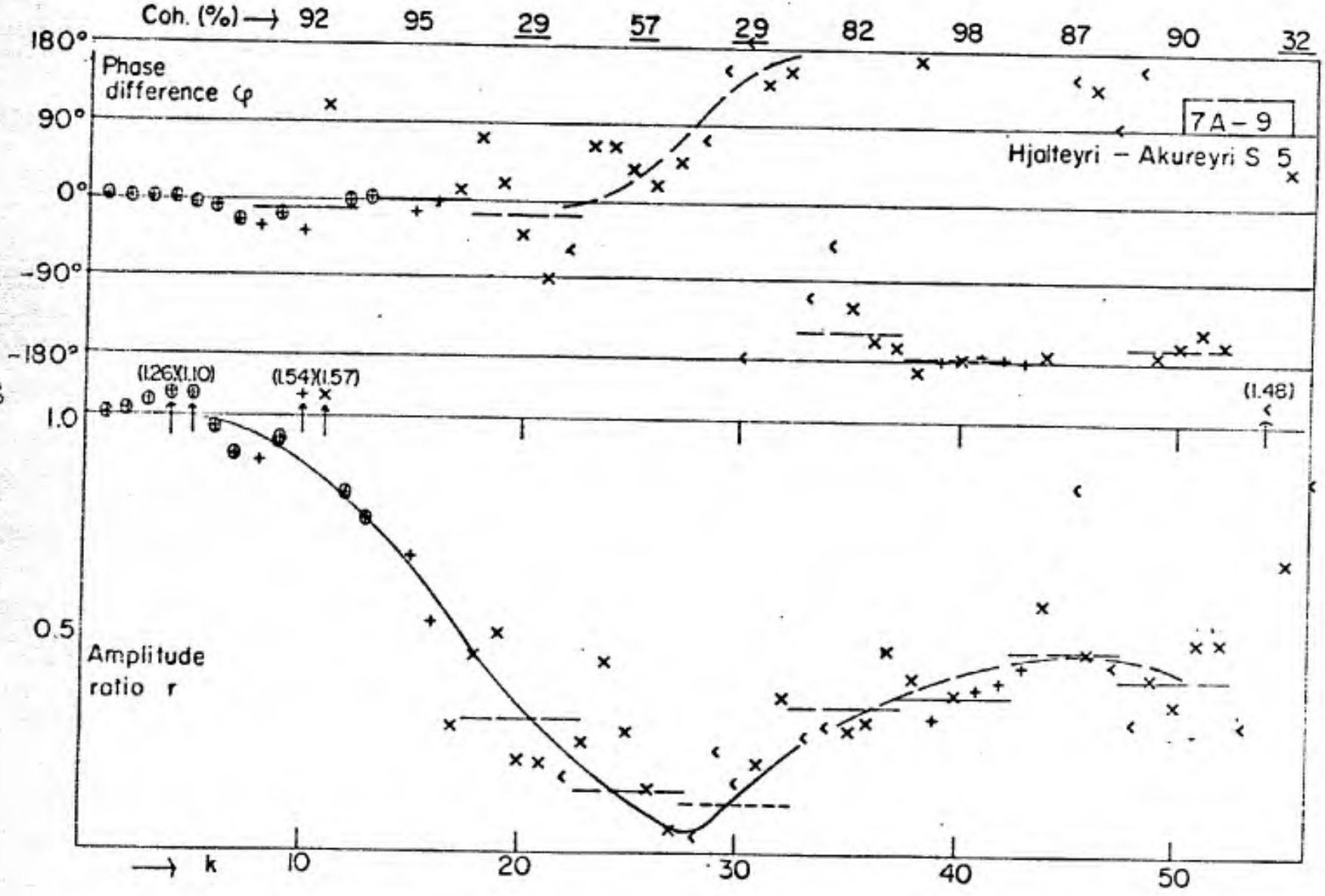
Coh. (%) → 92 95 29 57 29 82 98 87 90 32
180°
Phase difference φ
90°
0°
-90°
-180°
7A-9
Hjalteyri – Akureyri S 5
(1.26X1.10)
(1.54X1.57)
(1.48)
1.0
0.5
Amplitude ratio r
→ k
10
20
30
40
50
99
66

Figure 7A-9

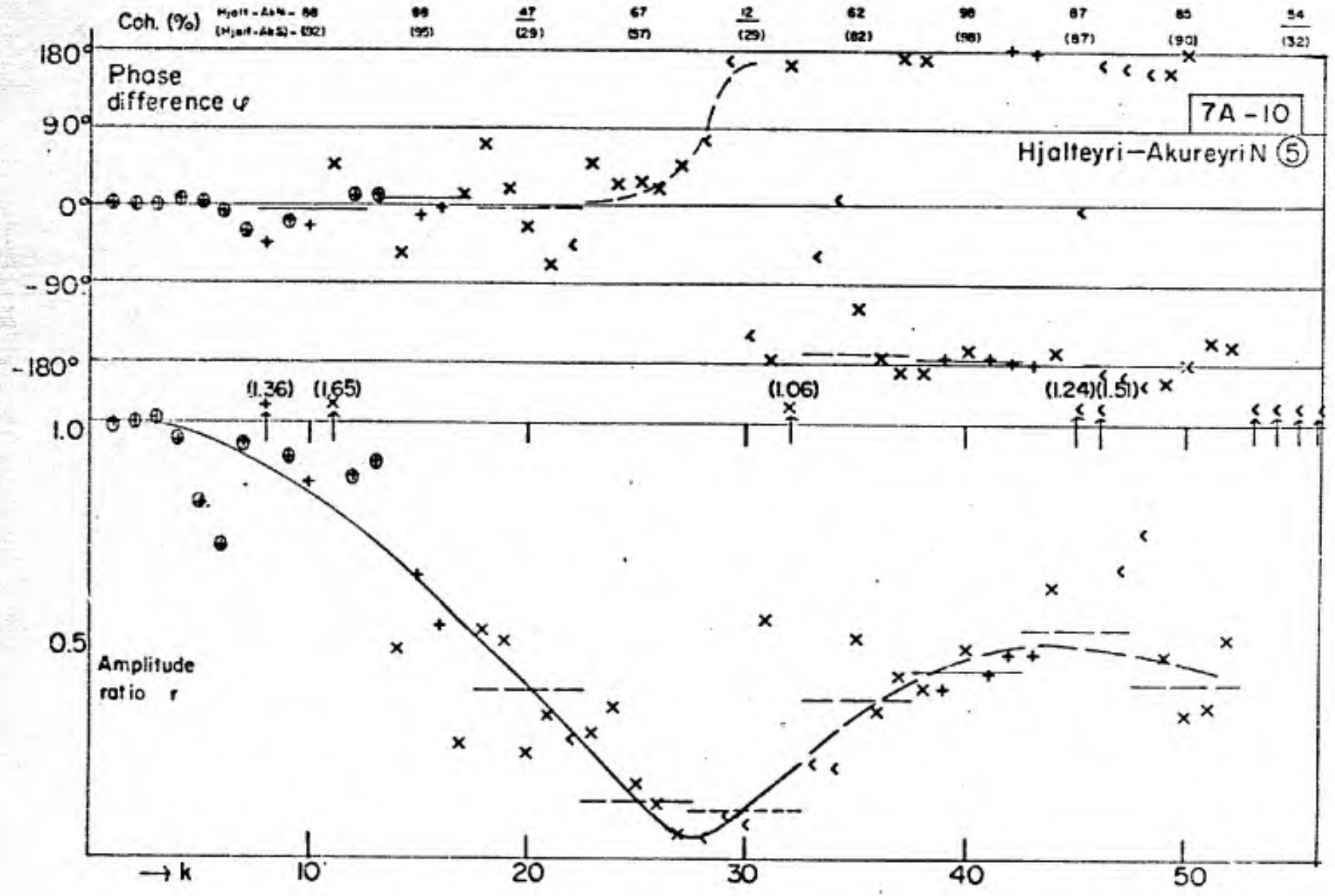
Coh. (%)
88
(95)
47
(29)
67
(57)
12
(29)
62
(82)
98
(98)
87
(97)
85
(90)
54
(32)
180°
Phase
difference φ
90°
0°
-90°
-180°
7A-10
Hjalteyri—Akureyri N ⑤
(1.36)
(1.65)
(1.06)
(1.24)
(1.51)
1.0
0.5
Amplitude
ratio r
→ k
10
20
30
40
50

Figure 7A-10

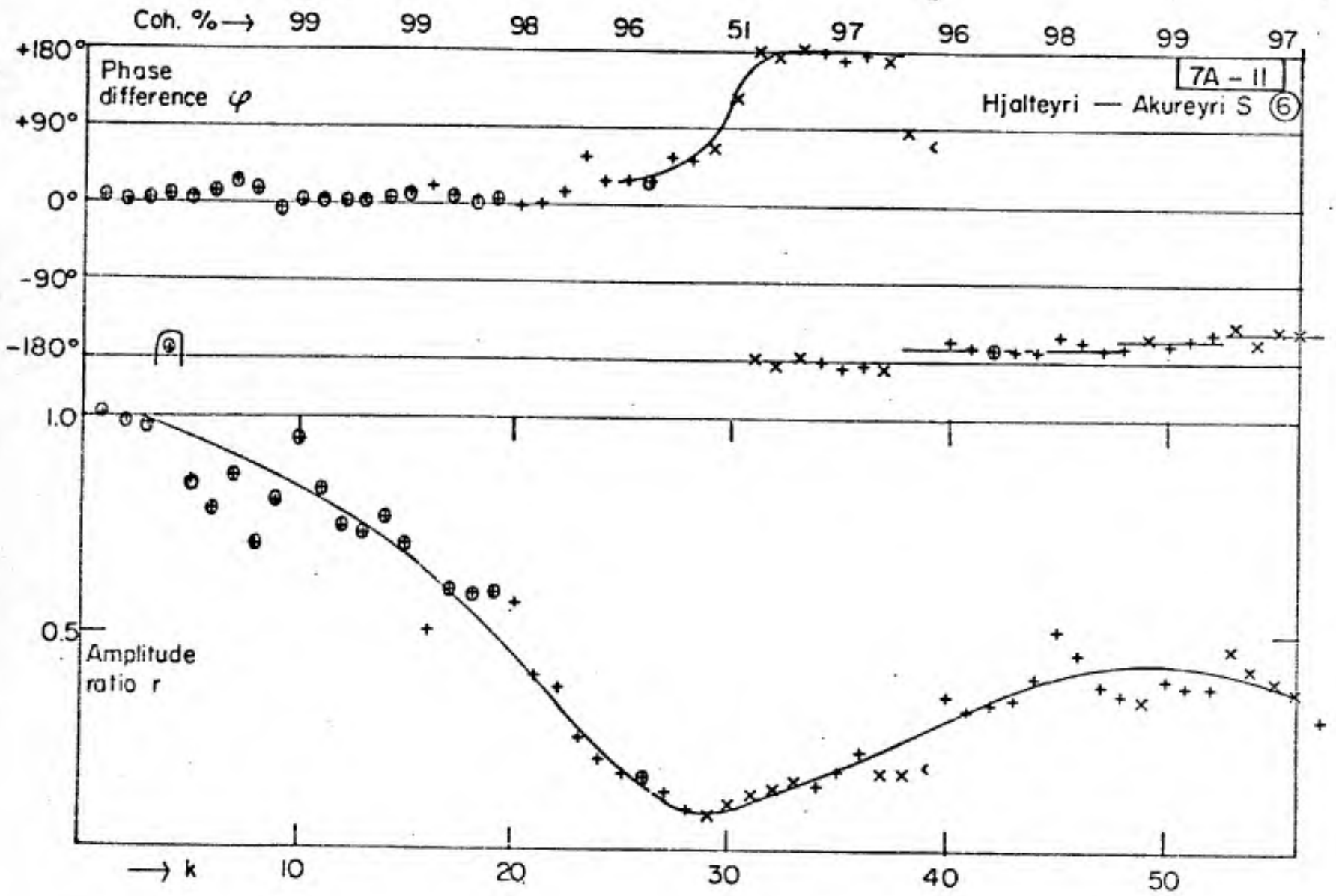
Coh. % →
99
99
98
96
51
97
96
98
99
97
+180°
+90°
0°
-90°
-180°
Phase
difference φ
7A - II
Hjalteyri — Akureyri S ⑥
1.0
0.5
Amplitude
ratio r
→ k
10
20
30
40
50

Figure 7A-11

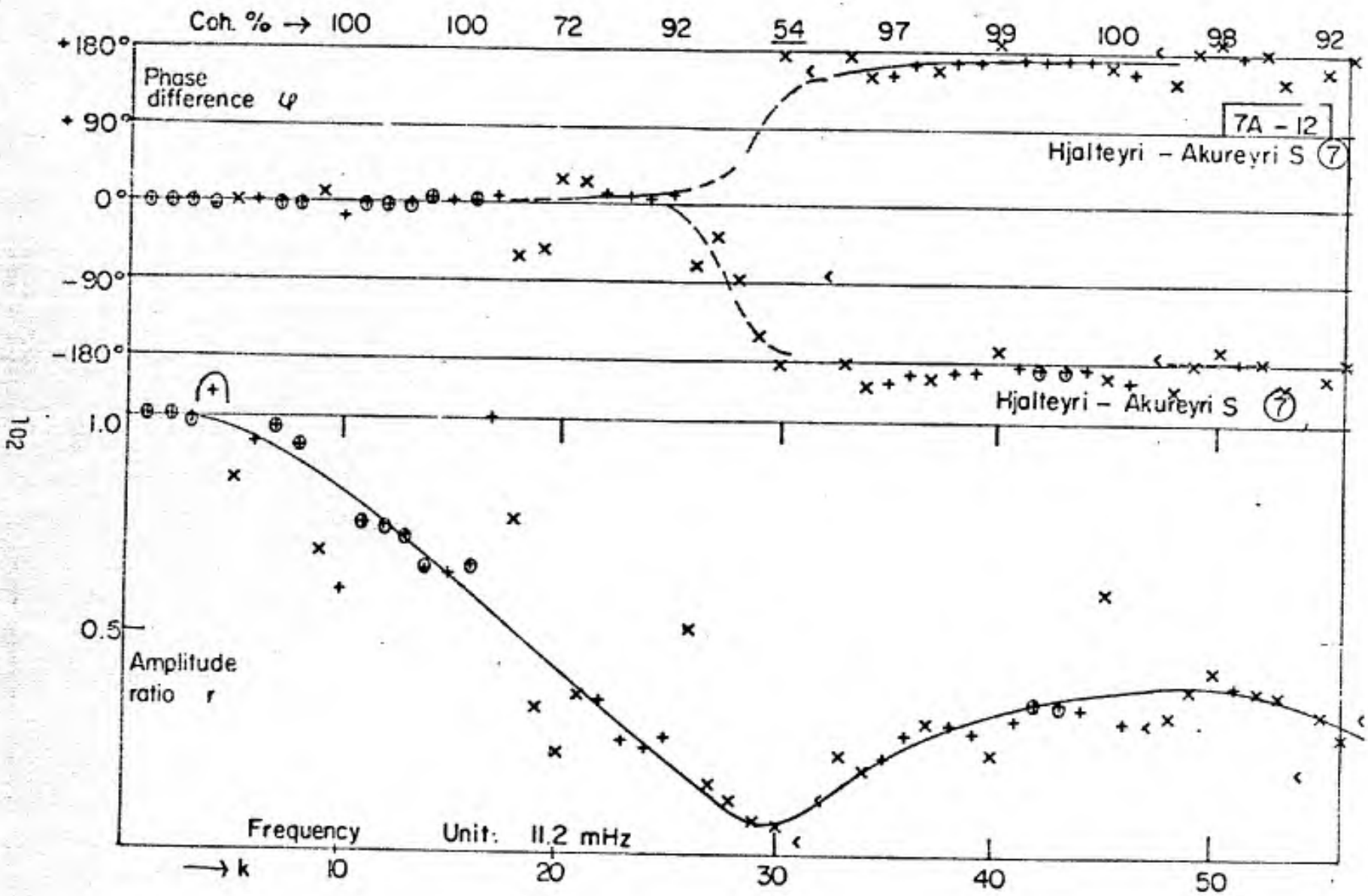
Coh. % → 100 100 72 92 54 97 99 100 98 92
+180°
Phase
difference φ
+ 90°
0°
-90°
-180°
7A - 12
Hjalteyri – Akureyri S (7)
Hjalteyri – Akureyri S (7)
log
1.0
0.5
Amplitude
ratio r
Frequency Unit: 11.2 mHz
→ k
10
20
30
40
50

Figure 7A-12

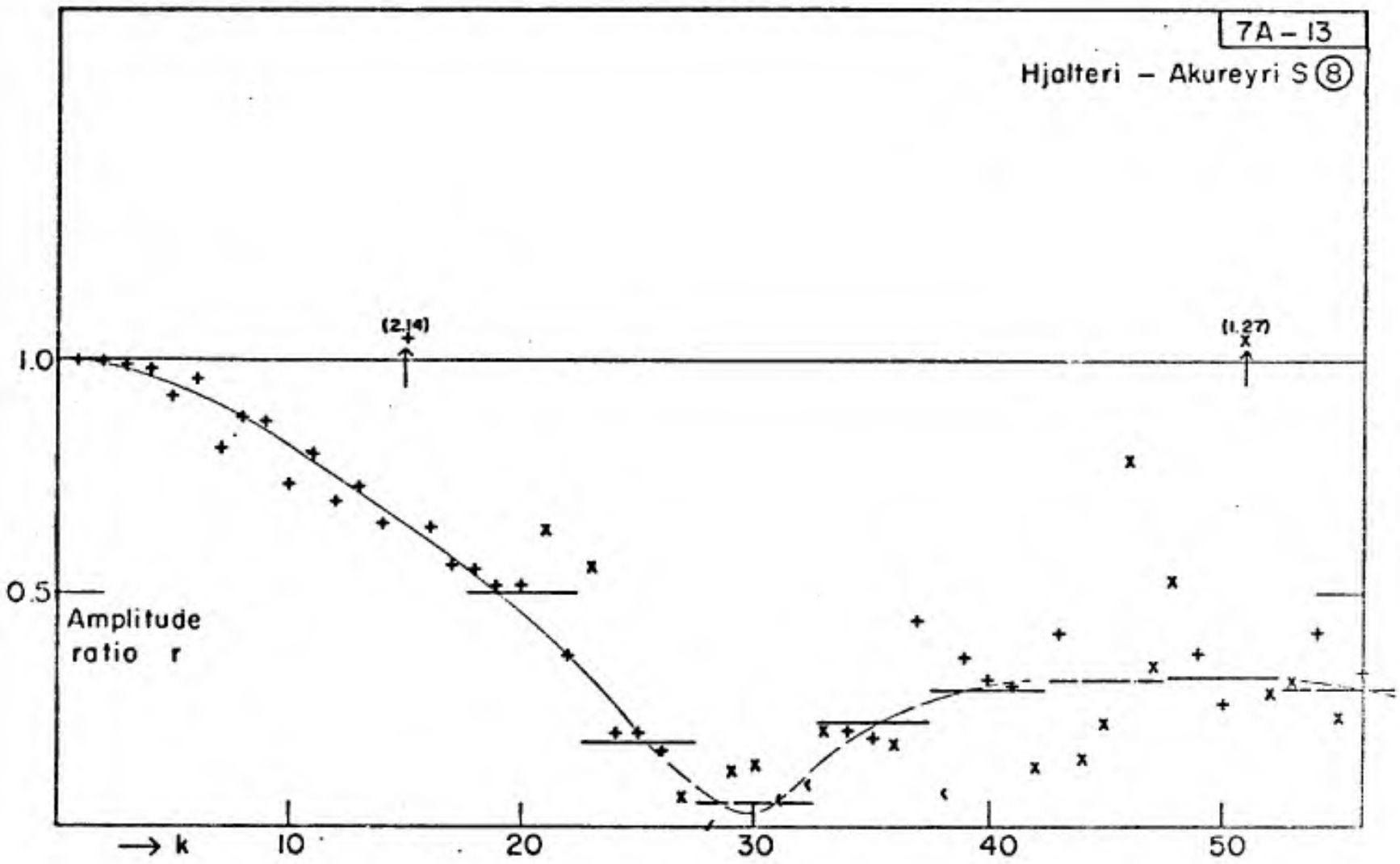
7A – 13
Hjalteri – Akureyri S ⑧
(2.14)
(1.27)
1.0
0.5
Amplitude
ratio r
→ k
10
20
30
40
50

Figure 7A-13

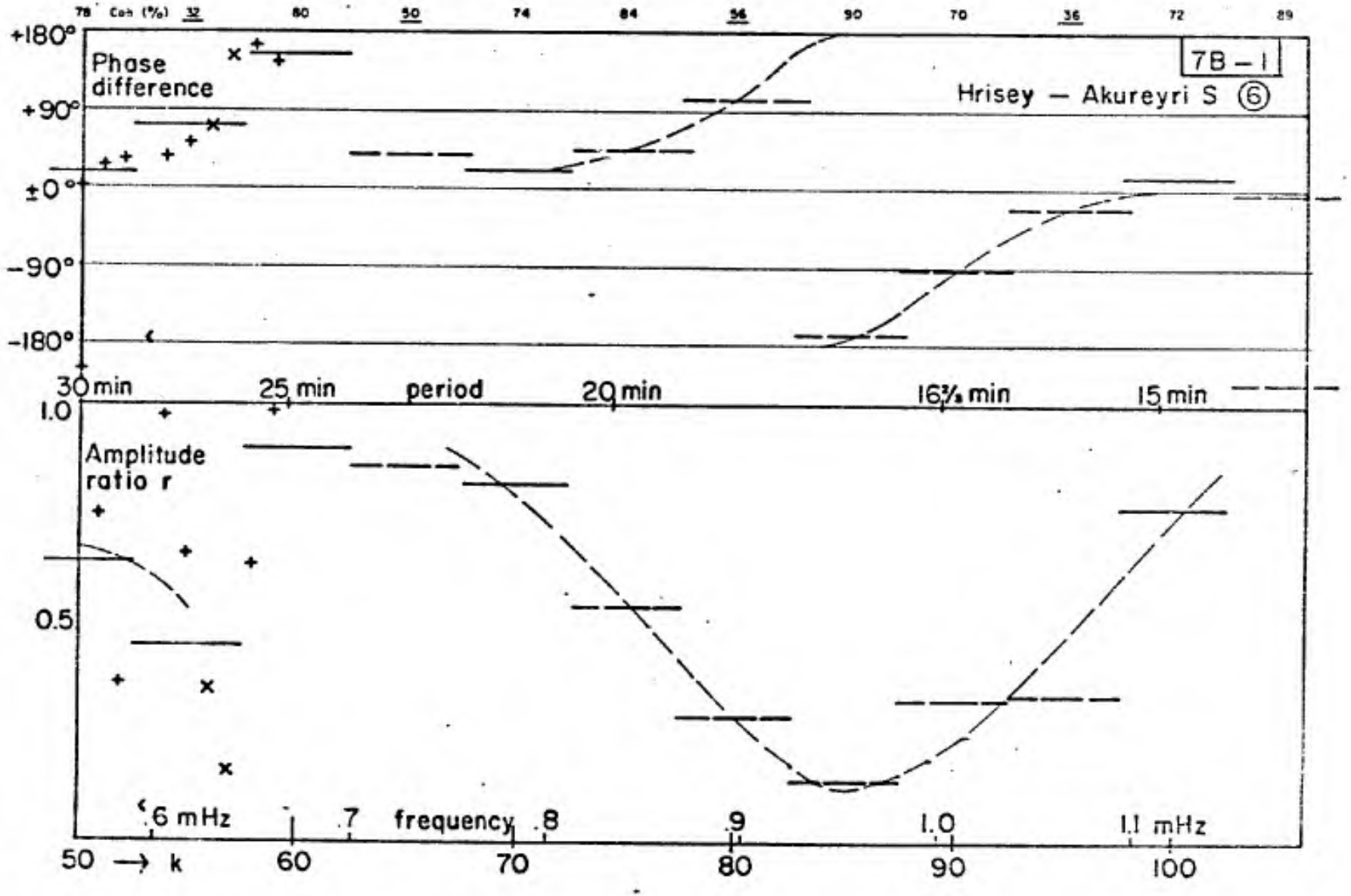
Coh (%) 32 80 50 74 84 56 90 70 36 72 89
+180°
+90°
±0°
-90°
-180°
Phase difference
7B – 1
Hrisey — Akureyri S ⑥
30 min
25 min
period
20 min
16⅔ min
15 min
1.0
0.5
Amplitude ratio r
.6 mHz
.7
frequency
.8
.9
1.0
1.1 mHz
50 → k
60
70
80
90
100

Figure 7B-1

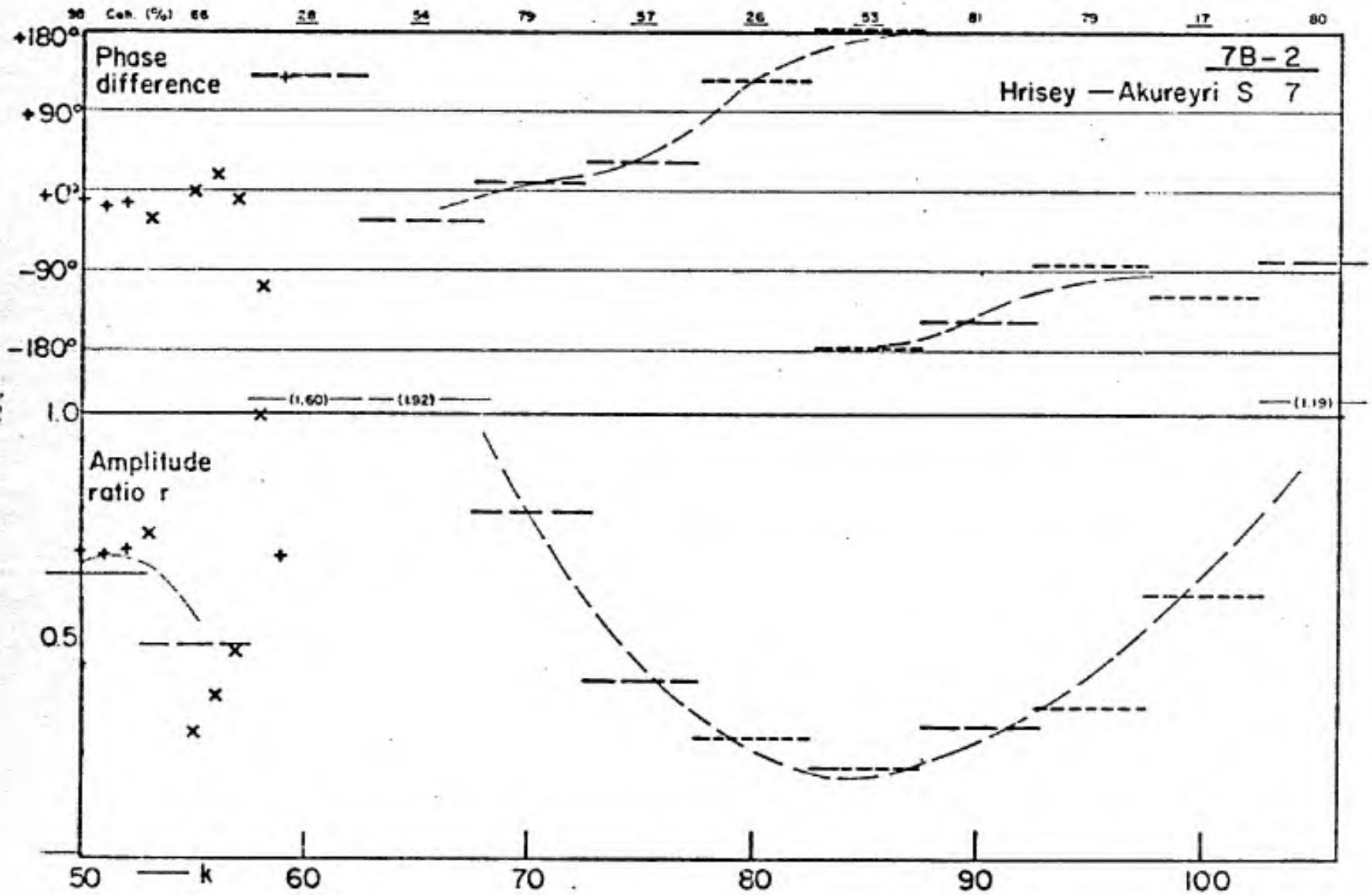
Coh. (%)
Phase difference
7B-2
Hrisey — Akureyri S 7
+180°
+90°
+0°
-90°
-180°
(1.60)
(1.92)
(1.19)
1.0
Amplitude ratio r
0.5
50
k
60
70
80
90
100

Figure 7B-2

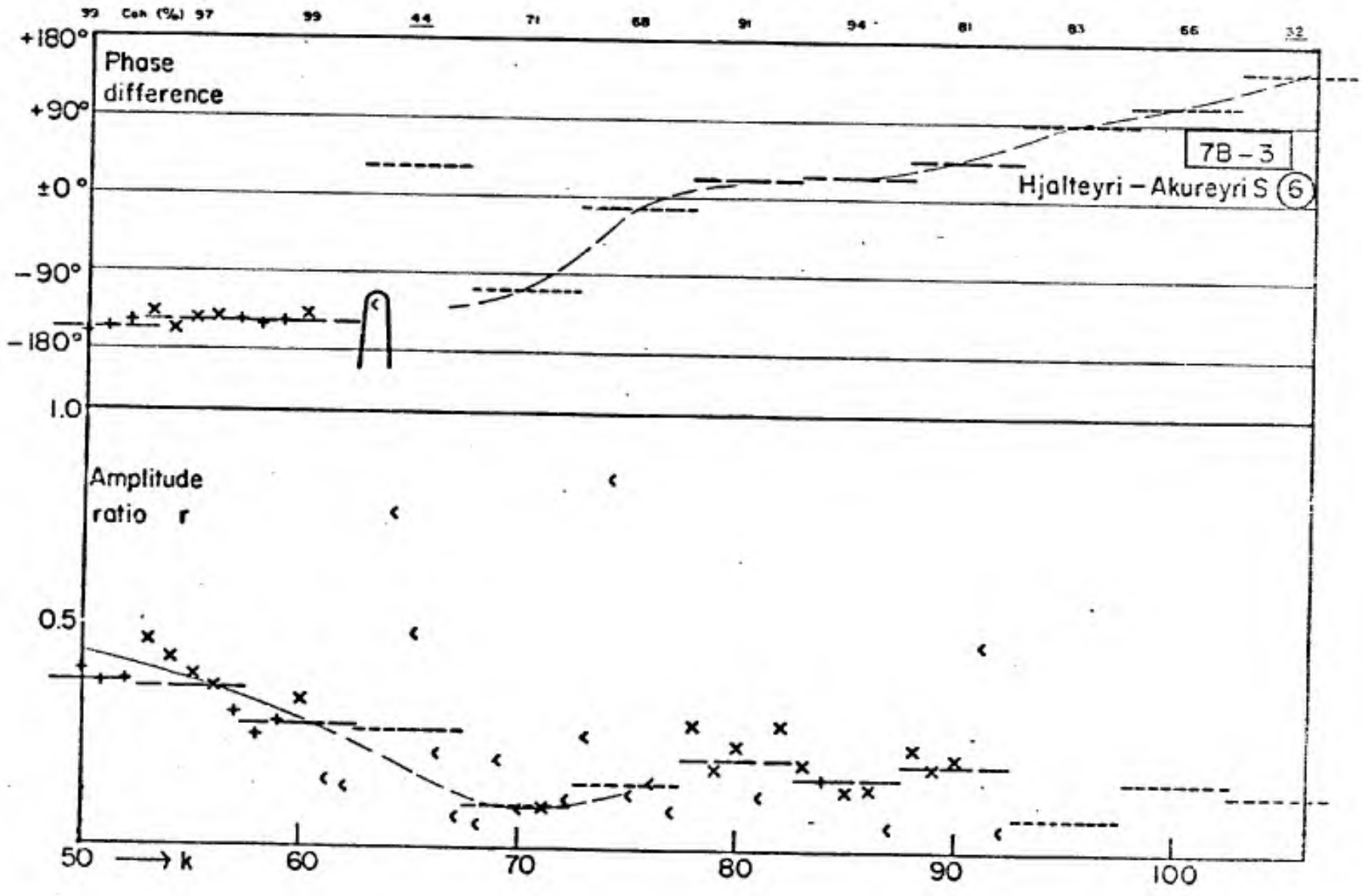
Con (%) 97 99 44 71 68 91 94 81 83 66 32
+180°
Phase
difference
+90°
±0°
-90°
-180°
7B-3
Hjalteyri – Akureyri S (6)
1.0
Amplitude
ratio r
0.5
50 → k
60
70
80
90
100

Figure 7B-3

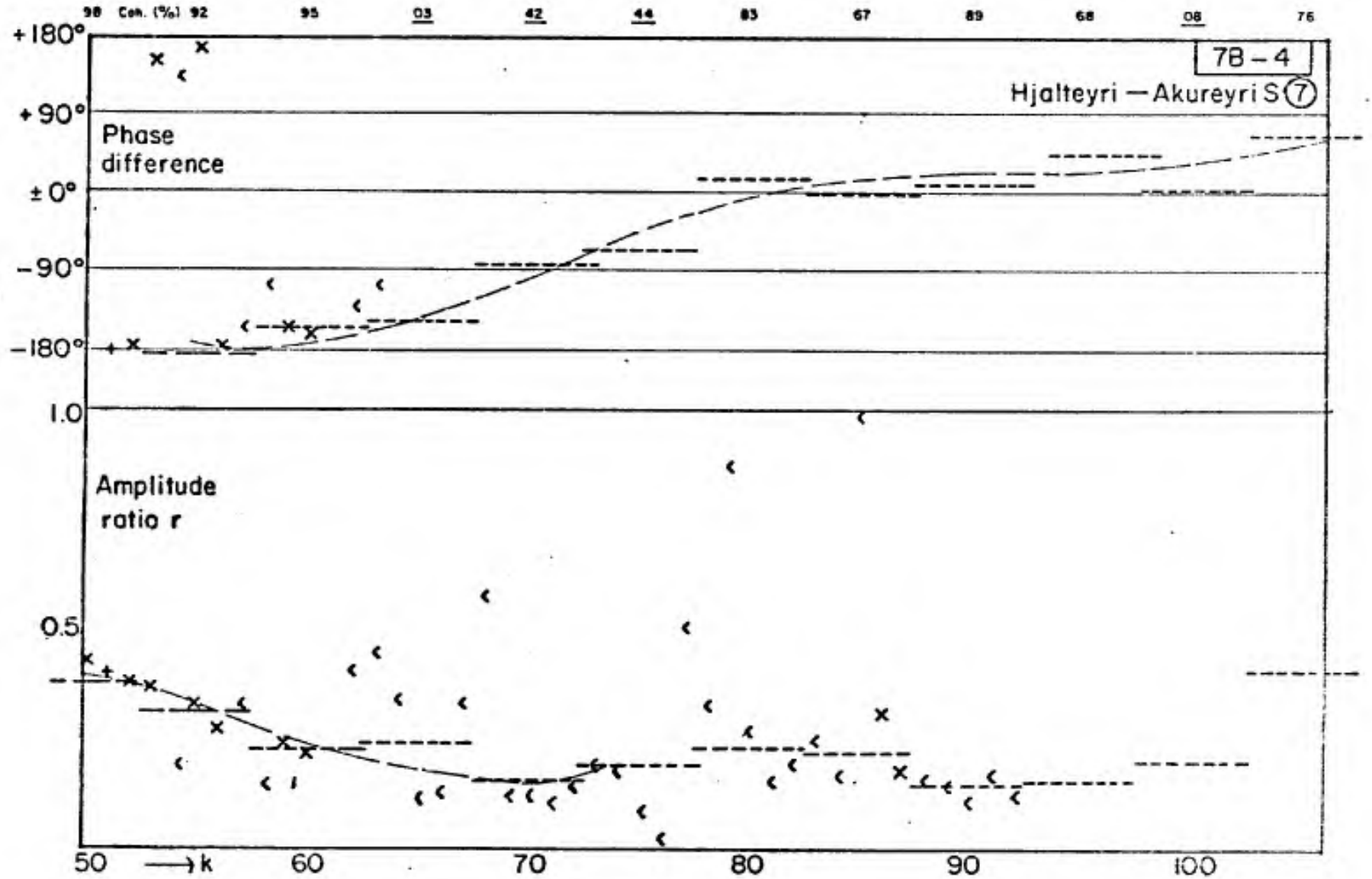
98 Con. (%) 92
95
03
42
44
83
67
89
68
08
76
+180°
+90°
Phase
difference
±0°
-90°
-180°
1.0
Amplitude
ratio r
0.5
7B-4
Hjalteyri — Akureyri S⑦
50
→k
60
70
80
90
100

Figure 7B-4

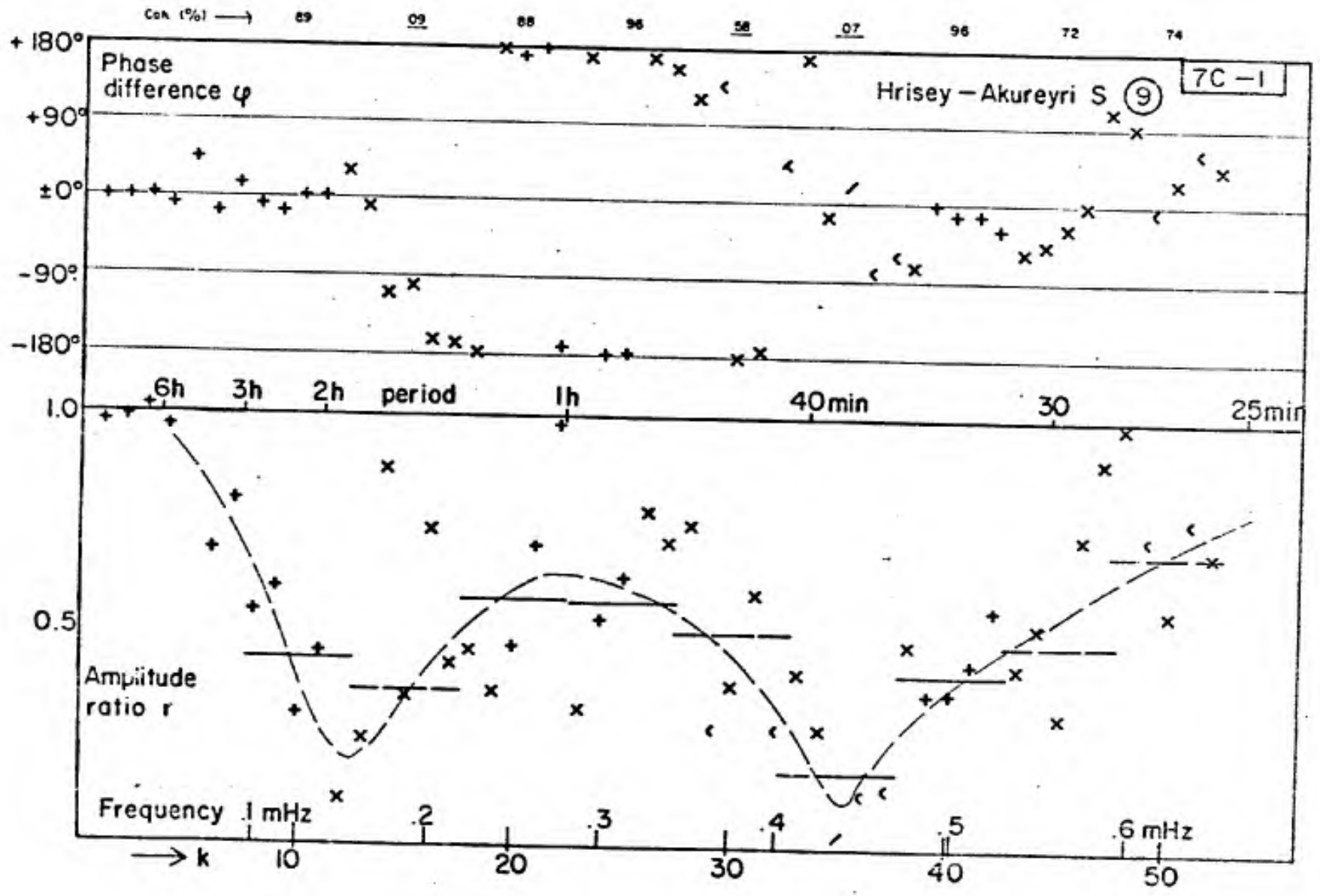
Coh (%) → 69 09 88 96 58 07 96 72 74
+180°
Phase
difference φ
Hrisey – Akureyri S (9)
7C –1
+90°
±0°
-90°
-180°
6h 3h 2h period 1h 40min 30 25min
1.0
0.5
Amplitude
ratio r
Frequency .1 mHz .2 .3 .4 .5 .6 mHz
→ k 10 20 30 40 50

Figure 7C-1

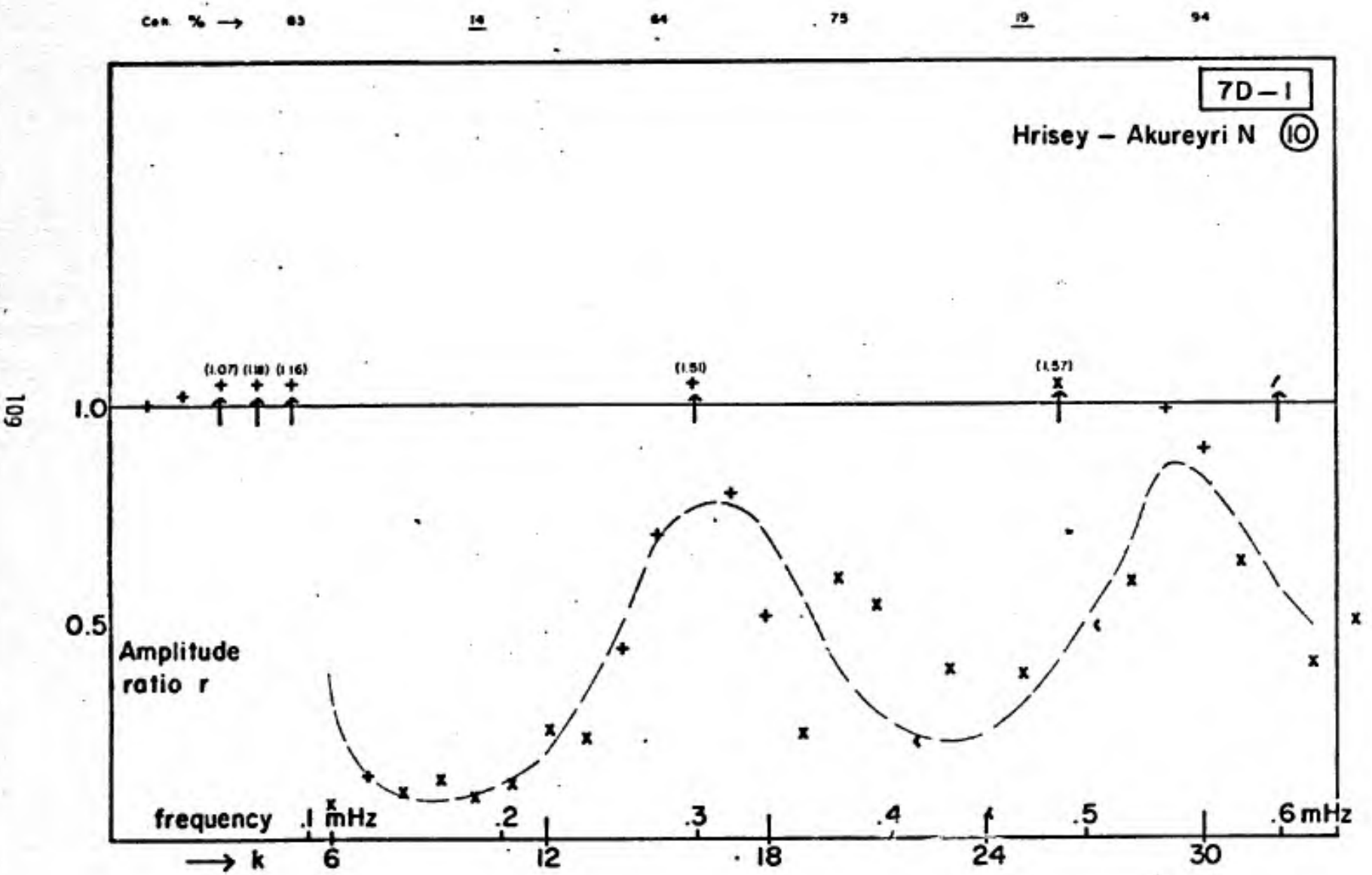
Con. % →
83
14
64
75
19
94
7D–1
Hrisey – Akureyri N
10
(1.07) (1.18) (1.16)
(1.50)
(1.57)
1.0
0.5
Amplitude ratio r
frequency
.1 mHz
.2
.3
.4
.5
.6 mHz
→ k
6
12
18
24
30

Figure 7D-1

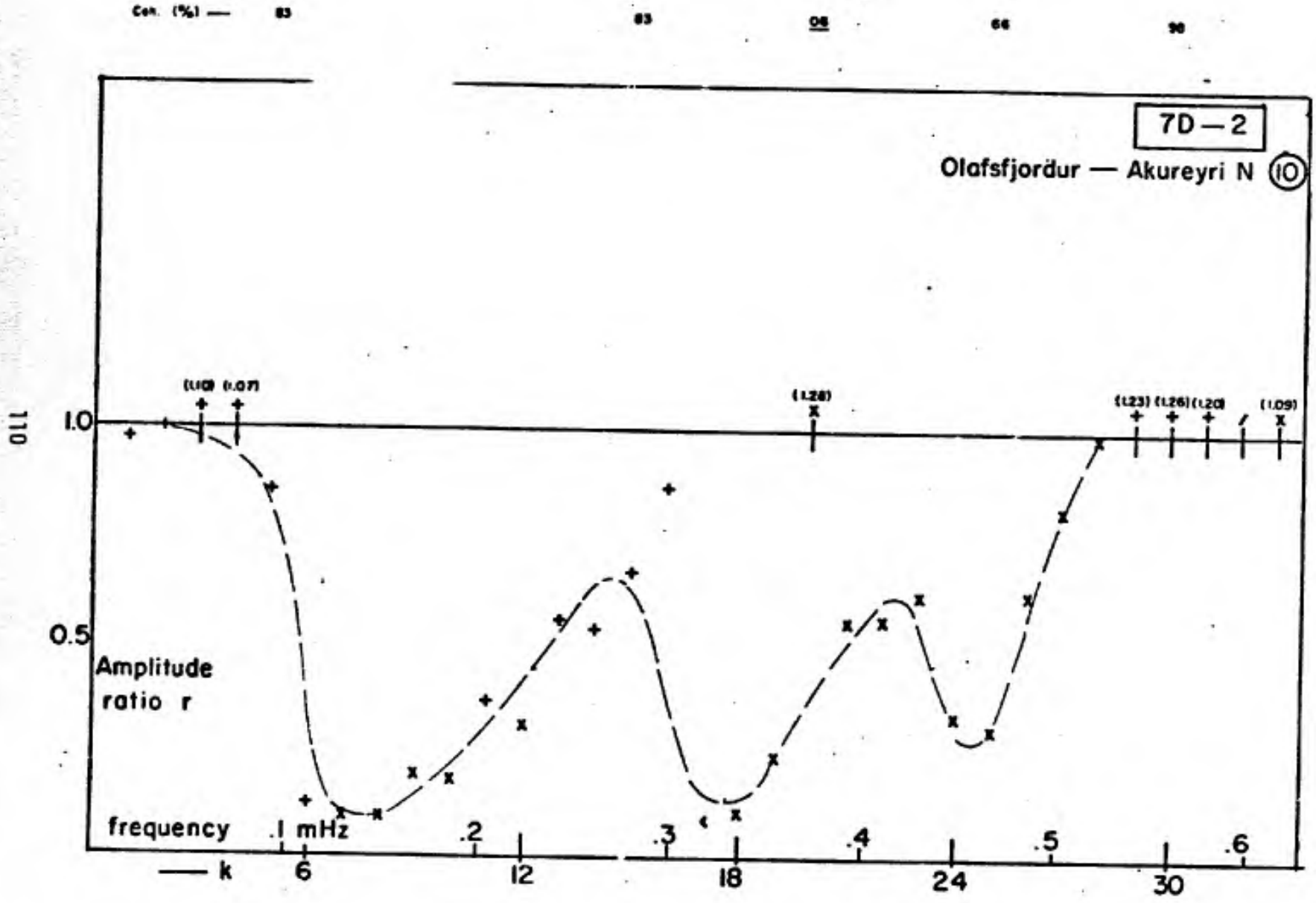
7D—2
Olafsfjordur — Akureyri N (10)
110
1.0
0.5
Amplitude
ratio r
frequency .1 mHz .2 .3 .4 .5 .6
— k 6 12 18 24 30

Figure 7D-2

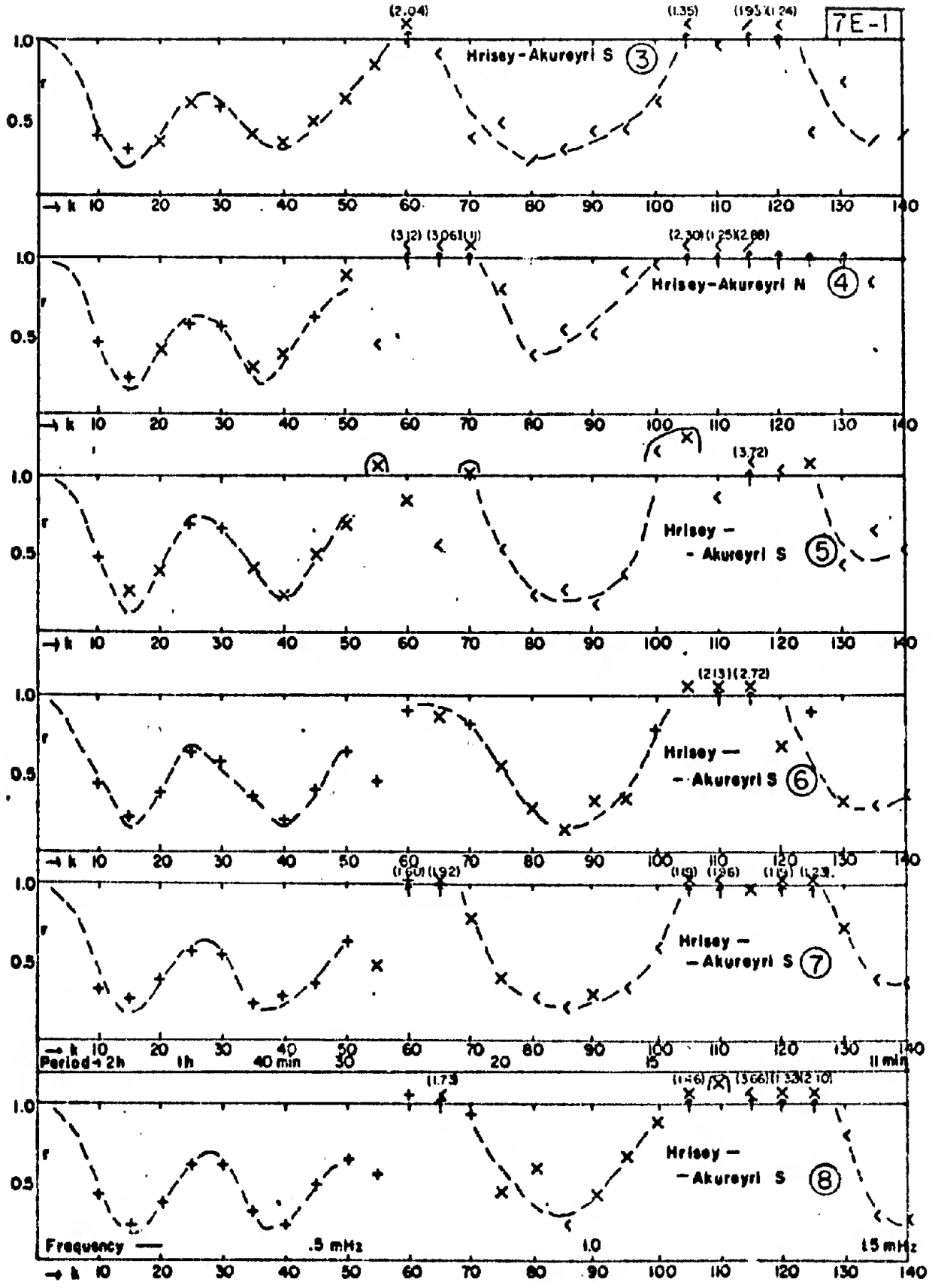
7E-1
Hrisey-Akureyri S ③
Hrisey-Akureyri N ④
Hrisey – Akureyri S ⑤
Hrisey – Akureyri S ⑥
Hrisey – Akureyri S ⑦
Hrisey – Akureyri S ⑧
r
k
Period → 2h
1h
40 min
30
20
15
11 min
Frequency —
.5 mHz
1.0
1.5 mHz

Figure 7E-1

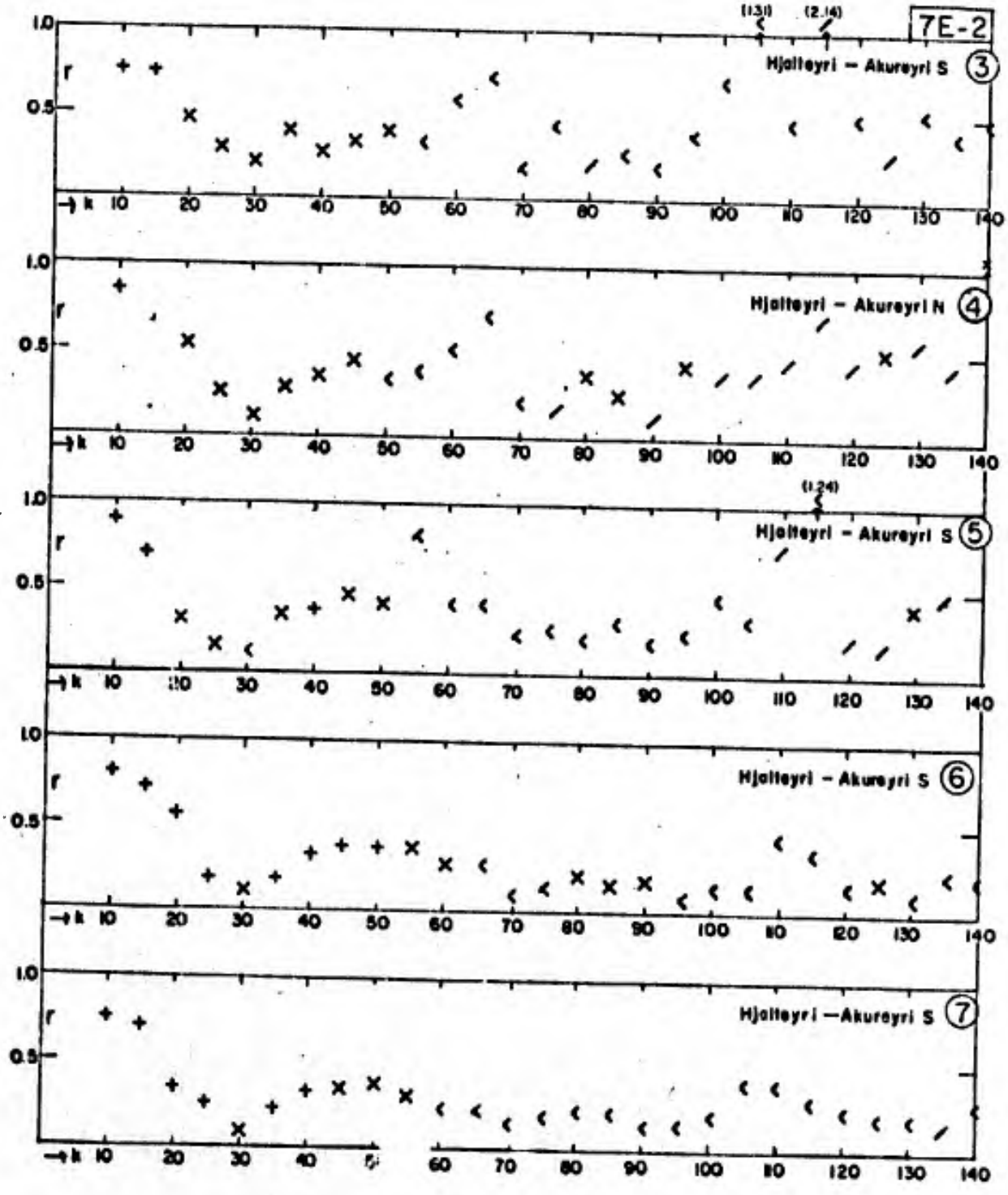
7E-2
(1.31)
(2.14)
Hjalteyri – Akureyri S ③
Hjalteyri – Akureyri N ④
(1.24)
Hjalteyri – Akureyri S ⑤
Hjalteyri – Akureyri S ⑥
Hjalteyri –Akureyri S ⑦
r
k
1.0
0.5
10
20
30
40
50
60
70
80
90
100
110
120
130
140

Figure 7E-2

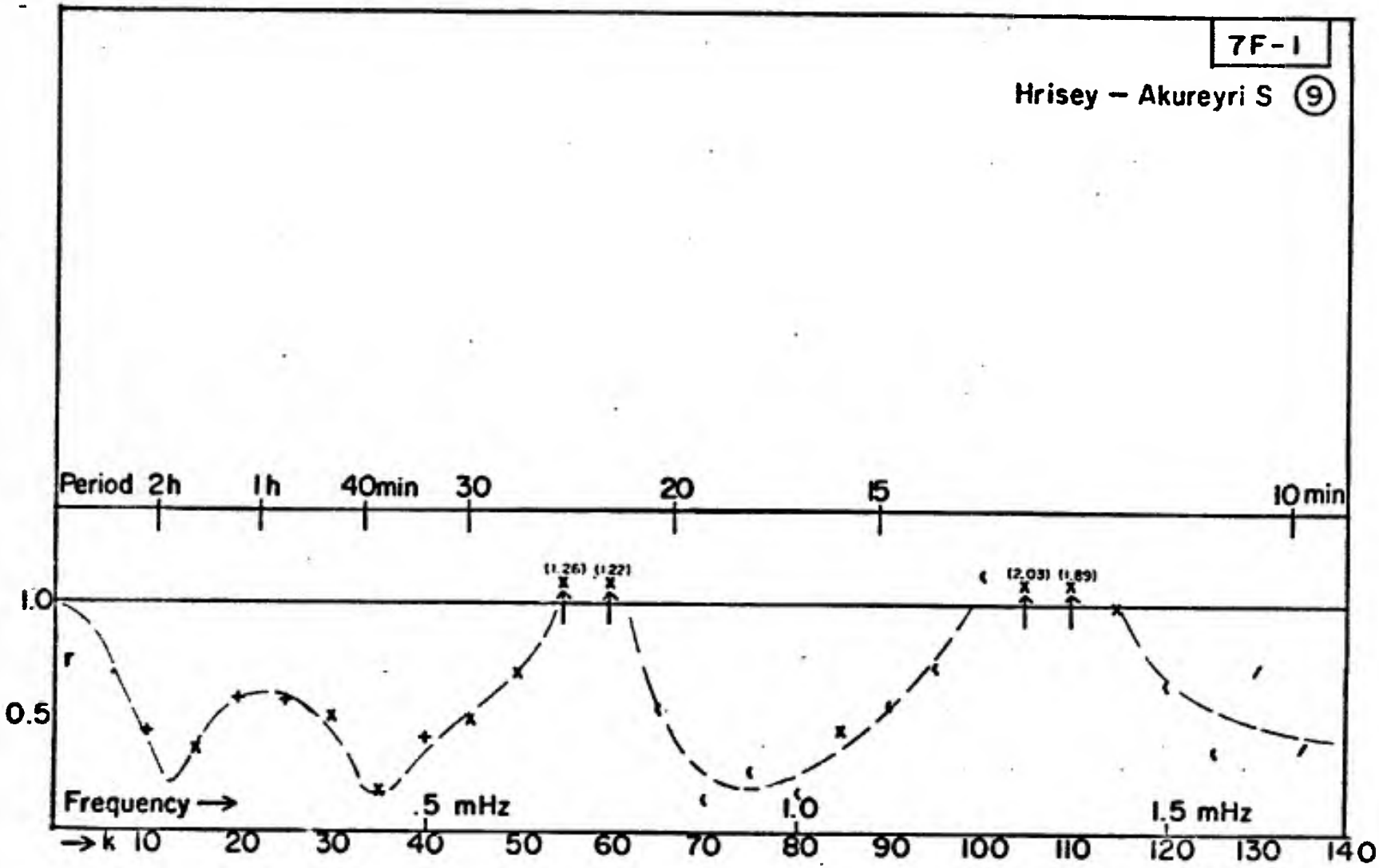
7F-1
Hrisey – Akureyri S (9)
Period 2h
1h
40min
30
20
15
10min
(1.26) (1.22)
(2.03) (1.89)
1.0
0.5
r
Frequency →
.5 mHz
1.0
1.5 mHz
→k 10
20
30
40
50
60
70
80
90
100
110
120
130
140

Figure 7F-1

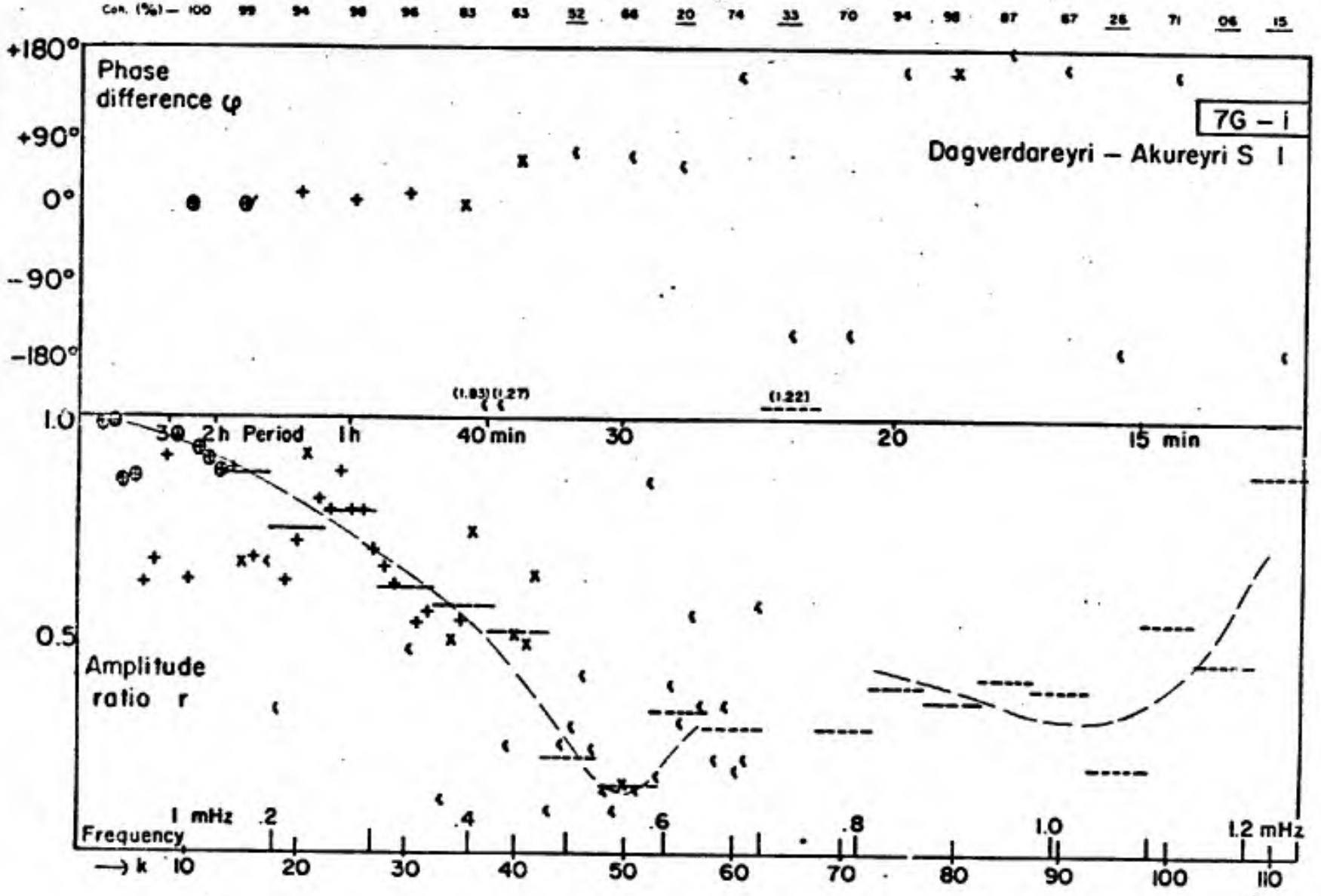
Coh. (%) — 100 99 94 98 96 83 63 52 66 20 74 33 70 94 98 87 87 25 71 06 15
+180°
Phase
difference φ
7G – i
Dagverdareyri – Akureyri S I
+90°
0°
-90°
-180°
(1.83) (1.27)
(1.22)
1.0
2h Period 1h
40 min
30
20
15 min
0.5
Amplitude
ratio r
1 mHz .2 .4 .6 .8 1.0 1.2 mHz
Frequency
→ k 10 20 30 40 50 60 70 80 90 100 110

Figure 7G-1

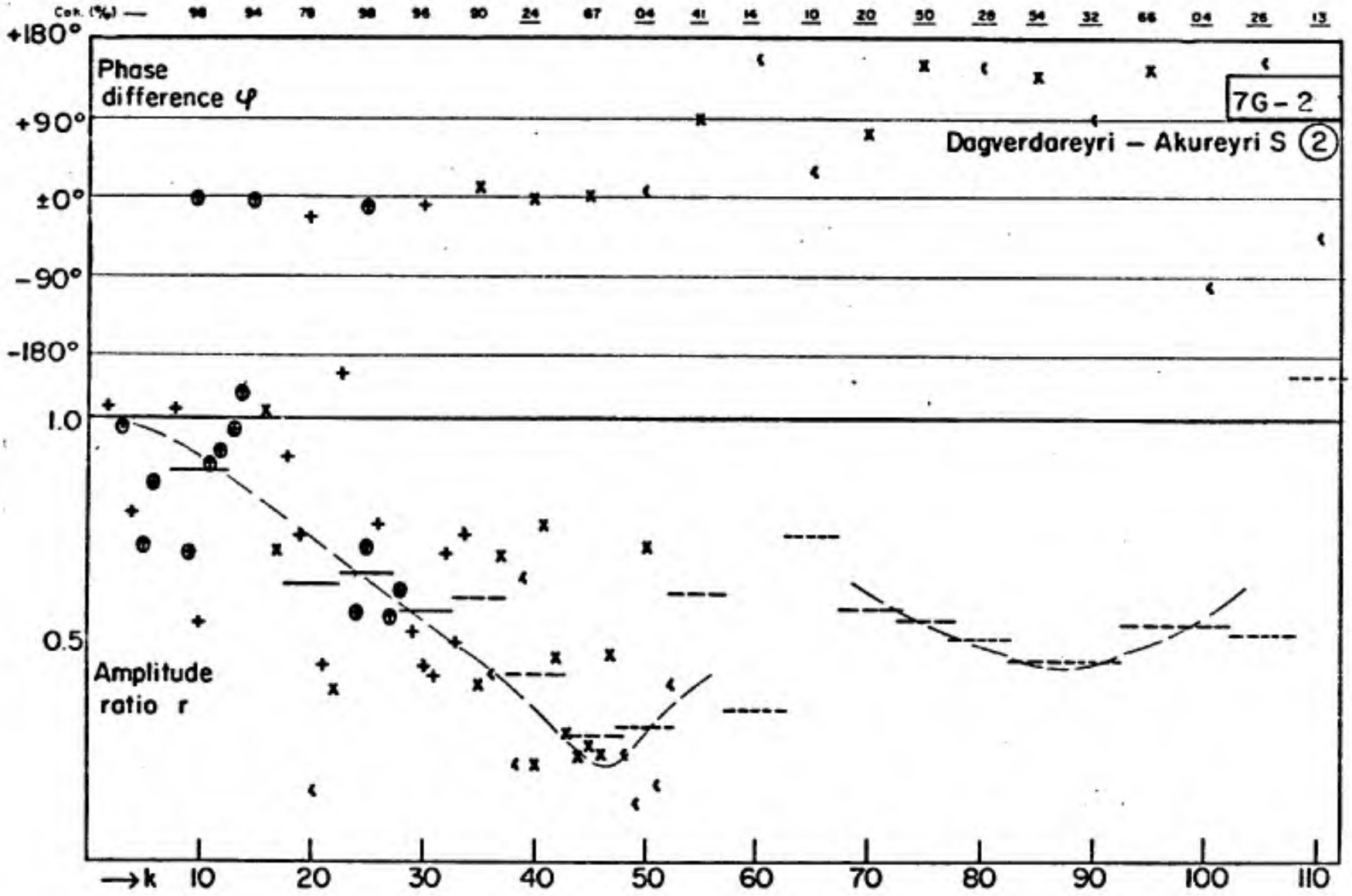
Coh. (%) — 98 94 78 98 96 90 24 67 04 41 16 10 20 50 28 54 32 66 04 26 13
+180°
Phase
difference φ
7G-2
+90°
Dagverdareyri – Akureyri S (2)
±0°
-90°
-180°
1.0
0.5
Amplitude
ratio r
→k 10 20 30 40 50 60 70 80 90 100 110

Figure 7G-2

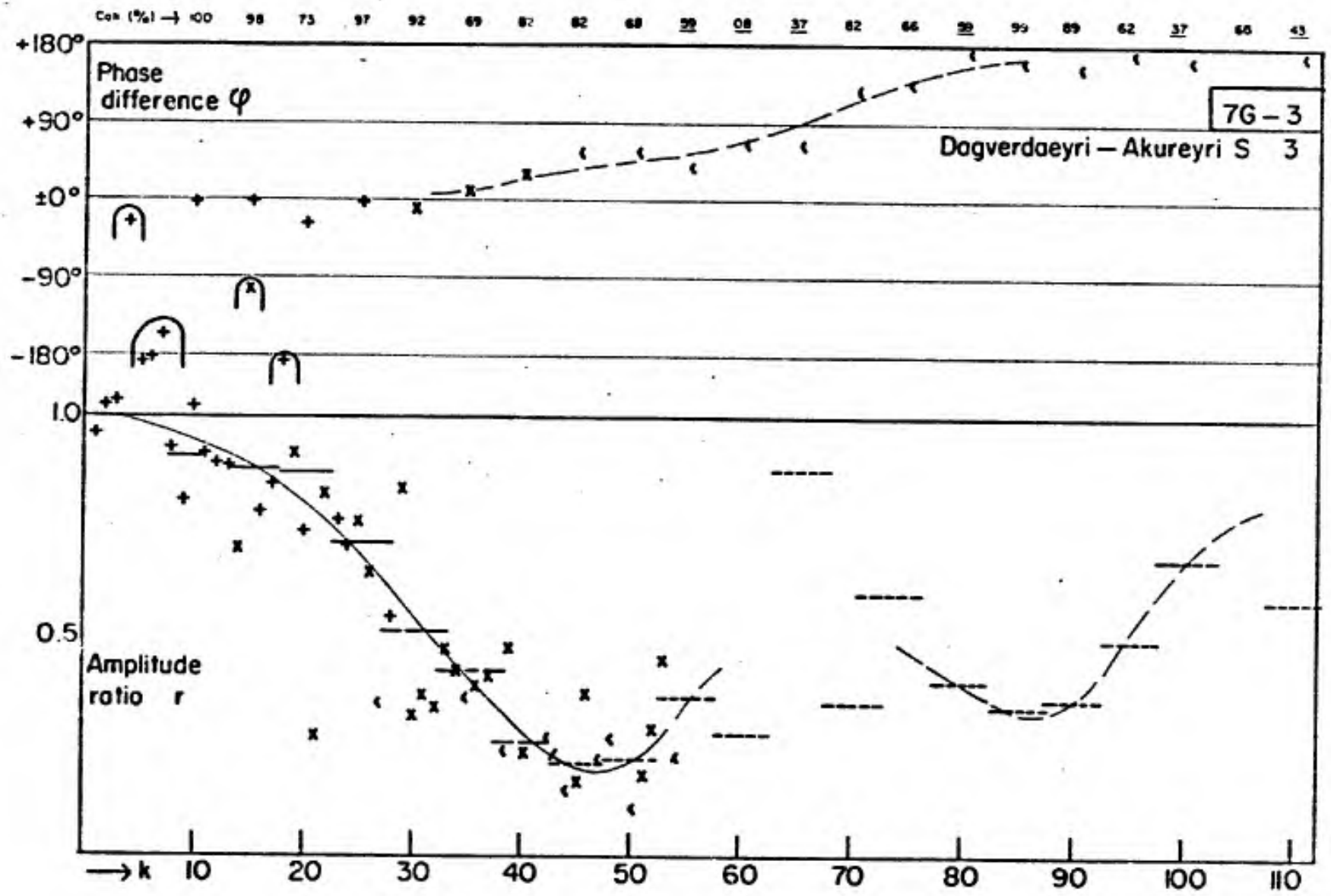
Coh (%) → 100 98 73 97 92 69 82 82 68 39 08 37 82 66 39 99 89 62 37 66 43
+180°
Phase
difference φ
+90°
±0°
-90°
-180°
7G – 3
Dagverdaeyri – Akureyri S 3
1.0
0.5
Amplitude
ratio r
→ k 10 20 30 40 50 60 70 80 90 100 110

Figure 7G-3

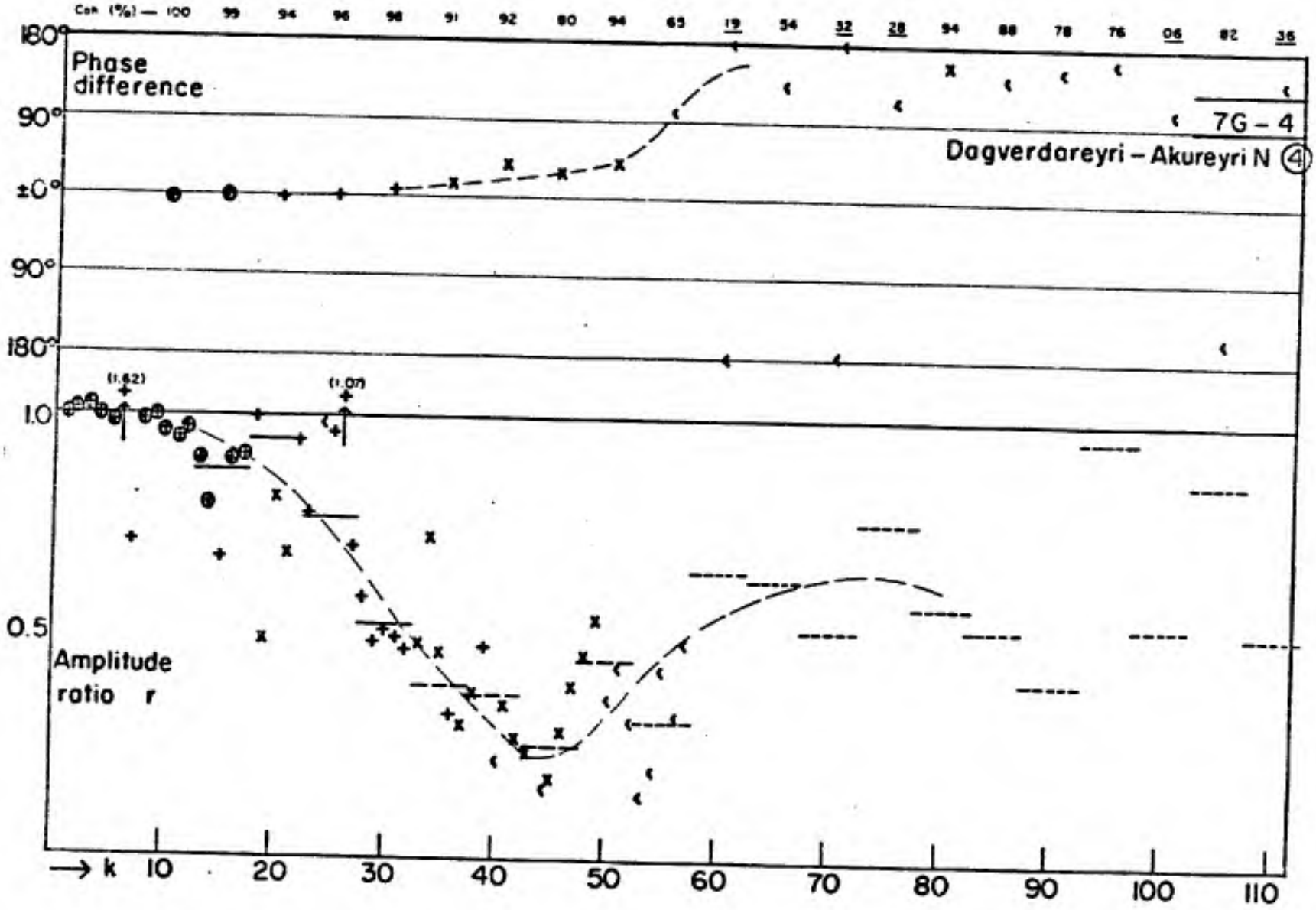
Coh (%) — 100 99 94 96 98 91 92 80 94 65 19 54 32 28 94 88 78 76 06 82 36
180°
Phase difference
90°
±0°
90°
180°
7G - 4
Dagverdareyri – Akureyri N ④
(1.62)
(1.07)
1.0
0.5
Amplitude ratio r
→ k 10 20 30 40 50 60 70 80 90 100 110

Figure 7G-4

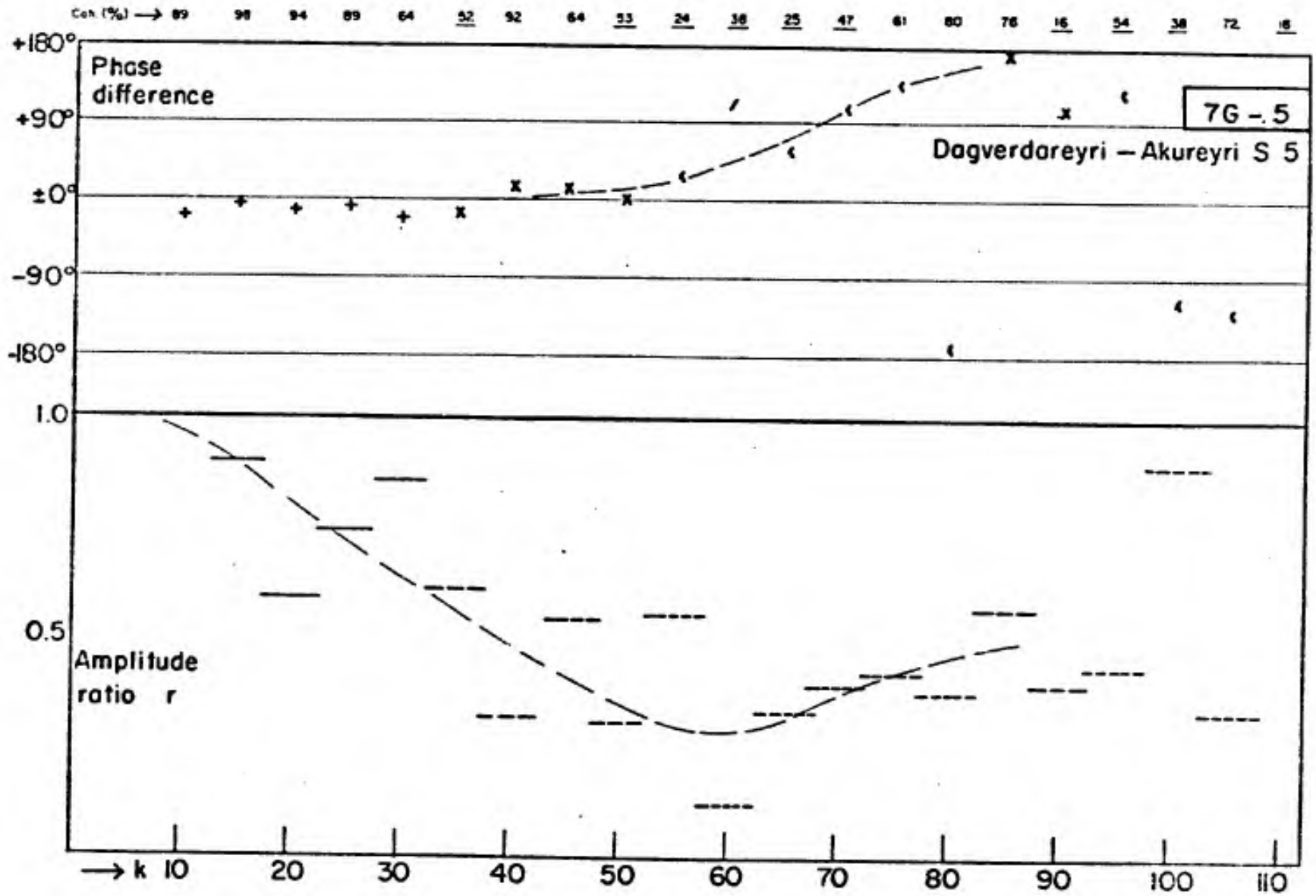
Coh. (%) → 89 98 94 89 64 52 92 64 53 24 38 25 47 61 80 76 16 54 38 72 18
+180°
Phase difference
+90°
±0°
-90°
-180°
7G -.5
Dagverdareyri – Akureyri S 5
1.0
0.5
Amplitude ratio r
→ k 10 20 30 40 50 60 70 80 90 100 110

Figure 7G-5

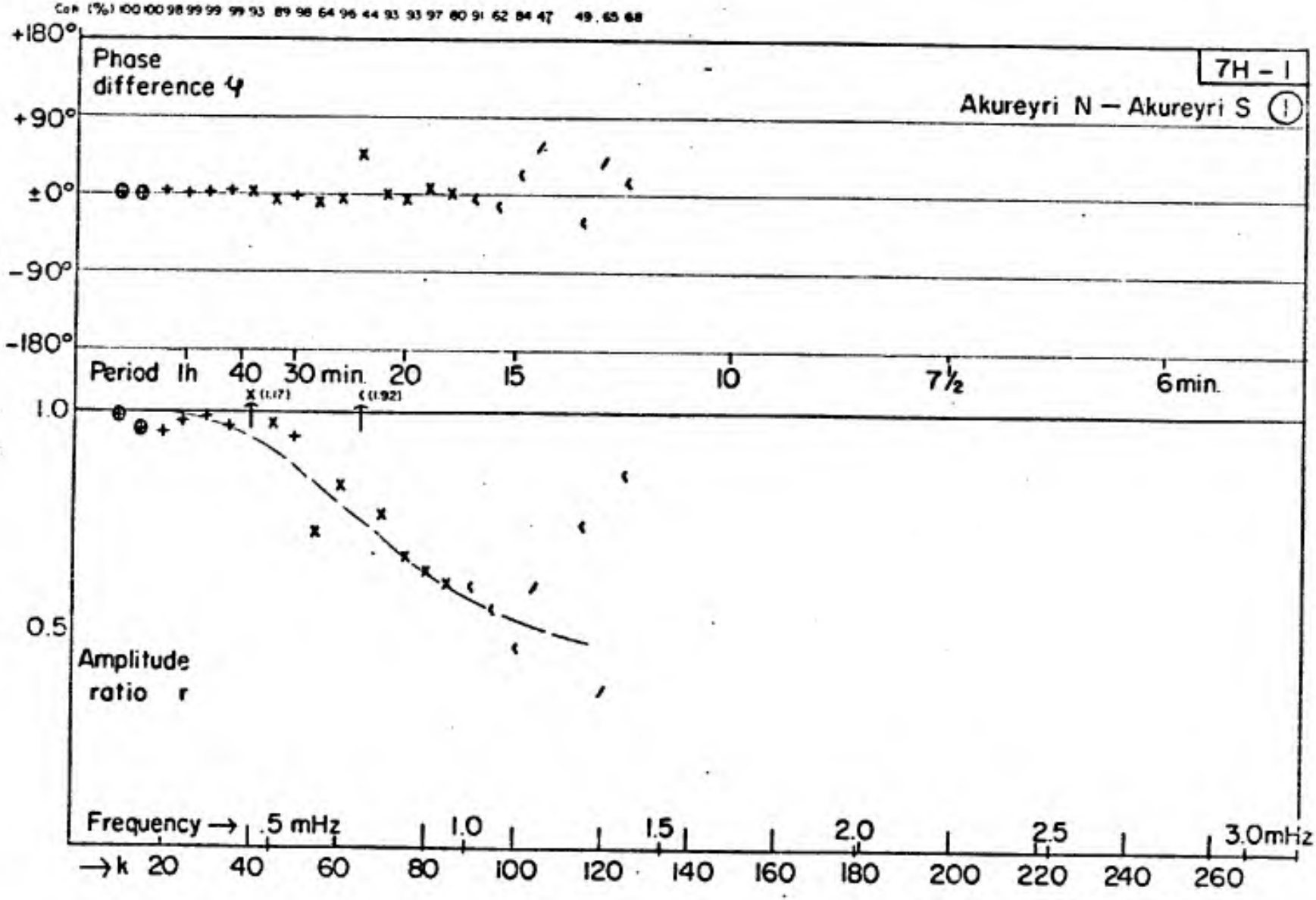
Coh (%) 100 100 98 99 99 99 93 89 98 64 96 44 93 93 97 80 91 62 84 47 49 65 68
+180°
Phase
difference φ
7H - 1
Akureyri N — Akureyri S (1)
+90°
±0°
-90°
-180°
Period 1h 40 30 min. 20 15 10 7½ 6 min.
X (1.17)
(1.92)
1.0
0.5
Amplitude
ratio r
Frequency → .5 mHz 1.0 1.5 2.0 2.5 3.0mHz
→k 20 40 60 80 100 120 140 160 180 200 220 240 260

Figure 7H-1

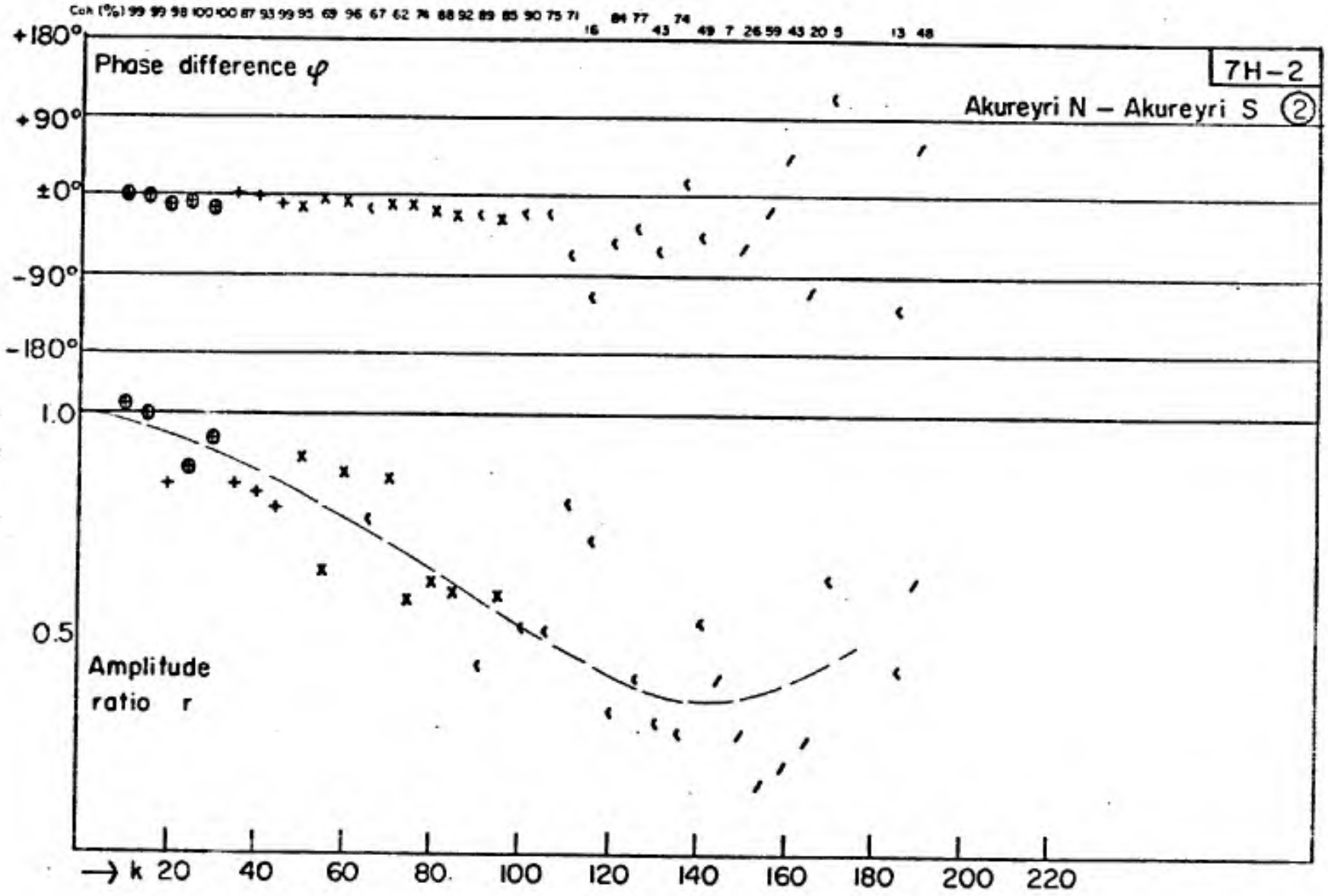
Coh (%) 99 99 98 100 100 87 93 99 95 69 96 67 62 76 88 92 89 85 90 75 71 16 84 77 43 74 49 7 26 59 43 20 5 13 48
+180°
Phase difference φ
7H-2
Akureyri N – Akureyri S ②
+90°
±0°
-90°
-180°
1.0
0.5
Amplitude ratio r
→ k 20 40 60 80 100 120 140 160 180 200 220

Figure 7H-2

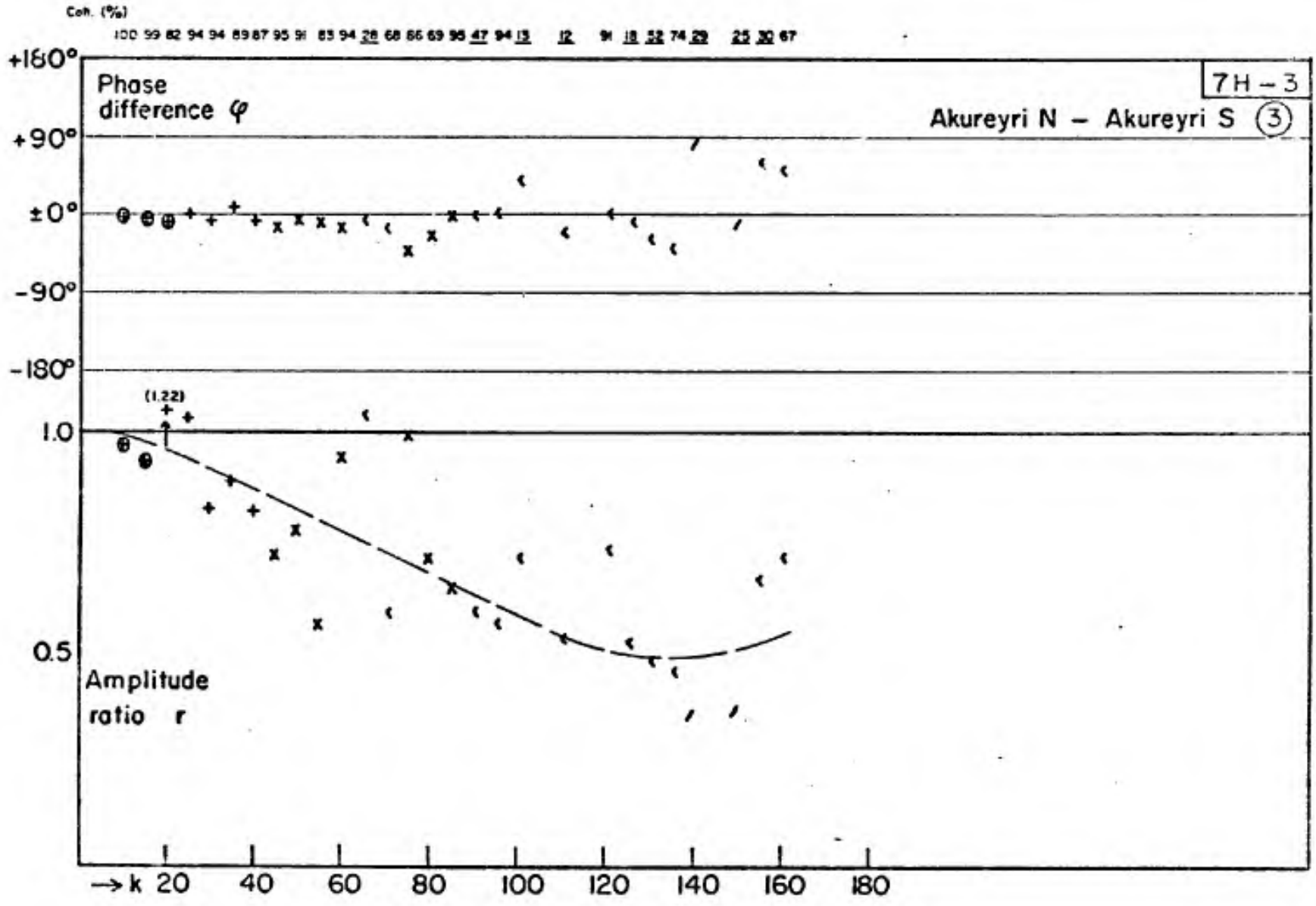
Coh. (%)
100 99 82 94 94 89 87 95 91 85 94 28 68 86 69 96 47 94 13 12 91 18 52 74 29 25 30 67
+180°
+90°
±0°
-90°
-180°
1.0
0.5
Phase
difference φ
7H – 3
Akureyri N – Akureyri S (3)
(1.22)
Amplitude
ratio r
→k 20 40 60 80 100 120 140 160 180

Figure 7H-3

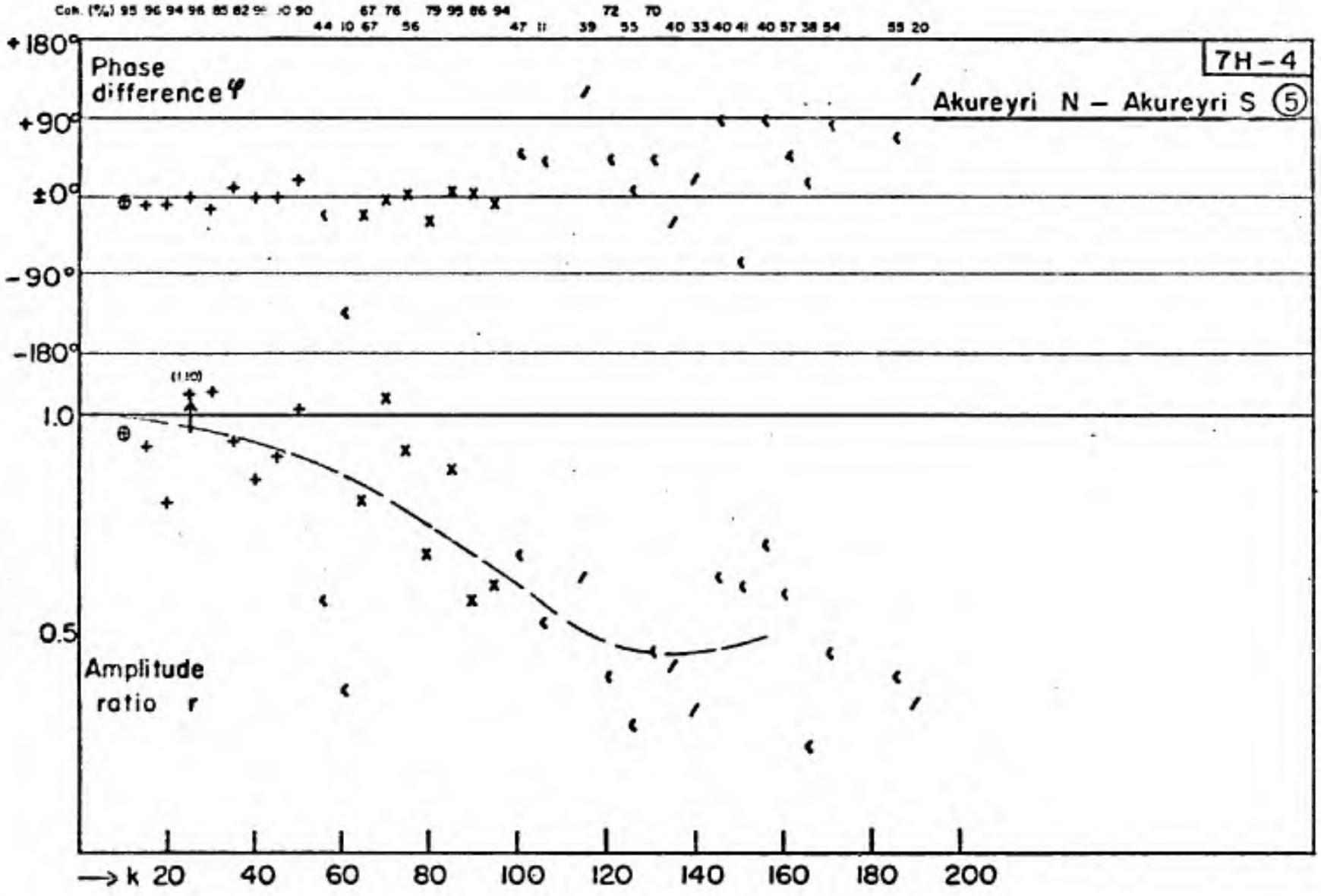
Coh. (%) 95 96 94 96 85 82 90 90 90
44 10 67 56 67 76
47 11 79 95 86 94
39 72 55 70
40 33 40 41 40 57 38 54
55 20
+180°
+90°
±0°
-90°
-180°
1.0
0.5
Phase difference φ
Amplitude ratio r
7H-4
Akureyri N – Akureyri S ⑤
→ k 20 40 60 80 100 120 140 160 180 200

Figure 7H-4

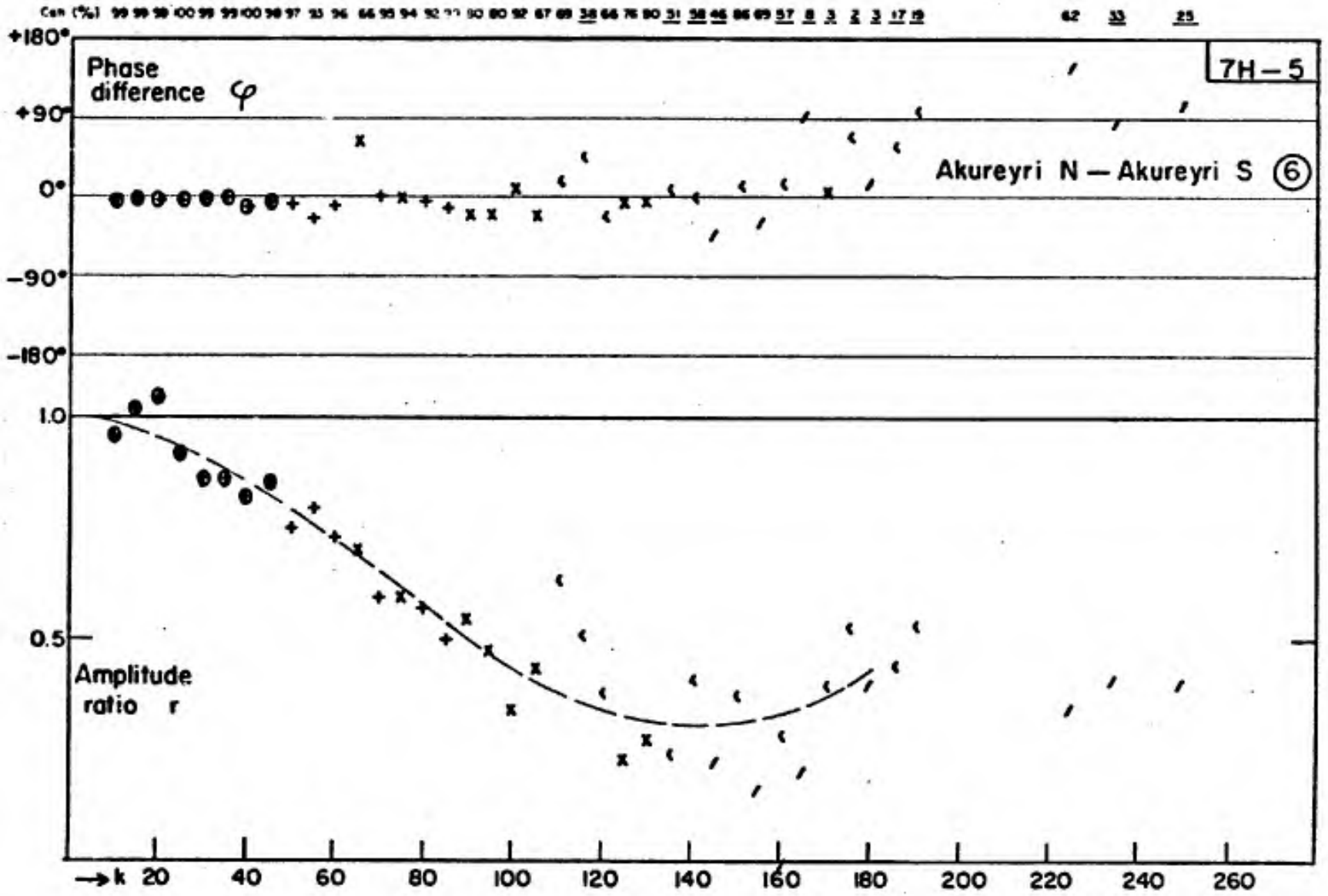
Coh (%)
+180°
Phase
difference φ
7H–5
+90°
Akureyri N — Akureyri S ⑥
0°
-90°
-180°
1.0
0.5
Amplitude
ratio r
→k 20
40
60
80
100
120
140
160
180
200
220
240
260

Figure 7H-5

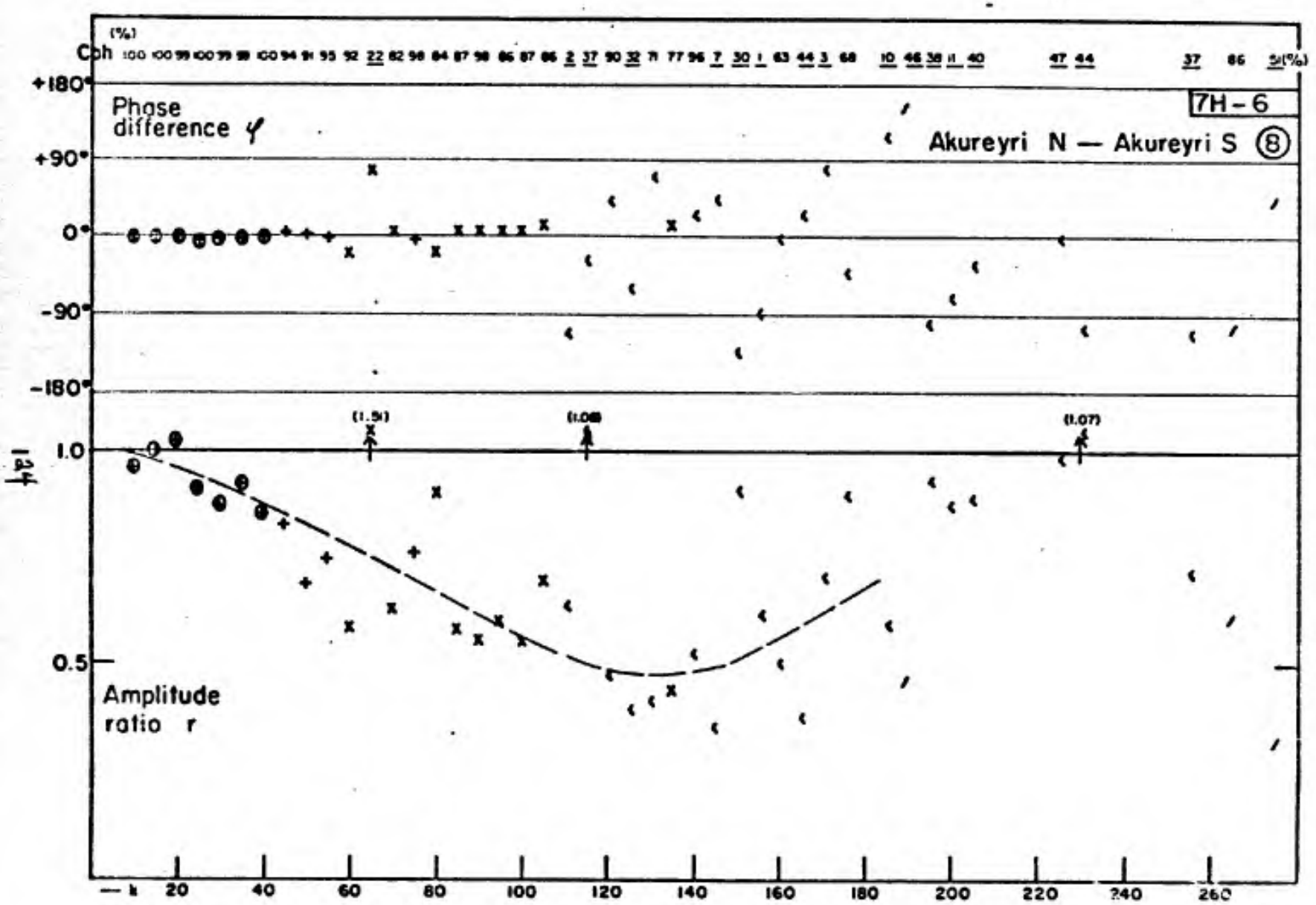
(%)
Coh
+180°
Phase
difference φ
7H-6
Akureyri N — Akureyri S ⑧
+90°
0°
-90°
-180°
(1.51)
(1.08)
(1.07)
1.0
0.5
Amplitude
ratio r
— k
20
40
60
80
100
120
140
160
180
200
220
240
260

Figure 7H-6

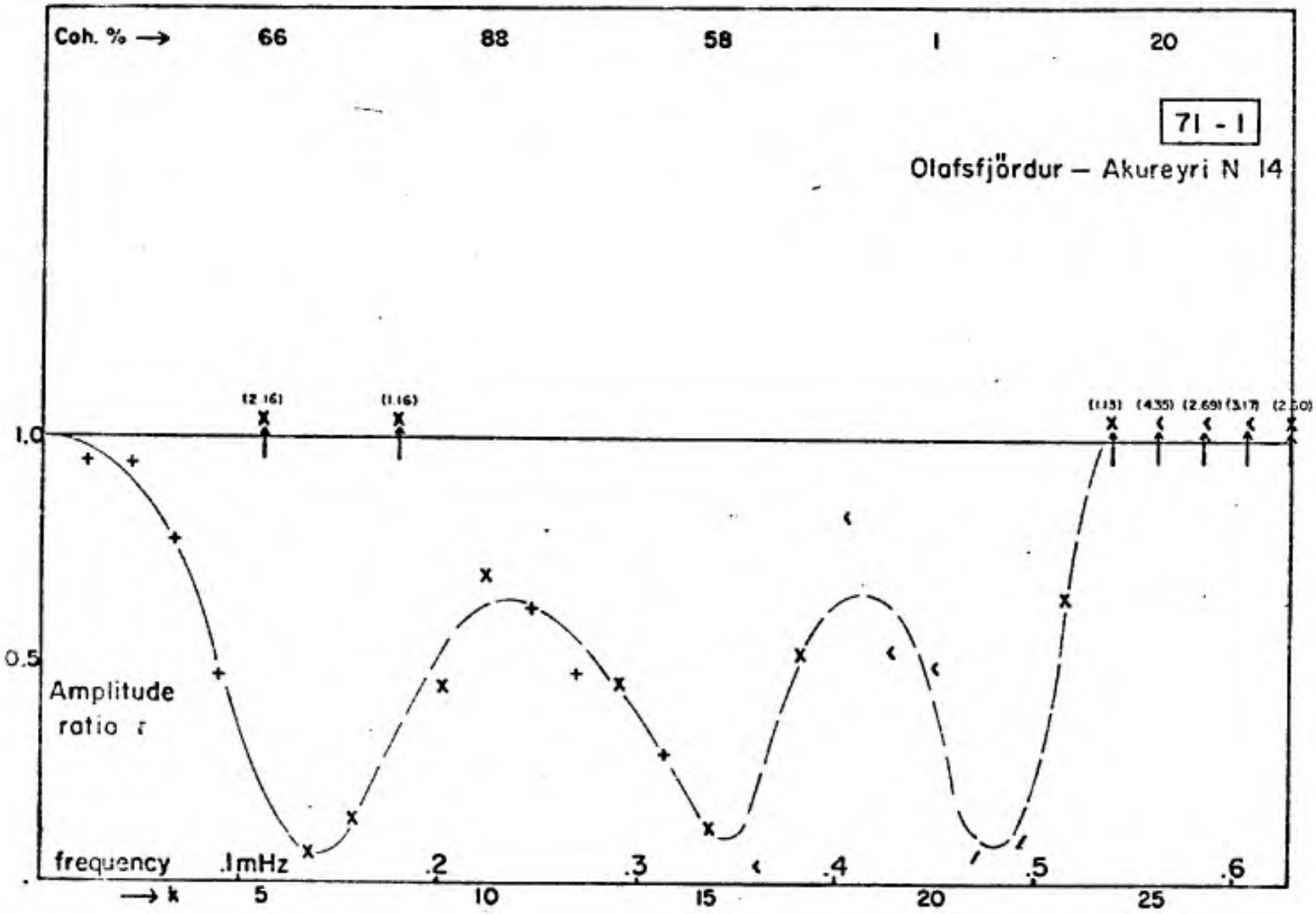
Coh. % →
66
88
58
1
20
71 - 1
Olafsfjördur – Akureyri N 14
(2.16)
(1.16)
(1.13)
(4.35)
(2.69)
(3.17)
1.0
0.5
Amplitude
ratio r
frequency
.1mHz
.2
.3
.4
.5
.6
→ k
5
10
15
20
25

Figure 7I-1

8. Closer Analysis of Resonance Peaks

8.1 General

In the previous chapter, it was clearly demonstrated that a reasonable description of the wave motion in the fjord is possible, at least for the lower frequencies up to about 0.6 mHz, by considering the water in the fjord as a linear passive system responding to the long waves entering from the sea. For these frequencies at least, the incoherent parts of the water level variations at the various stations in the fjord were shown to be of relatively minor importance in most records and average amplitude ratios and phase differences for pairs of stations in the fjord could be well established as functions of frequency.

This being so, an obvious question to ask next is: is it possible to deduce from the available data, some information on the amplitude ratios and phase differences for a station in the fjord, say Akureyri, the head of the fjord, and some place at sea outside the mouth of the fjord, where the wave motion can be considered as to approximate the "input signal" for the passively acting fjord. In short, we are interested in the shape of the (complex) frequency response function of the fjord as a whole with respect to the waves at sea. The behavior of this response function around the resonance peaks is of special interest.

In recent years, much theoretical and model work has been done to obtain a better understanding of the response characteristics of harbors on long waves incident upon an entrance gap; see the list of references [8]. The theoretical work has started with analytical treatments of oscillations in and close to harbors of simple geometry, mainly circular or rectangular basins with constant depth. More recently, numerical calculation schemes have been

worked out for basins of arbitrary geometry.

It has become clear that the shape of the resonance peaks in these cases is determined by two quite different mechanisms provoking dissipation of the wave energy in the basin: first, the associated oscillating currents in the basin lose momentum by friction with the bottom and with the sides of the basin, moreover, large eddies may form if the basin is irregularly shaped; second, the region of the basin entrance acts as a source of waves propagating more or less radially outward to the open sea. Depending on the conditions, either the first or the second process may account for the major part of the energy dissipation. The relative importance of the first process will increase as the basin is shallower, or narrower, or more irregularly shaped, or has a narrower entrance gap. In relatively deep basins with a regular geometry and with an entrance that is not very narrow, the second process may dominate. In fact, in much of the recent theoretical work referred to above [8], the effect of friction was neglected altogether and for several cases, good agreement with the results of hydraulic model experiments was found.

In the case of Eyjafjördur, it can be expected that both dissipation mechanisms play a non-negligible role. The problem may be posed as to the magnitude of both effects. Estimates of the magnitude of the friction effect in the inner parts of the fjord (inward of Hrisey) can be derived from the q-values estimated from the minima in the amplitude ratio curves dealt with in Chapter 7; see also the next Chapter 9. In order to investigate this dissipation problem further, the first thing we need to know is the shape of the frequency response function, especially the shape of the resonance peaks, of the fjord with respect to the long waves occurring outside the fjord. In

the next sections, we shall make an attempt to deduce the shape of the first resonance peak from the available data.

The difficulty, of course, is that no good water level records were available from outside the fjord taken simultaneously with records at stations in the fjord. The island of Grimsey, situated about 20 miles NNE from the mouth of Eyjafjördur, would have been a good place but, as already stated in Section 5.1, attempts to obtain reliable records there have not been successful. We, therefore, are forced to proceed in an indirect way.

8.2 The First Resonance Peak at Akureyri

In Section 6.2, dealing with autospectra, estimates were already made of the central frequencies of the first three resonance peaks. That of the first one was 0.135 mHz, corresponding with k = 12.0 and with a period of 124 minutes. Also a rough idea of the shapes of the resonance peaks was obtained, see Fig. 6F.

The shapes of these peaks, however, deviate from the shapes of the real power response functions for, at least, the following four reasons:

1o. The spectral estimates have only two "degrees of freedom" (see Sections 4.1 and 6.1) and the averages of Fig. 6F are based on only 8 spectra;

2o. The estimated average relative autospectra of Fig. 6F are biased estimates (this is shown in Appendix 5);

3o. These approximated averge relative autospectra would equally approximate the power response functions (in relative measure) only if the average input spectrum (of the waves outside the fjord) would be white over the k-ranges concerned; this is certainly not true.

4o. The frequency resolution in Fig. 6F is clearly so low that a correction in the frequency domain is needed.

The following analysis of the first resonance peak will be made in two steps:

1o. The ratios of the amplitudes of the waves outside the fjord and at Akureyri S for k = 10, 11, 12, 13 and 14 will be estimated from 8 available autospectra of records nrs. 1 to 8 incl. (record nr. 4 is for Akureyri N) and by the use of a Bessel-type approximation for the amplitude ratios;

2o. The maximum and the bandwidth of a simplified resonance peak will be fitted to these five amplitude ratios by means of the "spectral window" function of Section 4.4.

8.2.1 Estimation of Amplitude Ratios in the Resonance Peak for "Sea" and Akureyri S

It is appropriate to write down a few simple relations first. Let:

A (suffix) refer to Akureyri, i.e., the head of the fjord;

M (suffix) refer to the area just inside the mouth of the fjord, where the equations of Chapter 2 may be assumed to be still applicable;

S (suffix) refer to the sea area in front of the fjord, outside the zone of disturbance caused by the mouth of the fjord;

p (suffix) indicate the number of the set of records; p = 1, 2,...8;

k (suffix) indicate the Fourier number.

Then, if we assume complete coherencies for each set of records, we have for the spectral densities from records nr. p:

$$A_{Akp} = r_{Sk}^{-2} W_{Skp} = r_{Mk}^{-2} W_{Mkp} \, , \qquad (1)$$

where we have assumed that the amplitude ratios r_{Sk} and r_{Mk} are independent of p. In this double equation, only the W_{Akp} are known; the problem is to estimate r_{Sk}.

Let us next consider the two causes of variability of the spectral densities already mentioned in Section 5.1.

One cause of variability is connected with the low number of "degrees of freedom" (only two) of the spectral estimates, as was explained in Section 4.1. It is usual to conceive a given record as being one sample of the (infinite) ensemble of records corresponding to the given complex of "macroscopic conditions" (wind fields, atmospheric pressures, etc.) determining this ensemble of records, cf. e.g., [9]. If an asterisk (*) denotes the expected value for this ensemble, we can write for the p-th record:

$$W_{Skp} = W^*_{Skp}\ (1 + \varepsilon_{kp}) \tag{2}$$

and similar for W_{Mkp} and W_{Akp} ,

where the random variates $(1 + \varepsilon_{kp})$ are exponentially distributed between 0 and ∞ such that the ε_{kp} have expected values $\varepsilon^*_{kp} = 0$ and variances $V(\varepsilon_{kp}) = 1$; ε_{kp}-values for different p are uncorrelated, but with p given, they are positively correlated for consecutive k-values (Section 4.2, last paragraph).

Except for the lowest k-values ($k \leq 6$ hours, periods > hours, say) where the main tidal components play a major role, we may expect that the ensemble averages W^*_{Skp} are rather smooth functions of k. This will not always be true for W^*_{Mkp} and W^*_{Akp}, due to the frequency dependent response of the fjord.

The other variability is the natural variability due to the ever changing "macroscopic conditions". This means that the W^*_{Skp}, and similarly the W^*_{Mkp} , will have a large variability with respect to p, as is, indeed, indicated by the spectra obtained from the various records.

From (1) and (2), we have:

$$(1 + \varepsilon_{kp}) r_{Sk}^{-2} = \frac{W_{Akp}}{W^*_{Skp}} \tag{3}$$

The W_{Akp} are known. Then, if we could make rather accurate estimates of W^*_{Skp}, an averaging over the 8 records of the estimated right-hand member of Eq. (3), would yield unbiased estimates of r^2_{Sk} .

The estimates of W^*_{Skp} were arrived at in a number of steps, for which various assumptions had to be made.

Step 1. For two k-ranges on either side of the peak, k = 7, 8, 9 and K = 15, 16, 17, respectively, it was assumed that the amplitude ratios r_{Mk} are approximated by the function $|H_\alpha(s)|$ (cf. Section 2.2, Eq. (16)) with $\alpha = 0$, approximating the value -0.05 found in Section 6.2 for the main fjord as a whole, and with s (real) equal to $(k/12.0)\, s_1$ where s_1 is the first zero of $J_0(s)$.

The following Steps 2 to 6 inclusive were made for each of the eight autospectra individually.

Step 2. For both k-ranges W_{Mkp} was calculated as $r^2_{Mk}\, W_{Akp}$.

Step 3. Estimates of W^*_{Mkp} for k = 8 and for k = 16 were made, respectively as

$$\frac{1}{3}\sum_{k=7}^{9} W_{Mkp} \text{ and as } \frac{1}{3}\sum_{k=15}^{17} W_{Mkp} .$$

Step 4. In both k-ranges W^*_{Mkp} was assumed to equal W^*_{Skp} ; this implies for these k-ranges, the assumptions $W_{Mkp} = W_{Skp}$ (Eq. (2)) and $r_{Mk} = r_{Sk}$ (Eq. (1)).

Step 5. Since W^*_{Skp} can be assumed to be a smooth function of k, W^*_{Skp} for the range k = 10 to 14 incl. was estimated by plotting the W^*_{Mkp} - values for k = 8 and 16 in a double-logarithmic plot against k and connecting both points by a straight line.

Finally, to find estimates of r_{Sk} from W_{Akp} and the estimates just found for W_{Skp} , we can average over p in a number of ways. Instead of using Eq. (3)

to find unbiased estimates of r_{Sk}, we might also use (for example):

$$r_{Sk}^{-1} (1 + \varepsilon_{kp})^{\frac{1}{2}} = (\frac{W_{Akp}}{W^*_{Skp}})^{\frac{1}{2}} \quad , \tag{3a}$$

leading to the following relation between expected values for many records p:

$$0.886\ E(r_{Sk}^{-1}) = E\ \{(\frac{W_{Akp}}{W^*_{Skp}})^{\frac{1}{2}}\} \quad , \tag{3a'}$$

since $\quad E\ \{1 + \varepsilon_{kp})^{\frac{1}{2}}\} = \int_0^\infty x^{\frac{1}{2}} \exp(-x)\ dx = \frac{1}{2}\sqrt{\pi} = 0.886$

or we might use (for example):

$$r_{Sk}\ (1 + \varepsilon_{kp})^{-\frac{1}{2}} = (\frac{W_{Akp}}{W^*_{Skp}})^{-\frac{1}{2}} \ , \tag{3b}$$

leading to the following relation between expected values for many records p:

$$1.772\ E(r_{Sk}) = E\ \{(\quad)^{-\frac{1}{2}} \quad , \tag{3b'}$$

since $\quad E\ \{1 + \varepsilon_{kp})^{-\frac{1}{2}} = \int_0^\infty x^{-\frac{1}{2}} \exp\ (-x)\ dx = \sqrt{\pi} = 1.772$

Still, other possibilities exist.

It was found that the three averaging methods led to results that differed only slightly, except for two k-values where the method using (3b) yielded larger deviations from the results found from (3) and (3a). It was thought that Eq. (3a) would yield the most reliable result. Thus the following steps were made:

Step 6. For k = 10 to 14 incl., the square root of the quotient of W_{Akp} and W^*_{Skp} (estimated by step 5) was taken to find estimates for $r_{Sk}^{-1}\ (1 + \varepsilon_{kp})^{\frac{1}{2}}$ according to Eq. (3a).

Step 7. For each of these five k-values, these estimates were averaged over the eight cases and divided by 0.886 to find the estimates for r_{Sk}^{-1} according to Eq. (3a').

As an example to illustrate the whole procedure, the full set of data is given here for one of the spectra, that of the record nr. 7 with the highest resonance peak (cf. Fig. 6A-6).

Step nr. →		1	2	3	4	5	6
k	W_{Ak7} (cf.fig.6A-6)	r_{Mk}	W_{Mk7}	W^*_{Mk7}	W^*_{Sk7}	W^*_{Sk7}	$r_{Sk}^{-1}\ (1+\varepsilon_{k7})^{\frac{1}{2}}$
7	78.9	.565	25.1				
8	129.7	.454	26.6	17.3	17.3		
9	1.7	.338	0.2				
10	19.2					7.8	1.6
11	1314.8					5.5	15.4
12	4368.0					4.0	33.1
13	1894.2					3.0	25.2
14	99.3					2.3	6.6
15	18.7	.262	1.3				
16	22.9	.322	2.4	1.4	1.4		
16	3.6	.366	0.5				

The following table presents the estimates for $r_{Sk}^{-1}\ (1+\varepsilon_{kp})^{\frac{1}{2}}$, their averages over the eight cases and the resulting estimates for r_{Sk}^{-1} and r_{Sk} and r_{Sk}^{-2} in accordance with Step 7.

k Record nr.	10	11	12	13	14
1	2.3	16.3	29.3	17.2	4.0
2	3.5	17.6	17.5	10.3	9.8
3	3.5	10.7	13.8	7.1	1.1
4	3.8	8.1	5.4	3.1	3.4
5	0.9	0.4	6.1	6.1	0.3
6	3.5	6.3	8.4	10.0	5.2
7	1.6	15.4	33.1	25.2	6.6
8	2.8	5.9	7.9	7.8	5.0
$\{r_{Sk}^{-1}\ (1 + \epsilon_{k,})^{\frac{1}{2}}\}$ave.	2.74	10.1	15.2	10.8	4.43
r_{Sk}^{-1} estimate	3.10	11.4	17.1	12.2	5.00
r_{Sk} estimate	0.332	0.089	0.059	0.082	0.200
r_{Sk}^{-2} estimate	10	130	292	149	25

The values of the second and third lines from below in this table were plotted against k in Fig. 8A (crosses), together with the pre-assumed values on both sides of the resonance peak (cf. Steps 1 and 4).

The degree of accuracy of the estimates obtained for r_{Sk} in the k-range of resonance is obviously very questionable as it is affected by uncertainties associated with, at least, the Steps 1, 3, 4 and 5.

In Step 1, we have chosen $\alpha = 0$. With reference to the values for α estimated from the amplitude ratio plots for Hrisey-Akureyri S (see Section 7.2.1) we might also have chosen $\alpha \simeq + 0.25$. This choice would result in higher values for r_{Mk} in Step 1 and thus, in the end, in higher estimates for r_{Sk}. The relative increase would be 10 percent for k = 10, 15 percent for

k = 12, 20 percent for k = 14. The choice $\alpha = 0$, however, seems to be the better justified one.

Step 3 implies a sampling error whose relative standard error is no less than about $3^{-\frac{1}{2}} \approx 58$ percent.[1] By the interpolation, however, the relative sampling standard error in W^{*}_{Skp} (Step 5) will be reduced to roughly $58/2^{\frac{1}{2}} \approx 41$ percent. This leads to a relative standard error in the final estimates for r_{Sk} of about $20/8^{\frac{1}{2}} \approx 7$ percent.

The degree of justification of Step 4, according to the references [8], will strongly depend on the value of the parameter $\eta = \frac{1}{2}b\omega(gd)^{-\frac{1}{2}}$ at the mouth of the fjord, where the meaning of the symbols is given in the list of notations, Section 1.4. (This parameter is more usually denoted as kd, where k is the wave number and 2d is the entrance width of the harbor or bay, etc.). For the mouth of Eyjafjördur, we may take: width b = 13 km, mean depth d = 100 m. The parameter η then takes the values 0.12 for the Fourier component number k = 8, 0.18 for k = 12 and 0.24 for k = 16. Although these values are rather small, they do not exclude the possibility that a non-negligible error is introduced by Step 4. It is impossible to estimate the magnitude of this error here. Only a numerical calculation could solve this problem.

The method of interpolation proposed in Step 5 is arbitrary and merely justified by the experience that many continuous spectra in a restricted frequency range can be approximated by a power law. The results of Steps 4 and 5 for the eight spectra have been illustrated in Fig. 8B,[2]) which gives a

---

(1) Due to the positive correlation between consecutive k-values, this standard error will even be ca 70 percent.

(2) For the small circles connected by broken lines, see Chapter 10.

good impression of the estimated spectral levels at sea in this frequency range and of their variability. An alternative way of interpolation between the estimated W^*_{Skp} - values at k = 8 and k = 16 would be to assume an exponential decrease: $W^*_{Skp} \sim$ exp. (- const. k). This would have led to higher interpolated W^*_{Skp} - values and, in the end, to 4 to 10 percent higher estimates for r_{Sk}, the percentage increasing with the slope in the plot 8B. The assumption of a power law, however, seems to be preferable.

Finally, with reference to the last Steps 6 and 7, even if the estimates for W^*_{Skp} would be correct, the final estimates of r^{-1}_{Sk} would still have a sampling error due to the variability of the ε's, whose relative standard value is given by $(\frac{4 - \pi}{8\pi})^{\frac{1}{2}} \approx 18$ percent.

It must be concluded from all these arguments that the estimates arrived at for the amplitude ratios r_{Sk} in the k-range of the resonance peak have a rather large degree of uncertainty. It should be noted, however, that the uncertainties associated with the Steps 1 and 5 affect the mutual ratios between the 5 estimated r_{Sk}-values only very little.

8.2.2 Estimation of the Shape of the "Real" Resonance Peak

In this section, the "real" resonance peak is defined as the energy amplification factor between the sea area in front of the fjord and the head of the fjord (Akureyri), considered as a continuous function of frequency in a restricted frequency range including the "half-power points"; these are the two frequencies (on either side of the top) at which the energy amplification factor is half its maximum value. The difference between these two frequencies is the "half-power bandwidth".

The thus defined "real" resonance peak is obviously identical with the "real" spectral density distribution at the head of the fjord if the "input"

spectrum "at sea" is white in the frequency range considered with spectral density 1, and if there is no "noise".

To begin with, the central frequency of the "real" resonance peak is not affected by the "blurring" associated with the Fourier analysis. This can be deduced by using the relation (16) of Section 4.4. In other words, we can derive this central frequency from the estimated r_{Sk}^{-2} - values in the second table of the previous Section 8.2.1 (possibly extended to lower and higher k-values) as

$$\bar{k} = \Sigma\, k \cdot r_{Sk}^{-2} \cdot (\Sigma n_{Sk}^{-2})^{-1} \quad .$$

The result is k = 12.1, with estimated standard error 0.05. This value of k corresponds with a wave frequency 12.1 x 0.0112 = 0.1355 mHz, or with a wave period of 123 minutes.

In order to estimate the "real" shape from the amplitude ratios estimated in the previous section, by means of the spectral window function of Section 4.4, we need a "parameterization" of this shape.

It is usual to approximate the shape of any resonance peak by an expression of the form

$$\frac{\text{const.}}{1 + (\delta/q)^2} \quad , \qquad (4)$$

in which $1 + \delta$ is the frequency divided by the resonant frequency and the constant 2q is the half-power bandwidth divided by the resonant frequency, so that $(2q)^{-1}$ satisfies the usual definition for the "Q-factor" of the resonator. Except for the constant in the numerator, $(2q)^{-1}$ is the only characterizing parameter.

For a narrow fjord or bay, etc. in which the long-wave motion can be described by the Bessel-type expression (16) of Section 2.2 with s given by Eq. (12) of Section 2.1, the energy amplification factor between the "sea" and the head of the fjord (or any other station in the fjord) close to resonance, in fact, can be approximated by an expression like (4). This can be easily shown as follows. The energy amplification factor is assumed to be given by $|H_\alpha(s)|^{-2}$ with the real part s_r of s proportional to ω and with a relatively small imaginary part $- is_r q$ (section 2.1, eq. (12)). Now put $s_r/s_b = \omega/\omega_n = 1 + \delta$, where s_n and ω_n refer to the n-th resonance point (s_n is the n-th zero of $H_\alpha(s)$) and δ has the same meaning as in the expression (4) just given. We than have $s = s_n\ (1 + \delta)\ (i - iq) \approx s_n(1 + \delta - iq)$ if $|\delta|$ and $|q|$ are small compared to 1. Since $H_\alpha(s)$ is analytic in an area of the complex s-plane around s_n, it can be developed in a Taylor's series (omitting the suffix α):

$$H\{s_n*i + \delta - iq)\} = H(s_n) + s_n(\delta - iq)\,H' + \frac{1}{2}\,s_n^2\,(\delta - iq)^2H'' + \ldots$$

in which $H(s_n) = 0$ by definition of s_n and H', H'', ... are the derivatives of H(s) at $s = s_n$. If we stop the series after the term with H' (also observing that H" is small for s_n) we obtain for the energy amplification factor close to resonance the approximation:

$$|s_n(\delta - iq)H'(s_n)|^{-2} = \text{const.}(\delta^2 + q^2)^{-1}\ , \qquad (5)$$

i.e. an expression like (4). We see, moreover, that the dissipation parameter q introduced much earlier in Section 2.1, Eq. (12) is identical with the q just introduced in (4). The maximum energy amplification factor according to (5) is $(qs_nH'(s_n))^{-2}$, corresponding with a minimum "amplitude ratio" (in the sense

of Section 8.2.1) given by $qs_n|H'(s_n)|$, in accordance with Section 2.2, Eq. (19) and Section 8.2.1, Eq. (5).

It may be observed here that the well known expression for the energy amplification factor for the standard "single degree of freedom oscillator" (ref. [10]):

$$\{(1 - \frac{\omega^2}{\omega_o^2})^2 + \frac{1}{Q^2}\frac{\omega^2}{\omega_o^2}\}^{-1} ,$$

in which ω_o is the natural frequency of the undamped system, after putting $\omega/\omega_o = 1 + \delta$, assuming $|\delta| << 1$, retaining only the terms of lowest order in δ and putting $q = (2q)^{-1}$, is also approximated by an expression like (4): $(4\delta^2 + 4q^2)^{-1}$.

We shall now adopt a "real" first resonance peak at Akureyri of the form (4) and estimate the parameter q in (4) from the amplitude ratios r_{Sk} estimated in the previous Section 8.2.1.

In general, if $W(f) \cdot d(f/2T)$ is the coherent real spectral energy at Akureyri per frequency interval $d(f/2T)$ with a white "input" spectrum "at sea" of density 1, we have in good approximation from Section 4.4:

$$r_{Sk}^2 = \int_0^\infty d(\frac{f}{2T}) \cdot W(f) \cdot P(|k-f|) , \qquad (6)$$

where $P(|k-f|)$ is the "spectral window" function defined in Section 4.4 Eqs. (14a) and (13a), see Figure 4A. For Eq. (6) to be valid, it is necessary that non-zero values of the integrand are concentrated in a f-range for which $|k-f| << (k+f)$; since $P(|k-f|)$ converges rapidly to zero for $|k-f| > 3$, say (see small table in Section 4.4), this is always true if $k >$ say, 8.

For W(f) we put:

$$W(f)\,df = CW^*(f)\,df = \frac{c\,df}{\pi q f_o \{1 + (\frac{f - f_o}{q f_o})^2\}} \qquad (7)$$

or

$$W^*(\delta)\,d\delta = \frac{d\delta}{\pi q\,(1 + \frac{\delta^2}{q^2})} \quad , \qquad (7a)$$

in which f_o indicates the central frequency, $1 + \delta = f/f_o$ as in (4) and $q << 1$. Expressions (7) and (7a) are normalized such that

$$\int_0^{\infty} W^*(f)\,df \text{ and } \int_{-\infty}^{+\infty} W^*(\delta)\,d\delta \text{ are approximately 1.}$$

As the central frequency of the resonance peak happened to correspond approximately with k = 12, we have simply put $f_o = 12.0 = k_o$ (integer) in Eq. (7). By numerical integration, we then have calculated the integral over f of $W^*(f) \cdot P(|k-f|)$ for k = 10, 11, 12, 13 and 14, for three values of $qf_o = 12.0\ q$: 1/6, 1/3 and ½. According to Eq. (6) and from the definitions of $W^*(f)$ and $P(|k-f|)$, these integrals should yield, for these three assumed bandwidths, the <u>fractions</u> of the total energy that show up in the different Fourier components k, to be abbreviated as fr(k). Or also, they should yield r_{Sk}^{-2} values in <u>relative</u> measure, such that the sum of these overall k is 100 percent. The result was as follows:

$k_o q$	Fractions of total energy fr(k) (in percent) found for k =			Sum of fr(k) for 5 components	$\frac{fr(k_o \pm 1)}{fr(k_o)}$	$\frac{fr(k_o \pm 2)}{fr(k_o)}$
	k_o	$k_o \pm 1$	$k_o \pm 2$			
0	66.7	16.7	0.0	100	0.25	0.00
1/6	54.5	18.7	1.9	95.7	0.35	0.03^5
1/3	45.4	19.4	3.5^5	91.3	0.42^5	0.08
1/2	38.5	19.4	4.9	87.1	0.50^5	0.12^5

For $k_o q = 0$, see Section 4.2, Eq. (6) and Section 4.4, case 2o.

The distribution of these fractions over k should be compared with the estimated r_{Sk}^{-2} - values of the second table in Section 8.2.1 to estimate the value of $k_o q$ giving the best fit. We have plotted the ratios $fr(k_o \pm 1)/fr(k_o)$ and $fr(k_o \pm 2)/fr(k_o)$ against $k_o q$ and have taken the values of $k_o q$ at which these ratios equalled the ratios

$$\frac{\frac{1}{2}(r_{S11}^{-2} + r_{S13}^{-2})}{r_{S12}^{-2}} \text{ and } \frac{\frac{1}{2}(r_{S10}^{-2} + r_{S14}^{-2})}{r_{S12}^{-2}}, \text{ respectively,}$$

following from the second table in Section 8.2.1, these ratios being 0.48 and 0.060, respectively. The values of $k_o q$ found then are 0.44 and 0.27, respectively.

There is only a moderate agreement between these two values. We attached the greater weight to the first value and estimate 0.38 as the best value of $k_o q$, with an estimated standard error of 15 percent, and since $k_o = 12$, the estimate for q is 0.032.

The estimated half-power bandwidth of the "real" resonance peak in the k-scale, $2k_o q$, then becomes 0.76, corresponding with 0.76 x 0.0112 = 0.0085 mHz. The estimated "Q-factor", $(2q)^{-1}$, (see Eq. (4)), becomes 16.

We now have estimated the parameter q and have thus found an estimated approximation for the relative shape of the "real" resonance peak according to Eq. (7). The next problem is to estimate the absolute shape of this peak. We have to find the factor C by which the normalized function W*(f) in Eq. (7) has to be multiplied to give the absolute resonance peak W(f).

We have estimated the absolute shape of the "real" peak in two ways.

1o. According to Eq. (5), the maximum of the "real" energy amplification

factor should equal $\{qs_1 H'_\alpha(s_1)\}^{-2}$. If we put $\alpha = 0$ and $q = 0.032$, this becomes (ref. Fig. 2C) $= (0.032 \times 1.25)^{-2} = \underline{625}$. The estimate for the maximum amplitude amplification factor then is $625^{\frac{1}{2}} = \underline{25}$.

2o. We consider the k-range from 10 to 14 inclusive and make use of the following relation (see Equations (7) and (7a)):

$$\sum_{k=10}^{14} r_{Sk}^{-2} \approx C \int_{9\frac{1}{2}}^{14\frac{1}{2}} W^*(f)\, df = C \int_{-0.208}^{+0.208} W^*(\delta)\, d\delta = 0.90\, C$$

This relation must hold in good approximation since both the sum and the integrals include the major part of the resonance peak and the "spectral window" function P(k-f) (see (6)) has a rather small range of (k-f).

Since we estimated for the left-hand member (see second table of Section 8.2.1) the value 606, we find an estimated value of 673 for the factor C.

The maximum value of W*(f) in (7), $(\pi q f_0)^{-1}$ was estimated to be $(\pi \times 0.38)^{-1} = 0.84$. The maximum value of the "real" resonance peak is thus estimated to be $673 \times 0.84 \approx \underline{570}$, and the estimated maximum amplitude amplification factor is $570^{\frac{1}{2}} \approx \underline{24}$.

This second method of estimating the absolute shape of the "real" peak seems to be the more reliable one.

The r_{Sk}^{-2} - values of Section 8.2.1 and the approximated "real" resonance peak have been plotted together against k, or f, in Figure 8C. The corresponding "real" amplitude ratio r as a function of the frequency number f has been indicated as a dashed line in Fig. 8A.

8.3 Other Resonance Peaks

Some apparent average values of half-power bandwidths $2qf_0$ and of "Q-factors" $(2q)^{-1}$, directly derived from various Fourier autospectra, have

been collected in the following table (see next page for table). For Akureyri S, the apparent values read from the average relative spectra and the results from the detailed analysis of the previous section have been added.

Attempts to make more accurate estimates for other peaks than the first peak of Akureyri have not been made. For that peak, it is clear that the "real" value of the dissipation parameter q is considerably smaller than the apparent value as read directly from the Fourier spectra. The same will be certainly true also for the other resonance peaks, so that also here the "real" "Q-factors" will be considerably higher than those given in the table.

The narrowness of the first resonance peak of Ólafsfjördur is especially conspicuous; it is apparent in all of the four available spectra. We would estimate a "real" "Q-factor" of the order of 50 here.

	Records nr	Central frequency f_o (k-unis)	Estimated half-power bandwidths $2qf_o$ (in k-units) and "Q-factors" $(2q)^{-01}$					
			from "raw" spectra (very roughly average)		from average relative spectra (fig. 6F)		"real" value from detailed analysis	
			$2qf_o$	$(2q)^{-1}$	$2qf_o$	$(2q)^{-1}$	$2qf_o$	$(2q)^{-1}$
Akureyri S (figs. 6A-1 to 7, 6F)								
first peak	1,2,3,4, 5,6,7,8	12.0-12.1	2.0	6	2.2	5½	0.76	16
second peak	3,4,5,6 8	27	2.0	13	5	5½	-	-
third peak	2,6,7,8	42	2.4	18	5½	7½	-	-
Hialteyri (figs. 6A-8 to 10)								
first peak	3,4,5,6, 7,8	12	2.2	5½	-	-	-	-
Ólafsfjördur (fig. 6D)								
first peak	10,11,12, 14	0.76 5mHz	0.033 mHz	23	-	-	-	-

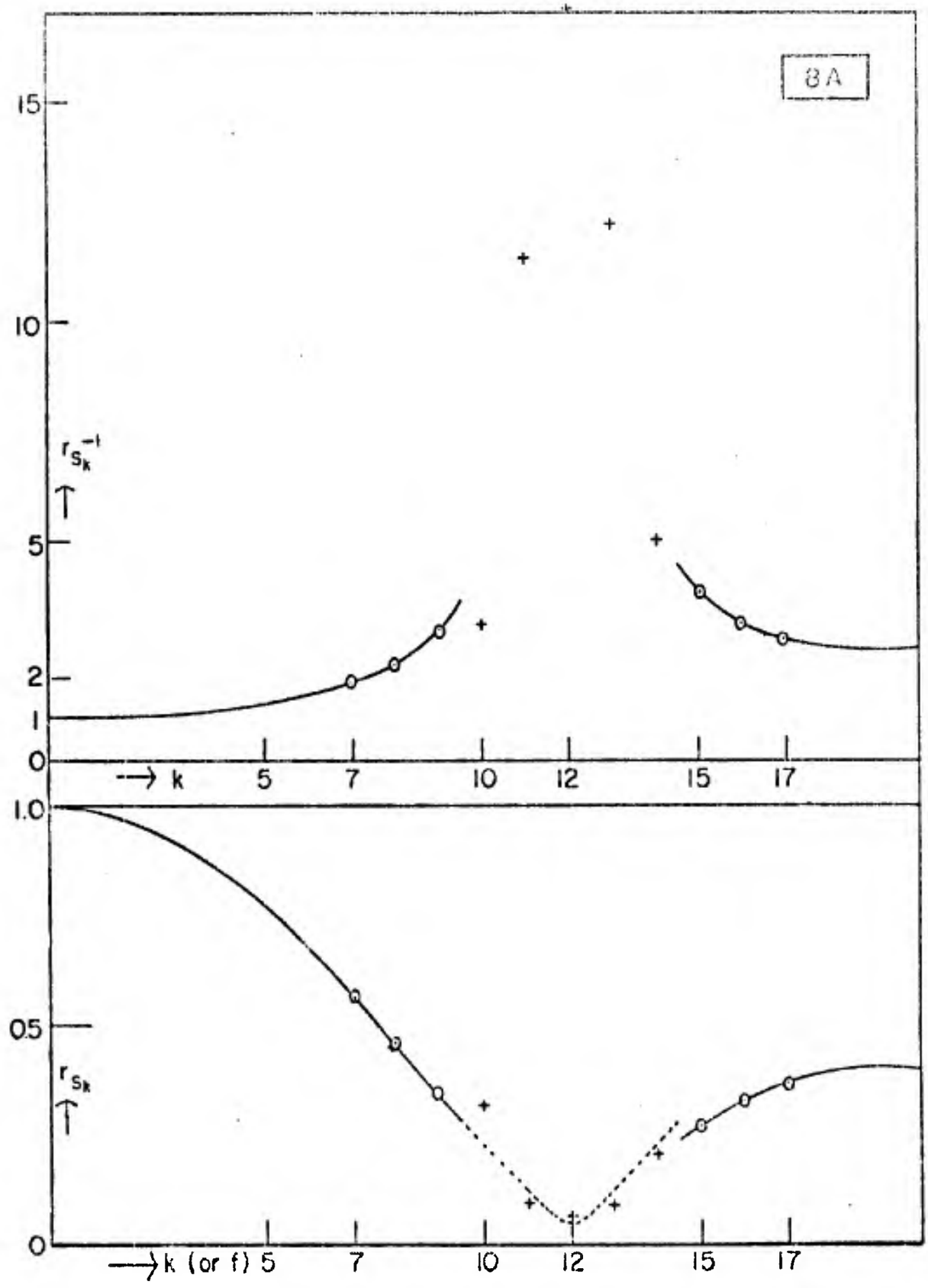

Figure 8A

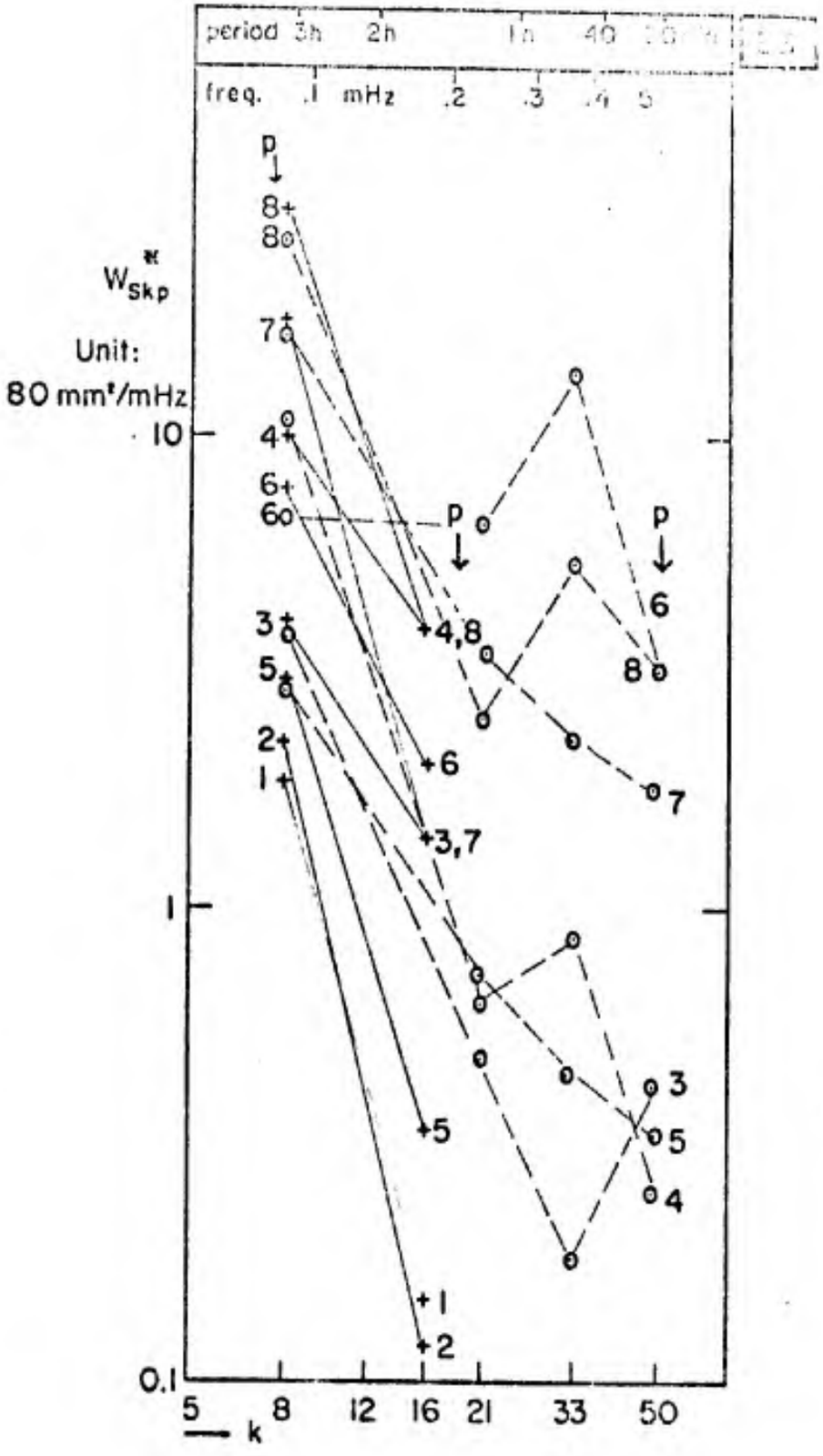
period 3h 2h 1h 40
freq. .1 mHz .2 .3 .4 .5
W^{*}_{Skp}
Unit:
80 mm²/mHz
10
1
0.1
5 8 12 16 21 33 50
k
p
8+
8o
7+
7o
4+
4o
6+
6o
3+
3o
5+
5o
2+
1+
+4,8
+6
+3,7
+5
+1
+2
8o
6o
7o
3o
5o
4o

Figure 8B

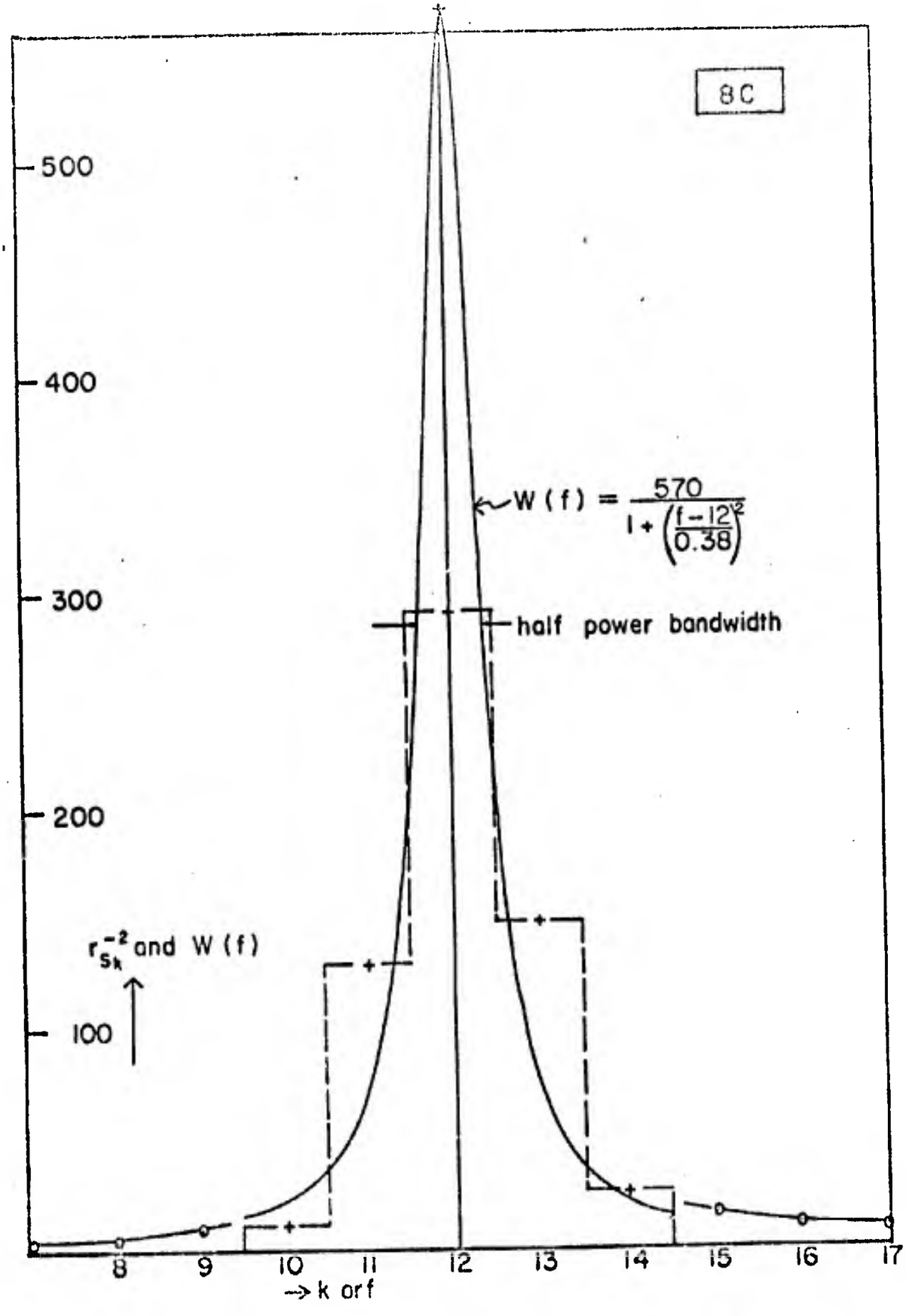
8C
500
400
300
200
100
$W(f) = \frac{570}{1+\left(\frac{f-12}{0.38}\right)^2}$
half power bandwidth
r_{Sk}^{-2} and W (f)
8
9
10
11
12
13
14
15
16
17
→ k or f

Figure 8C

9. The Dissipation Parameter c and the Current Velocities in the Fjord

9.1. General Discussion

The "Q-factor" $(2q)^{-1}$ of 16 and the maximum amplification factor, 24 for the amplitudes, both values referring to the response of the main fjord as a whole and resulting from the estimation in the previous chapter, appear to be rather high. They are higher than the values following from calculations and model experiments for rectangular harbors of constant depth and of a similar entrance width-length ratio as that of Eyjafjördur; see [8]. For such harbors, with entrance gap equal to the width of the harbor itself, the maximum amplification factor theoretically increases roughly inversely proportional with decreasing parameter η = wave number half width (ref. the discussion of "Step 4" in Section 8.2.1). Momoi (paper mentioned under [8], p. 884) found theoretical amplitude amplification factors 5.3 for $\eta = 0.20$, 10.2 for $\eta = 0.10$, 20.2 for $\eta = 0.05$. (These factors also refer to the amplitudes at the closed head of the channel-like harbor). For Eyjafjördur, however, the parameter η at the mouth for the first resonant frequency is about 0.18 (see Section 8.2.1); in the interior of the fjord, η is smaller, but it is still about 0.10 near Hjalteyri. And then we have to remember that the effect of friction of the currents in the harbor has been neglected in the theoretical calculations, so that the theoretical amplification factors are, in reality, upper limits. An explanation of the discrepancy can probably be found in the particular funnel-like shape of Eyafjördur which is actually not at all a rectangular basin with constant depth.

For the Bay of Fundy together with the Gulf of Maine (Atlantic coast of North America) the amplitude amplification factor for the M2-tide between the open sea (shelf edge) and the most inner part is 10 to 12; see [11]. Since it is highly improbable that this system is exactly "tuned" to the frequency of the

M2-tide, the maximum amplification factor at resonance of this system will be most probably still higher and could be comparable with that estimated for Eyjafjördur.

The parameter q, introduced in Section 2.1, Eq. (12), and discussed in more detail in Section 8.2.2 and just above, not only is a measure of the sharpness of the resonance peak but also is a measure of the dissipation of energy in the fjord, as usual in the description of linear resonant systems. For the present case, this can be shown from the original equations of Section 2.1 but it does not seem necessary to elucidate this here.

In Section 8.1, it was explained that the dissipation of wave energy consists of two different parts: a "frictional" part (including the dissipation caused by the formation of turbulent eddies) and a "radiational" part.

The part of the dissipation parameter q that is due to the frictional forces acting on the currents in the fjord is related to the dimensionless friction coefficient (= g/C^2, see Section 2.1, Eq. (2)) by the relation given by Eq. (12) of Section 2.1, and by Eq. (4) of Section 7.1, which we shall repeat here:

$$s_r q_f = \frac{1}{2} \int_0^x d\xi \, \frac{\gamma v_m}{d\sqrt{gd}} \quad , \tag{1}$$

where the symbols have their usual meaning and the suffix f is added to q to indicate that this quantity refers to the effect of friction only.

For the fjord as a whole, the detailed analysis of the previous Chapter 8 led to an estimated value 0.032 for q at k = 12. Since the associated value of s_r is 2.4 to 2.5 (see also Section 6.2), we find an estimated value 0.08 for $s_r q$.

Since some outward radiation of wave energy certainly occurs, it follows

that $s_r q_f$ in Eq. (1) for the whole fjord should be smaller than 0.08. But according to Eq. (1), $s_r q_f$ should be a monotonously increasing function of x, so that $s_r q_f$ for the inner parts of the fjord should be still smaller than for the whole fjord. In Section 7.2.1, however, we have estimated for Hrisey a value 0.2 for $s_1 q$ from the average first minimum of the amplitude ratio plots, at k = about 15, and in Section 7.2.2, similarly, for Hjalteyri a value 0.11 for $s_1 q$, at k = about 29. And for these inner parts of the fjord, we would expect the outward radiation of wave energy to be small. So, there is a discrepancy here.

9.2 Estimation of the Current Velocities in the Fjord and of the "Frictional" Part q_f of the Dissipation Parameter q.

Assuming γ to be independent of x, we shall try to roughly evaluate the integral in Eq. (1) to find a quantitative estimate for the ratio between q_f and γ. To this purpose, we first need to put in values for the velocity v_m.

9.2.1 Approximation for the Velocity v_m.

In this section, the proposition already made in Section 2.1 (after Eq. (7)) will be elucidated.

A general method for the linearization of the friction terms (and other non-linear terms) in the case that several frequencies are present in the long-wave motion, can be found in a book by Dronkers [12]. We shall, however, apply a simple reasoning here.

Assume the longitudinal velocity at a given location x, averaged over the cross-sectional area, to be given by a sum of harmonic terms with angular frequencies ω_1, ω_2 :

$$v = V_1 \cos \phi_1 + V_2 \cos \phi_2 \ldots$$

where

$$\phi_1 = \omega_1 t + X_1 \quad , \phi_2 = \omega_2 t + X_2, \text{ etc.}$$

For the frictional force exerted on a vertical slice of water across the fjord of thickness 1, we then put the approximations (apart from the sign):

not linearized:

$$\begin{aligned} F &= b \times \gamma\rho v^2 \\ &= b \times \gamma\rho \, (V_1 \cos \phi_1 + V_2 \cos \phi_2 + \ldots)^2 \end{aligned} \tag{2}$$

linearized:

$$F = b \times \gamma\rho \, (v_{m1} V_1 \cos \phi_1 + v_{m2} V_2 \cos \phi_2 + \ldots) \tag{2a}$$

where ρ is the density of the water in the fjord and v_{m1}, v_{m2}, ... are the positive time-independent velocities to be determined. It has been implicitly assumed that there is a more or less homogeneous distribution of the velocity over the cross-section which may be not true in reality, e.g., if there is some density stratification in the water.

From these equations, we have for the average energy dissipation per unit of time:

friction not linearized:

$$b \times \gamma\rho \times \text{ave} \, |V_1 \cos \phi_1 + V_2 \cos \phi_2 + \ldots|^3 \quad , \tag{3}$$

friction linearized:

$$\begin{aligned} &b \times \gamma\rho \times \text{ave} \, (v_{m1} V_1^2 \cos^2 \phi_1 + v_{m2} V_2^2 \cos^2 \phi_2 + \ldots) \\ &= b \times \gamma\rho \times \tfrac{1}{2} \, (v_{m1} V_1^2 \, v_{m2} V_2^2 + \ldots) \end{aligned} \tag{3a}$$

where the averages have to be taken over a "sufficiently long" time interval. We have to find v_{m1}, v_{m2}, ... now from the usual criterion of equal energy dissipation in both cases.

If only one harmonic long wave is present with $v = V_1 \cos \phi_1$, we have ave$|\cos \phi_1|^3 = 4/3\pi$ and v_{m1} becomes $8/3\pi \times V_1$.

With more harmonic components simultaneously present, the evaluation of (3) is difficult since the sum $V_1 \cos \phi_1 + V_2 \cos \phi_2 \ldots$ will, in most cases, change of sign in an irregular way.

In the situation considered in this report, there is a large tidal motion upon which many components of higher frequencies and of much lower amplitudes are superimposed. (A rough estimate indicates that, not only for the vertical wave motion but also for the currents, the components with frequencies below (6 hours)$^{-1}$ dominate by far). We are interested here only in the v_m for the higher frequencies. We, therefore, take for v the simplified form

$$v = V_1 \cos \phi_1 + V_2 \cos \phi_2 \quad , \quad \phi_1 = \omega_1 t + X_1, \text{ etc.} \qquad (4)$$

in which $V_1 >> V_2$ and $\omega_1 << \omega_2$; $V_1 \cos \phi_1$ represents the tidal stream and $V_2 \cos \phi_1$ the small component. Under these conditions, the sign of v is nearly always given by the sign of $\cos \phi_1$ and we can write approximately:

$$\text{ave}|V_1 \cos \phi_1 + V_2 \cos \phi_2|^3 \approx \text{ave}(V_1|\cos \phi_1| + V_2 \cos \phi_2)^3$$

It is adequate to average over one period of the major component. The last expression then yields approximately:

$$\text{ave}\,\{V_1^3|\cos \phi_1|^3 + 3V_1V_2^2|\cos \phi_1|\cos \phi_2^2\}$$

$$\approx \frac{4}{3\pi} V_1^3 + \frac{3}{\pi} V_1V_2^2 \ .$$

It will be seen then that (3) can be made equal to (3a) if

$$v_{m1} = \frac{8}{3\pi} V_1 \quad \text{and} \quad v_{m2} = \frac{6}{\pi} V_1 \tag{5}$$

If many relatively small components of higher frequencies are taken, v_m for all of these will be the same: $\frac{6}{\pi} V_1$; thus for v_m in Equation (1), we may substitute $\frac{6}{\pi}$ times the local amplitude of the main tidal current.

9.2.2 The Magnitude of the Currents in the Fjord

Assume the presence of only one major tidal component in the fjord. Since the fjord is short compared with the length of this tidal wave, in the fjord we have only small variations of the vertical tidal amplitude H_1 and of the phase. In that case, the continuity equation can be applied in a simple form, in order to express the amplitude of the tidal flow, $Q_1(x) = A(x) \cdot V_1(x)$, in H_1:

$$Q_1(x) = \omega_1 H_1 \int_0^x d\xi \cdot b(\xi) \quad , \tag{6}$$

where ω_1 is the angular frequency of the tidal component.

The integral in this expression is readily determined from Fig. 1A. If we consider the M2-tide, $\omega_1 = 2\pi/44700 = 1.4 \times 10^{-4}$ sec^{-1}, with a vertical amplitude (half range) $H_1 = 0.5$ m, Eq. (6) yields for 3 cross-sections in the main fjord:

	Unit	Hjalteyri	Hrisey	Mouth of Olafsfjördur
Distance x	km	20.5	37.5	51
$\int_0^x d\xi \cdot b(\xi)$	km^2	73	172	310
Tidal flow amplt. Q_1	m^3/sec	5100	12000	21.700
Cross-sect. area A	10^3m^2	370	440	930
Tidal current ampl. $V_1=Q_1/A$	cm/sec	1.4	2.7	2.3

The resulting tidal current velocities appear to be quite small; only a few centimeters per second. We have to keep in mind, however, that these values for V_1 represent amplitudes of the average velocity over a large cross-section and that locally higher velocities will occur.

In fact, the "Arctic Pilot" of the British Admiralty [13] mentions the occurrence in the fjord of a "fairly strong out-going current during the great thaw in the spring, especially in the channels abreast Hrisey and in the vicinity of Latur" due to "the many rivers debouching into the fjord and the great quantity of melted snow that drains into it; this outgoing stream is always strongest on the eastern side of the fjord." All this refers, obviously to the current in the upper few meters.

The results of a number of serial observations of salinity and temperature were made available by the Institue for Marine Research at Reykjavik. On eight days, rather regularly spaced over the period from October 1959 to December 1960, such observations were made at three stations in the fjord: at x = 2 (off Oddeyri = Akureyri N, depth about 30 m), at x = 13 (near Dagverdareyri, depth about 75 m), and at x = 20 (off Hjalteyri, depth about 83 m). These data indicate the presence of strong vertical gradients of temperature, salinity and density in the upper 10 to 30 meters in the months of May to August, incl., which can be brought into accordance with the information of the "Arctic Pilot" given above. For the months October to March, incl., however, these data show that the water in the fjord was nearly homogeneous, with average salinities of 34.7 promilles (approximately the salinity in the ocean off the fjord) and salinity differences between surface and bottom of only 0.1 to 0.8 promilles. The water level records analyzed in this report were all taken in one of the months October to March, incl. It may thus be assumed that, at the times of recording, the quantity of fresh water in the fjord and the amount of density stratification were negligible

so that there were neither strong out-going surface currents nor internal waves in the fjord.

It may be concluded from the above that the currents in the fjord were very small indeed, which suggests that the energy dissipation by friction in the fjord would have been quite small too.

9.2.3 The Relation Between the Friction Coefficient γ and the Dissipation Parameter q_f.

The relevant formula is Eq. (1) of Section 9.1. If we assume γ to be independent of x, Eq. (1) can be written:

$$s_r q_f = \frac{\gamma}{2} \int_0^x d\xi \, \frac{v_m}{d\sqrt{gd}} \qquad (1a)$$

We have made a rough evaluation of the integral by considering the hypothetical simplified fjord whose width b and mean depth d are given by $b = b_0 x^m$ and $d = d_0 x^n$, respectively, the assumptions leading to the Bessel-type solution for the long-wave motion (Section 2.2). Eq. (6) of Section 9.2.2 then gives, for the amplitude of the tidal flow:

$$Q_1(x) = \frac{\omega_1 H_1 \, b(x) \cdot x}{m + 1}$$

or for the amplitude of the tidal current:

$$V_1(x) = \frac{\omega_1 H_1 x}{(m+1) \cdot d(x)}$$

Here we note that for small x, V_1 behaves as x^{1-n} so that it is necessary to assume $n < 1$ if V_1 is to approach zero at the head of the fjord ($x = 0$).

Fortunately, all the values for n previously estimated for the main fjord (see Sections 6.2, 7.2.1, and 7.2.2) are smaller than 1.

Moreover, if we put $v_m = \frac{6}{\pi} V_1$ according to Section 9.2.1, we see that the ratio v_m/d behaves as x^{1-2n} for small x. The form $\gamma v_m/(\omega d)$ appears in the Equations (7a) and (12) of Section 2.1 and it has been assumed there that this form is << 1 throughout. Therefore, it is even necessary to assume here $n < \frac{1}{2}$. Fortunately, this condition too is satisfied by the n-values previously estimated.

We then substitute in (1a):

$$v_m = \frac{6}{\pi} \cdot \frac{\omega_1 H_1 x}{(m+1)\, d} \quad \text{and} \quad d = d_o x^n$$

and find, with $\omega_1 = 2\pi/44700$ sec^{-1} (M2-tide), tidal amplitude $H_1 = 0.5$ m, $g = 9.82$ m.sec^{-2} for the integral in (1a):

$$\frac{43.10^{-6}}{(m+1)(2-\frac{5}{2}n)} \times \frac{x^2}{d^{5/2}}$$

The value is not very sensitive to changes in m and n.

The following table contains the values assumed for m, n and d and the resulting values of the integral in (1a) for three cross-sections in the fjord.

	Unit	Hjalteyri	Hrisey	Mouth of Olafsfjördur
Distance x	km	20.5	37.5	51
α for Hja and Hri	-	+0.15	+0.24	+0.06
m from chapter 7	-	0.53	0.40	0.6
n	-	0.20	0.15	0.3
d (smoothed)	m	55	60	70
Integral in Eq. (1a)	-	0.35	0.95	1.36

The values in the last line thus give the ratio $2s_r q_f/\gamma$.

9.3 Evaluation and Conclusion

In the end of Section 9.1, we pointed to an apparent discrepancy: the s_{1q} -values found for the inner parts of the fjord were larger than the $s_r q$-values 0.08 found for the whole fjord.

This discrepancy may be explained for a major part by the fact, already noted in Section 7.2.1, that the s_{1q}-values derived from the average first minimum of the amplitude ratio plots are over-estimated due to the "noise" in these plots. In addition, the smoothing effect due to the finite width of the "spectral window" function dealt with in Section 8.2.2 plays a role. The "best" ratio plots with relatively little noise (Figs. 7A-4 and 7A-5) suggest that these effects may account for a factor not higher than about 3. If the factor would be 3, the estimate for s_{1q} for Hrisey would become 0.07, which is still high with respect to the estimate for $s_r q$, 0.08, for the whole fjord. This might be an indication that the latter estimate is too low.

Now consider again the inner parts of the fjord, where we would expect the dissipation parameters q and s_{1q} to be merely determined by the effect of the friction and where the outward radiation of wave energy would not be expected to play a role.

A commonly occurring value for $\gamma = g/C^2$ with a sandy bottom is 4.10^{-3}, corresponding with a Chezy coefficient C = 50; for rough, rocky bottoms, γ may be about 10^{-2} and C about 30. If we consider Hrisey, for example, the latter value would, according to the table in Section 9.2.3, correspond with a value 0.005 for $s_r q_f$. This is far less than the already reduced value 0.07 for s_{1q} roughly estimated from the amplitude ratio plots in Section 7.2.1. We still have to explain a discrepancy factor of about 14 here.

The explanation may be found in the combined effect of several factors.

1. The non-uniform lateral and vertical distribution of the tidal currents will lead to a higher effective value for v_m in (1a) than that according to (5), due to the quadratic character of the friction law. Possibly this effect may account for a factor 2 to 3.

2. More important may be the increase in energy dissipation by the formation of large horizontal eddies caused by irregularities in the coastal and the bottom topography of the fjord.

3. The same irregularities may indeed give rise to some outward radiation of wave energy, even from the inner parts of the fjord.

4. Local winds may set up smaller scale water circulations in the fjord, which interfere with the long-wave motion and thus lead to an extra dissipation of the energy in the long waves.

5. In the estimation of s_{1q} from the amplitude ratio plots, we have used Eq. (5) of Section 7.2, which was based on the theory of Section 2.2. This equation therefore is an approximation only. It does not seem, however, that a large error has been introduced here.

It appears likely that the effects 2 and 3 mentioned above will account for the major part of the apparent discrepancy. It may be concluded that it is clearly impossible to separate quantitatively the "frictional" and the "radiational" parts of the energy dissipation. For Hrisey, the actual value of the total dissipation factor $s_r q$ may be roughly 0.06; this would give for the total dissipation parameter q, at k = 15, an estimate of 0.03; the effective value of the friction coefficient γ may be somewhere between 0.02 and 0.12.

10. Spectral Densities at Sea

Since no good water level records from outside the fjord could be obtained, spectral densities of the sea level variations off the mouth of the fjord could be estimated only indirectly and roughly. Some estimates were already presented in Section 8.2.1 and plotted in Fig. 8B (crosses); these estimates were used in the analysis of the first resonance peak at Akureyri.

It was considered that, in order to estimate spectral densities in the mouth of the fjord, perhaps Hrisey would be the best station to start from, because Hrisey is the most seaward located station with a good many reliable records. The coherency between the water level variations in the mouth of the fjord and at Hrisey would be expected to be better than the coherency between the water level variations in the mouth and at the more inward stations.

Adopting again the notation of Section 8.2.1, and introducing the suffix H for Hrisey, we have for the spectral density ratio between the mouth and Hrisey:

$$\frac{W^*_{Mkp}}{W^*_{Hkp}} = \frac{W_{Mkp}}{W_{Hkp}} = \left(\frac{r_{Mk}}{r_{Hk}}\right)^2 \quad , \tag{1}$$

where the asterisk (*) again denotes the expected value for the ensemble from which record nr · p is considered to be a sample, and where the amplitude ratios r_{Mk} and r_{Hk} (both with respect to Akureyri) are independent of p if we ignore the inchoerent parts of the records.

By means of this equation, then, W_{Mkp} can be estimated from observed values of W_{Hkp} and from assumed values for r_{Mk} and r_{Hk}, according to

$$W_{Mkp} = \left(\frac{r_{Mk}}{r_{Hk}}\right)^2 W_{Hkp} \tag{1a}$$

We shall only consider here k-values below 60 (where the coherencies are still reasonably good) and we shall use the W_{Hkp}-values of the records nr · 3, 4, 5, 6, 7 and 8 (plotted in Figures 6A-11 and 6A-12).

We assume, as we did in Section 8.2.1, that the spectral densities W_{Mkp} in the mouth and W_{Skp} in the open sea do not differ much if k is outside the k-ranges of fjord resonance, that is, if k is <u>not</u> in the ranges 10 to 14, 24 to 30, 39 to 45, etc. (compare Section 8.2.1 (Step 1): $r_{Mk} = |J_o(s)|$ with $s = (k/12.0) \times 2.405 = 0.200\ k$.

The amplitude ratios r_{Hk} were dealt with in Section 7.2.1. It was found there that r_{Hk} has minima at k about 15 and about 39, two k-values at which the longitudinal wave motion in the fjord apparently has a node near Hrisey and for which r_{Hk} is determined to a large extent by the dissipation and thus is less certain. Considering that r_{Hk}^2 appears in the denominator in (1a), we therefore have excluded the k-ranges 15 to 18 and 36 to 38 as well. Only the following four k-ranges were finally considered for estimating W_{Mkp}: 7 to 9 incl., 19 to 23 incl., 31 to 35 incl. and 48 to 52 incl.

In Section 7.2.1, the best fitting Bessel-type expression for the amplitude ratios r_{Hk} of Hrisey was found to be that with $\alpha = +0.24$. That result, of course, is strictly incompatible with the assumption that the wave motion in the whole fjord can be described by the Bessel function $J_o(\alpha = 0)$, which reminds us of the fact that these Bessel-type expressions can only be more or less rough approximations for a real fjord. For the present purpose, it was considered better to approximate r_{Hk} by a J_o-function as well, but adapted as follows: for k = 7-9 and 19-23: $r_{Hk} = |J_o(s)|$ with $s = 0.158\ k$, the constant being chosen such that r_{Hk} is zero at k = 15.2; for k = 31-35 and 48-52: $r_{Hk} = |J_o(s)|$ with $s = 0.143\ k$, the constant being chosen such that r_{Hk} is zero at k = 38.6; compare the table in Section 7.2.1.

The following table shows the assumed values for r_{Mk} and r_{Hk}.

k	Assumed values of $\pm r_{Mk}$	$\pm r_{Hk}$	
	$J_o(0.200k)$	$J_o(0.158k)$	$J_o(0.143k)$
7	.567	.715	
8	.455	.639	
9	.340	.556	
19	- .403	- .260	
20	- .397	- .309	
21	- .377	- .349	
22	- .342	- .377	
23	- .296	- .395	
31	.202		- .336
32	.243		- .303
33	.274		- .264
34	.293		- .222
35	.300		- .178
48	- .209		.296
49	- .232		.300
50	- .246		.297
51	- .250		.289
52	- .243		.274

The simple calculation according to (1a) was executed for each of the 18 k-values selected and for each of the 6 Hrisey spectra considered. For each of the six spectra, the resulting W_{Mkp}-values were averaged for each of the 4-k ranges to obtain estimated W^*_{Mkp}-values for k = 8, 21, 33 and 50, respectively. The results were plotted in Fig. 8B as small circles which were connected by broken lines. It should be noted that, apart from the uncertainties in r_{Mk} and r_{Hk}, there is a standard sampling error of about 55 percent in the spectral estimates at k = 8. The wiggles shown for the records 3, 4, 6, and 8 may therefore not be significant and a general decrease of spectral density with increasing frequency is indicated.

It will be seen that the estimates obtained for k = 8 do not deviate much

from the estimates (indicated by crosses) derived from the Akureyri spectra in Section 8.2.1.

Interpolation between the W-values for k = 8 and k = 21 might present an alternative, and thus a check, for Step 5 of the procedure described in Section 8.2.1. The following table compares the estimated values of $r_{Sk}^{-1} (1 + \varepsilon_{kp})^{\frac{1}{2}}$ for k = 12 according to both interpolation methods (compare the second table of Section 8.2.1).

Record nr.	Interpolation based on spectral data of: Akureyri (Section 8.2.1)	Hrisey
1	29.2	-
2	17.5	-
3	13.8	16.3
4	5.4	7.2
5	6.1	4.6
6	8.4	6.2
7	33.1	22.5
8	7.9	7.8
Average for 6 last records	12.4	10.8
Average for 8 records	15.2	13.9

(In the last Figure (13.9), the estimates of the first column for records 1 and 2 were also used). The second method thus gives roughly 10 percent lower values for the amplitude amplification factors in the first resonance peak. A deviation of this order of magnitude is not at all surprising. The relative shape of the peak, however, will be hardly affected.

Returning now to Fig. 8B, we can see by looking at the wind data given in Appendix 3 that the records with the highest wind forces at Grimsey (nrs. 6, 7 and 8) have the highest spectral densities and the records with the lowest wind forces (nrs. 1, 3 and 4) have spectral densities that are among the lowest.

The following table presents estimated spectral densities (ranges) as found here, together with data from some published sample spectra from other locations. All densities have been expressed in mm^2/mHz.

Frequency, mHz Period	0.05 5.6h	0.1 2.8h	0.2 1.4h	0.33 50 min	0.5 33 min	1 17 min
Off Eyjafjördur (Fig. 8B)	-	100-2000	10-500	5-500	5-300	4-60(1)
La Jolla, Calif [14]	200-500	50-200	10-50	10-20	3-10	3-10
San Clemente Isl. Cal. [14]	200-500	50-100	3-10	5-10	2-5	2-5
Guadelupe Isl. Mex. [14] [15]	-	-	0.5-1	0.5-1	0.5-1	0.5-1
La Jolla, Calif. [16]	150	-	-	-	-	-
Oceanside, Calif. [17]	-	-	-	40-60	20-50	20-50
Thorlakshofn, S.W. Icel. [18]	-	-	-	70	50	100
Texas Tower Nr. 4 [18]	-	-	-	70	30	40
Azores [18]	-	-	-	4	1	<1

(1) Estimates for Hrisey (see Fig. 6C).

Our estimates for the shelf of Eyjafjördur are not inconsistent with the various spectral densities observed earlier at other locations, if it is

remembered that our estimates refer mainly to gale conditons. The low values for the small oceanic island of Guadelupe are considered by Munk, Snodgrass e.a. to be representative of the overall long-wave activity in the deep ocean.

It is not appropriate here to speculate further about the properties of the long waves off Eyjafjördur.

REFERENCES

1. Schonfeld, J.C., "Tides in Funnel-Shaped Channels," Rijkswaterstatt Nota CSD 55-16 N, (The Hague), 1955.

2. Schuster, A. "The Periodogram and its Optical Analogy", Proc. Roy. Soc. A (London) 77, 1906, pp. 136-40.

3. Jones, R. H., "A Reappraisal of the Periodogram in Spectral Analysis", Technometrics 7 (4), 1965, pp. 531-42.

4. Bendat, J. S. and Piersol, A. G., "Measurement and Analysis of Random Data", 1966, 390 pp. (Wiley), See p. 213.

5. Blackman, R. B. and Tukey, J. W., "The Measurement of Power Spectra", 1958, (Dover Publications).

6. Defant, A., "Physical Oceanography", Vol. II, 1961 (Pergamon) See p. 174.

7. Raichlen, F., "Harbor Resonance", Estuary and Coastline Hydrodynamics, Chapter 7, A. T.Ippen, Editor, 1966, McGraw-Hill, pp 307-309.

8. For work published prior to 1966, see Raichlen, F., "Harbor Resonance", Chapter 7 in Estuary and Coastline Hydrodynamics, (A.T. Ippen, Editor) 1966, (McGraw Hill), pp 292-340.
   Some later publications
   Momoi, T., "A Long Wave in a Rectangular Bay - Case of Normal Incidence", Bull. Earthquake Res. Inst. Univ. of Tokyo, 48(5), 1970, pp. 871-91 and earlier publications of this author in the same journal;

   Hwang, Li-San, and Tuck, E. O., "On the Oscillations of Harbours of Arbitrary Shape", J. Fluid Mechanics, 42(3), 1970, pp. 447-64;

   Lee, Jiin-Jen, "Wave Induced Oscillations in Harbours of Arbitrary Geometry", J. Fluid Mechanics, 45(2), 1971, pp. 375-94.

9. Kinsman, B., "Wind Waves", 1965 (Prentice Hall, Inc.), pp. 325-329.

10. Raichlen, F. as ref. (7), pp. 281-283 and 304-305. Note: formula (7.77) on p. 304 is incorrect.

11. Duff. G., "Tidal Resonance and Tidal Barriers in the Bay of Fundy System", J. Fish. Res. Bd. Canada 27(10), 1970, pp. 1701-1728.

12. Dronkers, J. J., "Tidal Computations in Rivers and Coastal Waters", 1964 (North Holland Publishing Company), see Chapter VIII, Sections 3.1-3.3.

13. British Admiralty, Arctic Pilot Vol. II, 6th Edition, 1961. p. 270, line 31.

14. Snodgrass, F. E., Munk, W. H., and Miller, G. R., "Long period Waves over California's Continental Borderland", Part I, Background Spectra, J. Marine Res. 20(1), 1962, pp. 3-30, See Fig. 2.

15. Munk, W. H., Snodgrass, F. E., and Tucker, M. J., "Spectra of Low-Frequency Ocean Waves", Bull. Scripps Inst. Oceanography, 7(4), 1959, pp. 283-361. See Chart 2.11.

16. Munk, W. H., and Bullard, E. C., "Patching the Long-Wave Spectrum Across the Tides", J. Geophysical Res. 68(12), 1963, pp. 3627-3634. See Fig. 2.

17. Munk, W. H., Snodgrass, F. and Gilbert, F., "Long Waves on the Continental Shelf: An Experiment to Separate Trapped and Leaky Modes", J. Fluid Mech., 20(4), 1964, pp. 529-554, See. Fig. 5.

18. Donn, W. L., Pattulo, J. G., Sham, D. M., "Sea Level Fluctuations and Long Waves", Research in Geophysics, (M.I.T. Press), Vol. 2, 1964, pp. 243-269. See. Fig. 15.

19. Munk, W. H., Cartwright, D. E., "Tidal Spectroscopy and Prediction", Phil. Trans. Roy. Soc. London Series A No. 1105, Vol. 259, 1966, pp. 533-581, See Appendix B, p. 580.

APPENDIX 7

1. Computation procedures

1.1 The records analyzed are continuous ink records on paper chart, of water level against time; height scale is 1:10, nominal time scale is 6 inches per hour. The records have been digitized by means of a curve follower with punched paper tape as output. The sampling interval of the curve follower can be varied with steps of 0.1 mm; in this case, 5.1 mm was taken corresponding with a time interval of approximately 2 minutes.

For the computation of cross-correlations between various simultaneous records, it is necessary that the samples of these records are taken at exactly equal points of time. Because of the fact that for each registration the time scale was not quite a constant due to slight irregularities in the frequency of the a.c. electric generator and to slight length variations of the paper chart, it was judged necessary by means of interpolation to compute from the output of the curve follower a new record in which the various values occur at well defined points of time.

The structure of a record after digitizing is as follows:

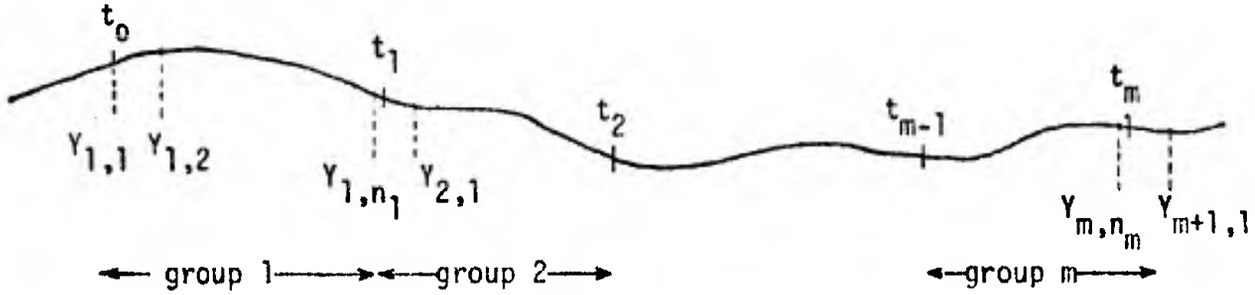

t_1, t_2, ... t_{m-1} are time marks given on the record with indicated exact time from a chronometer reading of the Icelandic operator. In a record of 24 hours duration, there are generally 3 to 5 such time checks. Suppose, it was decided that the record to be analyzed is to start at time t_0 and to end at

time t_m. These two points were indicated in the record, as deduced from a linear interpolation between t_1 and the previous time mark, and between t_{m-1} and the next time mark, respectively.

The values $y_{1,1}$ (at t_o), $y_{1,2}$ ... $y_{m+1,1}$ are ordinate samples of the record, obtained by means of the curve follower. The intervals between successive samples are constant as expressed in millimeters, viz., 5.1 mm. It was assumed that within each group 1, 2, ..., m, of samples lying between two consecutive time checks, the time interval was constant. These intervals are denoted by Δt_1 , Δt_2 ,... Δt_m (all close to 2 minutes).

The time marks, in general, situated between the values of the record, are distinguished from them by means of a separation mark. The points of time of the first samples coming after each time mark, $y_{2,1}$, $y_{3,1}$ ... $y_{m+1,1}$, are deduced by the operator from the values t_1, t_2 ... t_m and are punched. Then, by counting the number of values n_j occurring in each group j, the time interval Δt_j between the samples within each group can easily be computed.

By linear interpolation, a new series of values f'_{-n}, ... f'_n is then computed from the values $y_{1,1}$ ... $y_{m+1,1}$. The time interval Δt between any two successive elements of this series is supposed to be constant. For all computations Δt has been chosen as Δt = 2 minutes.

1.2 In order to avoid undesirable effects in the spectra (see par. 4 of the main report), the values f_j, j = -n ... n were multiplied by the function

$$\tfrac{1}{2}(1 + \cos \frac{\pi j}{n}) \qquad j = -n \ldots n$$

Thus, f_j was replaced by

$$f_j = \tfrac{1}{2} f_j (1 + \cos \frac{j}{n}) \qquad j = -n \ldots n$$

1.3 The whole computation consists of the following steps:

A varying number pb of simultaneous records are read. By linear interpolation values of these records are known at the same points of time for each of these records. The records are denoted by

$$f_{-n}^{(k)}, \ldots f_{n}^{(k)} \qquad k = 1,2 \ldots pb.$$

One wants to compute the following properties of these functions.

- The spectrum $g_k(f)$ $\quad k = 1, 2, \ldots pb$

  for $f = 0, (\frac{1}{2n\,\Delta t}), \frac{1}{2\Delta t}$.

- The cross-spectra $S_{\ell,j}(f) = C_{\ell,j}(f) + iQ_{\ell,j}(f)$, $i,j = 1, 2, \ldots pb$. $C_{\ell,j}(f)$ and $Q_{\ell,j}(f)$ being the cospectrum and the quadspectrum of the functions $f^{(1)}$ and $f^{(j)}$.

- Average values of $g_k(f)$, $C_{\ell,j}(f)$ and $Q_{\ell,j}(f)$ over a number of different frequencies. It is well known that periodogram estimates, as are computed here, may be considered as variates having approximately a χ^2 distribution with only two degrees of freedom. An average over m successive periodogram estimates gives a variate with 2m degrees of freedom. This averaging has been carried out for both spectra and cross-spectra.

Denoting the average values as

$$\overline{g}_k(f,m),\ \overline{C}_{\ell,j}(f,m),\ \overline{Q}_{\ell,j}(f,m),$$

the coherency function can be found by

$$r^2_{\ell,j}(f,m) = \frac{\overline{C}^2_{\ell,j}(f,m) + \overline{Q}^2_{\ell,j}(f,m)}{\overline{g}_{\ell}(f,m)\ \overline{g}_{j}(f,m)}$$

1.3.1 The computation of the spectra and the cross-spectra for $f = 0, \left(\frac{1}{2n\Delta t}\right), \frac{1}{2\Delta t}$.

The energy spectrum of a finite, continuous function of $f^{(k)}(t)$ can be obtained by

$$\beta_k(f) = \frac{1}{T}\left[\int_{-T/2}^{T/2} f^{(k)}(t)\, e^{2\pi i f t}\, dt\right]^2$$

$$= \frac{1}{T}\left[\int_{-T/2}^{T/2} f^{(k)}(t) \cos 2\pi f t\, dt\right]^2$$

$$+ \frac{1}{T}\left[\int_{-T/2}^{T/2} f^{(k)}(t) \sin 2\pi f t\, dt\right]^2$$

The cross-spectrum $S_{\ell,j}$ of two functions $f^{(\ell)}(t)$ and $f^{(j)}(t)$ can be obtained by

$$S_{\ell,j}(f) = \frac{1}{T}\int_{-T/2}^{T/2} f^{(\ell)}(t)\, e^{2\pi i f t}\, dt \int_{-T/2}^{T/2} f^{(j)}(t)\, e^{-2\pi i f t}\, dt$$

The spectrum and the cross-spectrum are computed for $f = 0, \left(\frac{1}{2n\Delta t}\right), \frac{1}{2\Delta t}$.

Let $\frac{1}{2n\Delta t} = \Delta f$ and $\beta_k(s\Delta f) = \beta_{k,s}$ and $S_{\ell,j}(s\Delta f) = S_{\ell,j;s}$.

For the digitized functions, the integrals from the above mentioned formulae are approximated by

$$\Delta t\, a_{k,s} = \Delta t\left\{\frac{1}{2}\left(f^{(k)}_{-n} + f^{(k)}_{n}\right)\cos \pi s + \sum_{r=-n+1}^{n-1}\left(f^{(k)}_{-r} + f^{(k)}_{r}\right)\cos\frac{\pi s r}{n}\right\}$$

$$s = 0, 1, 2, \ldots, n$$

$$\Delta t\, b_{k,s} = \Delta t \sum_{r=-n+1}^{n-1} (f^{(k)}_{-r} - f^{(k)}_{r} \sin \frac{\pm sr}{n}$$

$$s = 1, 2, \ldots, n-1$$

$$b_{k,o} = b_{k,n} = 0$$

By means of the coefficients $a_{k,s}$ *and* $b_{k,s}$, the spectra and the cross-spectra can be expressed as

$$\beta_{k;s} = \frac{\Delta t}{2n} (a^2_{k;s} + b^2_{k;s})$$

$$C_{\ell,j;s} = \frac{\Delta t}{2n} (a_{\ell;s}\, a_{j;s} + b_{\ell;s}\, b_{j;s})$$

$$Q_{\ell,j;s} = \frac{\Delta t}{2n} (a_{\ell;s}\, b_{j;s} - a_{j;s}\, b_{\ell;s})$$

1.3.2 The computation of the averaged values.

Let for $f = ms\Delta f$ $\overline{\beta}_k(f;m)$ be denoted as

$\overline{\beta}_k(f;m) = \overline{\beta}_{k;ms,m}$ and in the same way

$\overline{C}_{\ell,j}(f;m) = \overline{C}_{i,j;\, ms,\, m}$

$\overline{Q}_{\ell,j}(f;m) = \overline{Q}_{i,j;\, ms,\, m}$

These values are found from

$$\overline{\beta}_{k;ms,m} = \frac{1}{m} \sum_{\ell=0}^{m-1} \beta_{k;ms\, -\, \frac{m-1}{2}\, +\, \ell}$$

$$\overline{\beta}_{k;o,m} = \frac{\beta_{k;o} + 2(\beta_{k;1} + \ldots. + \beta_{k;\, \frac{m-1}{2}})}{m}$$

$$\overline{C}_{\ell,j;ms,m} = \frac{1}{m} \sum_{\ell=0}^{m-1} C_{\ell,j;ms - \frac{m-1}{2} + \ell}$$

$$\overline{Q}_{\ell,j;ms,m} = \frac{1}{m} \sum_{\ell=0}^{m-1} Q_{\ell,j;ms - \frac{m-1}{2} + \ell}$$

$$r^2_{\ell,j;ms,m} = \frac{\overline{C}^2_{\ell,j;ms,\,m} + \overline{Q}^2_{\ell,j;ms,\,m}}{\overline{\beta}_{\ell;ms,m} + \overline{\beta}_{j;ms,m}}$$

These computations have been carried out for the three values of m: m = 5, m = 11, m = 21.

2. Description of the Algol programme.

2.1 The flow-chart

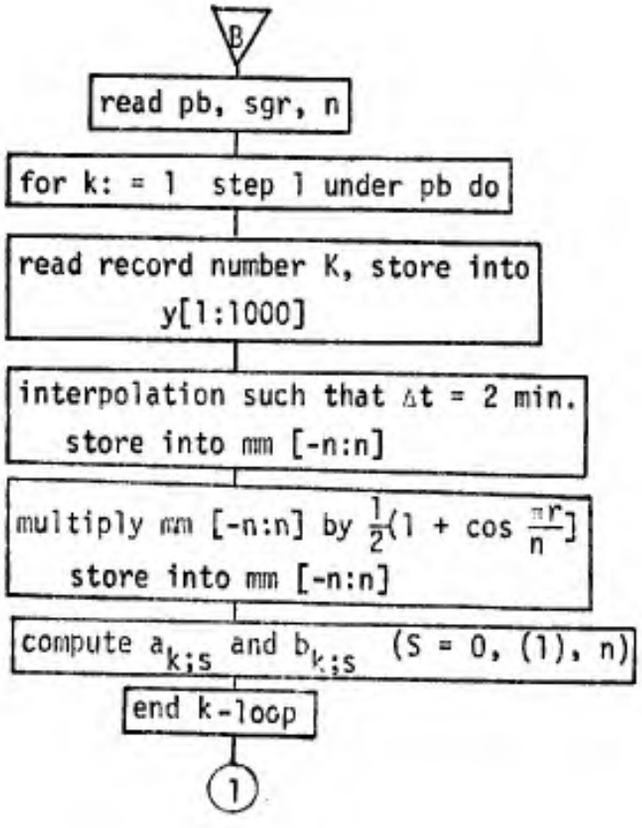

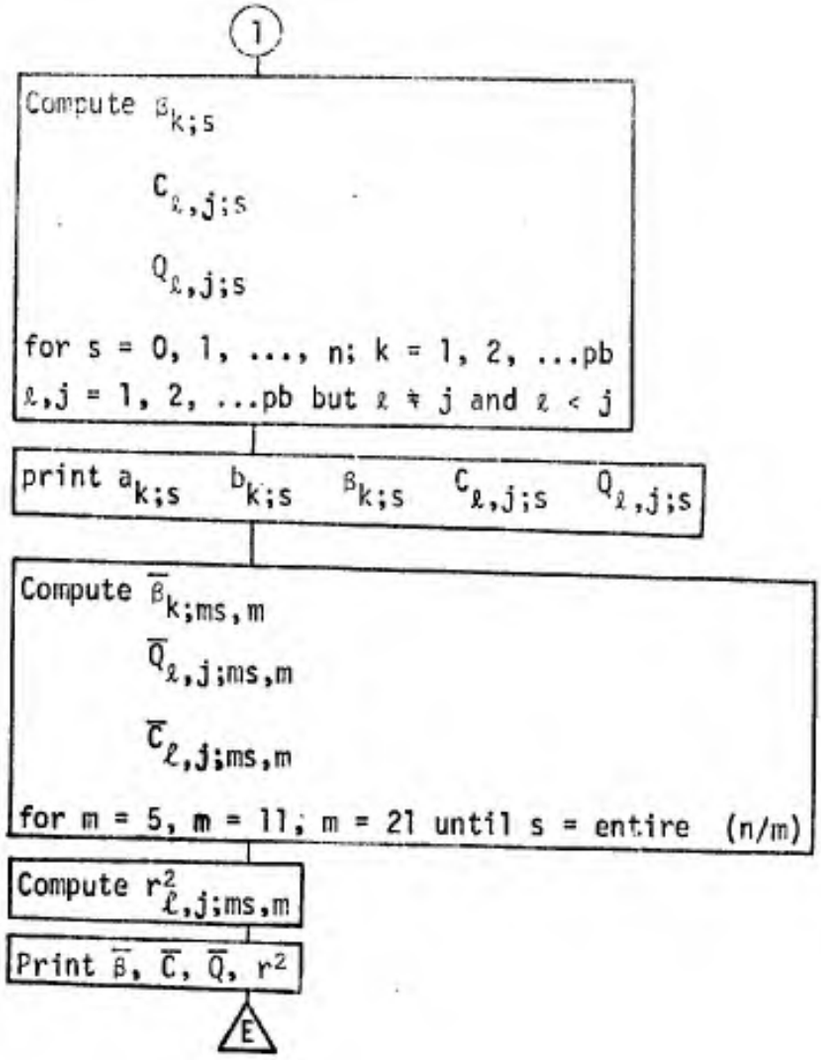

2.2 Procedures

- The procedure gepucona, which is a procedure written in the external code of the T.R.-4 computer, reads and interpretes a number which is in the code of the curve follower, moreover, it checks the number being read whether it is a value of the registration, a point of time or the end mark of the registration.
- The procedure uitvoer (cv, ca, gr, og, bg, zz, sf) provides for the output of an array zz(og:bg) as fixed point values with cv locations before the decimal point and ca locations after it. gr is the desired number of elements of zz to be printed on one line. sf is a scaling factor.

- vasko (a, b, $c_1 \ldots c_n$) prints $c_1 \ldots c_n$ as fixed point values with a locations before the decimal point and b locations after it. $c_1 \ldots c_n$ may be arithmetic expressions or elements of an array.

2.3 Some important variables

(a) pb, is the number of records to be processed simultaneously.

(b) sgr, because of the limited core storage of the actual computer not all of the computation could be performed in one run. sgr defines the number of spectral and cross spectral estimates that could be computed successively. The complications which were caused by the storage limitations are not treated here, having no essential influence on the results.

(c) n, a record consists of 2n + 1 numbers.

(d) y(0:1000), in this array, the numbers as they are read from the paper tape are stored.

(e) mm(-n:n), in this array, the interpolated values $f'_{-n} \ldots f'_n$ are stored and after the multiplication by $\frac{1}{2}(1 + \cos \frac{\pi j}{n})$, the values, such as $f_{-n} \cdots f_n$.

(f) tijdstip (1:2), the points of time defining the beginning and the end of any group $y_j \ldots y_{j+l,l}$ are stored in this array.

(g) deltat (1:10), the intervals Δt_j are stored in deltat (1:10), the programme accepts records with up to 10 groups with different intervals.

(h) a, b(1:pb, o:n), $a_{k;s}$ and $b_{k;s}$ are stored in these arrays.

(i) c, q, gec, gec, gamma, gebet, bet, in these arrays are stored $C_{\ell,j;s}$, $Q_{\ell,j;s}$, $\overline{c}_{\ell,j;ms,m}$, $\overline{Q}_{\ell,j;ms,m}$, $r^2_{\ell,j;ms,m}$, $\overline{s}_{k;ms,m}$, $s_{k;s}$. The complicated structure is caused by the under sgr mentioned, limited storage of the computer and the measures that have been taken to cope with this situation.

APPENDIX 2

List of Figures with Explanatory Notes

1A Plot of width b and mean depth d against distance x for Eyjafjördur. Linear - linear.

1B The same but double logarithmic.

2A Zeros s_1, s_2 and s_3 of Bessel function $J_{-\alpha}(s)$ against α.

2B Ratios between zeros and levels of secondary maxima of $|H_\alpha|$ against α.

2C $|s \frac{dH_\alpha}{ds}|$ in zeros against α; α as a function of the geometric parameters m and n.

2D Modulus and argument of $J_0\{s_r(1 - iq)\}$ with q = 0 (curves (a)) and q = .199 (curves (b)) respectively, against s_r. Four small circles in lower graph: approximation of $|J_0\{s_r(1 - .199\ i)\}|$ by Expression (5) or (6) in Section 7.2.

4A "Spectral window function" P(|k-f|) after use of cosine square taper, against k-f.

5A Plots of digitized simultaneous records (samples). Abscissa: time. Ordinate: water level with respect to the mean level for the analyzed segment, after correction of time deviations by the computer (ref. App. 1) at intervals of 2 minutes.

1. Part from records nr. 7: Hrisey, Hjalteyri, Akureyri S.
2. Part from records nr. 10: Hrisey, Akureyri N, Olafsfjördur.

6A Autospectra. Abscissa k from 4 to 56 (frequency from about .04 to .63 mHz). Ordinate linear, spectral density W_k in uts of 80 mm^2/mHz. For k > 30, W_k-values lower than 1 unit not plotted.

- Akureyri S, record nr. 1
- Akureyri S, record nr. 2
- Akureyri S, record nr. 3
- Akureyri N, record nr. 4
- Akureyri S, records 5 and 6
- Akureyri S, record nr. 7
- Akureyri S, record nr. 8
- Hjalteyri, records 3 and 4
- Hjalteyri, records 5 and 6
- Hjalteyri, records 7 and 8
- Hrisey, records 3, 4, 5 and 6
- Hrisey, records 7 and 8

6B Autospectra. Abscissa k from 10 to 160 (frequency from about .11 to 1.80 mHz). Ordinate logarithmic, spectral density W_k averaged over 5 successive k-values, in units of 80 mm^2/mHz.

- Akureyri S, record nr. 6
- Akureyri S, record nr. 8

6C Autospectra. Abscissa k from 10 to 140 (frequency from about .11 to 1.57 mHz). Ordinate logarithmic, same as B above.

- Hrisey, records 3, 4, 5, 6, 7 and 8
- Hjalteyri, records 3, 4, 5, 6 and 7

6D Autospectra Olafsfjördur. Abscissa k' with common frequency scale, about .06 to 3.5 mHz. Ordinate linear, spectral density W_k, partly per k' number, partly W_k averaged over 5 successive k'-values, in units of 80 mm^2/mHz.

- Olafsfjördur, records 10, 11, 12 and 14

6E Autospectra Olafsfjördur. Abscissa frequency from about .2 to 4.17 mHz (Nyquist freq.). Ordinate logarithmic, spectral density W_k averaged over 5 successive k'-values, in units of 80 mm^2/mHz.

- Olafsfjördur, records 10, 11, 12 and 14

6F Average relative spectra Akureyri S for records 1 to 8 incl., and for three k-ranges; 7 to 17, 18 to 35 and 36 to 53. Abscissa k. Ordinate: over all 8 records averaged value of the ratio: β_k divided by β_k averaged, per spectrum, over the k-range considered.

- Akureyri S, records 1 - 8 combined (record 4: AkN).

The leading number 7 refers to plots of amplitude ratios and phase differences for pairs of stations against the Fourier component number ("ratio plots"). The second station is normally Akureyri S (head of the fjord) or, in a few cases,

Akureyri N. Note: one k-unit corresponds with .0112 mHz. For convenience, the first plot in each category in general also gives frequency and period scale.

Several plots give values derived from average W- (or ϕ-), C- or Q-values over five consecutive k- (or k'-) numbers; in the Figures 7A, B, C and G, this was done as horizontal line segments.

Wherever relevant, coherencies as calculated over 5 consecutive k- or k'- numbers (according to Eq. (5) of Section 4.1) are given along the top side of the figures. Coherency values lower than .60 were underlined or were put a little lower than the others.

Different symbols are used for the points and line segments, according to the order of magnitude of the smallest W_k- or average W-value of the pair concerned, to indicate the increasing influence of incoherent noise as this magnitude decreases:

smallest W- or W-value	symbols
> 10 x 80 mm²/mHz	⊕ ———
1 to 10 x 80 mm²/mHz	+ ———
.1 to 1 x 80 mm²/mHz	x — — —
.01 to .1 x 80 mm²/mHz	< - - - - - - -
.001 to .01 x 80 mm²/mHz	, - - - - -

Curves have been drawn subjectively to show, or to suggest, a probable shape of the curve if there were no noise.

7A Ratio plots. Abscissa k from 1 to 56 (frequency from about .01 to .63 mHz). Ordinates 1o amplitude ratio r; 2o phase difference ϕ.

(1) Hrisey - Akureyri S, records nr. 3
(2) Hrisey - Akureyri N, records nr. 4
(3) Hrisey - Akureyri S, records nr. 5
(4) Hrisey - Akureyri S, records nr. 6

(5) Hrisey - Akureyri S, records nr. 7
(6) Hrisey - Akureyri S, records nr. 8
(7) Hjalteyri - Akureyri S, records nr. 3
(8) Hjalteyri - Akureyri N, records nr. 4
(9) Hjalteyri - Akureyri S, records nr. 5
(10) Hjalteyri - Akureyri N, records nr. 5
(11) Hjalteyri - Akureyri S, records nr. 6
(12) Hjalteyri - Akureyri S, records nr. 7
(13) Hjalteyri - Akureyri S, records nr. 8 (no ϕ plot)

7B Ratio plots. Abscissa k from 50 to 107 (frequency from .56 to 1.20 mHz). Ordinates as above.

(1) Hrisey - Akureyri S, records nr. 6
(2) Hrisey - Akureyri S, records nr. 7
(3) Hjalteyri - Akureyri S, records nr. 6
(4) Hjalteyri - Akureyri S, records nr. 7

7C Ratio plot. Abscissa k' from 1 to 52 (frequency from about .01 to .62 mHz). Ordinates as above.

(1) Hrisey - Akureyri S, records nr. 9

7D Ratio plot. Abscissa k' from 1 to 34 (frequency from about .02 to .64 mHz). Ordinate amplitude ratio r.

(1) Hrisey - Akureyri N, records nr. 10
(2) Olafsfjördur - Akureyri N, records nr. 10

7E Ratio plots. Abscissa k from 10 to 140 (frequency from about .11 to 1.57 mHz). Ordinate amplitude ratio, from average W-values over five consecutive k-numbers.

(1) Hrisey - Akureyri S, records nr. 3, 4, 5, 6, 7 and 8
Hrisey - Akureyri N, records nr. 4
(2) Hjalteyri - Akureyri S, records nr. 3, 5, 6, 7
Hjalteyri - Akureyri N, records nr. 4

7F Ratio plot. Abscissa k' from 10 to 140 (frequency from about .11 to 1.75 mHz). Ordinate as above.

(1) Hrisey - Akureyri S, records nr. 9

7G Ratio plots. Abscissa k from 1 to 110 (frequency from about .01 to 1.23 mHz). Ordinates lo amplitude ratio r; 2o phase difference ϕ.

(1) Dagverdareyri - Akureyri S, records nr. 1
(2) Dagverdareyri - Akureyri S, records nr. 2
(3) Dagverdareyri - Akureyri S, records nr. 3
(4) Dagverdareyri - Akureyri N, records nr. 4
(5) Dagverdareyri - Akureyri S, records nr. 5

7H Ratio plots. Abscissa k from 10 to 280 (frequency from about .1 to 3.1 mHz). Ordinates from average values over five consecutive k-numbers, plotted only if W_k for Akureyri S is .02 x 80 = 1.6 mm^2/mHz at least: 1o. amplitude ratio r; 2o. phase difference ϕ.

(1) Akureyri N - Akureyri S, records nr. 1
(2) Akureyri N - Akureyri S, records nr. 2
(3) Akureyri N - Akureyri S, records nr. 3
(4) Akureyri N - Akureyri S, records nr. 5
(5) Akureyri N - Akureyri S, records nr. 6
(6) Akureyri N - Akureyri S, records nr. 8

7I Ratio plot. Abscissa k' from 1 to 28 (frequency from about .02 to .63 mHz). Ordinate amplitude ratio r.

(1) Olafsfjördur - Akureyri N - records nr. 14

8A Crosses: estimated values for amplitude ratio r_{Sk} between the sea off the fjord entrance and Akureyri, and for r_{Sk}^{-1}. Circles: pre-assumed values for r_{Sk} and for r_{Sk}^{-1}: $r_{Sk} = |J_0(s)|$ with s = .2004 k. Dotted line: estimated "real" amplitude ratio as function of f. Abscissa: k = Fourier component number, or f = wave frequency in units of .0112 mHz.

8B Double logarithmic plots of estimated spectral densities W^*_{Skp} at sea off the fjord entrance against the Fourier component number k. Crosses connected by full lines: estimated from Akureyri spectra; ref. Section 8.2.1. Circles connected by broken lines: estimated from Hrisey spectra, ref. Chapter 10. p is number of record.

8C Crosses: estimated values for r_{Sk}^{-2} = inverse square of amplitude ratio between the sea off the fjord entrance and Akureyri. Circles: pre-assumed values for r_{Sk}^{-2} : $r_{Sk} = |J_0(s)|$ with s = .2004 k. Symmetrical high topped curve: estimated "real" energy amplification factor as

function of f; ref. section 8.2.2. Abscissa: k = Fourier component number, or f = wave frequency in units of .0112 mHz.

APPENDIX 3

Atmospheric Pressure and Wind Data

Atmospheric pressure at Akureyri, in millibar, either obtained from the Icelandic meteorological service, or read from surface weather maps.

Wind direction and force in Beaufort scale at Grimsey and Akureyri, data obtained from the Icelandic meteorological service.

Record Nr.	Year	Date	Local Time h	Barom. mbar	Wind Grimsey	Wind Akureyri
	1966	8 Dec.	23	996	NNE 9	N 6
		9 Dec.	2	998		NW 6
			5	1001		NNW 6
			8	"	NNW 8	NNW 5
			11	"	NW 6	N 6
			14	"	NW 4	W 3
1			17	1002	N 5	SE 3
1			20	1001		SSW 1
1			23	"	N 5	Calm
1		10 Dec.	2	"		SE 1
1			5	"		SE 2
1			8	1002	W 4	SSE 2
1			11	"	NNE 4	SSE 2
1			14	"	NNE 4	SSE 2
			17	"	ENE 3	SSE 1
			20	"		Calm
14			23	1001	ESE 3	Calm
14		11 Dec.	2	1000		SSW 1
14			5	999		SSW 1
14			8	998	ESE 5	Calm
			11	"	ESE 5	Calm

Record Nr.	Year	Date	Local Time h	Barom. mbar	Wind Grimsey	Wind Akureyri
	1967	20 Feb.	2			NW 2
			5			N 3
			8		E 7	N 3
			11	984	ENE 7	NW 3
2			14		ENE 8	NNE 3
2			17		NE 8	NW 3
2			20			NW 3
2			23	985	NNE 8	NNW 3
2		21 Feb.	2			NNW 3
2			5			NNW 3
2			8		NE 8	NNW 3
2			11	995	ENE 7	NNW 3
2/3			14		E 7	W 1
3			17		E 6	Calm
3			20			Calm
3			23	1000	E 5	W 1
3		22 Feb.	2			W 2
3			5			Calm
3			8		E 4	Calm
3/4			11	1002	E 5	Calm
3/4			14		E 5	Calm
4			17		E 5	SSE 1
4			20			Calm
4			23	1003	ESE 4	S 1
4		23 Feb.	2			Calm
4			5			Calm
4			8		ESE 2	SSE 2
4			11	1002	ESE 2	SE 2

Record Nr.	Year	Date	Local Time h	Barom. mbar	Wind Grimsey	Wind Akureyri
	1967	14 Mar.	2			W 1
			5	992		W 3
			8		E 10	W 2
			11	985	E 9	N 4
			14		E 8	N 4
5			17	987	ENE 8	NW 6
5			20		NE 8	N 5
5			23	993	NE 8	N 4
5		15 Mar.	2			N 4
5			5	1000		NNW 5
5			8		NNE 5	NW 5
5			11	1005	NNE 4	NW 4
5			14		NE 2	NNE 2
5			17	1008	NE 2	NNW 3
			20		NE 3	Calm
			23	1010	E 3	Calm
		16 Mar.	2			NNW 2
			5	1007		SSE 3
			8		SE 2	SE 3
			11	1002	SE 2	Calm
			14		ESE 3	NW 2
			17	985	ESE 6	SSE 4
			20		ESE 4	Calm
			23	970	SE 2	Calm
		17 Mar.	2			SSE 6
			5	966		N 8
			8		N 10	NNW 6
6			11	984	N 9	N 7
6			14		N 9	N 7
6			17	1001	NNE 8	NNW 5
6			20		NNE 6	NNW 2
6			23	1015	N 3	SE 3
6		18 Mar.	2			SE 4
6			5	1011		SSW 2
6			8		ESE 5	SE 7

Record Nr.	Year	Date	Local Time h	Baro. mba	Wind Grimsey	Akureyri
			11	995	ESE 5	SSE 8
7			14		ESE 3	S 9
7			17	982	W 3	S 4
7			20		W 5	S 3
7			23	978	WNW 6	S 4
7		19 Mar.	2			W 8
7			5	981		W 4
7			8		WNW 9	W 5
7			11	992	WNW 8	W 9
7/8			14		NW 5	SSW 3
8			17	998	WNW 7	S 3
8			20		NW 5	Calm
8			23	994	NW 3	S 4
8		20 Mar.	2			SE 3
8			5	979		S 4
8			8		WNW 9	WSW 5
8			11	980	WNw 9	W 4
			14		NNE 5	W 3
	1967	26 Oct.	2			NNW 5
			5			N 5
			8		NNE 8	N 6
			11	985	NNE 8	NNW 5
			14		NNE 8	NW 5
			17		NNE 8	NNW 5
13			20			N 4
13			23	989	N 9	N 3
13		27 Oct.	2			SSE 2
13			5			N 6
13			8		NNE 9	N 4
13			11	991	NNE 9	NNW 4
			14		NNE 9	N 4
			17		NNE 9	NNW 5
			20			N 4
			23	1003	ENE 8	N 4

Record Nr.	Year	Date	Local Time h	Barom. mbar	Wind Grimsey	Wind Akureyri
		28 Oct.	2			NW 3
			5			N 2
			8		E 7	Calm
			11	1010	E 5	Calm
12			14		E 5	Calm
12			17		ESE 5	Calm
12			20			WNW 1
12			23	1009	ESE 2	Calm
12		29 Oct.	2			
12			5			
12			8			
			11	1010		
	1968	16 Mar.	23	964	NE 10	N 4
		17 Mar.	2	970		N 5
			5	977		N 5
			8	982	N 8	NNE 5
			11	985	N 8	NNW 5
9			14	990	NNE 7	NNW 5
9			17	992	NNE 5	NNW 4
99			20	994	NNE 4	SE 2
9			23	994	NNE 3	S 3
9		18 Mar.	2	"		W 2
9			5	"		W 2
9			8	"	NE 4	WNW 2
11			11	"	NE 4	WNW 2
11			14	993	ENE 4	NW 2
11			17	"	NE 6	N 3
11			20	"	NE 6	NE 4
11			23	"	NE 6	ENE 4
10		19 Mar.	2	"		ENE 4
10			5	"		W 3
10			8	991	NE 6	NE 7
10			11	995	NE 6	NE 5
10			14	996	NE 7	NE 4

APPENDIX 4

Illustration of the Effect of Atmospheric Pressure on Sea Level

Reference is made to Section 4.3, third paragraph.

The effect of atmospheric pressure on the water level in Eyjafjordur is most strikingly demonstrated in the accompanying fugire, indicated "Figure going with App. 4", for the recording period 14 to 20 March 1967. In that period of six days no less than four deep depressions successively passed over, or close to, Eyjafjordur.

In the figure various data were plotted against time.

The lower part gives:

1o. crosses (+), the approximate times and levels (relative) of high water (HW) and low water (LW), as roughly read from the paper chart of Hrisey; the levels were estimated as the maximum and minimum average levels over some 20 minutes, with respect to the edge of the chart; the height of the corsses indicate a measure of uncertainty;

2o. circles (°), for each HW or LW, the average level of (a:) that level and (b:) the average of the preceeding and the following LW or HW level; these circles approximating the mean level over one tidal cycle;

3o. half-crosses (⊢ and ⊣) connected by dashed lines, the times and approximate levels of beginning and end of the analyzed segments nrs. 5, 6, 7 and 8.

The upper part of the figure gives:

1o. crosses (+), atmospheric pressures over Eyjafjordur, as read from six-hourly synoptic surface weather maps;

2o. winds as observed at Grimsey Island (about 20 miles NNE of the mouth of Eyjafjordur) at 09, 11, 14, 17, 20, 23 h local time (direction and force Beaufort);

3o. Indications of passing depressions and ridges.

The negative correlation between atmospheric pressure and mean sea level is most conspicuous. The sea level obviously responded to the varying air pressure without a notable time lag. A plot (not shown here) of the air pressures (averaged over 12 hours similarly as the water levels) against the simultaneous mean sea levels (interpolated) reveals all points except three lying within 4 cm from a straight line given by: air pressure (mbar) + sea level (cm) = 1074. This indicates an almost purely isostatic inverse barometer effect according to the thecretical relation: 1 mbar corresponds with 1.01 cm of sea water.

The outlying three points refer to 17 March, 5, 11 and 17 h, for which the levels are about 10 cm low. That day was characterized by strong northerly winds and a very steep rise of air pressure. A direct wind effect on the sea level in this case would rather be expected to pile up the water in the fjord, contrary to the observation; the direct wind effect on the sea levels in the fjord, however, can account for a few centimeters only due to the large water depths in the fjord. The moving depressions may also have generated edge waves, propagating with the depressions along the Icelandic north coast, with large periods of order $\frac{1}{2}$ day, thus affecting notably the HW and LW levels, a rough estimate from the speed of the depressions and the shelf slope, however, suggests rather periods of 1 h and less for such edge waves. A plausible explanation for these three outlying points cannot be given.

The consequence of the large, meteorologically induced, long-period variations of mean water level for the analyzed 24h 48min segments is clearly demonstrated in the figure; level differences between beginning and end going up to 30 centimeters. The resulting "saw-tooth effect" on the Fourier analysis was dealt with in Section 4.3.

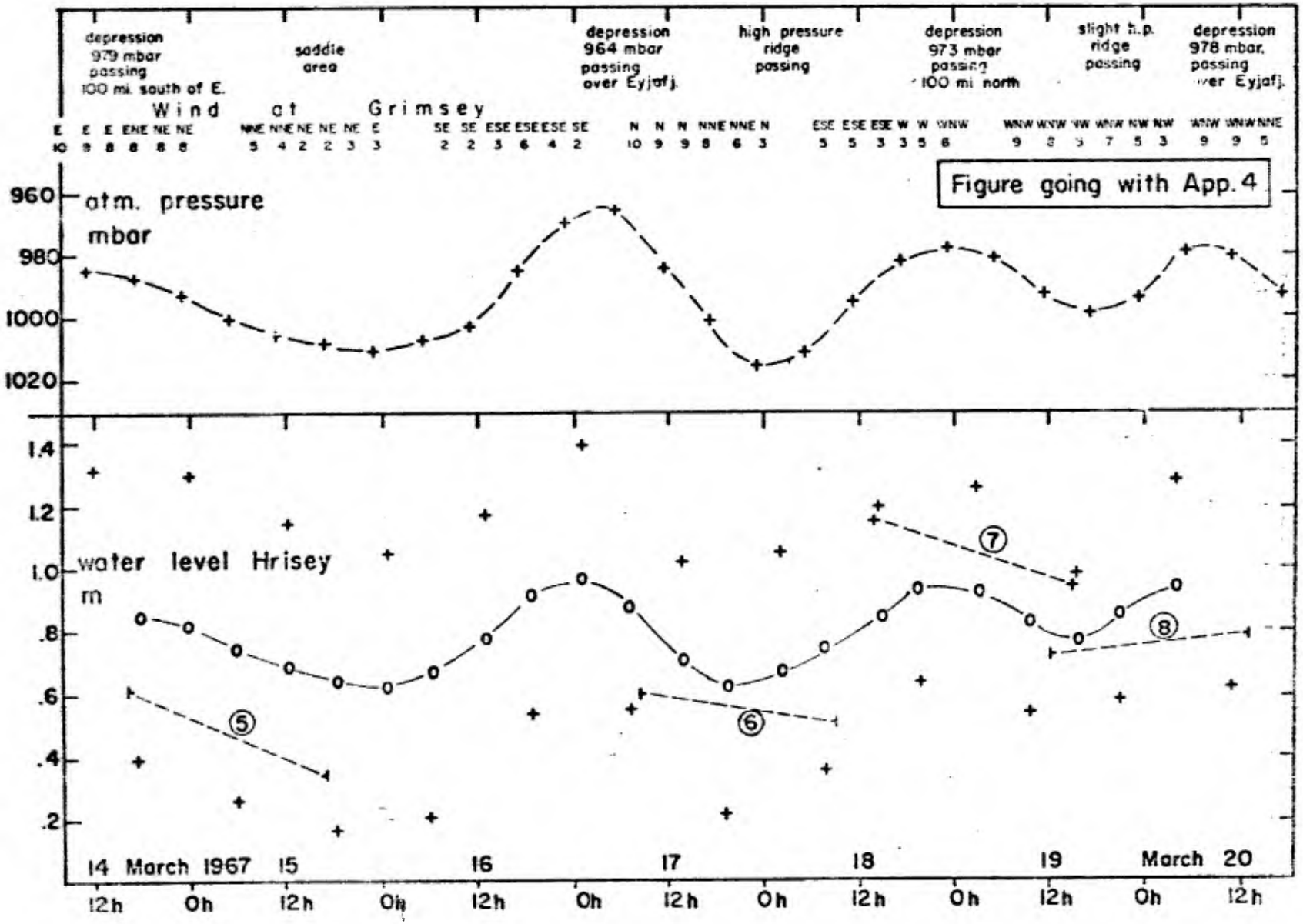
depression 979 mbar passing 100 mi. south of E.
saddle area
depression 964 mbar passing over Eyjafj.
high pressure ridge passing
depression 973 mbar passing 100 mi north
slight h.p. ridge passing
depression 978 mbar passing over Eyjafj.
Wind at Grimsey
E E E ENE NE NE NNE NNE NE NE NE E SE SE ESE ESE ESE SE N N N NNE NNE N ESE ESE ESE W W WNW WNW WNW NW NW NW WNW WNW NNE
10 9 8 8 8 8 5 4 2 2 3 3 2 2 3 6 4 2 10 9 9 8 6 3 5 5 3 3 5 6 9 8 5 7 5 3 9 9 5
Figure going with App. 4
960
980
1000
1020
atm. pressure
mbar
1.4
1.2
1.0
.8
.6
.4
.2
water level Hrisey
m
⑤
⑥
⑦
⑧
14 March 1967
15
16
17
18
19
March 20
12h
0h
12h
0h
12h
0h
12h
0h
12h
0h
12h
0h
12h

APPENDIX 5

Bias in the estimates of the relative spectral densities in the resonance peaks (Section 6.2, Fig. 6F).

The notations used are those introduced in Section 8.2.1.

In Section 6.2 (Fig. 6F), we estimated average relative shapes of the resonance peaks in the autospectra of Akureyri S as averages over p of the fraction:

$$\frac{W_{Anp}}{\sum_{k_1}^{k_2} W_{Akp}} = f_{np}, \text{ say,} \tag{1}$$

where n denotes a particular value of k and the sum in the denominator was taken over a k-range including the resonance peak with its wings. A better estimate would be the average over p of the fraction:

$$\frac{W^*_{Anp}}{\sum_{k_1}^{k_2} W_{Akp}} = f^*_{np}, \text{ say,} \tag{2}$$

To compare both expressions (1) and (2), we can write, from Section 8.2.1, Eq. (2), and after omitting (for simplicity) the suffices A and the letters k_1 and k_2:

$$f_{np} = \frac{W^*_{np}\,(1 + \epsilon_{np})}{\sum_k \{W^*_{kp}\,(1 + \epsilon_{kp})\}} = \frac{W^*_{np}}{\sum_k W^*_{kp}} \times \frac{1 + \epsilon_{np}}{1 + X_p} = f^*_{np}\,\frac{1 + \epsilon_{np}}{1 + Xp} \tag{3}$$

where we have put

$$\frac{\sum_k (W^*_{kp}\,\epsilon_{kp})}{\sum_k W^*_{kp}} = \sum_k f^*_{kp}\,\epsilon_{kp} = Xp \tag{4}$$

representing a weighed average of ϵ_{kp} over the k-range considered. The expected values of ϵ_{np} and Xp for many records p are zero, the variances of ϵ_{np} are 1 and the varance of Xp is $\sum_k (f^*_{kp}) < 1$. From (3), we obtain for the expected values for many records p, approximately:

$$E(f_{np}) = E(f^*_{np}) \times E\left(\frac{1 + \epsilon_{np}}{1 + Xp}\right) \tag{5}$$

This is an approximation because, though ϵ_{np} is not correlated with f^*_{np}, Eq. (4) shows that Xp and f^*_{np} are positively correlated. The variability in the fractions f^*_{kp} with respect to p, however, will be relatively small. Let us assume, to proceed, that f^*_{kp} does not depend on p; thus $f^*_{kp} = f^*_k$. Then we have

$$E(f_{np}) = f^*_n \cdot E\{(1 + \epsilon_{np})\ (1 - Xp + \frac{Xp^2}{1 + Xp})\}$$

$$= f^*_n[1 - E(\epsilon_{np} Xp) + E(\frac{Xp^2}{1 + Xp}) + E(\epsilon_{np}\ \frac{Xp^2}{1 + Xp})] \tag{6}$$

The second term in the square brackets, from (4), with the assumptions made, is simply $-f^*_n$.

The fourth term is seen to be small compared to the third term and may be neglected.

The third term is positive since all Xp are > -1. It will not deviate much from $E(Xp^2) = \Sigma(f^{*2}_k)$.

Thus we arrive at, approximately:

$$E(f_{np}) = f^*_n[1 - f^*_n + \Sigma(f^{*2}_k)] \tag{7}$$

The confidence we can put in this equation is strengthened by the fact

that, by taking the sum over n from k_1 to k_2, it yields the relation $\sum_n \{E(f_{np})\} = \sum_n f_n^* = 1$, as it should be.

Now consider different cases:

1o. f_n^* is relatively <u>small</u>, i.e., n lies outside the resonance peak; in that case, we see that the estimator $E(f_{np})$ is <u>positively</u> biased;

2o. f_n^* is relatively <u>large</u>, i.e., n lies at or near the top of the resonance peak; in that case we have a good chance that in fact, if f_n is the largest of all f_k in the k-range considered, this can be shown to be true; this means that the estimator $E(f_{np})$ is <u>negatively</u> biased.

Example. Consider the range k = 7 to 17 incl.

k or n	7-10 incl.	11	12	13	14-17 incl.	
Assume f_k^*	.025	.18	.44	.18	.025	(sum = 1) sum of squares .263
Eq. (7) gives $E(f_{np})$	.031	.195	.362	.195	.031	(sum = 1)

This example very roughly corresponds with the plot in Fig. 6F (the ordinates there having been divided by 11).

It is clear that the estimator procedure used for Fig. 6F smoothens out the real resonance peak to some extent.

It would be possible to correct the plots given in Fig. 6F by solving the $k_2 - k_2 + 1$ equations (7) ($n = k_1, k_1 + 1 \ldots k_2$) with the left-hand members considered as being vien by the averages of f_{np} over 8 records. For the first resonance peak this has been done very roughly in the example just given.